

https://dspace.org/

Bioremediation of Acid Mine Drainage Using Grass

Smith, Janet

2025-10
University of the Witwatersrand, Johannesburg
https://hdl.handle.net/10539/50094
Smith, Janet. (2025). Bioremediation of Acid Mine Drainage Using Grass. [PhD thesis, University of the Witwatersrand, Johannesburg]. WIReDSpace. https://hdl.handle.net/10539/50094

Downloaded from a DSpace repository. https://dspace.org/



UNIVERSITY OF THE
WITWATERSRAND,
JOHANNESBURG

Bioremediation of Acid Mine Drainage Using Grass

Prepared by

Janet Smith (819988)

A dissertation submitted to the School of Chemical and Metallurgical Engineering, Faculty of Engineering and the Built Environment, University of the Witwatersrand, in fulfilment of the requirements for the degree Doctor of Philosophy

Supervisors

Prof. Lizelle van Dyk

Prof. Kevin Harding

Prof. Craig Sheridan

October 2025

Acknowledgements

Financial Acknowledgements

I would like to acknowledge Professor Craig Sheridan for his financial support of this research.

Personal Acknowledgements

I am deeply grateful to my academic supervisors, Professor Lizelle van Dyk, Professor Craig Sheridan, and Professor Kevin Harding for their guidance and support, and making this research possible.

To my family, my husband Steve and daughter Nicole for their love, encouragement, and support during my many years of studies; to Aunty Rose for taking such good care of our family and allowing us the time to pursue our dreams; to my brother Gerald, for his encouragement and unwavering belief in my abilities; and to my parents, Mary and Neil Wright, whose deep belief in the power of education taught me that no dream was impossible.

To Motlatsi Phali for his friendship, exceptional technical support and analytical assistance.

To the many others, not individually mentioned, that have helped me to fulfil this dream, I am truly grateful to everyone and am again reminded of a quote by George Matthew Adams: “There is no such thing as a “self-made man.” We are made up of thousands of others. Everyone who has ever done a kind deed for us, or spoken one word of encouragement to us, has entered into the make-up of our character and our thoughts, as well as our success.”

Declaration

I declare that this dissertation is my own unaided work. It is being submitted for the degree of Doctor of Philosophy to the University of the Witwatersrand, Johannesburg. It has not been submitted before for any degree or examination to any other University.

Janet Smith
3rd October 2025

Summary

Large-scale mining of South Africa's gold in the Witwatersrand, and coal in the Mpumalanga areas has contributed substantially to economic wealth and energy provision for the South African economy. Unfortunately, these operations have also resulted in considerable damage to surrounding environments. One of the largest sources of this large-scale mining-induced environmental damage in South Africa is acid mine drainage (AMD). AMD is formed when sulfidic rock is exposed to oxygen and water, and results in highly mineralised, acid water, which can infiltrate and contaminate surrounding groundwater, land, and surface watercourses (McCarthy, 2011a; Simate and Ndlovu, 2014). Where AMD volumes surpass the natural dilution effects, plants, animals, humans, and economic activities such as agriculture suffer negative impacts. Since South Africa is a water-stressed country, remediating AMD is critical to protect limited water resources.

Active chemical treatment options for AMD remediation are generally implemented owing to their ease of control; however, these treatment options carry high capital and operating costs and produce large volumes of hazardous sludge waste. A more sustainable and cost-effective alternative to chemical treatment is biological treatment via the dissimilatory reduction (DSR) remediation process. DSR uses sulfate reducing bacteria (SRB) to reduce sulfates (SO_4^{2-}) to hydrogen sulfide (H_2S). The alkalinity produced from the reaction increases the pH and precipitations metals present in the system as metal sulfides (Ruehl and Hiibel, 2020; Burman, Harding and Sheridan, 2021).

The DSR process requires supplementation with an organic carbon source to drive the remediation process (Van Rooyen, Van Staden and Du Preez, 2021). Grass can be used as a lignocellulosic substrate to provide the organic carbon and electron donor source to drive the DSR process. Grass is a renewable, secondary waste resource that is readily available as natural growth, garden waste, and roadside vegetation, and thus does not compete with primary agricultural output for food production, a particularly important consideration for countries which experience food insecurity (Magowo, Rumbold and Sheridan, 2015). However, the complex organic structure of the grass needs to be broken down to release the monomeric sugars in a form amenable to SRB before it can be used in the DSR process. In this work, the acidity of AMD is used as a weak acid source to disrupt the grass lignocellulosic structure. This disrupted lignocellulosic structure would render the cellulosic component in the grass amenable to subsequent enzymatic hydrolysis and fermentation for biofuel production. Using the grass residue from AMD bioremediation for bioethanol production provides a means to derive value from the remediation process which can help to offset the remediation costs.

This study aimed to contribute to existing knowledge for the development of a more sustainable process for the biological remediation of AMD. The study also sought to assess the effects of varying AMD bioremediation process conditions on subsequent biofuel production.

This research commenced with a characterisation of AMD from two AMD receiving dams in the Mpumalanga coalfields region in South Africa, and an evaluation of the seasonal variations on the physical and chemical parameters present in the AMD. Spatial and temporal trends presented changes in physio-chemical

concentrations, which provides valuable information to inform remediation process development, and to identify possible limitations in prospective remediation processes. Data showed the presence of several metal(oid)s that were in excess of legislative limits. The removal of elevated concentrations of manganese (Mn) and zinc (Zn) are difficult by adsorption and are thus not easily supported by passive treatment systems. High concentrations of aluminium are difficult to remove via precipitation mechanisms owing to the amphoteric nature of aluminium hydroxides and would thus be less suited to active chemical treatment processes. This work demonstrated a strong correlation between electrical conductivity (EC) and total dissolved solids (TDS). Other major AMD parameters, such as iron (Fe) and sulfate (SO_4^{2-}), showed similar temporal trends to EC and TDS.

The research continued with a statistical evaluation of all the data from the two Mpumalanga AMD sites. This confirmed the strong EC/TDS correlation noted in the previous work and identified further EC correlated parameters which included total acidity (TA), dissolved iron (Fe), and dissolved sulfur (S). EC was thus identified as a useful correlative measurement for the prediction of TA, Fe and S concentrations in these acidic AMD waters. These empirical correlations were then leveraged to derive regression equations which were used to calculate EC values corresponding to legislative water quality limits and thus provide a novel rapid method for testing compliance. In a similar manner, EC can also be used as a control measure in remediation processes, particularly in the event of an uncontrolled AMD breach, where real-time measurements could trigger a fast response to minimise potential environmental harm.

In the next part of the work, locally sourced grass types that were co-located with AMD sites in the Mpumalanga coalfields region, South Africa were identified, classified, and their physical and chemical properties determined. Experimental test work was conducted to assess the amenability of these grass types to increase the pH of AMD, thereby indicating their suitability for use in AMD bioremediation. Grass types, *Chrysopogon zizanioides* and *Hyparrhenia hirta* achieved the greatest increase in pH after single and multiple grass additions. Renewing the organic substrate improved the performance of the more poorly performing grass types. This was supported by an improvement in the anticipated positive correlation between the hydrogen ion concentration (H^+) and oxidation-reduction potential (ORP). Decreased inorganic cation concentrations observed in the grass samples after contact with AMD indicated the likelihood of an ion-exchange reaction between the H^+ ions in the AMD and inorganic cations associated with the anions present in the grass.

In the next component of the study, naturally occurring sources of SRB cultures were experimentally evaluated to determine their suitability to support SRB growth and activity in AMD remediation. The performance of the selected SRB culture sources was assessed at three different pH environments. Raw sewage (RS) collected from the Bushkoppies wastewater treatment facility near Soweto, and mud inoculum sampled from the reed beds (RM) surrounding a Mpumalanga AMD source, achieved the greatest conversion of sulfate to sulfide. The reduction of sulfate to sulfide is indicative of the DSR process which was shown to improve at neutral pH.

Lastly, experimental work was conducted to evaluate the effect of hydraulic retention time (HRT) on AMD bioremediation using grass, and subsequent bioethanol production. To produce bioethanol from grass, the lignocellulosic structure of the grass must first be broken down to render the grass amenable to enzymatic hydrolysis. The premise for this work was that If grass were used for AMD remediation, the acidity from the AMD would be sufficient to disrupt the lignocellulosic structure of the grass. The opened grass structure will facilitate enzyme access to the remaining sugars in the grass in a subsequent simultaneous hydrolysis and fermentation (SSF) process to produce bioethanol products. This would provide a dual use for the grass, whereby it is first used for AMD remediation, and subsequently the waste grass from this process is used for bioethanol production, thereby creating an opportunity to derive value from the overall process. Various investigations into grass contacted with AMD (to achieve optimal AMD remediation, and to achieve the greatest conversion to bioethanol after SSF were performed. The AMD remediation and grass pre-treatment experiments were conducted with and without SRB addition. Data showed that the synthetically prepared weak acid AMD solution was sufficient to disrupt the grass lignocellulosic structure at ambient temperature. Extending the retention times to eleven and thirteen days improved the pH increase and sulfide production, particularly in filtered AMD solutions after grass had been removed. SRB amendment improved pH increase, and sulfide production was increased by orders of magnitude more than in non-amended samples. An untreated grass sample that had not had prior exposure to acid hydrolysis by AMD, produced marginally higher ethanol concentrations during SSF than the non-amended pre-treated day eleven sample, but less than the SRB-amended day eleven HRT sample. As such, SRB amendment and longer grass-AMD contact times, favoured improved AMD remediation as well as bioethanol production.

Testwork was successfully carried out to address all objectives. The outcomes from each study bring new knowledge to improve the sustainability and potentially improve the cost-effectiveness of AMD bioremediation techniques.

Table of Contents

List of Acronyms 12

CHAPTER 1 14

1 Introduction 14
1.1 Background 14
1.2 Problem Statement 15
1.3 Research Objectives 16
1.4 Novelty of this research 16
1.5 Structure of Dissertation 18
1.6 References 21

CHAPTER 2 23

2 Literature Review 23
2.1 Energy in South Africa 23
2.2 Mining in South Africa 23
2.3 Water in South Africa 24
2.4 The Impacts of Mining on Water 27
2.4.1 The formation of Acid Mine Drainage (AMD) 28
2.4.2 Environmental, social, and other impacts of AMD 30
2.5 Physico-chemical Properties of AMD in the Mpumalanga Coalfields South Africa 32
2.6 Current Treatment of Acid Mine Drainage 35
2.6.1 Abiotic AMD remediation technologies 36
2.6.2 Passive AMD remediation processes 38
2.7 Biological sulfate reduction (BSR) 40
2.7.1 Factors affecting the success of the dissimilatory sulfate remediation (DSR) processes 40
2.8 Grass as an alternate organic carbon source for AMD remediation 43
2.9 Bioethanol production using lignocellulosic biomass 45
2.10 The pursuit of a sustainable, cost-effective biological process for AMD remediation 46
2.11 References 48

CHAPTER 3. 56

3 Seasonal characterisation of acid mine drainage in Mpumalanga coalfields region 56
3.1 Abstract 57
3.2 Introduction 57
3.3 Experimental Procedure 58
3.3.1 Sampling Procedure 58
3.3.2 Analytical Methods 58

3.3.3 Results and Discussion 59
3.4 Conclusions 65
3.5 References 66

CHAPTER 4. 68

4 Critical evaluation of the chemical composition of acid mine drainage for the development of statistical correlations linking electrical conductivity with acid mine drainage concentrations 68
4.1 Abstract 69
4.2 Introduction 70
4.3 Method 72
4.3.1 Sampling and Preservation 72
4.3.2 Analytical Methods 72
4.3.3 Calibration and data quality control 73
4.3.4 Comparison of data with legislative and advisory guides 74
4.4 Results and Discussion 74
4.4.1 Analytical Data 74
4.4.2 Potential Health Effects 75
4.4.3 Seasonal Variability 75
4.4.4 Correlation Analysis 75
4.4.5 Regression Analysis 77
4.5 Conclusion 82
4.6 Acknowledgements 82
4.7 Recommendations 82
4.8 References 83

CHAPTER 5. 85

5 Classification of grasses in the Mpumalanga coalfields region and assessment of their suitability to increase the pH of acid mine drainage, for potential use in passive acid mine drainage remediation systems 85
5.1 Abstract 86
5.2 Introduction 87
5.2.1 Acid mine Drainage and Remediation 87
5.2.2 Lignocellulose biomass 88
5.3 Methodology for grass classification 89
5.3.1 Sampling and classification of grass 89
5.3.2 Determination of the structural and chemical composition of grasses 90
5.3.3 Determination of extractives, structural carbohydrates, and lignin 90
5.3.4 Ultimate composition analysis 91
5.3.5 Proximate analysis 91

5.3.6 Calorific value analysis 92
5.3.7 Determination of pH, oxidation-reduction potential (ORP), and dissolved oxygen (DO) 92
5.4 Methodology for determination of suitability of different grass types from the Mpumalanga coalfields region, (South Africa) to increase the pH of AMD for use in AMD remediation 92
5.4.1 Single grass addition experiment – Procedure for sample and reactor preparation 92
5.5 Testwork to establish the effects of multiple additions of fresh grass to AMD on solution pH, ORP, and DO 93
5.5.1 Multiple grass addition experiment - Sample and reactor preparation 93
5.5.2 Chemical analysis of grass samples before and after contact with AMD 93
5.6 Results 94
5.6.1 Grass classification 94
5.6.2 Composition of grass 95
5.7 Single grass addition - Determination of the suitability of grass for AMD remediation 96
5.8 Multiple grass addition - The effects of multiple additions of fresh grass to AMD on solution pH, ORP, and DO 98
5.9 Elemental concentration data for grass samples before and after subsequent addition to AMD 101
5.10 Discussion 103
5.11 Conclusions 107
5.12 Recommendations 108
5.13 Acknowledgements 108
5.14 References 108

CHAPTER 6. 111

6 Investigation of suitable, readily available, sources of sulfate-reducing bacteria inoculum, and evaluation of sulfate reduction rates achieved at different pHs 111
6.1 Abstract 112
6.2 Introduction 113
6.3 Materials and Methods 114
6.4 Reactor set-up 114
6.5 Parameters evaluated 116
6.6 Results and Discussion 116
6.6.1 Results 117
6.7 Testwork performed at pH 2 117
6.8 Testwork performed at pH 4 118
6.9 Testwork performed at pH 7.5 120
6.10 Discussion 122
6.11 Conclusions 123
6.12 Acknowledgements 124
6.13 References 124

CHAPTER 7. 127

7 The effects of grass pre-treatment time on acid mine drainage bioremediation potential, and bioconversion of sugars to ethanol 127
7.1 Abstract 128
7.2 Introduction 128
7.3 Materials and Methods 131
7.3.1 Grass collection and preparation 131
7.3.2 Pre-treatment of grass 131
7.3.3 Simultaneous hydrolysis and fermentation of pre-treated grass 132
7.4 Results and discussion 133
7.4.1 Acid mine drainage grass pre-treatment results 133
7.4.2 Enzymatic hydrolysis and fermentation data 149
7.5 Conclusions 159
7.6 Acknowledgements 160
7.7 References 160

CHAPTER 8. 163

8 Discussion and Concluding remarks 163
8.1 Discussion of objectives 163
8.1.1 Objective a: Characterisation of acid mine drainage (AMD) 163
8.1.2 Objective b: Characterisation of grasses 164
8.1.3 Objective c: Naturally occurring sources of sulfate reducing bacteria (SRB) inoculum 165
8.1.4 Objective d: Grass pre-treatment time and SRB addition for acid mine drainage remediation and bioconversion of sugars to ethanol 166
8.2 Concluding remarks 167
8.3 Recommendations 168

Appendix I - Supplementary data for Chapter 4 170

Appendix II - Supplementary data for Chapter 5 210

Appendix III - Supplementary data for Chapter 6 228

Appendix IV - Supplementary data for Chapter 7 233

List of Figures

Figure 1.1 Summary diagram of the individual investigations included in chapters three to seven, and their relation to the dissertation objectives. 20

Figure 2.1 Map of southern Africa, showing the six river basins, their main rivers and tributaries, and the approximate extent of the seven aquifer systems shared between South Africa and neighbouring countries. Data for map taken from Kistin et al. (2009), data from (Ashton et al., 2006; Struckmeier and Richts, 2006; Kistin et al., 2009). 25

Figure 2.2 Republic of South Africa Proposed Water Management Areas. Department of Water and Sanitation (DWS) (2022). 26

Figure 2.3 A conceptual model of AMD pollution. Data from (Jiao et al., 2023). 30

Figure 2.4 AMD generation and related contamination pathway. Data from (Naidu et al., 2019). 31

Figure 2.5 The locality of the Witbank Coalfield and geochemical sample sites. Data from (Cairncross, Hart and Willis, 1990) 32

Figure 2.6 Pathways and relationships between total metal in an earth material and toxicity. Data from (Smith, 2007). 34

Figure 2.7 Abiotic and biological remediation technologies for acid mine drainage water. Data from (Simate and Ndlovu, 2014). 35

Figure 2.8 Schematic diagram showing the effect of pre-treatment on lignocellulosic biomass. Data from (Tong, Cheng and Pullammanappallil, 2013). 44

Figure 3.1 Variation in rainfall and total acidity, electrical conductivity, and dissolved aluminium (Al), iron (Fe), and sulfur (S) concentrations for Site 1 over the sampling period. 64

Figure 3.2 Variation in rainfall and total acidity, electrical conductivity, and dissolved aluminium (Al), iron (Fe), and sulfur (S) concentrations for Site 2 over the sampling period 65

Figure 4.1 Visual Abstract: Critical evaluation of the chemical composition of acid mine drainage for the development of statistical correlations linking electrical conductivity with acid mine drainage concentrations 69

Figure 4.2 Location of coal mines in South Africa (MineralscouncilSouthAfrica, 2019) 71

Figure 4.3 Linear regression equations with the intercept set to zero for total dissolved solids, total acidity, dissolved iron and sulfur as a function of electrical conductivity 79

Figure 4.4 Linear regression with the intercept set to zero, and power regression equations used for total dissolved solids total acidity, dissolved iron and sulfur as a function of electrical conductivity. 80

Figure 4.5 Total dissolved solids total acidity, dissolved iron and sulfur as a function of electrical conductivity: Linear regression with the intercept set to zero, and power regression equations after rejection of outliers 81

Figure 5.1 Graphical Abstract: Classification of grasses in the Mpumalanga coalfields region and assessment of their suitability for potential use in passive acid mine drainage remediation systems 86

Figure 5.2 The location of the grass samples collected in the Mpumalanga coalfields region of South Africa (Scale 1:2 200 000 cm). 90
Figure 5.3 pH and ORP data for synthetic and receiving dam (RD) AMD solutions after grass addition 97
Figure 5.4 pH and Eh data for synthetic and return dam (RD) AMD solutions after subsequent grass addition 99
Figure 5.5 K, Mg, Ca, P, Na and S concentrations in grass samples before and after subsequent addition to AMD. Samples 13, 13 (2), and 12 are classified as Hyparrhenia hirta, grass 15 is classified as Chrysopogon zizanioides, G5 as Hyparrhenia filipendula, and G6 as Eragrostis curvula 102
Figure 5.6 Oxidation-reduction potential (ORP) plotted as a function of hydrogen ion concentration (H^+) for single and multiple grass additions 106
Figure 6.1 Visual abstract: The investigation of suitable, readily available, sources of sulfate-reducing bacteria inoculum, and evaluation of sulfate reduction rates achieved at different pHs 112
Figure 6.2 Reactor arrangement for experimental work 115
Figure 6.3 Experimental data for test work performed at pH 2 showing the change in pH, S^{2-}, SO_4^{2-}, and COD concentrations over time. 117
Figure 6.4 Experimental data for test work performed at pH 4 showing the change in pH, S^{2-}, SO_4^{2-}, and COD concentrations over time. 119
Figure 6.5 Experimental data for test work performed at pH 7.5 showing the change in pH, S^{2-}, SO_4^{2-}, and COD, concentrations over time. 121
Figure 7.1 SEM secondary electron images of (i) grass before pre-treatment; (ii) grass pre-treated without SRB amendment; and (iii) grass pretreated with SRB amendment. 134
Figure 7.2 Glucose and xylose concentrations produced for non- and SRB-amended samples, at each grass-AMD contact hydraulic retention time (HRT), using a 30 g/L grass-AMD ratio. Error bars represent the standard deviation of duplicate analyses 135
Figure 7.3 Acetate and propionate concentrations produced for non- and SRB-amended samples, at each grass-AMD contact hydraulic retention time (HRT), using a 30 g/L grass-AMD ratio. Error bars represent the standard deviation of duplicate analyses. 137
Figure 7.4 pH values for AMD blanks and for non- and SRB-amended samples, for each of the selected grass-AMD hydraulic retention times (HRT), using a 30 g/L grass-AMD ratio, and 24 mL/L of SRB. Error bars represent the standard deviation of duplicate analyses 139
Figure 7.5 pH values for (a) non-amended filtrate samples and (b) SRB-amended filtrate samples vs the number of days after grass removal for initial grass hydraulic retention times (HRT). Error bars represent the standard deviation of duplicate analyses. 140
Figure 7.6 Average COD concentrations with standard deviations for non- and SRB-amended samples and AMD blank samples for each selected grass-AMD hydraulic retention

times (HRT), using a 30 g/L grass-AMD ratio. Error bars represent the standard deviation of duplicate analyses. 141
Figure 7.7 COD concentrations for (a) non-amended filtrate samples and (b) SRB-amended filtrate samples plotted against the number of days after grass removal. Error bars represent the standard deviation of duplicate analyses. 143
Figure 7.8 Sulfide concentrations for AMD blanks and for non- and SRB-amended samples, for each for the selected grass-AMD hydraulic retention times (HRT), using a 30 g/L grass-AMD ratio. Error bars represent the standard deviation of duplicate analyses. 144
Figure 7.9 Sulfide concentrations for (a) non-amended filtrate samples and (b) SRB-amended filtrate samples plotted against the number of days after grass removal. Error bars represent the standard deviation of duplicate analyses. 145
Figure 7.10 Fe concentrations for blanks and for non- and SRB-amended samples, for each of the selected grass-AMD hydraulic retention times (HRT), using a 30 g/L grass-AMD ratio. Error bars represent the standard deviation of duplicate analyses. 147
Figure 7.11 Fe concentrations for (a) non-amended filtrate samples and (b) SRB-amended filtrate samples plotted against the number of days after grass removal. Error bars represent the standard deviation of duplicate analyses. 148
Figure 7.12 Glucose concentrations produced during SSF hydrolysis of untreated and pre-treated grass samples, for non- and SRB-amended samples. Error bars represent the standard deviation of duplicate analyses. 149
Figure 7.13 HPLC chromatograms showing (a), the assumed glucose isomer peak at RT 3.68, and a separate glucose peak at RT 4.00 and (b), a possible glucose isomer peak overlapping glucose peak 150
Figure 7.14 The glucose-isomer/glucose peak showing an initial increase in concentration, followed by a decrease in concentration over time for non- and SRB-amended samples. Error bars represent the standard deviation of duplicate analyses. 151
Figure 7.15 Xylose concentrations produced during SSF hydrolysis of untreated and pre-treated grass samples, for non- and SRB-amended samples. Error bars represent the standard deviation of duplicate analyses. 152
Figure 7.16. Lactate concentrations produced during SSF hydrolysis of untreated and pre-treated grass samples, for non- and SRB-amended samples. Error bars represent the standard deviation of duplicate analyses. 153
Figure 7.17 Acetate concentrations produced during fermentation of untreated, and pre-treated grass samples, for non- and SRB-amended samples. Error bars represent the standard deviation of duplicate analyses. 154
Figure 7.18 Propionate concentrations produced during fermentation of untreated, and pre-treated grass samples, for non- and SRB-amended samples. Error bars represent the standard deviation of duplicate analyses. 155

Figure 7.19 Valerate concentrations produced during fermentation of untreated, and pre-treated grass samples, for non- and SRB-amended samples. Error bars represent the standard deviation of duplicate analyses. 156
Figure 7.20 Isovalerate concentrations produced during fermentation of untreated, and pre-treated grass samples, for non- and SRB-amended samples. Error bars represent the standard deviation of duplicate analyses. 156
Figure 7.21 Ethanol concentrations produced during fermentation of untreated and pre-treated grass samples, for non- and SRB-amended samples. Error bars represent the standard deviation of duplicate analyses. 157

List of Tables

Table 2.1 Comparison of trace elements in South African coals - adapted from: (Wagner and Hlatshwayo, 2005). 33
Table 3.1 Physical and chemical parameters as measured for Site 1 in Mpumalanga 59
Table 3.2 Physical and Chemical parameters as measured for Site 2 in Mpumalanga 60
Table 3.3 Site 1 and 2 data – major cations and anions 61
Table 3.4 Dissolved Metals Concentrations 63
Table 4.1 Methodology and/or instrumentation used for sample analysis 72
Table 4.2 Separate and pooled correlations between electrical conductivity, calculated total dissolved solids, total dissolved solids, total acidity, dissolved iron and dissolved sulfur concentrations 76
Table 4.3 Summary of ANOVA test results at a 95 % confidence level 77
Table 4.4 A comparison of the R-squared values achieved for each parameter using the different regression options and after rejection of outliers 79
Table 5.1 Grass name and classification 94
Table 5.2 The averaged structural, proximate, ultimate, and calorific value analysis concentration ranges of the collected grass samples 95
Table 5.3 Percentage change in hydrogen ion concentration (H^+) from initial H^+ concentration after each successive grass addition to synthetic AMD, and after the experiment. 104
Table 6.1 Reactor conditions. 116
Table 7.1 The Increase in ethanol concentration produced during SSF 158

List of Acronyms

Acronym	Definition
ABC	Alkaline–barium–calcium
AMD	Acid mine drainage
ANOVA	Analysis of variance
APHA	American Public Health Association
AWARD	Association for Water and Rural Development
BSR	Biological sulfate reduction
CD	Cow dung
CHNS	Carbon, hydrogen, nitrogen, and sulphur
CMA	Catchment management agency
COD	Chemical oxygen demand
CRM	Certified reference material
CV	Calorific value
DBS	De Bruyn Spectroscopic
DI	Deionised water
DMR	South African Department of Minerals and Energy
DO	Dissolved oxygen
DSR	Dissimilatory sulfate reduction
DWAF	South African Department of Water Affairs
DWEL	Drinking Water Equivalent Level
DWS	Department of water and sanitation
EC	Electrical conductivity
EPA	United States Environmental Protection Agency
GCI	Global Change Institute
GDP	Gross domestic product
GF	Glass fibre
CoGTA	South Africa Department of Cooperative Governance and Traditional Affairs
HRT	Hydraulic retention time
ICP	Inductively coupled plasma
ICP-OES	Inductively coupled plasma - optical emission spectrometry
IMWA	International Mine Water Association
MA	Methanogenic archaea
MCL	Maximum Contaminant Level
MIW	Mine impacted water
MJ	Megajoules
MS	Mass spectrometry
MUD	AMD mud

Acronym	Definition
MW	Microwave
NECOM	South African National Energy Crisis Committee
NIC	Nanotechnology Innovation Canter at Mintek, South Africa
NMD	Neutral mine drainage
NTU	Turbidity
NWA	South African National Water Act 36 of 1998
NWRIA	National Water Resource Infrastructure Agency
ORP	Oxidation-reduction potential
PP	Polypropylene
PTE	Potentially toxic element
RD	Received dam
REE	Rare earth elements
RM	Mud inoculum sampled from the reed beds
RO	Reverse osmosis
RS	Raw sewage
RSD	Relative standard deviation
SACEC	South African Chemical Engineering Congress
SAHRC	South African Human Rights Commission
SANS	South African National Standard
SEM	Scanning electron microscope
SEMA	Specific Environmental Management Act
SFF	Simultaneous saccharification and fermentation
SHE	Standard hydrogen electrode
SHF	Separate hydrolysis and fermentation
SPR	Source-pathway-receptor
SRB	Sulfate reducing bacteria
TA	Total acidity
TDS	Total dissolved solids
TGA	Thermogravimetric analysis
TSS	Total suspended solids
TWQR	Target Water Quality Range
UJ	University of Johannesburg
VFA	Volatile fatty acids
WMA	Water management agencies
WSA	South African Water Services Act 108 of 1997
WSP	Water Service Providers

CHAPTER 1

1 Introduction

1.1 Background

Earth's finite water supply is affected by several factors, such as changing climatic conditions, population growth, industrialization, and urbanization amongst others (Bogardi *et al.*, 2012a). South Africa is ranked amongst the 20 most water-scarce countries in the world and receives an estimated 500 mm of annual precipitation compared to the world-wide average of 860 mm. As such, water security and sustainability are of increasing concern, particularly as increased industrial and agricultural production are required to support a growing population (Woodford, Rosewarne and Girman, 2006; Bogardi *et al.*, 2012a). Mining has historically been central to South Africa's economic, social, and political environment; however, particularly evident in gold and coal mining activities is the formation of acid mine drainage (AMD), which has had a deleterious impact on water quality (Simate and Ndlovu, 2014). South Africa is heavily reliant on coal to satisfy economic revenue generation from coal exports, and for use in coal-fired power generation. Continued mining activity, and the predicted generation of significant quantities of AMD post mine closure are compounded by the prohibitive costs and commercial technology limitations of remediating these mine-impacted waters (Woodford, Rosewarne and Girman, 2006; Bogardi *et al.*, 2012b; Simate and Ndlovu, 2014). Thus, there is a need for the development of sustainable, and cost-effective, technologies to remediate AMD to produce clean water and to reduce the negative impacts of AMD on land and water resources.

Indigenous and other grasses are abundantly co-located in areas around mining operations in the Mpumalanga region, South Africa, and are considered a potential sustainable and renewable source of both carbon and energy, that can be used for biological AMD treatment (Westensee *et al.*, 2018; Chamoli *et al.*, 2024). Magowo and others (2015) conducted preliminary research to investigate the potential of using South African indigenous grasses to remediate AMD through a biologically mediated dissimilatory sulfate reduction (DSR) process. It was postulated that grass acts as the carbon source and electron donor, necessary to drive the dissimilatory reduction process required to remediate AMD water. The AMD water provides a weak-acid source to break down the lignocellulosic structure of the grass to release monomeric sugars for sulfate reducing bacteria (SRB) to use in the DSR reduction of sulfates to sulfides. The disruption of the recalcitrate cellulosic structure also renders the grass amenable to subsequent enzymatic hydrolysis for the production of sugars, and fermentation of these sugars for conversion to bioethanol (Magowo, Rumbold and Sheridan, 2015; Ramla and Sheridan, 2015).

If remediation technologies could be combined with processes to produce value added products such as biofuels from lignocellulosic waste, this would make a significant contribution towards lessening the country's dependence on coal for energy production while at the same time reducing waste. Additionally, the successful recovery of valuable minerals from AMD such as rare earth elements (REE) could create further

benefit as the re-sale of these recovered minerals could be used to further offset the costs of remediation (Naidu *et al.*, 2023; Smith *et al.*, 2023; Hardwick *et al.*, 2024).

AMD acid-hydrolysed grass has been subjected to enzymatic hydrolysis for the successful production of fermentable sugars (Magowo, Rumbold and Sheridan, 2015; Ramla and Sheridan, 2015). Burman et al. (2019) explored the techno-economic feasibility of various design options for bioethanol production using indigenous South African grass that had been pretreated with AMD. Although this research confirmed that the simultaneous remediation of AMD and bioethanol production was technically possible; a techno-economic evaluation of a combined process concluded that the process was not economically feasible. Further investigation of options to reduce the minimum ethanol selling price are required to improve viability of a combined process (Burman, 2020).

The focus of this research is to explore the use of locally sourced grasses and readily available sulfate reducing bacteria in such a process. This research will aim to contribute to existing knowledge on the use of grass in the bioremediation of AMD by addressing knowledge gaps such as what the underlying chemical/biological processes that underpin a process like this are. Various opportunities will be explored to improve the process sustainability and to potentially improve the cost-effectiveness of AMD bioremediation, and subsequent bioethanol production processes.

1.2 Problem Statement

Previous research confirmed the feasibility of using grass in a DSR process that could combine the remediation of AMD with the production of fermentable sugars for the subsequent production of second generation biofuels (Magowo, Rumbold and Sheridan, 2015; Ramla and Sheridan, 2015; Burman, Sheridan and Harding, 2019). These studies have either been as stand-alone processes or as limited combined processes.

Burman's (2020) investigation of process design options focused primarily on the optimisation of the grass pretreatment conditions for subsequent enzymatic hydrolysis and fermentation for production of biofuels. Further investigation is needed to assess the extent of AMD remediation that can be achieved during the pretreatment process. Previous studies did not provide information on the chemical and physical composition of AMD sources, and the influence of these unique characteristics on the development of a viable remediation process. In a comparison of sulfate removal technologies, van Rooyen et al. (2021) concluded that access to, and the cost of reagents were key components of any remediation process. The cost of organic carbon source is considered a major limitation to the general acceptance of bioremediation processes in the market (van Hille *et al.*, 2016; Van Rooyen, Van Staden and Du Preez, 2021). In a techno-economic evaluation of a combined AMD bioremediation and bioethanol production process, Burman (2020), concluded that the grass feedstock constituted the largest operating cost, owing to the large volumes required. This was followed by heating, enzyme, and then cooling costs. The suitability of locally sourced

grasses co-located with AMD sources in the Mpumalanga coalfields region, their characteristics, and their potential for use in the bioremediation process have not been fully explored. The use of readily available and naturally occurring inoculum sources in different pH environments, simulating different AMD sources, have also not been investigated.

Alternate strategies to improve the economic viability of a combined AMD bioremediation and biofuel processes such as optimal grass-AMD contact or hydraulic retention time at ambient temperature, with and without SRB amendment, has not been previously investigated.

This work seeks to add to the body of knowledge of AMD bioremediation and bioethanol production by the experimental evaluation of varying conditions and factors that were not previously considered. This research aims to address these specific areas in the following research objectives:

1.3 Research Objectives

a. To characterise and critically evaluate the physical and chemical composition of Acid Mine Drainage (AMD) sourced from coal mining operations in the Mpumalanga region, South Africa and determine geographical and temporal variability.

b. To identify and characterise various commonly occurring grass types that are readily available and co-located with AMD sites and compare these for use in AMD bioremediation.

c. To source naturally occurring sulfate reducing bacteria (SRB) inoculum in different pH environments and compare then in the production of sulfides.

d. To investigate the effects of conducting biological AMD remediation at ambient temperature (with no additional heating), and the effects of grass-AMD contact time, with and without SRB amendment, on the extent of both a bioremediation process using grass as an organic substrate, and on subsequent bioethanol production using the spent grass residue.

1.4 Novelty of this research

This research is significant in that it is multidisciplinary and addresses the water-food-energy nexus. Remediated AMD water can be re-used for crop irrigation or in other mining and industrial processes to reduce dependence on freshwater resources and thereby contribute to water resource sustainability. The production of fermentable sugars from lignocellulosic waste material for bioconversion into biofuels does not impact primary agricultural crops used for food production and has potential for sustainable energy creation. The sale of biofuels can also potentially offset remediation costs.

This research provides baseline knowledge for use in the development of a sustainable, circular economy, that utilise waste to produce clean water and other valuable products. The novel aspects of this research include:

a. The characterisation of AMD to evaluate the seasonal changes of two in-situ AMD sources in relation to rainfall patterns in the Mpumalanga region in South Africa.

b. The derivation of regression equations from statistically established empirical correlations between electrical conductivity, total alkalinity, total dissolved solids, dissolved iron, and dissolved sulfur. Followed by the use of these correlations to derive electrical conductivity values corresponding to water quality limits, for a rapid, and novel, method for testing compliance to legislated environmental standards. This work also provides a novel methodology for data evaluation to establish site-specific statistical correlations.

c. The identification and classification of grass types in the Mpumalanga coalfields, South Africa. This work presents a study of the suitability of various uncultivated grass types, that are co-located with coal mine AMD sources in the area for use in AMD bioremediation. The study is novel in that it includes grasses that span the entire Witbank coalfields region that extends from Springs in the west to Belfast in the North-east. This work also considers the merits of Vetiver grass (*Chrysopogon zizanioides*), because of its previously reported success in phytoremediation of AMD. Further novelty is added by the experimental confirmation of an ion-exchange mechanism occurring between hydronium ions in AMD and inorganic cations associated with anions present in lignocellulosic material. The finding of a pH-ORP relationship presents a useful tool for bioremediation process control.

d. The evaluation of the suitability of readily available natural sources of sulfate reducing bacteria (SRB) in differing pH environments. These provide a novel, alternate and sustainable sources of SRB amendment that can be used to reduce costs and improve the economic feasibility of biologically mediated AMD bioremediation processes.

e. The investigation of grass pretreatment, and AMD bioremediation, using weak acid concentration AMD, with and without SRB inoculation, at ambient temperature. This is the first time that grass and SRB have been combined experimentally to compare with grass only AMD treatment. Additionally, previous experimental research explored the combination of AMD remediation and the production of sugars from lignocellulose while employing high temperatures and/or acid concentrations.

f. This study demonstrates that the hydraulic retention time of AMD-grass contact influences both the extent of AMD bioremediation and subsequent bioethanol production, confirming that synergies exist between the two processes.

1.5 Structure of Dissertation

This dissertation is divided into eight chapters. The objectives of this dissertation were primarily in the style of publication outputs. As each publication contributes either partially or fully to a specific research objective, the author requests the readers' indulgence where information is repeated in this dissertation as a consequence of this publication process. An overview of chapters one to eight is described.

Chapter 1: Introduction

Chapter one includes a background to this topic, which introduces the problem statement, research objectives and novelty of this topic.

Chapter 2: Literature review

Chapter two gives an extended literature review to provide background to water and energy in South Africa, AMD formation and impacts thereof, remediation, and biofuel production.

Chapters three to seven describes the individual investigations conducted to address the specific research objectives. The publications derived from these investigations are included in each respective chapter.

Chapter 3: Seasonal characterisation of acid mine drainage in Mpumalanga coalfields region

Chapter three addresses objective (a), where the physical and chemical parameters of two AMD sources in the Mpumalanga coalfields, South Africa were experimentally characterised and temporal changes were evaluated over twelve months. These data were compared with regulatory discharge and drinking water limits, and potential limitations of active and passive treatment systems related to elevated concentrations of certain metal(oid)s were noted. Seasonal (rainfall) variability and data trends were explored. This paper was presented virtually by the author at the South African Chemical Engineering Congress (SACEC), 2021 conference, and the paper was published in the SACEC 2021 book of proceedings (Smith *et al.*, 2021).

Chapter 4: Critical evaluation of the chemical composition of acid mine drainage for the development of statistical correlations linking electrical conductivity with acid mine drainage concentrations

Chapter four builds on chapter three and addresses objective (a) and statistically evaluates the strong correlations noted between electrical conductivity (EC) and other main components in AMD. These empirical correlations are useful to formulate a quick check measure for testing compliance to water quality limits. This article was published in Environmental Advances, 2022 (Smith *et al.*, 2022).

Chapter 5: Classification of grasses in the Mpumalanga coalfields region and assessment of their suitability to increase the pH of acid mine drainage, for potential use in passive acid mine drainage remediation systems

Chapter five addresses objectives (b) to identify and characterise various grass types that are readily available and co-located with AMD sites for use as a substrate and carbon source in the bioremediation of AMD. This

work experimentally determines the physical and chemical properties of grass samples collected from Mpumalanga coalfield region, South Africa. Evaluation of the extent of pH increase achieved when contacting the different grass types with AMD, to establish a range of grass types that may be used in the remediation process. The results of changing process conditions by observing differences between single and multiple grass additions to synthetically prepared and "real" AMD are also evaluated. The feasibility of the pH change resulting from an ion exchange reaction between hydrogen ions (H^+) in AMD and inorganic cations associated with anions present in grass content of grass samples is explored. This article was published in Ecological Engineering, 2024 (Smith *et al.*, 2024).

Chapter 6: Investigation of suitable, readily available, sources of sulfate-reducing bacteria inoculum, and evaluation of sulfate reduction rates achieved at different pHs

Chapter six addresses objective (c), to explore alternative and naturally occurring sources of sulfate reducing bacteria (SRB) inoculum, that would be suitable to use in AMD bioremediation. This study experimentally investigated the use of readily available and naturally occurring sources of sulfate-reducing bacteria (SRB) inoculum for AMD bioremediation. The suitability of these naturally occurring inoculum to support the growth and activity of SRB was evaluated by comparison of the conversion ratios of sulfide produced to sulfate removed at three different pH conditions. This article was published in Environmental Microbiology Reports, 2025 (Smith *et al.*, 2025).

Chapter 7: **The effects of grass pre-treatment time on acid mine drainage bioremediation potential, and bioconversion of sugars to ethanol**

Chapter seven addresses objective (d) that explores the generation of additional value from AMD remediation by investigating a combined process whereby grass is used for AMD remediation, and the spent AMD-pretreated grass is used for subsequent enzymatic conversion to biofuels. This work investigates the effects of varying hydraulic retention times (HRT) for grass-AMD contact on the efficacy of AMD bioremediation at ambient temperature, with and without the addition of SRB inoculum, and also explores the suitability of using the pretreated grass residue for subsequent hydrolysis and fermentation. The suitability of using a weak-acid AMD to breakdown the lignocellulosic structure of grass is assessed, and the HRT of AMD-grass contact is explored for synergies in both the remediation of AMD, and in the bioconversion to bioethanol during the hydrolysis and fermentation process. This article will be submitted to a journal for publication.

Chapter 8: **Discussion and concluding remarks**

Chapter eight presents a discussion of the main findings of each investigation and conclusions reached, with limitations and recommendations for future work.

A summary diagram of the individual investigations included in chapters three to seven, and their relation to the dissertation objectives is presented in Figure 1.1.

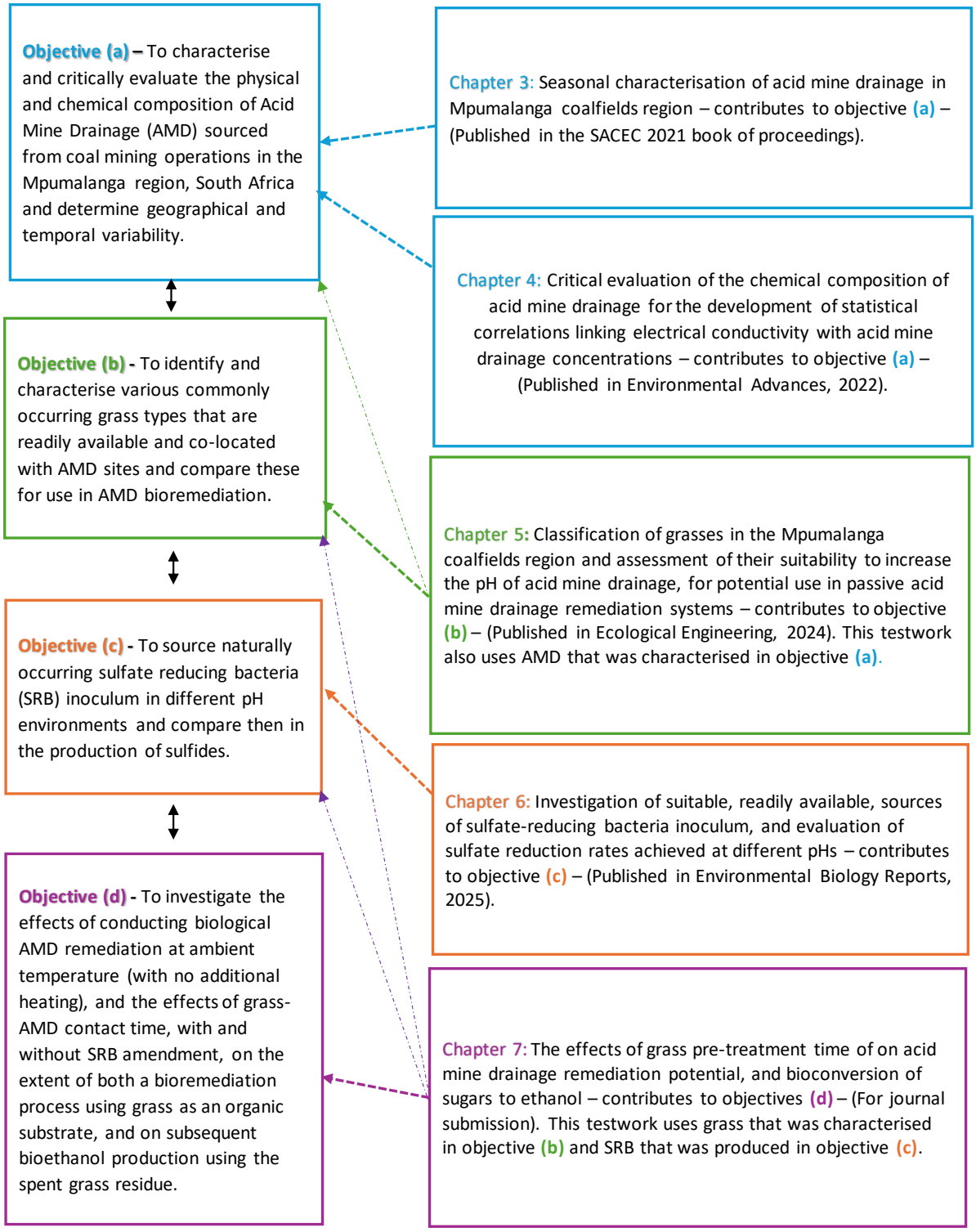


Figure 1.1 Summary diagram of the individual investigations included in chapters three to seven, and their relation to the dissertation objectives.

1.6 References

Bogardi, J.J. et al. (2012a) 'Water security for a planet under pressure: interconnected challenges of a changing world call for sustainable solutions', Current Opinion in Environmental Sustainability, 4(1), pp. 35–43. Available at: https://doi.org/10.1016/j.cosust.2011.12.002

Bogardi, J.J. et al. (2012b) 'Water security for a planet under pressure: interconnected challenges of a changing world call for sustainable solutions', Current Opinion in Environmental Sustainability, 4(1), pp. 35–43. Available at: https://doi.org/10.1016/j.cosust.2011.12.002

Burman, N.W. et al. (2018) 'Evaluation of a combined lignocellulosic / waste water bio-refinery for the simultaneous production of valuable biochemical products and the remediation of acid mine drainage', Biofuels, Bioproducts and Biorefining, 12(4), pp. 649–664. Available at: https://doi.org/10.1002/bbb.1880

Burman, N.W. (2020) Design and optimization of a bioprocess to simultaneously produce biochemicals and remediate acid mine drainage using indigenous South African grasses. Doctoral dissertation. University of the Witwatersrand. Available at: https://hdl.handle.net/10539/30088

Burman, N.W., Harding, K.G. and Sheridan, C.M. (2021) 'Evaluation of two different reactor configurations for the simultaneous remediation AMD and pretreatment of lignocellulosic biomass', in. South African Chemical Engineering Congress (SACEC), At: Virtual.

Burman, N.W., Sheridan, C.M. and Harding, K.G. (2019) 'Lignocellulosic bioethanol production from grasses pre-treated with acid mine drainage: Modelling and comparison of SHF and SSF', Bioresource Technology Reports, 7, p. 100299. Available at: https://doi.org/10.1016/j.biteb.2019.100299

Chamoli, P. et al. (2024) 'Recent advances in the processing of Napier grass (Pennisetum purpureum Schumach) as a potential bioenergy crop for bioethanol production', Journal of Applied Biology & Biotechnology [Preprint]. Available at: https://doi.org/10.7324/JABB.2024.154513

Greenway, N. et al. (2017) 'Process design for the treatment of acid mine drainage utilising lignocellulosic material as the organic carbon source for dissimilatory sulfate reduction'. Available at: https://doi.org/10.13140/RG.2.2.21804.77449

Hardwick, E. et al. (2024) 'Recovery of rare earth elements from acid mine drainage using strong acid cation resin, and separation by green chemistry methods'. Available at: https://doi.org/10.13140/RG.2.2.13453.35048

van Hille, R. et al. (2016) 'Development of a pilot-scale semi-passive system for the bioremediation of ARD', in IMWA, 2016, pp. 957–964. Available at: http://www.mwen.info/docs/imwa_2016/IMWA2016_Hille_247.pdf (Accessed: 07 March 2025).

Magowo, E., Rumbold, K. and Sheridan, C. (2015) 'The Utilization of Cellulosic Biomass in treating AMD and the Subsequent Generation of Fermentable Sugars', in. 10th International Conference on Acid Mine Drainage & IMWA Annual Conference, Santiago, Chile. Available at: http://www.imwa.de/docs/imwa_2015/IMWA2015_Sheridan_168.pdf (Accessed: 26 August 2024).

McCarthy, T.S. (2011) 'The impact of acid mine drainage in South Africa', South African Journal of Science, 107, pp. 01–07.

Naidu, Tamlyn, S. et al. (2023) 'Exploring the Potential for Rare Earth Element Recovery from Coal Mine Acid Mine Drainage using Ion Exchange Technology', in. Y Dyfodol | The Future, Newport, Wales, UK, (International Mine Water Association): IMWA, pp. 376–382. Available at: https://www.imwa.info/docs/imwa_2023/IMWA2023_Naidu_376.pdf

Ramla, B. and Sheridan, C. (2015) 'The Potential Utilisation of Indigenous South African Grasses for Acid Mine Drainage Remediation', Water SA, 41(2), p. 247. Available at: https://doi.org/10.4314/wsa.v41i2.10

Ruehl, M.D. and Hiibel, S.R. (2020) 'Evaluation of organic carbon and microbial inoculum for bioremediation of acid mine drainage', Minerals Engineering, 157, p. 106554. Available at: https://doi.org/10.1016/j.mineng.2020.106554

Simate, G.S. and Ndlovu, S. (2014) 'Acid mine drainage: Challenges and opportunities', Journal of Environmental Chemical Engineering, 2(3), pp. 1785–1803. Available at: https://doi.org/10.1016/j.jece.2014.07.021

Smith, J. et al. (2021) 'Seasonal characterisation of acid mine drainage in Mpumalanga coalfields region', in. South African Chemical Engineering Congress (SACEC), Virtual, p. 118.

Smith, J. et al. (2022) 'Critical evaluation of the chemical composition of acid mine drainage for the development of statistical correlations linking electrical conductivity with acid mine drainage concentrations', Environmental Advances, 8, p. 100241. Available at: https://doi.org/10.1016/j.envadv.2022.100241

Smith, J. et al. (2023) 'The Development of a Sample Preparation Technique for the Analysis of Trace Elements in Mine Impacted Waters containing High Levels of Iron', in IMWA 2023 Y DYFODOL | THE FUTURE. Newport, Wales, UK, (International Mine Water Association): IMWA, pp. 484–490. Available at: https://www.imwa.info/docs/imwa_2023/IMWA2023_Smith_484.pdf (Accessed: 23 January 2025).

Smith, J. et al. (2024) 'Classification of grasses in the Mpumalanga coalfields region and assessment of their suitability to increase the pH of acid mine drainage, for potential use in passive acid mine drainage remediation systems', Ecological Engineering, 209, p. 107424. Available at: https://doi.org/10.1016/j.ecoleng.2024.107424

Smith, J. et al. (2025) 'Investigation of Suitable, Readily Available, Sources of Sulfate-Reducing Bacteria Inoculum, and Evaluation of Sulfate Reduction Rates Achieved at Different pHs', Environmental Microbiology Reports, 17(2), p. e70081. Available at: https://doi.org/10.1111/1758-2229.70081

Smith, K.S. (2007) 'Strategies to predict metal mobility in surficial mining environments', in DeGraff, J. V., Understanding and Responding to Hazardous Substances at Mine Sites in the Western United States. Geological Society of America. Available at: https://doi.org/10.1130/2007.4017(03)

Van Rooyen, M., Van Staden, P.J. and Du Preez, K.A. (2021) 'Sulphate removal technologies for the treatment of mine-impacted water', Journal of the Southern African Institute of Mining and Metallurgy, 121(10), pp. 1–7. Available at: https://doi.org/10.17159/2411-9717/1541/2021

Westensee, D.K. et al. (2018) 'The availability of second generation feedstocks for the treatment of acid mine drainage and to improve South Africa's bio-based economy', Science of The Total Environment, 637–638, pp. 132–136. Available at: https://doi.org/10.1016/j.scitotenv.2018.04.410

Woodford, A., Rosewarne, P. and Girman, J. (2006) '"How much groundwater does South Africa have?" Internal discussion document.' SRK. Available at: http://www.srk.co.za/files/File/newsletters/groundwater/PDFs/1_A_Woodford.pdf

CHAPTER 2

2 Literature Review

This chapter provides the background for the research conducted for this dissertation. Discussion including: the water and energy landscape in South Africa; the contribution of mining to the country's economy, and the unintended consequences of AMD formation and pollution of the surrounding environment from mining; the impacts of AMD and various remediation options; and the need to develop sustainable remediation options that address a circular economy concept, to resolve the water-energy-food-nexus that affects not only South Africans, but the global community.

2.1 Energy in South Africa

Currently, South Africa relies primarily on coal supplied to power stations for energy generation, which fulfils 72.1% of the country's energy needs. After export, 53% of coal production is supplied to power stations for electricity the generation, the remaining supply is shared between Sasol (33%), ArcelorMittal (12%), and only domestic activities (2%) (Eskom, 2021). Ageing power stations, combined with poor maintenance, has resulted in disruption to electricity supply in South Africa, which started in 2007, and required the implementation of load-shedding to balance the energy supply and demand (Mostert, Van Den Berg and Kengni, 2021). The implementation of the South African governments Energy Action Plan announced by the president, Cyril Ramaphosa in 2022, and implementation of the National Energy Crisis Committee (NECOM), has brought about some alleviation to the energy crisis (Government of Republic of South Africa, 2024). However, South Africa's continued reliance on fossil fuels for energy generation, with associated socio-economic and environmental ramifications caused by mining, necessitates the implementation of alternate means of power generation (Strambo, Button and Atteridge, 2019; Mostert, Van Den Berg and Kengni, 2021).

2.2 Mining in South Africa

Mining has historically supported the South African economy, facilitating economic, political, and social development. Copper mining was the first mining type in South Africa and commenced in 1852, in the Northern Cape. This was followed in 1864 by commercial coal mining in the Eastern Cape, which was later expanded to Vereeniging and Witbank (Casey, 2019). The discovery of diamonds in the 1860s lead to the diamond rush and the establishment of diamond mines, and the notorious "Big Hole" in the Kimberley area (Casey, 2019). The Kimberly diamond fields received their coal supplies from coal mined from the Vereniging area (Eskom, 2021). The discovery of gold in South Africa in 1885 resulted in extensive mining in the Witwatersrand region, and the demand for coal increased for use in the generation of steam, compressed air, and electricity (McCarthy, 2011b; Habashi, 2016; Eskom, 2021). Approximately 90% of Africa's coal reserves are located in Southern Africa, and South Africa is the fifth largest global coal producer, and third largest coal exporter, with 25% of coal production exported to other countries (Eskom, 2021; Mostert, Van

Den Berg and Kengni, 2021). In recent times, the diminishing gold reserves, increased operational costs, and reduced capital investment have been cited as causes for the decline in the contribution of mining to the national gross domestic product (GDP), which reported an 8.2% contribution in 2020, compared with the 21% contribution in 1980 (Cole *et al.*, 2024).

2.3 Water in South Africa

South Africa has 1.22 million square kilometres of semi-arid landscape and is ranked amongst the 20 most water-scarce countries with an estimated average 456 mm/a annual precipitation compared to the world-wide average annual rainfall of 860 mm per annum. (Woodford, Rosewarne and Girman, 2006; Turton, A, 2008; Egoh *et al.*, 2009; Mwendera and Atyosi, 2018; The World Bank Group, 2021; Department of Water and Sanitation (DWS), 2023). Rainfall variability, low annual precipitation, combined with evaporation rates that exceed precipitation rates, and instances of extreme drought resulting from rising average temperatures, all contribute to South Africa having scarce water resources in global terms (Woodford, Rosewarne and Girman, 2006; Turton, A, 2008; The World Bank Group, 2021; GCIS, 2022).

The influence of varying climatic conditions and geology have the greatest impact on South Africa's complex groundwater and surface water interactions. The south African climate ranges from desert in the far northwest, semi-desert in the west, subtropical/tropical in the east, and Mediterranean in the Southwest of the country. The seasonality, and variability of rainfall volumes between, and within, the different regions result in an uneven distribution of water resources South Africa (Levy, J and Xu, Y, 2011; WWF-SA, 2016, 2016; Nel *et al.*, 2017; Department of Water and Sanitation (DWS), 2022, 2023). Four of South Africa's major river systems, the Orange-Senqu, Limpopo, Inkomati and Usutu/Pongola-Maputo system are shared with six other neighbouring states, and effective transboundary water resource management is vital to ensuring equitable sharing of these resources between the different countries (WRC, 2009; Mwendera and Atyosi, 2018; Department of Water and Sanitation (DWS), 2022, 2023). The Orange-Senqu River is shared with Botswana, Lesotho, and Namibia; the Limpopo River with Botswana, Mozambique, and Zimbabwe; the Inkomati and the Usuthu/Pongola-Maputo Rivers are shared with Mozambique and Eswatini (Figure 2.1) (Kistin *et al.*, 2009).

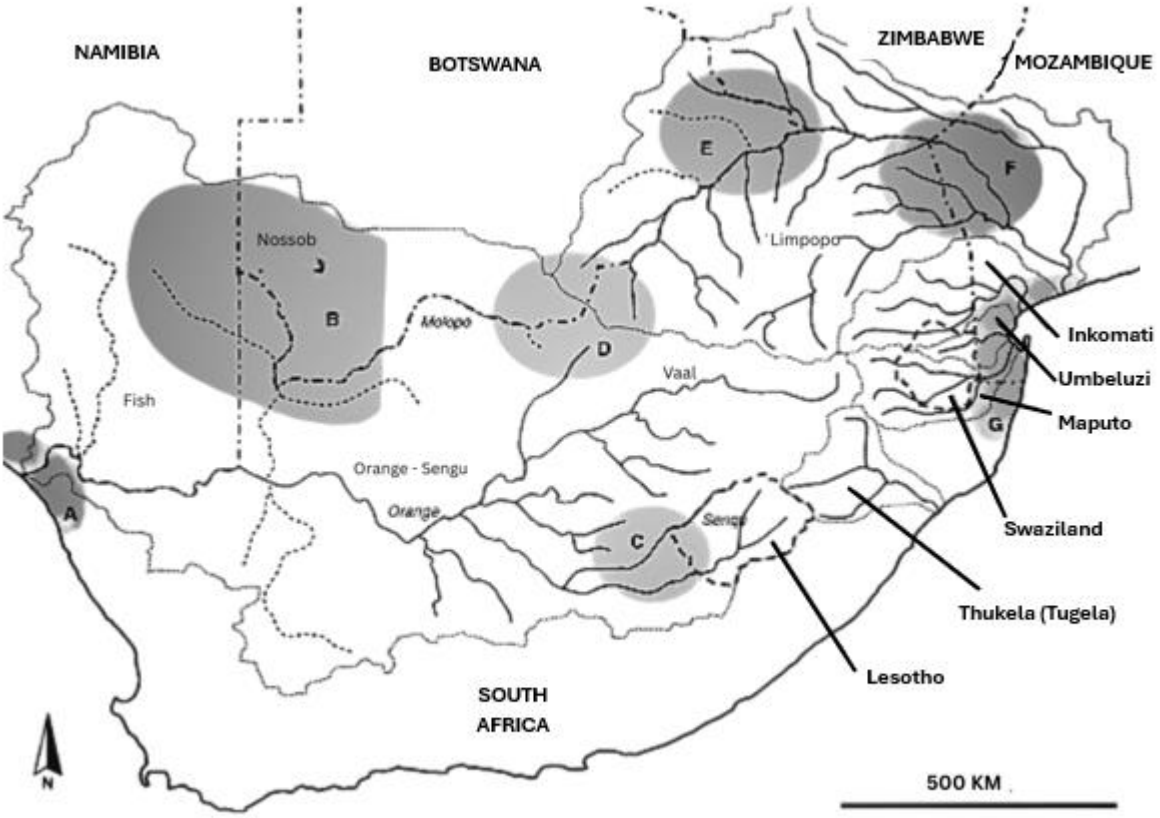


Figure 2.1 Map of southern Africa, showing the six river basins, their main rivers and tributaries, and the approximate extent of the seven aquifer systems shared between South Africa and neighbouring countries. Data for map taken from Kistin et al. (2009), data from (Ashton et al., 2006; Struckmeier and Richts, 2006; Kistin et al., 2009).

South Africa has developed sufficient dam capacity to store approximately two thirds of the countries average annual rainfall, and in excess of 90% of the countries' water supply is drawn from surface water resources (Department of Water and Sanitation (DWS), 2023). Half of the countries' surface run-off water is sourced from twenty two strategic catchment areas (GCIS, 2022). All of South Africa's surface reserves are allocated, and current water use is dominated by agriculture irrigation (66%), and municipal/domestic use (27%). Power generation, afforestation, livestock, industry and mining each consume between two and three percent portions of the countries' remaining water resource (Department of Water and Sanitation (DWS), 2023).

Enshrined in the South African constitution is everyone's right "to have access to sufficient food and water" (SAHRC, 2018). Specific Environmental Management Acts (SEMA) to support water security include the Water Services Act (WSA) (Act 108 of 1997), which defines the provision of potable water and sanitation on a municipal basis, the National Water Act (NWA) (Act 36 of 1998) legislates the protection, management, use, development, and control of these use of all water sources at a national and catchment level, and the Water Research Act, 1971 (Act 34 of 1971, to promote water related research (Claassen, 2013; Kruger *et al.*, 2022;

Department of Water and Sanitation (DWS), 2023). The National Department of Water and sanitation (DWS) is responsible for water resource management (WRM) functions which delegates water resource functions to Catchment Management Agencies (CMAs) (Department of Water and Sanitation (DWS), 2022). Nationally, the National Water Resource Infrastructure Agency (NWRIA) is responsible for water infrastructure development and management. At a local level, municipalities or Water Service Authorities (WSAs), provide water services or outsource these to private Water Service Providers (WSPs), and these institutions fall under the control of the Department of Cooperative Governance and Traditional Affairs (CoGTA) (Department of Water and Sanitation (DWS), 2022). Water Management Areas (WMAs) which are primarily identified based on catchment boundaries (except for catchments that share international borders) are managed by CMAs. Initially 19 WMAs were identified (October 1999), these were reduced to nine in July 2012 and further reduced to six in September 2023 to promote improved operational efficiencies. The six WMAs include the Limpopo-Olifants (Polokwane/Mpumalanga Province), Inkomati-Usuthu (Mpumalanga), Pongola-Mtamvuna (KwaZulu Natal), Vaal-Orange, Mzimvubu-Tsitsikamma (Eastern Cape), and Breede-Olifants (Western Cape) (Claassen, 2013; Department of Water and Sanitation (DWS), 2023). (Figure 2.2).

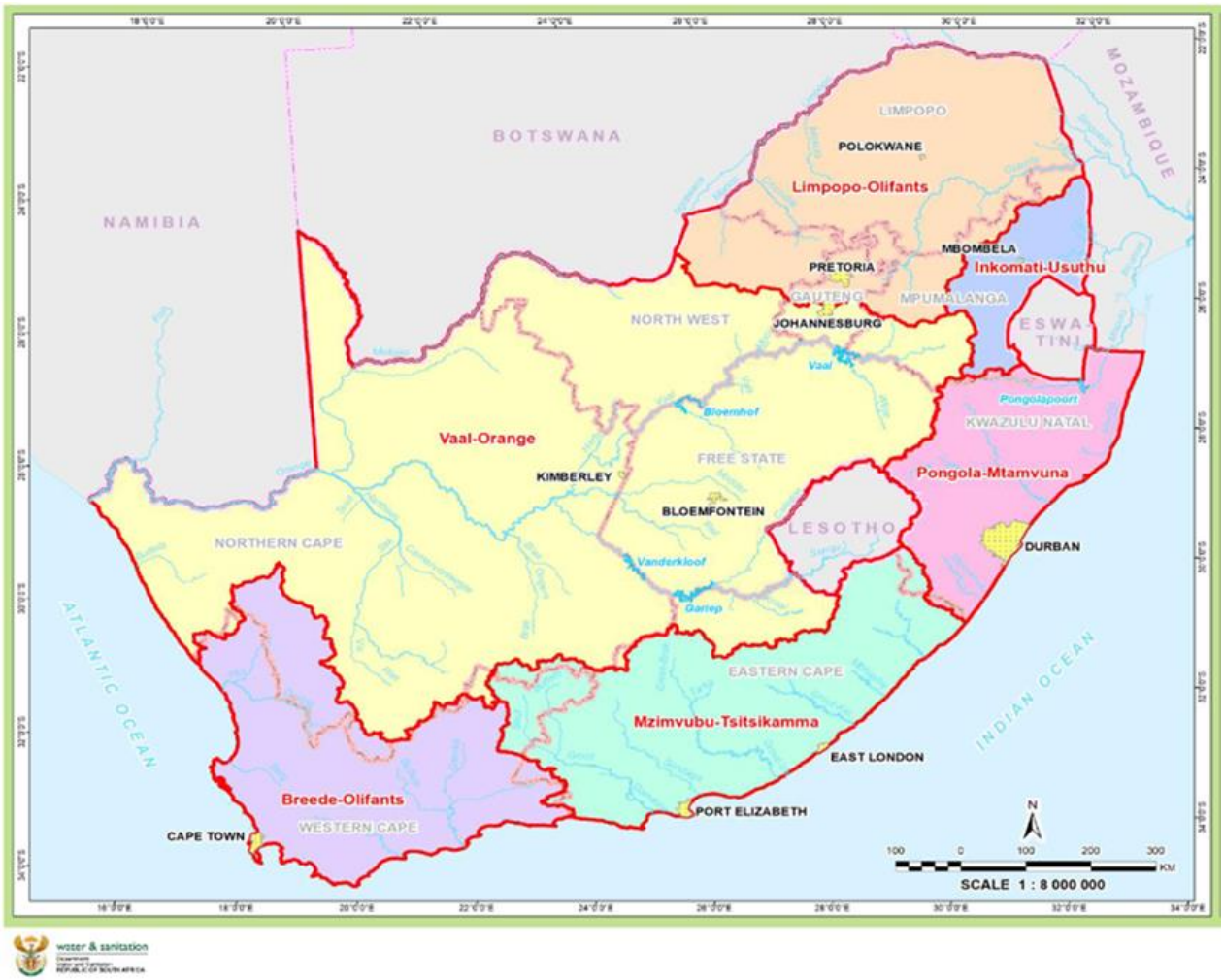


Figure 2.2 Republic of South Africa Proposed Water Management Areas. Department of Water and Sanitation (DWS) (2022).

The management of water quality is supported by a series of South African Water Quality guidelines which are contained within the NWA, and define the Target Water Quality Range (TWQR) for the various water uses (Kruger *et al.*, 2022). Further regulatory initiatives to measure drinking water and waste water management performance of municipalities against a standardised scorecard, the Blue Drop, and the Green Drop Certification Programme were introduced in 2008 (Burgess, J, 2016; Kruger *et al.*, 2022).

South Africa's water scarcity is compounded by climate change which is anticipated to increase the variability of rainfall, and water quality challenges, which include acid mine drainage (AMD), heavy metal, and radionuclide contamination resulting from gold and coal mining; Eutrophication resulting from increased nutrient load from urban, agricultural, and industrial waste (which is exaggerated by the favourable conditions created from the development of dams and inter-basin transfer systems for toxic cyanobacterial bloom); and contamination from increased use of medication, and failing infrastructure (Turton, A, 2008; WWF-SA, 2013).

In the 2022 National state of Water Report a 1% deficit of National water supply systems is estimated and this is predicted to increase to 3.4% by 2040 (Department of Water and Sanitation (DWS), 2022). Effective water demand management initiatives such as the improvement of infrastructure can reduce physical losses which are estimated at 36%. Some groundwater capacity is available as only six percent of the anticipated fifteen percent resource availability is utilised (Department of Water and Sanitation (DWS), 2023). There are however, limited major groundwater aquifers for large scale abstraction owing to the predominantly hard rock nature of the South African geology. Care must however be exercised to prevent over-extraction of this resource and detailed assessment of all interrelated surface and groundwater flows must be compiled to give a full water balance to ensure that recharge rates are not exceeded. (Department of Water and Sanitation (DWS), 2023). Additional to this, the treatment, and reuse of water will be necessary to provide sufficient capacity to meet current and future water demands and ensure ongoing water security (Department of Water and Sanitation (DWS), 2022, 2023).

2.4 The Impacts of Mining on Water

Mining processes result in the disturbance of soil and exposure of underlying minerals to surface natural elements such as oxygen, water, wind, vegetation, and microbial communities. The chemistry of mine impacted water (MIW) can vary and factors such as, geological formation, geochemical conditions, and the chemical composition of the ore deposit, and can result in either acidic or neutral impacted water (Prepilková *et al.*, 2022). Neutral mine drainage (NMD) typically comprises medium to high dissolved metals and sulfate content, low dissolved oxygen and has pHs of between 6–8 (Prepilková *et al.*, 2022). In contrast, acid mine drainage (AMD) is characterised by low pH (0.5–4.5), and high concentrations of sulfate (SO_4^{2-}), iron (Fe), and other metal(oid)s, associated with the ore body and leached from surrounding environment (Akcil and Koldas, 2006; Simate and Ndlovu, 2014; Prepilková *et al.*, 2022; Daraz *et al.*, 2023).

2.4.1 The formation of Acid Mine Drainage (AMD)

AMD is a world-wide problem which is caused primarily by mining but it can also result from other deep excavation type process such as tunnelling, the by-products of industrial operations that discharge high SO_4^{2-} concentrations, waste water such as paper and pulp manufacture, galvanic processing, leather and food processing, and scrubbing of flue gasses at power stations (Gazea, Adam and Kontopoulos, 1996; Simate and Ndlovu, 2014; Rambabu et al., 2020; Zhang et al., 2023; Hasii and Gasii, 2024). Gold and coal ores are often associated with sulfide minerals such as pyrite (FeS_2) which are initially formed in the absence of oxygen under reducing conditions (McCarthy, 2011b; Habashi, 2016). The mining process, dictates the particle size and surface area, of the exposed sulfide ore (Daraz et al., 2023). Large quantities of fragmented rock are produced during mining activities, which result in the exposure of increased rock surface area, to the elements, which results in an increased potential for AMD generation (McCarthy, 2011b; Simate and Ndlovu, 2014).

AMD is formed when pyritic rock, is exposed to atmospheric oxygen and water, the sulfide minerals in the ore are oxidised to form oxidation products containing ferrous sulfate and acidity. These reactions occur in the presence of oxidising bacteria (Simate and Ndlovu, 2014; Skousen, Ziemkiewicz and McDonald, 2019; Rambabu *et al.*, 2020). The formation of AMD occurs in a two stage reaction; firstly, sulfide oxidation and then ferrous oxidation and the reactions are described in *Equations 2.1-2.4* (Akcil and Koldas, 2006; Simate and Ndlovu, 2014; Ojonimi *et al.*, 2021; Daraz *et al.*, 2023).

Sulfide Oxidation: Pyrite is oxidised to form dissolved ferrous iron, sulfate, and hydrogen ions when contacted with oxygen and water, (*Equation 2.1*).

$$2FeS_2 + 7O_2 + 7H_2O \rightarrow 2Fe^{2+} + 4SO_4{}^{2-} + 4H^+ \qquad \textit{Equation 2.1}$$

Ferrous iron oxidation: The ferrous iron (Fe^{2+}) produced in *Equation 2.1* may be oxidised to ferric iron (Fe^{3+}) if the pH is greater than 3.5, sufficient oxygen is available, and some bacterial activity exists (*Equation 2.2*). If insufficient oxygen is present, this reaction would only occur at pH 8.5. This is the rate-limiting step in pyrite oxidation, because under abiotic conditions, the conversion of ferrous to ferric is slow at pH values below 5 (Akcil and Koldas, 2006; Simate and Ndlovu, 2014; Ojonimi *et al.*, 2021; Daraz *et al.*, 2023).

$$4Fe^{2+} + O_2 + 4H^+ \leftrightarrow 4Fe^{3+} + 2H_2O \qquad \textit{Equation 2.2}$$

At pHs between 2.3 and 3.5 ferrous ions may precipitate as ferric hydroxide, removing most Fe^{3+} from the solution while simultaneously lowering the pH (*Equation 2.3*). Ferric hydrolysis products are unstable at pHs below pH 2 which would result in the Fe^{3+} remaining in solution (Akcil and Koldas, 2006; Simate and Ndlovu, 2014; Ojonimi *et al.*, 2021; Daraz *et al.*, 2023).

$$Fe^{3+} + 3H_2O \leftrightarrow FeOH_3 \downarrow + 3H^+ \qquad \textit{Equation 2.3}$$

Any remaining ferric iron from Equation 2.3 that does not precipitate as ferric hydroxide, may be used to oxidise additional pyrite resulting in a further decrease in pH (*Equation 2.4*) (Akcil and Koldas, 2006; Simate and Ndlovu, 2014; Ojonimi *et al.*, 2021).

$$FeS_2 + 14Fe^{3+} + 8H_2O \leftrightarrow 15Fe^{2+} + 2{SO_4}^{2-} + 16H^+ \qquad \textit{Equation 2.4}$$

Although oxygen is the primary oxidant, at pHs below pH 3, oxidation of pyrite by ferric iron is the dominant reaction and occurs 10 to 100 times faster than the oxygen reaction. Ferric oxidation of one mole of pyrite produces sixteen moles of H^+ compared with two moles of H^+ produced in *Equation 2.1*, and hence the oxidation of Fe^{2+} to Fe^{3+} is referred to as the acid generating rate determining step (Zagury, Kulnieks and Neculita, 2006; Simate and Ndlovu, 2014). This reaction will be in equilibrium under closed anaerobic conditions, however, in an open system, such as a mining environment, Fe^{3+} will be regenerated, and the reaction will shift strongly to the right. Acidophilic bacteria, such as *Thiobacillus ferrooxidans*, most commonly associated with the oxidation of Fe^{2+} in acidic mine-impacted waters and several other bacterium species, which are thought to be involved in pyrite weathering have also been shown to significantly increase iron conversion rate using a range of biological mechanisms. *(Simate and Ndlovu, 2014; Quatrini and Johnson, 2019; Ojonimi et al., 2021; Daraz et al., 2023).*

The increased acidity of AMD then results in secondary reactions where other metals are leached from the surrounding ore bodies and dissolved in the AMD, resulting in an acidic run-off that is contaminated with a range of heavy metals which could include; manganese, aluminium, iron, nickel, zinc, cobalt, copper, lead, and also radioactive materials such as radium, thorium, and uranium (Gazea, Adam and Kontopoulos, 1996; Simate and Ndlovu, 2014; Rambabu *et al.*, 2020; Daraz *et al.*, 2023; Zhang *et al.*, 2023). The rate of AMD generation is determined by factors including temperature, moisture, specific sulfide mineralogy, and the availability of natural neutralising minerals (Ramontja *et al.*, 2011). A conceptual model of AMD pollution sourced from Jiao *et al*. (2023), is presented in Figure 2.3. This model describes the transport of water from mining and industrial processes, and the resulting chemical, physical, and biochemical reactions that occur when the associated metal sulfide minerals in the ore body come into contact with water, oxygen and microorganisms (Jiao et al., 2023).

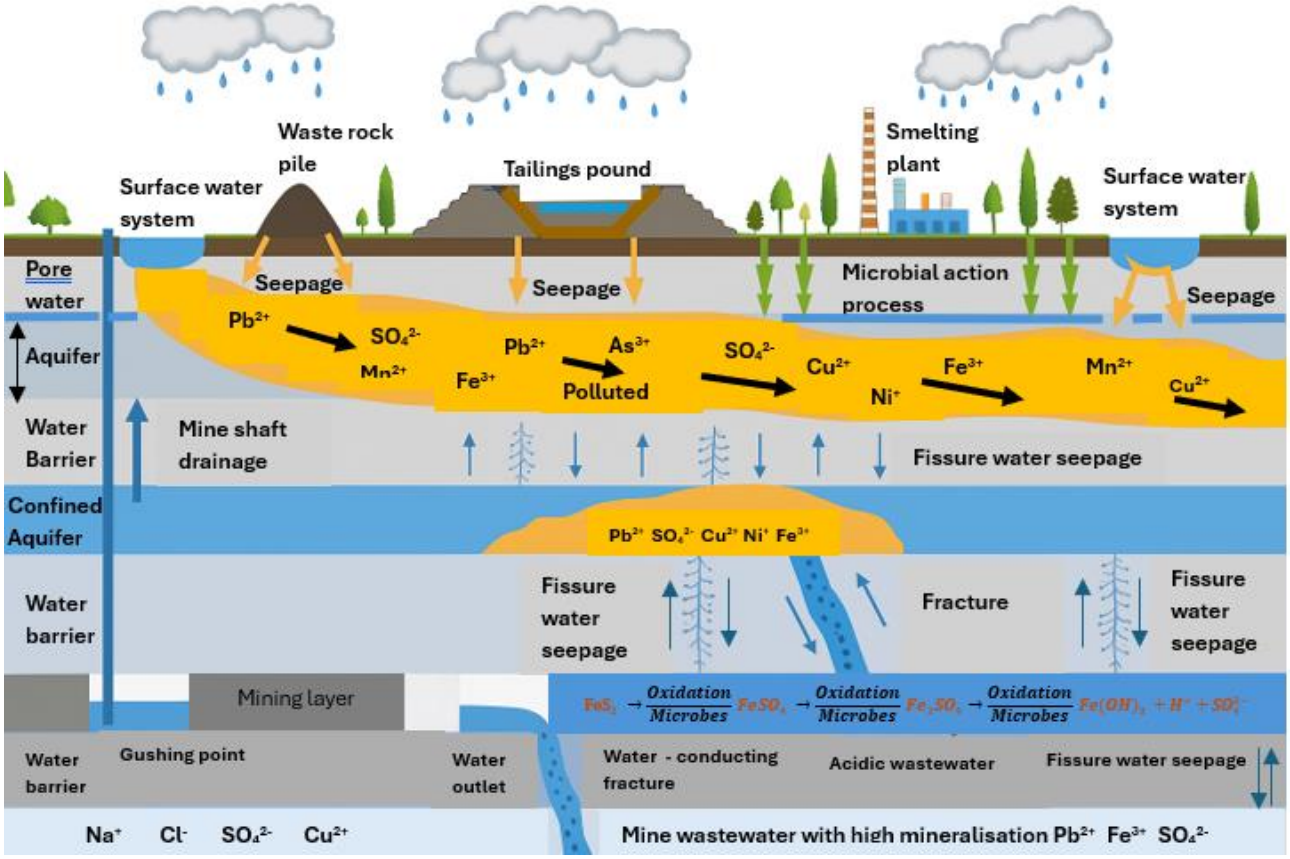


Figure 2.3 A conceptual model of AMD pollution. Data from (Jiao et al., 2023).

2.4.2 Environmental, social, and other impacts of AMD

While mining has contributed to job creation, economic growth and the countries dependence on fossil fuels for energy generation, coal (and other) mining has resulted in a plethora of adverse socio-economic consequences owing to its physical footprint. These include the social aspects of land dislocation, and environmental consequence of land and habitat destruction. Downstream pollution effects include adverse environmental and health consequences of air pollution caused from dust emissions, the release of toxic compounds such as carbon dioxide, methane, sulfur compounds, and volatile metals from spontaneous combustion of coal discard heaps, plus water and land pollution from mine run-off (Simate and Ndlovu, 2014; Belle, Schoeman and Oberholster, 2023; Ninomiya *et al.*, 2023; Cole *et al.*, 2024; Hasii and Gasii, 2024). Intensive mining activities has resulted in the formation of amplified quantities of AMD, which has exceed the natural neutralization processes (such as dilution) that would normally be sufficient to ameliorate any acid generation caused through the typical weathering process (McCarthy, 2011b). AMD is a global crisis and has been cited by the United Nations as “the second biggest problem facing the world after global warming” (Tuffnell, 2017). The highly acidic and mineralised AMD run-off can corrode infrastructure and if allowed to flow unchecked, can infiltrate ground and surface water bodies resulting in severe impact on the surrounding environment (Simate and Ndlovu, 2014; Belle, Schoeman and Oberholster, 2023; Mbae *et al.*, 2024). Figure 2.4, data from Naidu et al. (2019), illustrates AMD generation and the related contamination pathway.

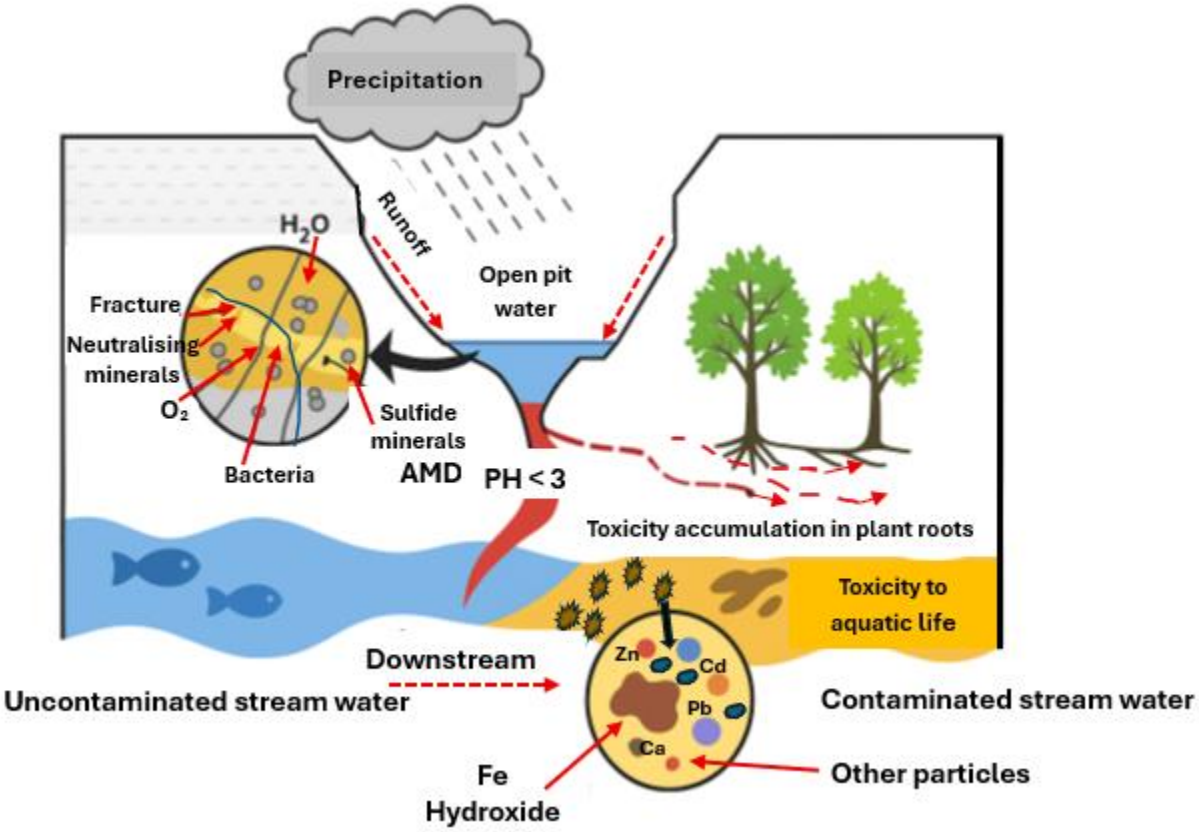


Figure 2.4 AMD generation and related contamination pathway. Data from (Naidu et al., 2019).

In the Mpumalanga region, South Africa, coal mining is located in the upper reaches of the Olifants catchment around eMalahleni, Middelburg and Delmas, and poses a significant risk of AMD generation. The degree of acidification and metal load in AMD are determined by the amount and type and of acid-producing sulfide minerals, and acid-neutralising carbonate minerals present in the exposed rock (Westensee *et al.*, 2018; Skousen, Ziemkiewicz and McDonald, 2019; Retief and Pollard, 2020). Rising salinity and sulfate levels in the Middelburg and Witbank dams provide evidence of the decant of AMD from coal mining operations in the Witbank–Middelburg area, into tributaries of the Olifants River (McCarthy, 2011b). The entire Olifants Water Management Area is considered as highly stressed with limited opportunity for further water resource development (McCarthy, 2011b; Retief and Pollard, 2020). The adverse impacts of mine activities continue past mine-closure, and mine closure efforts have historically been limited by insufficient planning and underestimation of potential post-closure environmental and social liability costs. However, despite the implementation of legislative frameworks for mine closure, and post-mine land use planning, mine closure remains an ongoing challenge in South Africa. This is highlighted by the legacy of AMD decant and defunct tailings storage facilities observed in the South African Witwatersrand goldfields. (Hobbs, Oelofse and Rascher, 2008; Cole *et al.*, 2024). Belle *et al*. (2023) noted the ecological and public health risks of potentially toxic element (PTE) contamination and proposed the implementation of a risk assessment framework based on a source-pathway-receptor (SPR) model to evaluate potential threats of PTE pollution to surface waters (Belle, Schoeman and Oberholster, 2023). Evaluation of the changing chemistry of the PTEs in the

surrounding environment owing to seasonal rainfall patterns, and other natural or industrial processes, requires regular monitoring to ensure adequate control and timeous response to ameliorate possible AMD breeches and infiltration (Smith, 2007; Belle, Schoeman and Oberholster, 2023). This in turn relies on robust analytical techniques to provide the data to facilitate long-term monitoring, as well as quick-turn-around analytical techniques that will allow a quick response to potential overflow crises (Smith *et al.*, 2022).

2.5 Physico-chemical Properties of AMD in the Mpumalanga Coalfields South Africa

Geologically, South Africa's coal reserves are predominantly hosted in the rocks for the Karoo Supergroup, where the sedimentary fraction is predominantly comprised of the Dwyka, Ecca, Beaufort, and Stormberg lithostratigraphic units (Hancox and Götz, 2014). The coal seams found in the Vryheid Formation of the Ecca subgroup also comprise sandstones, mudstones, siltstone and shale. The Witbank coalfield, is located in the northern part of the Karoo Basin, where the sedimentary layers of the Ecca Group thin out (Banks *et al.*, 2011; Hancox and Götz, 2014). The Witbank Coalfield extends ≈190 km from Springs in the south-west to Belfast in the north-east, and ≈50 km from Middelburg in the north to Rietspruit in the south. This is subdivided into three geographical areas that are formed by varying geological basement layers, which dictate the nature and quality of the coal deposit (Hobbs, Oelofse and Rascher, 2008; Hancox and Götz, 2014). The six coal seams in the Vryheid formation, and the five coal seams in the Witbank coalfield deliver high-value, export quality coal (Banks *et al.*, 2011; Hancox and Götz, 2014). Figure 2.5, data from Cairncross et.al. (1990) shows the locality of the Witbank and the geochemical sampling sites used in their research.

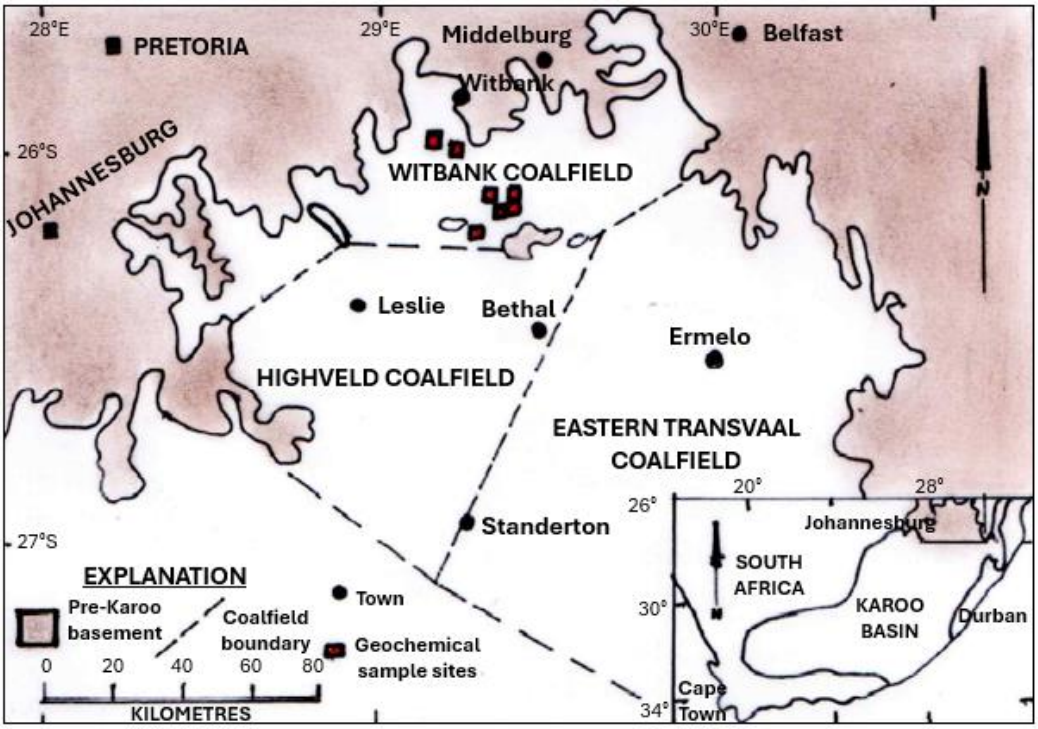


Figure 2.5 The locality of the Witbank Coalfield and geochemical sample sites. Data from (Cairncross, Hart and Willis, 1990).

Pyrite is an iron sulfide mineral commonly associated with gold and coal mining, and analysis of the pyrite content in different coal samples reported varied concentrations of between 11-50%, (Pinetown, Ward and Van Der Westhuizen, 2007). Wagner and Hlatshwayo (2005) postulated the likelihood of over 90% of the sulfur content in South African coals being associated with Pyrite, and that trace elements arsenic (As), cadmium (Cd), copper (Cu), lead (Pb), antimony (Sb), and zinc (Zn) have affinity either for pyrite, or accessory sulfide minerals (Wagner and Hlatshwayo, 2005). Wagner and Hlatshwayo (2004) compared trace metal concentrations of selected elements from Highveld coal samples with previously reported data from other South African, and international coals field data. These data are shown in Table 2.1 (Watling and Watling, 1982; Willis, 1983; Cairncross, Hart and Willis, 1990; Wagner and Hlatshwayo, 2005).

Table 2.1 Comparison of trace elements in South African coals - adapted from: (Wagner and Hlatshwayo, 2005).

Trace Element	Witbank No 2 Seam (Cairncross *et al*. 1990)	South African coals (Watling and Watling, 1982)	South African Coals (Willis, 1983)	Global range (Swaine, 1990)
Units	**ppm**	**ppm**	**ppm**	**ppm**
Antimony (Sb)	0.47			0.05–10
Arsenic (As)	4.6		0.9–8.2	0.5–80
Cadmium (Cd)		0.39		0.1–3
Chromium (Cr)	28	25	12–63	0.5–60
Cobalt (Co)	7.9	7.8	3.3–14	0.5–30
Copper (Cu)	9.7	10.9	4.2–16	0.5–50
Lead (Pb)	10	10.1	1.9–25	2–80
Manganese (Mn)		30		5–300
Mercury (Hg)		0.327		0.02–1
Molybdenum (Mo)			<1–2.7	0.1–10
Nickel (Ni)	17	15.5	6.9–32	0.5–50
Selenium (Se)	0.9		<0.4–0.9	0.2–10
Vanadium (V)	27		17–43	2–100
Zinc (Zn)	10	18.1	3.2–16	5–300

The trace elemental composition is not limited to the elements reported in Table 2.1. Cairncross, Hart and Willis, (1990) reported a total of 33 trace elements, which included rare earth elements (REE) for the Witbank No. 2 seam. Ruch et al., (1974) determined that arsenic (As), cobalt (Co), copper (Cu), nickel (Ni), phosphorus (P), and antimony (Sb) were commonly associated with sulfur in nature, and that the affinity of certain elements was partitioned in varying degrees between the organic and the inorganic portions of the coal (Ruch, Gluskoter and Shimp, 1974). Germanium (Ge), beryllium (Be) and boron (B) showed the greatest affinity to the organic portion of coal, while mercury (Hg), zirconium (Zr), zinc (Zn), cadmium (Cd), Arsenic

(As), lead (Pb), manganese (Mn), and molybdenum (Mo) were concentrated in the inorganic portion in coal (Ruch, Gluskoter and Shimp, 1974). The varied base layer sedimentology of different coal deposits results in different inorganic and organic compositions of coal seams, and varying concentrations of trace elements present (Bergh, 2009). As a result, the differences in AMD composition, and the relative concentrations of potentially toxic elements (PTEs) are unique to a particular region and are dependent on a number of factors including the water source, geology, mineralogy, microclimate, and microorganisms present in that area (Smith, 2007; Skousen, Ziemkiewicz and McDonald, 2019; Rambabu *et al.*, 2020).

Further to this, a comparison of the analytical data from a grab soil sample taken from the base of coal mine tailings with a reference soil sample taken from a non-mining location in the Mpumalanga coalfields region, showed significantly higher Fe, SO_4^{2-}, As, Cd, Co, Cr, Mn, Ni, P, Pb, and V concentrations in the tailings sample Thomas et. al. (2023). The low soil pH of pH 3.48 provided evidence of soil acidification, and the increased metal(oid) concentrations were indicative of the effects of AMD contamination (Thomas, Sheridan and Holm, 2023). Smith (2007) used a source, pathway, fate concept (on the right of Figure 2.6) to illustrate the pathway and relationship between the total metals and their potential toxicity to organisms. The orange scale on the left of Figure 2.6 shows that only a portion of the metal is transported from one stage to the next (Smith, 2007).

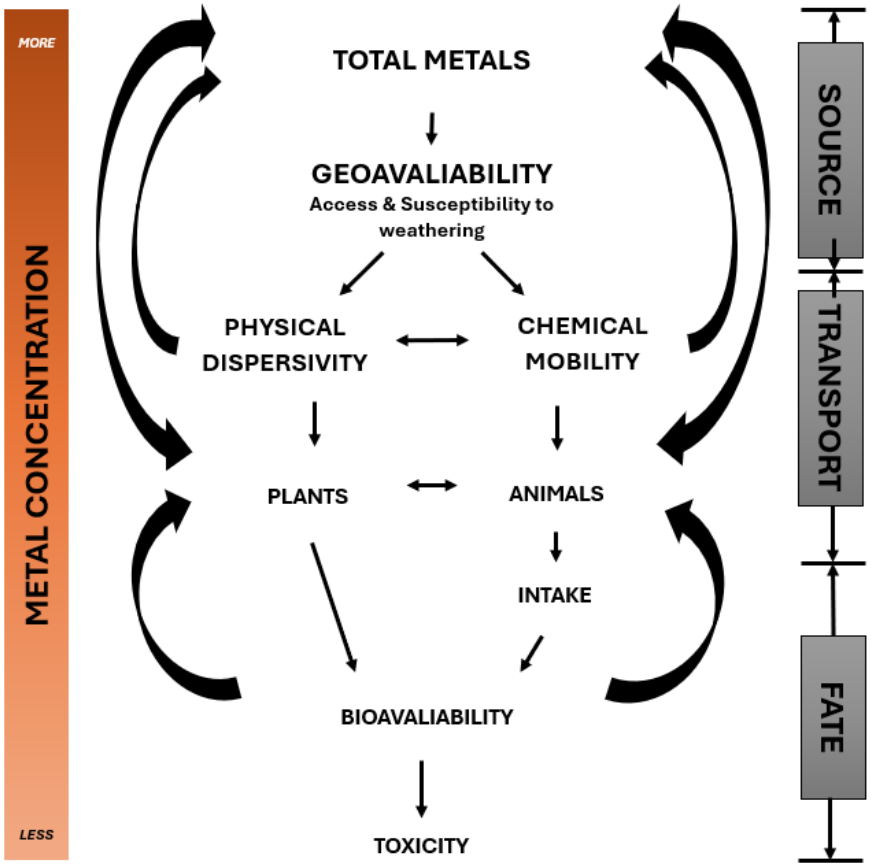


Figure 2.6 Pathways and relationships between total metal in an earth material and toxicity. Data from (Smith, 2007).

The release of potentially toxic elements (PTEs) from coal mining at point sources, and their impact on the downstream environment, highlights the urgent need for remediation of AMD in these affected mine impacted waters (MIWs) (Belle, Schoeman and Oberholster, 2023; Thomas, Sheridan and Holm, 2023; Mbae *et al.*, 2024). The sight specificity demonstrated, highlights the site specificity of AMD, and the need for adequate analytical monitoring to properly understand the differing composition and variances of different AMD bodies.

2.6 Current Treatment of Acid Mine Drainage

AMD is characterised by low pH, and high concentrations of sulfate, and iron and other metal(oid)s such as those described in Sections 2.4 and 2.5. Remediation of AMD is necessary to mitigate environmental ramifications of unchecked flow of these acidic waters, and provide water of suitable quality to alleviate water scarcity and to contribute to water security (Chen *et al.*, 2020).

AMD treatment can include either active or passive systems, with active systems requiring chemical amendment and passive systems relying on naturally occurring biological, geochemical and physical processes to achieve remediation of AMD (Akcil and Koldas, 2006; Ndlovu, 2017; Skousen *et al.*, 2017; Chen *et al.*, 2020). Active systems are generally abiotic and examples include "alkaline precipitation, ion exchange, solvent extraction, electrolytic techniques, membrane technologies and adsorption processes" (Ndlovu, 2017). Examples of passive treatment systems are anoxic limestone drains, aerobic wetlands, constructed wetlands, permeable reactive barriers, low-pH Fe oxidation, and bioreactors. While anoxic limestone drains are abiotic, geochemical passive systems, and rely on the reaction of water with limestone, most passive remediation systems are biological. Passive remediation systems and can be both active or passive (Johnson and Hallberg, 2005; Simate and Ndlovu, 2014; Ndlovu, 2017; Skousen *et al.*, 2017). Figure 2.7 provides an illustration of abiotic and biological remediation systems (Simate and Ndlovu, 2014).

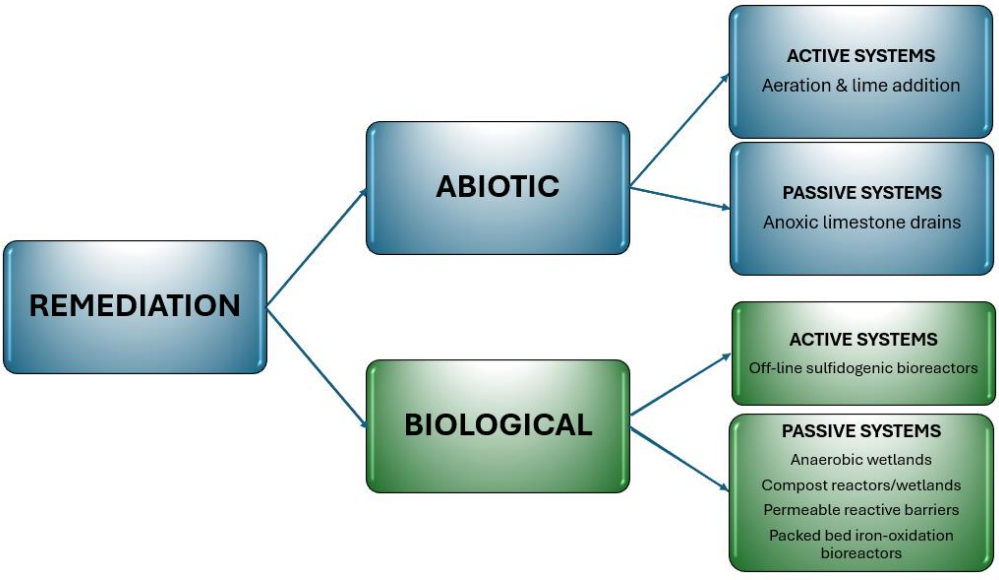


Figure 2.7 Abiotic and biological remediation technologies for acid mine drainage water. Data from (Simate and Ndlovu, 2014).

Some active abiotic technologies that have been trialled or are in operation in South Africa are described in more detail.

2.6.1 Abiotic AMD remediation technologies

2.6.1.1 Alkaline precipitation

The treatment of AMD seeks to achieve water of neutral pH and the removal of sulfates, iron and other metals to meet environmental compliance thresholds, or, to a sufficient quality to permit discharge into the environment (Gazea, Adam and Kontopoulos, 1996). If the treated water is intended for re-use either in mining or industrial processes, then treatment is targeted to produce water of sufficient quality to meet the "fit for purpose" requirements.

Conventional chemical AMD treatment relies on the addition of alkaline materials to achieve chemical neutralization of the pH; these materials can include: limestone (calcium oxide), hydrated lime ($Ca(OH)_2$, pebble quicklime (calcium oxide), soda ash (sodium carbonate), sodium hydroxide (caustic soda), ammonia, periclase (magnesium oxide), brucite (magnesium hydroxide), dolomite (calcium-magnesium-carbonate). These processes are limited by either high installation or operating costs and result in the precipitation of metals as either metal hydroxides or carbonates sludge, which incur prohibitive waste disposal costs. Some chemicals pose handling risks, the suitability of the alkaline source is dependent on the physio-chemical composition of the AMD, and high sulfate concentrations are not sufficiently removed to meet south African environmental discharge limits of between 250–500 mg/L (Johnson and Hallberg, 2005; Simate and Ndlovu, 2014; Skousen, Ziemkiewicz and McDonald, 2019; Van Rooyen, Van Staden and Du Preez, 2021; Zhang *et al.*, 2023). The addition of industrial byproducts such as slag, fly ash, lime kiln ash, and cement kiln ash can achieve a rapid increase in pH (Naidu, Sheridan and Van Dyk, 2020; Zhang *et al.*, 2023).

Membrane technologies include nanofiltration, ultrafiltration, and reverse osmosis (RO) (Mosai, Ndlovu and Tutu, 2024). Nano filtration uses membranes with pore sizes ranging from 1–10 nm to separate metals from AMD but requires a pretreatment step to remove particulate matter and prevent fouling. Ultrafiltration uses semi-permeable membrane and is efficient in removing suspended particles, colloids, and microorganisms, and can produce high quality water. It is the preferred technique for water treatment, owing to ease of operation and better cost and energy efficiencies compared with other membrane technologies. Reverse osmosis separates solution from impurities by using osmotic pressure to force a concentrated solute through a semi-permeable membrane. The process is costly as pretreatment is required to prevent fouling and scaling, and large quantities of brine are produced (Mosai, Ndlovu and Tutu, 2024). More recent developments to improve the efficiencies of nano and ultrafiltration technologies include the development of NIC Membrane™ a semi-permeable, low-fouling capillary ultrafiltration membrane by the Nanotechnology Innovation Centre (NIC), at Mintek, South Africa, and various modifications nanofiltration membranes have been implemented to improve performance (Mosai, Ndlovu and Tutu, 2024).

The low pH and high iron and sulfate concentrations present in AMD pose significant challenges in remediation efforts. While alkaline addition can effectively increase pH and precipitate metals, sulfate is not effectively removed. Van Rooyen et al., (2021) compared the efficiencies of four commercially developed AMD treatment process technologies for sulfate removal. These included two chemical processes, ettringite precipitation, and barium carbonate addition: reverse osmosis, a combined physiochemical process, and a biological process, biological sulfate reduction.

2.6.1.2 Ettringite precipitation

The ettringite process effectively enables the reduction of sulfate concentration to acceptable limits. An ettringite precipitate is formed when a water-soluble aluminium salt is added to a sulfate–saturated water. Ettringite is a calcium-aluminium-sulfate mineral (Ca-Al-SO_4, that is stable) and has a very low solubility constant. Mintek developed an improved process, whereby aluminium is recovered from the ettringite precipitate. The SAVMIN® process requires a neutralisation step, where $Ca(OH)_2$ is added to increase the pH and precipitate gypsum and metal hydroxides. Sulfate is then removed by adding soluble aluminium hydroxide to form the ettringite precipitate. A softening step uses carbon dioxide to precipitate calcium carbonate from the decant water which is then filtered to produce the treated water product. The aluminium is recovered from the ettringite precipitate by the addition of sulfuric acid followed by the decomposition to solid aluminium hydroxide and gypsum (Van Rooyen, Van Staden and Du Preez, 2021). Potentially high-quality, saleable by-products are produced from the process, however the saturated calcium sulfate medium presents scaling issues, and large quantities of sludge are produced (Simate and Ndlovu, 2014; Ndlovu, 2017; Van Rooyen, Van Staden and Du Preez, 2021).

2.6.1.3 Barium carbonate precipitation

A modified CSIR alkaline–barium–calcium (ABC) process can successfully remove sulfate to acceptable concentrations by forming a barium carbonate precipitate. This process follows several treatment stages which include neutralisation using calcium hydroxide, metals removal using hydrogen sulfide, magnesium removal using calcium hydroxide, and sulfate removal using barium carbonate. The effluent from the barium carbonate precipitation produces the treated water product and the resulting barium sulfate (barite)/calcium carbonate (calcite) sludge is then further processed to recover barium carbonate, calcium hydroxide and sulfur. A second sludge processing stage recovers calcium carbonate, magnesium carbonate and sulfur from the initial neutralisation, metals removal and magnesium stage. The process is able to successfully remove sulfates from AMD, however the extreme toxicity of barium carbonate is of concern, and reagent costs and scale-up equipment for thermal reduction of wastes are anticipated to be high (Simate and Ndlovu, 2014; Akinwekomi, Maree and Wolkersdorfer, 2017; Van Rooyen, Van Staden and Du Preez, 2021).

2.6.1.4 Reverse osmosis

A patented reverse osmosis (RO) technology, the High Recovery Precipitating Reverse osmosis (HIPRO®) process, is successfully employed at the eMalahleni Water Reclamation Plant in the Mpumalanga coalfields in South Africa. This is a multi-stage physiochemical process that combines clarification, ultrafiltration and RO to remove all monovalent ions and produce drinking quality water (Van Rooyen, Van Staden and Du Preez, 2021; Mosai, Ndlovu and Tutu, 2024). The first stage uses ozone to oxidise of iron and manganese to form oxide precipitates which then reports to a clarification stage for settling. Antiscalant is added to the clarified overflow which reports to reverse osmosis. The supersaturated ions in the RO brine are then precipitated using lime, followed by a second clarification and RO stage, and the same process is repeated through a third stage. Large quantities of gypsum, sludge, and brine are produced as either saleable or waste products (Simate and Ndlovu, 2014; Ndlovu, 2017; Van Rooyen, Van Staden and Du Preez, 2021). This process can achieve sulfate recoveries more than 95%, but has high operating costs, the RO process is limited by scaling, large quantities of waste brine are produced (Van Rooyen, Van Staden and Du Preez, 2021; Mosai, Ndlovu and Tutu, 2024).

The chemical ettringite and barium carbonate processes were able to achieve success in sulfate removal, and produce potable water, they were not able to remove monovalent sodium and chloride ions. The RO process was successful in removing all monovalent ions. The above-mentioned processes are commercially available abiotic processes and require high capital investment, large inputs of chemicals and energy, constant monitoring and control, and produce varying amounts of waste sludge (Johnson and Hallberg, 2005; Simate and Ndlovu, 2014; Zhang *et al.*, 2023). Although more favourable operating costs were reported for the SAVMIN® process, the biological sulfate reduction process offered the lowest operating cost (Van Rooyen, Van Staden and Du Preez, 2021).

Active remediation systems are generally favoured for active mines, owing to the smaller footprint required, and for their ability to accommodate operational changes during the life of mine, while passive systems provide a more economic long-term solution after mine closure (Ndlovu, 2017). Passive treatment processes often use bio-remediation technologies which may include several chemical and biological treatment mechanisms such as microbially mediated redox reactions, chemical and enzymatic hydrolysis, phytoextraction, and biosorption (Gazea, Adam and Kontopoulos, 1996). Examples of passive and semi-passive biological systems include aerobic and anaerobic wetlands, vertical flow wetlands, bioreactors and manganese removal beds (Gazea, Adam and Kontopoulos, 1996). Some passive and semi-passive processes are described.

2.6.2 Passive AMD remediation processes

2.6.2.1 Aerobic wetlands - Oxidation and hydrolysis

Aerobic wetlands employ a process of oxidation and hydrolysis for metals removal by precipitation. Vegetation is planted to mediate the flow of AMD through the shallow wetland by preventing channelling

and thus, providing the residence time for the oxidation of ferrous iron (Fe^{2+}) to the ferric iron form (Fe^{3+}). The Fe^{3+} is then hydrolysed to form a ferric hydroxide precipitate (Skousen *et al.*, 2017). The mechanism for iron oxidation has previously been described in Section 2.4, Equations 2.2–2.4. The addition of limestone is sometimes needed to create net-alkaline conditions and maintain the long-term efficiency of the system (Skousen *et al.*, 2017). Only minor uptake of metals has been observed in the wetland plants, and it is rather the diffusion of oxygen from the plant roots into the surrounding substrate that have benefit in providing localised oxidising zones within the wetland, thus facilitating subsequent oxidation and removal of the metal precipitates. Plants also function as a substrate for wildlife habitat, and additional attachment sites for metal precipitates. Organic material produced from decaying plants is used for further absorption and exchanged of metals. Plant cellulose provides nutrients for the sulfate reducing bacteria (Gazea, Adam and Kontopoulos, 1996).

2.6.2.2 Anaerobic wetlands - Reduction processes

Reducing conditions prevail in anaerobic systems and SRB use the sulfate from the AMD to oxidise the organic matter to release bicarbonate and hydrogen sulfide. The dissolved metals react with the hydrogen sulfide and form insoluble metal sulfide complexes (Gazea, Adam and Kontopoulos, 1996; Skousen *et al.*, 2017). Anaerobic wetlands are constructed by planting wetland vegetation into a permeable, organic substrate, and are sometimes underlain by limestone for alkalinity generation (Gazea, Adam and Kontopoulos, 1996; Skousen *et al.*, 2017).

Passive wetlands systems typically require a large land footprint and are more suited to small AMD flows of moderate acidity. These systems require some degree of maintenance and management, particularly for high metal loads as systems will eventually reach capacity. The long-term stability of accumulated deposits is not suitable for land rehabilitation use, and depending on the treatment mechanisms involved, care must be exercised in disposal. (Johnson and Hallberg, 2005; Skousen *et al.*, 2017). Wetlands can be costly to construct, are subject to seasonal changes, and are less easy to control.

Passive or semi-passive systems can be optimised by focussing on biological processes that require smaller footprint areas (Johnson and Hallberg, 2005; Zagury, Kulnieks and Neculita, 2006). Sulfidogenic bioreactors can be constructed using the same principles as anaerobic wetlands, but differ in the substrate used, and require additional organic amendment and inoculation with anaerobic bacteria (Greenway, 2019). Biological sulfate reducing (BSR) processes carry higher operating costs than passive wetland systems and some examples of active BSR plants that have been developed and/or trialled in South Africa include Mintek's THIOPAQ® and cloSURE® processes, the East Rand Water Care (ERWAT) Company's Ancor plant, VitaOne8's VitaSOFT Process, the THIOTEQ™ and SULFATEQ™ developed by Paques for zinc removal at Nyrstar Budel Zinc refinery (Sánchez-Andrea *et al.*, 2014; Van Rooyen, Van Staden and Du Preez, 2021).

2.7 Biological sulfate reduction (BSR)

Biological AMD remediation processes require less energy, produce less waste than physiochemical processes and the formation of metal sulfide precipitates provides significant potential for the recovery of valuable metals (Greben *et al.*, 2007; Zhang *et al.*, 2023). Metal sulfides present favourable densities, low solubility, and are easily dewatered. The varying solubility of metal sulfides at different pHs facilitates the selective recovery of metals (Sánchez-Andrea *et al.*, 2014). Metal sulfides are used in in a number of industrial applications including hydrocracking in fuel refineries, hydro processing, and oxygen reduction in fuel cells, and at nano-scale, in medical applications such as cancer therapy (Qian *et al.*, 2019). The biological sulfate reduction (BSR) process is mediated by microorganisms known as SRB, and the process includes by both assimilatory (ASR) as well as dissimilatory sulfate reducing (DSR) pathways (Liamleam and Annachhatre, 2007; Zhou *et al.*, 2021). The two BSR processes differ in the way they use sulfate; In DSR, SRB use organic compounds as a carbon and energy source and sulfate is used as terminal electron acceptor in anaerobic respiration to produce hydrogen sulfide; In ASR, sulfate is reduced to sulfide, which is then incorporated into sulfur-containing amino acids (Sánchez-Andrea *et al.*, 2014; Van Rooyen, Van Staden and Du Preez, 2021; Zhou *et al.*, 2022). The DSR reaction occurs in an anaerobic environment using formaldehyde (CH_2O) as the carbon source, as shown in Equation 2.5. The reaction shows the SRB oxidation of CH_2O to form bicarbonates, which then raise the pH and alkalinity of the media and reduce the available sulfates (SO_4^{2-}) to hydrogen sulfide (H_2S) (Gazea, Adam and Kontopoulos, 1996; Zagury, Kulnieks and Neculita, 2006; Kaksonen and Puhakka, 2007; Ruehl and Hiibel, 2020; Du Preez, 2021). The energy produced from the substrate oxidation coupled with the sulfate reduction is used by the SRB for growth and development (McMahon and Daugulis, 2008).

$$SO_4^{2-} + 2CH_2O + 2H^+ \rightarrow H_2S + 2HCO_3^- \qquad \textit{Equation 2.5}$$

The soluble sulfides formed then combine with metals present in the AMD and precipitate out as insoluble metal sulfides where Me^{2+} represents the cationic metal (Equation 2.6).

$$Me^{2+} + H_2S + 2H^+ \rightarrow MeS\downarrow + 2H^+ \qquad \textit{Equation 2.6}$$

In this instance, SRB activity consumes two moles of proton (H^+) per mole of SO_4^{2-} reduced and produces two equivalents of alkalinity (HCO_3^-) per mole of $SO4^{2-}$ reduced. The carbon source used, and the starting alkalinity (neutralising capacity) of the AMD will dictate the number of protons consumed and alkalinity produced (Liamleam and Annachhatre, 2007; Lindsay *et al.*, 2012; Zhou *et al.*, 2022).

2.7.1 Factors affecting the success of the dissimilatory sulfate remediation (DSR) processes

The success of the performance of SRB in the DSR process, is dependent on a range of factors including the concentration of SO_4^{2-}, SRB type, pH (proton (H^+) concentration) of the AMD, temperature, oxidation-reduction potential (ORP), hydraulic retention time (HRT), electron donor substrates, COD/SO_4^{2-} ratio,

concomitant ions (e.g. potassium and sodium and metal ions), syntropic or competitive bacteria, organic acid and sulfide inhibition at low pH, and reactor configuration (Sánchez-Andrea et al., 2014; Qian et al., 2019; Zhang et al., 2022). Neutrophilic SRB grow optimally between pH 6–7, and acid tolerant and acidophilic SRB operate best at low pH (Sánchez-Andrea et al., 2014) Optimal bacterial activity occurs if sufficient concentrations sulfate and organic matter are available, pHs are greater than four, and oxidising agents such as oxygen (O_2), ferric iron (Fe^{3+}) and manganese (Mn^{4+}) are not present (Gazea, Adam and Kontopoulos, 1996; Zhang *et al.*, 2022).

2.7.1.1 pH

SRB activity and growth is initially inhibited at low pH, but their activity results in an increase in pH, thus permitting their activity in the sediments beneath extremely acidic waters (Gazea, Adam and Kontopoulos, 1996). The hydrogen sulfide produced by bacterial sulfate reduction readily reacts with heavy metals at pH >3 to form virtually insoluble sulfide compounds, and sulfate reducing bacteria are also tolerant of high heavy metal concentrations. Iron sulfide precipitates are denser and form within the organic substrate, unlike the large blanketing sludge that results from iron oxidation and hydrolysis (Gazea et al., 1996). Neutrophil SRB function best between a pH range of 7.0–7.8 and are inhibited at low (<pH 5) and high (>pH 9) pHs, while eosinophil SRB function best at a pH range between 2.0–4.0. The chemical balance of sulfide species present in solution is affected by pH, H_2S species predominate between pH 4.5–5, and hydrosulfide ion (HS^-) species predominate at weak-alkaline or neutral pH (Zhang *et al.*, 2022). High concentrations of H_2S disrupt metabolic activity of SRB and competing microorganisms in the system. Acidic pHs also affect the form of metals and organics in the system, resulting in further inhibition of SRB activity (Zhang *et al.*, 2022). The success of dissolved metals removal as the metal sulfide is dependent on pH, solubility of the specific metal sulfide, and the concentrations of the metals (Zagury, Kulnieks and Neculita, 2006). Increasing the pH of the AMD, allows the selective precipitation of metal sulfide ions and metal sulfides with lower solubility product constants will precipitate before those of higher solubility (Gazea, Adam and Kontopoulos, 1996; Ramla and Sheridan, 2015).

2.7.1.2 Temperature

Different SRB types may function optimally at different temperatures (Qian *et al.*, 2019). Optimal temperatures for eliminating heavy metals in mesophilic systems is 37°C (Novair *et al.*, 2024). Low temperatures change the structure of cell membrane fats, resulting in reduction of SRB metabolism (Sánchez-Andrea *et al.*, 2014; Qian *et al.*, 2019).

2.7.1.3 Syntrophic/competitive bacteria

The presence of competitive and complimentary microorganism in a system affects the rate of biological sulfate reduction (Berrier, Neubauer and Franklin, 2022). Heterotopic SRB use organic substrates as electron donors to reduce sulfates, while autotrophic SRB use inorganic electron donors such as hydrogen (H_2) to

convert sulfate to sulfide (Liamleam and Annachhatre, 2007; Liu *et al.*, 2024). Competition between SRB and methanogens also play a role in the efficiency of anaerobic systems, and the choice of electron donor can affect the competition between the different microorganisms in a system, which in turn affects the treatment efficiency (Costa, De Castro, *et al.*, 2020; Ferraz *et al.*, 2021; Liu *et al.*, 2024).

2.7.1.4 Electron donor and COD/SO_4^{2-} ratio

The organic carbon concentrations in AMD are typically low, thus requiring amendment with additional organic source to enhance microbial activity (Sánchez-Andrea *et al.*, 2014). The organic carbon source is critical for SRB enrichment and acidic organic substrates such as glycerol are required for acidophilic sulfidogenic bioreactor that operate between pHs 2–5 (Qian *et al.*, 2019). The theoretical amount of organic matter (measured as the chemical oxygen demand (COD) required to complete the removal of sulfate by reduction is 0.67 g of COD for each 1 g of sulfate. (i.e. a COD:sulfate ratio of 0.67) (Liamleam and Annachhatre, 2007). Process conditions should be considered when selecting the organic substrate, for example propionate and ethanol are better suited to high salinity processes (Qian *et al.*, 2019). Organic sources can include synthetic organic compounds where low molecular weight compounds such as lactate, acetate, propionate, pyruvate and butyrate are favoured (Liamleam and Annachhatre, 2007). Organic and lignocellulosic wastes may also be used as a carbon source e.g. manure, corn cob, spent hops and grains, forestry residues, garden and agricultural wastes switch grass and lawn (Liamleam and Annachhatre, 2007; Zhang and Wang, 2014; Ramla and Sheridan, 2015; Ruehl and Hiibel, 2020).

2.7.1.5 Oxidation reduction potential (ORP)

In SRB metabolism, sulfates have a lower capacity to accept electrons than oxygen and nitric acid, and as such, appropriate ORP conditions are needed for the sulfate reaction to proceed. SRB are strictly anaerobic microorganisms but can tolerate trace amounts of oxygen (Sánchez-Andrea *et al.*, 2014). The presence of dissolved oxygen (DO), and some redox substances such as nitrates, nitrites and zero valent iron can result in an increase in ORP in an aerobic system which could then inhibit SRB metabolism. SRB metabolism was found to be optimal at ORPs below -100 mV, with inhibited metabolism occurring at ORPs above -100 mV (Sánchez-Andrea *et al.*, 2014). At low ORP, SRB have a competitive advantage over methanogenic archaea (MA) for electron acceptors such as hydrogen formate and acetate, and electron donors such as propionate and butyrate (Zhang *et al.*, 2022).

2.7.1.6 Hydraulic retention time

Reactor efficiencies are affected by hydraulic retention time (HRT). Optimisation of HRT is essential to balance the effective degradation of organic matter and sulfate reduction. Short HRTs may inhibit SRB metabolism owing to incomplete reactions resulting in unfavourable, acidic conditions within the anaerobic system. Extended HRTs may deplete the organic substrate and cause increase residual sulfide, and precipitated metals concentrations which may result in short circuiting the system (Zhang *et al.*, 2022).

2.7.1.7 Concomitant ions

Inhibitors that can affect the rate of sulfate reduction include oxidative substances such as oxygen, nitrates, nitrites. Toxic substances including Pb, and Se, molybdate and excessive organic acid or sulfide concentrations (Sánchez-Andrea *et al.*, 2014; Qian *et al.*, 2019). High concentrations of heavy metals are toxic to SRB and other microorganisms in anaerobic systems. The toxicity of the individual metals varies and is influenced by factors such temperature, pH, carbon source, and metal complexes that are formed (Zhang *et al.*, 2022).

2.8 Grass as an alternate organic carbon source for AMD remediation

While biological sulfate reduction provides an effective and more sustainable alternative than conventional AMD treatment technologies, the high operating costs associated with the provision of a suitable carbon and energy source remains a limiting factor (Greben et al., 2009; Van Rooyen, Van Staden and Du Preez, 2021). The need to improve the cost-efficiency of the process has prompted investigation into using alternative organic substrates such as lignocellulosic waste, to provide an abundant and renewable resource for this purpose (Demirbaş, 2001, Hsu et al., 1980, Petrova and Ivanova, 2010) (Demirbaş, 2001; Petrova and Ivanova, 2010; Niju, Swathika and Balajii, 2020; Cazier et al., 2024). Greben et al., (2009) investigated the use of grass as a potential carbon source for biological sulfate removal, due to its availability as garden waste and ease of cultivation (Greben et al., 2009). Investigation of grass types *Pennisetum clandestinum* (Kikuyu) *(Greben et al., 2009),* and indigenous grass types *Hyparrhenia hirta Setaria Sphacelata* (Ramla and Sheridan, 2015) and a mixture of *Digitaria eriantha* and *Eragrostis* (Greenway, 2019), demonstrated their suitability to use as feedstocks for AMD remediation (Greben et al., 2009; Ramla and Sheridan, 2015; Greenway, 2019). Grass has the added benefit of not impacting primary crops that are needed for food production (Demirbaş, 2001; Petrova and Ivanova, 2010; Humbird et al., 2011; Westensee et al., 2018; Niju, Swathika and Balajii, 2020; Cazier et al., 2024).

Vetiveria zizanioides or Chrysopogon zizanioides which is commonly known as Vetiver grass, originates from India, and the southern and south-eastern parts of Asia, is fast-growing with a deep root system. Gnansounou et al. (2017) describe Vetiver grass as highly tolerant to climate change, fire, pests, different soils and pHs. Vetiver grass has successfully been used for soil stabilization and phytoremediation of heavy metals pollution from mine impacted water (Gnansounou et al. 2017). Oils extracted from Vetiver roots are used in pharmaceutical and perfumery industries. This grass has also shown potential for biofuel and biogas production (Gnansounou et al., 2017).

Grass is a complex carbon source and cannot be used directly by SRB. (Andueza *et al.*, 2021). A pre-treatment step is required to disrupt the lignocellulosic structure of the grass to release monomeric sugars, glucose and xylose, which are subsequently converted to volatile fatty acids (VFA)s, which are used by the SRB for the

conversion of sulfates to sulfides (Meegoda *et al.*, 2018; Burman, Sheridan and Harding, 2019; van Hille *et al.*, 2021). The three main VFAs acetate, butyrate and propionate are formed during acidogenesis from the degradation of protein, carbohydrates and fats (Saratale *et al.*, 2022).

The chemical composition and nutritive value of grass can differ depending on the particular environment, growth cycle, and maturity stage of the grass (Andueza *et al.*, 2021). Delayed harvesting of grasses gives higher dry matter content and overall yield, as well as increased levels of organic matter, neutral and acid detergent fibre, and acid detergent lignin. In contrast with lower ash (mineral) content and crude protein levels (Bantihun *et al*., 2022; Barro *et al.*, 2022). Grass comprises mainly cellulose, hemicellulose and lignin with traces of inorganic elements and extractable compounds (Sun, Zhang and Loh, 2021; Wang *et al.*, 2024). Cellulose comprises mainly glucose, while hemicellulose comprises sugars such as glucose, mannose, galactose, xylose and arabinose. The products of sugars degradation include furan aldehydes: 5-hydroxymethylfurfural (HMF) and furfural; and aliphatic acids: acetic acid, formic acid and levulinic acid (Sluiter *et al.*, 2012; Jönsson, Alriksson and Nilvebrant, 2013; Niju, Swathika and Balajii, 2020). Volatile fatty acids (VFAs) which are produced during acidogenesis provide the electron donor required by SRB to facilitate the conversion of sulfate to sulfide by DSR (Meegoda *et al.*, 2018; van Hille *et al.*, 2021).

Pre-treatment methods can include physical, chemical, physio-chemical and biological processes and are varied based on the type of lignocellulosic material treated. Milling and grinding reduce particle size; dilute acids such as sulfuric (H_2SO_4) and phosphoric (H_3PO_4), or steam explosion, hydrolyse hemicellulose; while biological treatment using white-, brown- and soft-rot break down hemicelluloses and cellulose. Lignan is extracted using alkalis such as lime, sodium hydroxide (NaOH), and sodium carbonate (Na_2CO_3) or organic solvents such as ethanol and butanol. Polymers are fractionated using ionic liquids or deep-eutectic solvents which comprise mixtures of Lewis acids and bases (Galbe and Wallberg, 2019). The selected pretreatment method should ensure optimal recovery of the lignocellulosic polymers, while minimising the formation of toxic inhibitory products (Burman, Sheridan and Harding, 2019; Galbe and Wallberg, 2019). Figure 2.8 shows a schematic diagram in cellular structure and the effect of the pretreatment of lignocellulosic biomass (Tong, Cheng and Pullammanappallil, 2013).

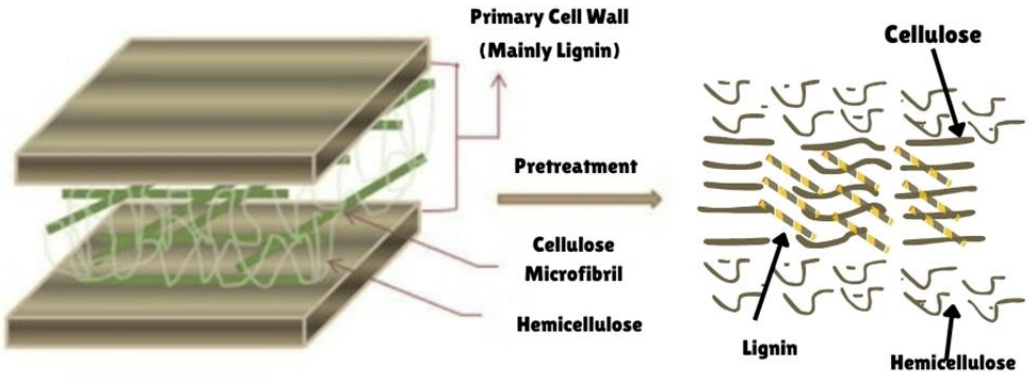


Figure 2.8 Schematic diagram showing the effect of pre-treatment on lignocellulosic biomass. Data from (Tong, Cheng and Pullammanappallil, 2013).

Magowo et al. (2014) successfully demonstrated the use of AMD as a weak sulfuric acid source to break down the lignocellulosic structure of the of the grass. This facilitated remediation of the AMD and rendered the grass susceptible to subsequent enzymatic hydrolysis and fermentation for ethanol production (Magowo, Rumbold and Sheridan, 2015).

2.9 Bioethanol production using lignocellulosic biomass

First-generation biofuel production using sucrose and starch containing raw materials has previously relied on the use of edible crops (Ab Rasid *et al.*, 2021). However, given the demands for increased food production to satisfy a growing population, reliance for bioethanol production should move to use of sustainable and renewable resources such as lignocellulose biomass or plant cell wall material as these are obtained as by-products of agricultural and forestry industries (Koppram et al., 2014; Ab Rasid et al., 2021; Mankar et al., 2021; Beluhan et al., 2023). As previously discussed, grass is an abundant and renewable feedstock, which can also be considered to produce biofuels (Chamoli *et al.*, 2024). The cellulose component in grass comprises primarily glucose, and hemicellulose component which comprises xylose and arabinose, which are the main contributors to the fermentation of lignocellulose biomass (Saratale *et al.*, 2022). The production of biofuels requires three processes, a pre-treatment, hydrolysis, and fermentation stage (Chamoli *et al.*, 2024). The pretreatment stage in this instance, is required to break down the strong ligno-hemicellulosic matrix to render the cellulose amenable to enzymatic hydrolysis for conversion to glucose (monosaccharides). During enzymatic hydrolysis cellulose and hemicellulose are converted to monomeric sugars using a buffer/cellulase mixture. The pre-treatment step contributes a substantial proportion of the total cost of the bioethanol production process thus necessitating development of efficient pre-treatment technologies (Koppram *et al.*, 2014; Chamoli *et al.*, 2024).

The fermentation stage uses an inoculum solution containing fermenting micro-organisms and prepared with added yeast extract and peptone nutrients to convert the monomeric sugars in the hydrolysis filtrate to alcohols, biogas and organic acids (Burman, Sheridan, *et al.*, 2018; Burman, Harding and Sheridan, 2021; Ojo, 2023). The separate hydrolysis and fermentation (SHF) process can be combined into a single step, known as simultaneous saccharification and fermentation (SSF), where the pre-treated grass is added to a combined mixture of buffer/cellulase and inoculum (Burman, Sheridan, *et al.*, 2018). The benefits of a combined SSF process include lower start-up costs and less risk of enzyme inhibition (Chamoli *et al.*, 2024).

The cellulose hydrolysis step is the rate limiting step in cellulosic fuel production as lignin monomers cannot be utilised directly for ethanol production (Petrova and Ivanova, 2010). Using grass in a combined process to remediate AMD (a pollutant), while at the same time using the AMD as a dilute acid as a resource to break down the lignocellulose structure of the grass for further enzymatic hydrolysis and fermentation to generate biofuels (creation of a value product) contributes to a circular economy in that it provides a sustainable use of grass (a naturally occurring waste product). As such, further investigation to improve the economic

feasibility of these processes by using grass types that are co-located with AMD sources, natural and readily available SRB sources, and optimising process conditions will provide a valuable contribution to the body of knowledge, that uses waste to generate both clean water and biofuels.

2.10 The pursuit of a sustainable, cost-effective biological process for AMD remediation

Water scarcity and the increasing energy demands stem from growing population, industrial, and agricultural needs. Acid mine drainage has resulted in contamination of local environment and watercourses and poses significant threat of further contamination which exasperates already evident water security issues. The development of a sustainable, cost-effective, AMD treatment process would provide some relief for mitigation of part of these liability issues and have the benefit of producing an improved water quality product that can be re-used for drinking, crop irrigation, process water or other purposes depending on the water quality achieved.

Biological AMD remediation has shown promise as an alternative remediation process to conventional, active processes that require high CAPEX and OPEX costs. The biological sulfate reduction process has the added benefit of the precipitation of metals as the metal sulfide, which facilitates easier metals recovery, than if metals were precipitated in the hydroxide form from alkaline chemical addition. The recovery of valuable minerals from AMD could provide a revenue source to offset the high costs of remediation. Although the recovery of metals is not part of this study, collaboration with researchers into the use of Ion Exchange for recovery of value minerals such as rare earth elements, resulted in the development of a methodology for rapid determination of REEs in high Fe/SO_4^{2-} matrix using inductively coupled plasma optical emission spectrometry (ICP-OES), rather than the using the favoured, but slower, ICP – Mass Spectrometry (ICP-MS) technique, and thus providing faster turn-around of data to expedite process development (Smith *et al.*, 2023).

The limiting factor in biological treatment systems is the cost of the organic substrate required to drive the DSR process, which necessitates the need for an inexpensive and sustainable carbon and energy source (Burman, 2020). Indigenous and other grass types are easily cultivated close to AMD source wastes or can be sourced from garden and roadside wastes. Research has demonstrated the success of various grass types as organic source in the biological sulfate remediation of mine impacted water (Ramla and Sheridan, 2015; Westensee *et al.*, 2018; Greenway, 2019; Magowo, Sheridan and Rumbold, 2023).

Grass has also shown success in the production of biofuels which could reduce our dependence on coal for fuel generation. This would realise health benefits, such as reduced exposure to particulate matter (P10) created from coal dust created during mining, and carbon dioxide and other volatile substances released in burning of coal to produce energy. Although South Africa has sufficient coal reserves for the next 200 years, there is a worldwide movement towards controlling the use of fossil fuels and adopting clean coal

technologies that will limit environmental and health issues resulting from the mining and burning of coal (Eskom, 2021).

The development of a combined remediation and bioethanol process presents an opportunity to use renewable waste products to produce clean water, and to produce biofuels which will reduce the use of fossil fuels with associated environmental benefits. Galbe and Wallberg, (2019), in their review of pretreatment methods for the efficient use of lignocellulosic materials for biorefineries, noted that it was not possible to conduct techno-economic evaluation without reliable experimental data (Galbe and Wallberg, 2019). This study thus endeavours to provide experimental verification of proposed processes that may be considered in the design of a combined AMD retreatment and bioethanol production process. Improving economic feasibility of bioprocesses and metals recovery presents a means of deriving further value from AMD remediation. While the resale of precious metals and rare earth elements (REE) can generate income, metals such as Co, Ni, Cu, Zn are classified as critical, owing to their scarcity and their industrial application to clean energy transition (Müller *et al.*, 2025).

The differing geochemical composition of ore types in a particular region based on geochemical stratigraphic layering, the type of ore being mined, the mining process used, the surrounding water chemistry and ecosystem, will directly influence the acid generating capacity of a soil and the resulting AMD composition. This highlights the site specificity of AMD, and the need for accurate characterisation of the AMD, and for continued monitoring to properly understand seasonal variances and other factors that might affect the chemistry of these waters. This information is necessary to maintain control of the AMD body, planning for managing an unintended breach event, prevention of contamination of the surrounding environment, and to understand the potential pathways of the contaminated water from point source. Understanding the chemistry underlying the AMD and seasonal variances is also important for the design specification of appropriate remediation processes. The high cost of remediation processes can be offset by incorporating locally sourced, naturally available, materials in the design of the process, which will also safeguard sustainability. This in turn requires an understanding of the naturally available resources such as grasses, and the assessment of the suitability of these grass types for use in the remediation process. If the products and by-products of the process could be recovered for resale, this would assist with offsetting the high costs of remediation.

This research focused on AMD resulting from coal mining operations in the Mpumalanga/Witbank region. AMD from this region was characterised to understand the distinct characteristics of the region's AMD and also the seasonal variations thereof, which can be used to inform treatment options and specification. Different grass types that are co-located with coal mines in the Mpumalanga area were characterised and experimentally tested to assess suitability for use in bioremediation. Natural sources of SRB inoculum were sought and tested for suitability to increase pH, and their ability to reduce sulfates and produce sulfides. Lastly, the effects of grass-AMD hydraulic retention time were assessed with and without SRB addition for the influence on both AMD bioremediation and subsequent bioethanol production.

2.11 References

Ab Rasid, N.S. et al. (2021) 'Recent advances in green pre-treatment methods of lignocellulosic biomass for enhanced biofuel production', Journal of Cleaner Production, 321, p. 129038. Available at: https://doi.org/10.1016/j.jclepro.2021.129038

Akcil, A. and Koldas, S. (2006) 'Acid Mine Drainage (AMD): causes, treatment and case studies', Journal of Cleaner Production, 14(12–13), pp. 1139–1145. Available at: https://doi.org/10.1016/j.jclepro.2004.09.006

Akinwekomi, V., Maree, J.P. and Wolkersdorfer, C. (2017) 'Using Calcium Carbonate/Hydroxide and Barium Carbonate to Remove Sulphate from Mine Water', Mine Water and the Environment, 36(2), pp. 264–272. Available at: https://doi.org/10.1007/s10230-017-0451-7

Andueza, D., Picard, F., Note, P. and Carrère, P., 2021. Relationship between the chemical composition, nutritive value and the maturity stage of six temperate perennial grasses during their first growth cycle along an altitude gradient. European Journal of Agronomy, 130, p.126364. Available at: https://doi.org/10.1016/j.eja.2021.126364

Ashton, P.J. et al. (2006) A compilation of all the international freshwater agreements entered into by South Africa with other states. 1515,1/06. WRC. Available at: https://www.wrc.org.za/wp-content/uploads/mdocs/1515-1-061.pdf (Accessed: 25 February 2025).

Banks, V.J. et al. (2011) Conceptual models of Witbank coalfield, South Africa : Earth observation for monitoring and observing environmental and societal impacts of mineral resources Exploration and Exploitation, CEC FP7 Project EO-MINERS, Deliverable D3.1-2. British Geological Survey, p. 107. Available at: https://nora.nerc.ac.uk/id/eprint/506746/ (Accessed: 20 January 2025).

Bantihun, A., Asmare, B. and Mekuriaw, Y., 2022. Comparative evaluation of selected grass species for agronomic performance, forage yield, and chemical composition in the highlands of Ethiopia. *Advances in Agriculture*, *2022*(1), p.6974681. Available at: https://doi.org/10.4314/jasem.v26i12.3

Barro, R., Cortés, R., Pérez, J., Ciria, C. S., Fernández, M. and Ciria, P., 2022. Nitrogen fertilisation and harvest time on biomass production and composition of tall wheatgrass in Mediterranean marginal conditions. Biomass & Bioenergy, 158, p.106382. Available at: https://doi.org/10.1016/J.BIOMBIOE.2022.106382

Belle, G., Schoeman, Y. and Oberholster, P. (2023) 'Potential Toxic-Element Pollution in Surface Water and Its Implications for Aquatic and Human Health: Source–Pathway–Receptor Model', Water, 15(17), p. 3100. Available at: https://doi.org/10.3390/w15173100

Beluhan, S. et al. (2023) 'The Production of Bioethanol from Lignocellulosic Biomass: Pretreatment Methods, Fermentation, and Downstream Processing', Energies, 16(19), p. 7003. Available at: https://doi.org/10.3390/en16197003

Bergh, J.P. (2009) The partitioning of trace elements in the no. 4 seam of the Witbank coalfield. MSc. Dissertation. University of the Witwatersrand. Available at: https://wiredspace.wits.ac.za/server/api/core/bitstreams/bfe98122-a8d5-4d05-8a2b-044cbfbbd800/content (Accessed: 21 January 2025).

Berrier, D.J., Neubauer, S.C. and Franklin, R.B. (2022) 'Cooperative microbial interactions mediate community biogeochemical responses to saltwater intrusion in wetland soils', FEMS Microbiology Ecology, 98(3), p. fiac019. Available at: https://doi.org/10.1093/femsec/fiac019

Burgess, J (2016) 'South African green drop certification for excellence in wastewater treatment plant operation'. Water Research Commission of South Africa. Available at: https://iwa-network.org/wp-content/uploads/2016/03/South-African-Green.pdf (Accessed: 25 February 2024).

Burman, N.W. et al. (2018) 'Modelling of low temperature dilute sulfuric acid pre-treatment of South African grass', Bioresource Technology Reports, 4, pp. 21–28. Available at: https://doi.org/10.1016/j.biteb.2018.08.014

Burman, N.W., Harding, K.G. and Sheridan, C.M. (2021) 'Evaluation of two different reactor configurations for the simultaneous remediation AMD and pretreatment of lignocellulosic biomass', in. South African Chemical Engineering Congress (SACEC), At: Virtual.

Burman, N.W., Sheridan, C.M. and Harding, K.G. (2019) 'Lignocellulosic bioethanol production from grasses pre-treated with acid mine drainage: Modelling and comparison of SHF and SSF', Bioresource Technology Reports, 7, p. 100299. Available at: https://doi.org/10.1016/j.biteb.2019.100299

Burman, N.W. (2020) Design and optimization of a bioprocess to simultaneously produce biochemicals and remediate acid mine drainage using indigenous South African grasses. Doctoral dissertation. University of the Witwatersrand. Available at: https://hdl.handle.net/10539/30088

Cairncross, B. and Cadle, A.B. (1988) 'Palaeoenvironmental control on coal formation, distribution and quality in the Permian Vryheid Formation, East Witbank Coalfield, South Africa', International Journal of Coal Geology, 9(4), pp. 343–370. Available at: https://doi.org/10.1016/0166-5162(88)90031-6

Cairncross, B., Hart, R.J. and Willis, J.P. (1990) 'Geochemistry and sedimentology of coal seams from the Permian Witbank Coalfield, South Africa; a means of identification', International Journal of Coal Geology, 16(4), pp. 309–325. Available at: https://doi.org/10.1016/0166-5162(90)90056-5

Casey, J.P. (2019) 'History of mining in South Africa'. Mining Technology. Available at: https://www.mining-technology.com/features/history-of-mining-in-south-africa/?cf-view (Accessed: 20 November 2024).

Cazier, E.A. et al. (2024) 'Exploring industrial lignocellulosic waste: Sources, types, and potential as high-value molecules', Waste Management, 188, pp. 11–38. Available at: https://doi.org/10.1016/j.wasman.2024.07.029

Chamoli, P. et al. (2024) 'Recent advances in the processing of Napier grass (Pennisetum purpureum Schumach) as a potential bioenergy crop for bioethanol production', Journal of Applied Biology & Biotechnology [Preprint]. Available at: https://doi.org/10.7324/JABB.2024.154513

Chen, G. et al. (2021) 'A critical review of prevention, treatment, reuse, and resource recovery from acid mine drainage', Journal of Cleaner Production, 329, p. 129666. Available at: https://doi.org/10.1016/j.jclepro.2021.129666

Chen, H. et al. (2020) 'In-situ remediation of acid mine drainage from abandoned coal mine by filed pilot-scale passive treatment system: Performance and response of microbial communities to low pH and elevated Fe', Bioresource Technology, 317, p. 123985. Available at: https://doi.org/10.1016/j.biortech.2020.123985

Claassen, M. (2013) 'Integrated Water Resource Management in South Africa', International Journal of Water Governance, 1(3), pp. 323–338. Available at: https://doi.org/10.7564/13-IJWG12

Cole, M. et al. (2024) Developing Mine Closure Risk Ratings and a Post-closure Opportunity Framework for South Africa. Report to the Water Research Commission. WRC Report No. TT 930/23. Available at: https://www.wrc.org.za/wp-content/uploads/mdocs/TT%20930%20final%20web.pdf

(Accessed: 19 January 2025).

Costa, J.M. et al. (2020) 'Anaerobic reactors for the treatment of sulphate and metal-rich wastewater: a review', International Journal of Environmental Analytical Chemistry, 102(4), pp. 923–934. Available at: https://doi.org/10.1080/03067319.2020.1728261

Daraz, U. et al. (2023) 'Remediation technologies for acid mine drainage: Recent trends and future perspectives', Chemosphere, 311, p. 137089. Available at: https://doi.org/10.1016/j.chemosphere.2022.137089

Demirbaş, A. (2001) 'Biomass resource facilities and biomass conversion processing for fuels and chemicals', Energy Conversion and Management, 42(11), pp. 1357–1378. Available at: https://doi.org/10.1016/S0196-8904(00)00137-0

Department of Water and Sanitation (DWS) (2022) National State of Water Report 2022. Integrated Water Studies Report. WII/IWS/NSoW 2022. Pretoria, South Africa. Available at: https://www.dws.gov.za/Projects/National%20State%20of%20Water%20Report/Documents/National%20State%20of%20Water%20Report%202022.pdf (Accessed: 22 February 2024).

Department of Water and Sanitation (DWS) (2023) NATIONAL WATER RESOURCE STRATEGY III (NWRS-3). Pretoria, South Africa. Available at: https://www.dws.gov.za/Documents/Gazettes/Approved%20National%20Water%20Resource%20Strategy%20Third%20Edition%20(NWRS3)%202023.pdf (Accessed: 16 February 2024).

Du Preez, K. (2021) 'Mintek's Integrated cloSURETM Technology for Treatment of Acid Mine Drainage', in Mine Water Management for Future Generations. Cardiff, Wales: Natural Resources Wales, The Coal Authority, Welsh Government, Cardiff University, pp. 129–135.

Egoh, B. et al. (2009) 'Spatial congruence between biodiversity and ecosystem services in South Africa', Biological Conservation, 142(3), pp. 553–562. Available at: https://doi.org/10.1016/j.biocon.2008.11.009

Eskom (2021) 'COAL IN SOUTH AFRICA: Fact Sheet'. Available at: https://www.eskom.co.za/wp-content/uploads/2021/08/CO-0007-Coal-in-SA-Rev-16.pdf (Accessed: 29 September 2024).

Ferraz, R.M. et al. (2021) 'Effects of the inoculum source, electron donor, and immobilization on the microbial community of sulfidogenic bioreactors', Chemical Engineering Journal, 404, p. 126549. Available at: https://doi.org/10.1016/j.cej.2020.126549

Galbe, M. and Wallberg, O. (2019) 'Pretreatment for biorefineries: a review of common methods for efficient utilisation of lignocellulosic materials', Biotechnology for Biofuels, 12(1), p. 294. Available at: https://doi.org/10.1186/s13068-019-1634-1

Gazea, B., Adam, K. and Kontopoulos, A. (1996) 'A review of passive systems for the treatment of acid mine drainage', Minerals Engineering, 9(1), pp. 23–42. Available at: https://doi.org/10.1016/0892-6875(95)00129-8

GCIS (2022) 'South Africa Yearbook 2021/2022 Water and Sanitation'. Available at: https://www.gcis.gov.za/sites/default/files/docs/gcis/21.%20Water%20and%20Sanitation.pdf.

Government of Republic of South Africa (2024) Energy Action Plan: 18 Month Progress Report: March 2024. The Presidency. Available at: https://www.stateofthenation.gov.za/priorities/growing-the-economy-and-jobs/just-transition-to-a-low-carbon-economy#the-energy-action-plan_12 (Accessed: 19 January 2025).

Greben, H. et al. (2007) 'Improved sulphate removal rates at increased sulphide concentration in the sulphidogenic bioreactor', Water SA, 31(3), pp. 351–358. Available at: https://doi.org/10.4314/wsa.v31i3.5206

Greben, H.A. et al. (2009) 'Bioremediation of sulphate rich mine effluents using grass cuttings and rumen fluid microorganisms', Journal of Geochemical Exploration, 100(2–3), pp. 163–168. Available at: https://doi.org/10.1016/j.gexplo.2008.01.004

Greenway, N. (2019) The bioremediation of acid mine drainage utilising Indigenous South African grass as the organic carbon source of dissimilatory sulphate reduction. MSc. Dissertation. University of the Witwatersrand. Available at: https://hdl.handle.net/10539/28938 (Accessed: 15 December 2024).

Habashi, F. (2016) 'Gold – An Historical Introduction', in Gold Ore Processing. Elsevier, pp. 1–20. Available at: https://doi.org/10.1016/B978-0-444-63658-4.00001-3

Hancox, P.J. and Götz, A.E. (2014) 'South Africa's coalfields — A 2014 perspective', International Journal of Coal Geology, 132, pp. 170–254. Available at: https://doi.org/10.1016/j.coal.2014.06.019

Hasii, O. and Gasii, G. (2024) 'Coal mining and water resources: impacts, challenges, and strategies for sustainable environmental management', IOP Conference Series: Earth and Environmental Science, 1348(1), p. 012017. Available at: https://doi.org/10.1088/1755-1315/1348/1/012017

van Hille, R. et al. (2021) Report to the Water Research Commission: PILOT-SCALE SEMI-PASSIVE TREATMENT OF ARD – EVALUATION OF TREATMENT PRODUCTS FOR DOWNSTREAM USE. WRC Report No. 2762/1/21. Pretoria, pp. 1–64. Available at: https://www.wrc.org.za/wp-content/uploads/mdocs/2762%20final.pdf

(Accessed: 11 January 2024).

Hobbs, P., Oelofse, S.H.H. and Rascher, J. (2008) 'Management of Environmental Impacts from Coal Mining in the Upper Olifants River Catchment as a Function of Age and Scale', International Journal of Water Resources Development, 24(3), pp. 417–431. Available at: https://doi.org/10.1080/07900620802127366

Humbird, D. et al. (2011) Process Design and Economics for Biochemical Conversion of Lignocellulosic Biomass to Ethanol: Dilute-Acid Pretreatment and Enzymatic Hydrolysis of Corn Stover. NREL/TP-5100-47764, 1013269, p. NREL/TP-5100-47764, 1013269. Available at: https://doi.org/10.2172/1013269

Jiao, Y., Zhang, C., Su, P., Tang, Y., Huang, Z., Ma, T., 2023. A review of acid mine drainage: Formation mechanism, treatment technology, typical engineering cases and resource utilization. Process Saf. Environ. Prot. 170, 1240–1260. https://doi.org/10.1016/j.psep.2022.12.083

Johnson, D.B. and Hallberg, K.B. (2005) 'Acid mine drainage remediation options: a review', Science of The Total Environment, 338(1–2), pp. 3–14. Available at: https://doi.org/10.1016/j.scitotenv.2004.09.002

Jönsson, L.J., Alriksson, B. and Nilvebrant, N.-O. (2013) 'Bioconversion of lignocellulose: inhibitors and detoxification', Biotechnology for Biofuels, 6(1), p. 16. Available at: https://doi.org/10.1186/1754-6834-6-16

Kaksonen, A.H. and Puhakka, J.A. (2007) 'Sulfate Reduction Based Bioprocesses for the Treatment of Acid Mine Drainage and the Recovery of Metals', Engineering in Life Sciences, 7(6), pp. 541–564. Available at: https://doi.org/10.1002/elsc.200720216

Kistin, E.J. et al. (2009) 'An overview of the content and historical context of the international freshwater agreements that South Africa has entered into with neighbouring countries', International Environmental Agreements: Politics, Law and Economics, 9(1), pp. 1–21. Available at: https://doi.org/10.1007/s10784-008-9086-2

Koppram, R. et al. (2014) 'Lignocellulosic ethanol production at high-gravity: challenges and perspectives', Trends in Biotechnology, 32(1), pp. 46–53. Available at: https://doi.org/10.1016/j.tibtech.2013.10.003

Kruger, A. et al. (2022) 'The role of effect-based methods to address water quality monitoring in South Africa: a developing country's struggle', Environmental Science and Pollution Research, 29(56), pp. 84049–84055. Available at: https://doi.org/10.1007/s11356-022-23534-3

Levy, J and Xu, Y (2011) 'Groundwater management and groundwater/surface-water interaction in the context of South African water policy'. Available at: https://repository.uwc.ac.za/handle/10566/825

Liamleam, W. and Annachhatre, A.P. (2007) 'Electron donors for biological sulfate reduction', Biotechnology Advances, 25(5), pp. 452–463. Available at: https://doi.org/10.1016/j.biotechadv.2007.05.002

Lindsay, M.B. et al. (2012) 'Long-term Biogeochemistry of Mine Tailings Amended with Organic Carbon for Water-quality Management', in Proceedings of the 9th International Conference on Acid Rock Drainage. I9th International Conference on Acid Rock Drainage, pp. 20–26. Available at: https://scholar.google.com/scholar?start=10&q=different+carbon+sources+on+amount+of+alkalinity+produced+in+DSR&hl=en&as_sdt=0,5 (Accessed: 26 January 2025).

Liu, Y. et al. (2024) 'Current regulates electron donors for heterotrophic and autotrophic microorganisms to enhance sulfate reduction in three-dimensional electrode biofilm reactors', Chemical Engineering Journal, 500, p. 157150. Available at: https://doi.org/10.1016/j.cej.2024.157150

Magowo, E., Rumbold, K. and Sheridan, C. (2015) 'The Utilization of Cellulosic Biomass in treating AMD and the Subsequent Generation of Fermentable Sugars', in. 10th International Conference on Acid Mine Drainage & IMWA Annual Conference, Santiago, Chile. Available at: http://www.imwa.de/docs/imwa_2015/IMWA2015_Sheridan_168.pdf (Accessed: 26 August 2024).

Magowo, E., Sheridan, C. and Rumbold, K. (2023) 'Fermentable sugars as bioprocessing feedstocks from lignocellulosic biomass pretreated with acid mine drainage', in Advances in Lignocellulosic Biofuel Production Systems. Elsevier, pp. 161–178. Available at: https://doi.org/10.1016/B978-0-323-91192-4.00006-7

Mankar, A.R. et al. (2021) 'Pretreatment of lignocellulosic biomass: A review on recent advances', Bioresource Technology, 334, p. 125235. Available at: https://doi.org/10.1016/j.biortech.2021.125235

Mbae, M. et al. (2024) 'Onsite sanitation systems and contamination of groundwater: A systematic review of the evidence for risk using the source-pathway-receptor model', PLOS Water. Edited by S.M. Tareq, 3(7), p. e0000167. Available at: https://doi.org/10.1371/journal.pwat.0000167

McCarthy, T.S. (2011) 'The impact of acid mine drainage in South Africa', South African Journal of Science, 107(5/6), p. 7 pages. Available at: https://doi.org/10.4102/sajs.v107i5/6.712

McMahon, M.J.L. and Daugulis, A.J. (2008) 'Enhancement of biogenic sulfide production in a packed-bed bioreactor via critical inoculum design and carrier material selection', Biotechnology and Bioengineering, 100(5), pp. 855–863. Available at: https://doi.org/10.1002/bit.21827

Meegoda, J.N. et al. (2018) 'A Review of the Processes, Parameters, and Optimization of Anaerobic Digestion', International Journal of Environmental Research and Public Health, 15(10), p. 2224. Available at: https://doi.org/10.3390/ijerph15102224

Mosai, A.K., Ndlovu, G. and Tutu, H. (2024) 'Improving acid mine drainage treatment by combining treatment technologies: A review', Science of The Total Environment, 919, p. 170806. Available at: https://doi.org/10.1016/j.scitotenv.2024.170806

Mostert, H., Van Den Berg, H.M. and Kengni, B. (2021) 'Chapter IX.21: Frameworks for energy governance and regulation in Africa', in, pp. 238–252. Available at: https://doi.org/10.4337/9781788119689.IX.21

Müller, D., Groves, D.I., Santosh, M. and Yang, C-X., 2025. Critical metals: Their applications with emphasis on the clean energy transition. Geosystems and Geoenvironment, 4(1), p.100310. Available at: https://doi.org/10.1016/j.geogeo.2024.100310

Mwendera, E. and Atyosi, Y. (2018) 'A Review of Water Storage for Socio-Economic Development in South Africa', Journal of Water Resource and Protection, 10(03), pp. 266–286. Available at: https://doi.org/10.4236/jwarp.2018.103016

Naidu, G. et al. (2019) 'A critical review on remediation, reuse, and resource recovery from acid mine drainage', Environmental Pollution, 247, pp. 1110–1124. Available at: https://doi.org/10.1016/j.envpol.2019.01.085

Naidu, T.S., Sheridan, C.M. and Van Dyk, L.D. (2020) 'Basic oxygen furnace slag: Review of current and potential uses', Minerals Engineering, 149, p. 106234. Available at: https://doi.org/10.1016/j.mineng.2020.106234

Ndlovu, S. (2017) Acid Mine Drainage Treatment Technologies. Management and Mitigation of Acid Mine Drainage in South Africa: Input for Mineral Beneficiation in Africa. Available at: https://books.google.co.za/books?hl=en&lr=&id=XF1DDgAAQBAJ&oi=fnd&pg=PA216&ots=LmKIfULM43&sig=T0utYWqKuZL7WYtvkyjTEer0eek&redir_esc=y#v=onepage&q&f=false (Accessed: 24 January 2025).

Nel, J.L. et al. (2017) 'Strategic water source areas for urban water security: Making the connection between protecting ecosystems and benefiting from their services', Ecosystem Services, 28, pp. 251–259. Available at: https://doi.org/10.1016/j.ecoser.2017.07.013

Niju, S., Swathika, M. and Balajii, M. (2020) 'Pretreatment of lignocellulosic sugarcane leaves and tops for bioethanol production', in Lignocellulosic Biomass to Liquid Biofuels. Elsevier, pp. 301–324. Available at: https://doi.org/10.1016/B978-0-12-815936-1.00010-1

Ninomiya, M.E.M. et al. (2023) 'Indigenous communities and the mental health impacts of land dispossession related to industrial resource development: a systematic review', The Lancet Planetary Health, 7(6), pp. e501–e517. Available at: https://doi.org/10.1016/S2542-5196(23)00079-7

Novair, S.B. et al. (2024) 'The role of sulphate-reducing bacteria (SRB) in bioremediation of sulphate-rich wastewater: Focus on the source of electron donors', Process Safety and Environmental Protection, 184, pp. 190–207. Available at: https://doi.org/10.1016/j.psep.2024.01.103

Ojo, A. (2023) 'An Overview of Lignocellulose and Its Biotechnological Importance in High-Value Product Production', Fermentation, 9(11), p. 990. Available at: https://doi.org/10.3390/fermentation9110990

Ojonimi, T.I. et al. (2021) 'Acid mine drainage (AMD) contamination in coal mines and the need for extensive prediction and remediation: a review', Journal of Degraded and Mining Lands Management, 9(1), pp. 3129–3136. Available at: https://doi.org/10.15243/jdmlm.2021.091.3129

Petrova, P. and Ivanova, V. (2010) 'Perspectives for the Production of Bioethanol from Lignocellulosic Materials', Biotechnology & Biotechnological Equipment, 24(sup1), pp. 529–546. Available at: https://doi.org/10.1080/13102818.2010.10817894

Pinetown, K.L., Ward, C.R. and Van Der Westhuizen, W.A. (2007) 'Quantitative evaluation of minerals in coal deposits in the Witbank and Highveld Coalfields, and the potential impact on acid mine drainage', International Journal of Coal Geology, 70(1–3), pp. 166–183. Available at: https://doi.org/10.1016/j.coal.2006.02.013

Prepilková, V. et al. (2022) 'Possibilities of remediation of neutral mine drainage - Removal and recovery of potentially hazardous elements', Soil and Water Research, 17(4), pp. 251–267. Available at: https://doi.org/10.17221/7/2022-SWR

Qian, Z. et al. (2019) 'Recent advances in dissimilatory sulfate reduction: From metabolic study to application', Water Research, 150, pp. 162–181. Available at: https://doi.org/10.1016/j.watres.2018.11.018

Quatrini, R. and Johnson, D.B. (2019) 'Acidithiobacillus ferrooxidans', Trends in Microbiology, 27(3), pp. 282–283. Available at: https://doi.org/10.1016/j.tim.2018.11.009

Rambabu, K. et al. (2020) 'Biological remediation of acid mine drainage: Review of past trends and current outlook', Environmental Science and Ecotechnology, 2, p. 100024. Available at: https://doi.org/10.1016/j.ese.2020.100024

Ramla, B. and Sheridan, C. (2015) 'The Potential Utilisation of Indigenous South African Grasses for Acid Mine Drainage Remediation', Water SA, 41(2), p. 247. Available at: https://doi.org/10.4314/wsa.v41i2.10

Ramontja, T. et al. (2011) Mine Water Management in the Witwatersrand Gold Fields With Special Emphasis on Acid Mine Drainage Inter-Ministerial-Committee on Acid Mine Drainage. Report of the Team of Experts for the Inter-Ministerial Committee on Acid Mine Drainage. Report of the Team of Experts for the Inter-Ministerial Committee on Acid Mine Drainage. Pretoria, p. 146. Available at: https://www.imwa.info/docs/imwa_2016/IMWA2016_Coetzee_66.pdf (Accessed: 21 January 2024).

Retief, H. and Pollard, S. (2020) 'Overview of Water Quality and Quantity Olifants River Catchment. AWARD series: Climate change impacts on the Olifants River Catchment'. © Association for Water and Rural Development (AWARD). Available at: https://award.org.za/wp/wp-content/uploads/2020/05/AWARD-BROCHURE-Overview-of-water-quality-and-quantity-in-Olifants-River-catchment-2020-v2.pdf (Accessed: 19 January 2025).

Ruch, R.R., Gluskoter, H.J. and Shimp, N.F. (1974) Occurrence and Distribution of Potentially Volatile Trace Elements in Coal: A Final Report. Illinois State Geological Society (Environmental Geology Notes, 72). Available at: https://books.google.co.za/books?hl=en&lr&id=BoqnqqSC_wUC&oi=fnd&pg=PA3&dq=Occurrence+and+distribution+of+potentially+volatile+trace+elements+in+coal:&ots=U6yxHgurDC&sig=O6tG5sVR7EgLDypx8H7H3Gmvr2Q&redir_esc=y&pli=1#v=onepage&q=Occurrence%20and%20distribution%20of%20potentially%20volatile%20trace%20elements%20in%20coal%3A&f=false (Accessed: 22 January 2025).

Ruehl, M.D. and Hiibel, S.R. (2020) 'Evaluation of organic carbon and microbial inoculum for bioremediation of acid mine drainage', Minerals Engineering, 157, p. 106554. Available at: https://doi.org/10.1016/j.mineng.2020.106554

SAHRC (2018) 'The Right to Water & Sanitation'. Available at: https://www.sahrc.org.za/home/21/files/SAHRC%20Water%20and%20Sanitation%20revised%20pamphlet%2020%20March%202018.pdf

Sánchez-Andrea, I. et al. (2014) 'Sulfate reduction at low pH to remediate acid mine drainage', Journal of Hazardous Materials, 269, pp. 98–109. Available at: https://doi.org/10.1016/j.jhazmat.2013.12.032

Saratale, R.G. et al. (2022) 'A critical review on biomass-based sustainable biorefineries using nanobiocatalysts: Opportunities, challenges, and future perspectives', Bioresource Technology, 363, p. 127926. Available at: https://doi.org/10.1016/j.biortech.2022.127926

Simate, G.S. and Ndlovu, S. (2014) 'Acid mine drainage: Challenges and opportunities', Journal of Environmental Chemical Engineering, 2(3), pp. 1785–1803. Available at: https://doi.org/10.1016/j.jece.2014.07.021

Skousen, J. et al. (2017) 'Review of Passive Systems for Acid Mine Drainage Treatment', Mine Water and the Environment, 36(1), pp. 133–153. Available at: https://doi.org/10.1007/s10230-016-0417-1

Skousen, J.G., Ziemkiewicz, P.F. and McDonald, L.M. (2019) 'Acid mine drainage formation, control and treatment: Approaches and strategies', The Extractive Industries and Society, 6(1), pp. 241–249. Available at: https://doi.org/10.1016/j.exis.2018.09.008

Sluiter, A. et al. (2012) Determination of Structural Carbohydrates and Lignin in Biomass Laboratory Analytical Procedure (LAP). Technical NREL/TP-510-42618. NREL. Available at: https://www.nrel.gov/docs/gen/fy13/42618.pdf (Accessed: 3 July 2024).

Smith, J. et al. (2022) 'Critical evaluation of the chemical composition of acid mine drainage for the development of statistical correlations linking electrical conductivity with acid mine drainage concentrations', Environmental Advances, 8, p. 100241. Available at: https://doi.org/10.1016/j.envadv.2022.100241

Smith, J. et al. (2023) 'The Development of a Sample Preparation Technique for the Analysis of Trace Elements in Mine Impacted Waters containing High Levels of Iron', in IMWA 2023 Y DYFODOL | THE FUTURE. Newport, Wales, UK, (International Mine Water Association): IMWA, pp. 484–490. Available at: https://www.imwa.info/docs/imwa_2023/IMWA2023_Smith_484.pdf (Accessed: 23 January 2025).

Smith, K.S. (2007) 'Strategies to predict metal mobility in surficial mining environments', in DeGraff, J. V., Understanding and Responding to Hazardous Substances at Mine Sites in the Western United States. Geological Society of America. Available at: https://doi.org/10.1130/2007.4017(03)

Strambo, C., Button, J. and Atteridge, A. (2019) The end of coal? Planning a "just transition" in South Africa, SEI report. Stockholm Environment Institute. Available at: https://www.sei.org/wp-content/uploads/2019/02/planning-a-just-transition-in-south-africa.pdf (Accessed: 19 January 2025).

Struckmeier, W. and Richts, A. (2006) 'WHYMAP and the World Map of Transboundary Aquifer Systems at the scale of 1 : 50 000 000 (Special Edition for the 4th World Water Forum, Mexico City, March 2006)', Episodes, 29(4), pp. 274–278. Available at: https://doi.org/10.18814/epiiugs/2006/v29i4/005

Sun, J., Zhang, L. and Loh, K.-C. (2021) 'Review and perspectives of enhanced volatile fatty acids production from acidogenic fermentation of lignocellulosic biomass wastes', Bioresources and Bioprocessing, 8(1), p. 68. Available at: https://doi.org/10.1186/s40643-021-00420-3

The World Bank Group (2021) Climate Risk Profile: South Africa. Available at: https://climateknowledgeportal.worldbank.org/sites/default/files/country-profiles/15932-WB_South%20Africa%20Country%20Profile-WEB.pdf (Accessed: 23 September 2024).

Thomas, G., Sheridan, C. and Holm, P.E. (2023) 'Arsenic contamination and rare earth element composition of acid mine drainage impacted soils from South Africa', Minerals Engineering, 203, p. 108288. Available at: https://doi.org/10.1016/j.mineng.2023.108288

Tong, Z., Cheng, N. and Pullammanappallil, P. (2013) 'Pretreatment of lignocellulosic biomass for biofuels and bioproducts. Dep Agric Biol Eng Univ Florida', AE 495, pp. 1–4.

Tuffnell, S. (2017) 'Acid drainage: the global environmental crisis you've never heard of', The Conversation UK. Available at: https://theconversation.com/acid-drainage-the-global-environmental-crisis-youve-never-heard-of-83515 (Accessed: 19 January 2025).

Turton, A (2008) 'Three strategic water quality challenges that decision-makers need to know about and how the CSIR should respond', in. Science real and relevant: 2nd CSIR Biennial Conference, CSIR International Convention Centre Pretoria, p. 28. Available at: https://researchspace.csir.co.za/dspace/handle/10204/2620

Van Rooyen, M., Van Staden, P.J. and Du Preez, K.A. (2021) 'Sulphate removal technologies for the treatment of mine-impacted water', Journal of the Southern African Institute of Mining and Metallurgy, 121(10), pp. 1–7. Available at: https://doi.org/10.17159/2411-9717/1541/2021

Wagner, N.J. and Hlatshwayo, B. (2005) 'The occurrence of potentially hazardous trace elements in five Highveld coals, South Africa. International Journal of Coal Geology, 63(3-4), pp.228-246.', International Journal of Coal Geology, (63(3–4)), pp. 228–246.

Wang, Y. et al. (2024) 'Composition of Lignocellulose Hydrolysate in Different Biorefinery Strategies: Nutrients and Inhibitors', Molecules, 29(10), p. 2275. Available at: https://doi.org/10.3390/molecules29102275

Watling, R.J. and Watling, H.R. (1982) 'Metal concentrations in some South African coals.', S.Afr. J. Sci.; (South Africa), 78(4), pp. 164–166.

Westensee, D.K. et al. (2018) 'The availability of second-generation feedstocks for the treatment of acid mine drainage and to improve South Africa's bio-based economy', Science of The Total Environment, 637–638, pp. 132–136. Available at: https://doi.org/10.1016/j.scitotenv.2018.04.410

Willis, J.P. (1983) 'Trace-element studies on South African coals and fly ash', in International congress on applied mineralogy, Johannesburg (South Africa)., 23-30 Jun 1981.

Woodford, A., Rosewarne, P. and Girman, J. (2006) '"How much groundwater does South Africa have?" Internal discussion document.' SRK. Available at: http://www.srk.co.za/files/File/newsletters/groundwater/PDFs/1_A_Woodford.pdf

WRC (2009) 'Transboundary waters: We all live downstream'. Water Research Council Organisation. Available at: https://www.wrc.org.za/wp-content/uploads/mdocs/WW_09_mar-apr_14_kidz_p_36-37.pdf (Accessed: 16 November 2024).

WWF-SA (2013) Defining South Africa's Water Source Areas. Cape Town, south Africa. Available at: https://www.wwf.org.za/?9321/Defining-South-Africas-Water-Source-Areas (Accessed: 26 February 2024).

WWF-SA (2016) Water: Facts & Futures. Cape Town South Africa. Available at: http://awsassets.wwf.org.za/downloads/wwf009_waterfactsandfutures_report_web__lowres_.pdf (Accessed: 4 March 2024).

Zagury, G.J., Kulnieks, V.I. and Neculita, C.M. (2006) 'Characterization and reactivity assessment of organic substrates for sulphate-reducing bacteria in acid mine drainage treatment', Chemosphere, 64(6), pp. 944–954. Available at: https://doi.org/10.1016/j.chemosphere.2006.01.001

Zhang, M. and Wang, H. (2014) 'Organic wastes as carbon sources to promote sulfate reducing bacterial activity for biological remediation of acid mine drainage', Minerals Engineering, 69, pp. 81–90. Available at: https://doi.org/10.1016/j.mineng.2014.07.010

Zhang, X. et al. (2023) 'Selective separation of metals from wastewater using sulfide precipitation: A critical review in agents, operational factors and particle aggregation', Journal of Environmental Management, 344, p. 118462. Available at: https://doi.org/10.1016/j.jenvman.2023.118462

Zhang, Zhao et al. (2022) 'A review of sulfate-reducing bacteria: Metabolism, influencing factors and application in wastewater treatment', Journal of Cleaner Production, 376, p. 134109. Available at: https://doi.org/10.1016/j.jclepro.2022.134109

Zhou, L. et al. (2021) 'Assimilatory and dissimilatory sulfate reduction in the bacterial diversity of biofoulant from a full-scale biofilm-membrane bioreactor for textile wastewater treatment', Science of The Total Environment, 772, p. 145464. Available at: https://doi.org/10.1016/j.scitotenv.2021.145464

Zhou, S. et al. (2022) 'A novel steady-state model to quantitively assess the effect of pH elevation by dissimilatory sulfate reduction process in acidic waters in mining areas', Water Research, 222, p. 118852. Available at: https://doi.org/10.1016/j.watres.2022.118852

CHAPTER 3.

3 Seasonal characterisation of acid mine drainage in Mpumalanga coalfields region

(Presented at South African Chemical Engineering Congress (SACEC) (Virtual)
Smith, J., Sheridan, C.M., Van Dyk, L.D., Harding, K.G., 2021. Seasonal characterisation of acid mine drainage in Mpumalanga coalfields region. Presented at the South African Chemical Engineering Congress (SACEC), Virtual, p. 118.

This chapter addresses objective (a): To characterise and critically evaluate the physical and chemical composition of Acid Mine Drainage (AMD) sourced from coal mining operations in the Mpumalanga region, South Africa and determine geographical and temporal variability.

The characterisation of AMD, and the experimental characterisation of the physical (pH, electrical conductivity (EC), turbidity (NTU), total dissolved solids (TDS), total suspended solids (TSS)), and chemical parameters (total acidity (TA), dissolved metals, (calcium (Ca^{2+}), magnesium (Mg^{2+}), sodium (Na^{+}), potassium (K^{+}), and dissolved sulfur (S), of two different AMD sources, collected from separate dams in the Mpumalanga coalfields, South Africa, is discussed. This is Followed by analyses demonstrating the spatial and temporal (over 12 months) nature of AMD. The elemental concentrations contained in the selected AMD dams were evaluated for compliance with the Department of Water Affairs (DWAF) general discharge limits set for Sections 21 (f), relating to the "discharge of waste or wastewater directly into a water resource" and (h), relating to the "disposal of water containing waste, or which has been heated in, any industrial or power generation process;" (DWAF, 2013)[*], and the South African National Standard (SANS) 241:2015[†] drinking water limits. The limitations to passive remediation systems relating to elevated concentrations of Mn, Zn, and Cd; and to active remediation systems relating to elevated concentrations of copper Cu, Sn, Pb, and Al were considered. Temporal trends in physio-chemical variables were noted, and changes in concentration owing to seasonal variability were highlighted.

CRediTs: Janet Smith: Conceptualization, Methodology, Investigation, Validation, Formal analysis, writing-Original Draft; Craig Sheridan: Funding acquisition, Conceptualization, Resources, Supervision, Writing – Review and editing; Lizelle van Dyk: Conceptualization, Supervision, Writing – Review and Editing; Kevin Harding: Conceptualization, Supervision, Writing – Review and Editing

[*] DWAF (2013) 'Department of Water Affairs and Forestry, Government Notice 665 in Government Gazette 36820, Revision of General Authorisations in Terms of Section 39 of The National Water Act, 1998 (Act No. 36 of 1998), DWAF general discharge limits set for Sections 21 (f) and (h)

[†] South African National Standard (2015) 'South African National Standard (SANS). 241-1: 2015 Drinking Water, Part 1: Microbiological, Physical, Aesthetic and Chemical Determinants. 241-2: 2015 Drinking Water, Part 2: Application of SANS 241-1.'

3.1 Abstract

In South Africa, sulfide is a large component of many of the natural ore bodies, in particular coal and gold ores. This results in large-scale problems such as acid mine drainage (AMD). AMD run-off or decant can corrode infrastructure and, if allowed to flow unchecked, will infiltrate ground and surface water bodies causing severe negative impacts on the surrounding environment. Sustainable, cost-effective treatment processes could mitigate such AMD problems. However, prior to designing treatment processes, the nature of the problem needs to be comprehensively quantified. In this study, the physical and chemical characteristics of AMD, emanating from two coal sites in Mpumalanga, are described and the ramifications of these properties, for the design of treatment processes, are discussed. The concentrations of total dissolved solids, total acidity, and dissolved iron varied by an order of magnitude between the sites. Reduced rainfall volumes were recorded during the winter months, and seasonal variability of AMD waters was shown in instances where reduced and increased concentrations coincided with increased and reduced rainfall volumes, respectively. Significant concentrations of aluminium, manganese and zinc could impact the effectiveness of active and passive treatment systems and should be considered in the design of a suitable treatment system.

Keywords: acid mine drainage (AMD), composition, correlation, regression

3.2 Introduction

Gold and coal mining activities in South Africa result in the formation of large quantities of acid mine drainage (AMD) (McCarthy, 2011). Given the immediacy of the decant issues, considerable attention has been given to AMD in the Western and Central Basins. A total of 126 coal mine operations have been identified in South Africa (DMR, 2017). Decant from coal mining sites in the Witbank–Middelburg area has historically flowed into the tributaries of the Olifants River causing significant increases in the salinity and sulfate levels of nearby dams, thus deleteriously affecting the quality of local water.

Mining operators are under a legal obligation to adhere to increasingly stringent environmental compliance regulations, as stipulated in their water use licenses. Strictly regulated industrial water discharge limits imposed to prevent environmental damage, compounded with a growing demand for a limited water supply, necessitate consideration of treatment options to ensure sustained quality of receiving water bodies into the future and to facilitate the reuse of water. Development of sustainable, cost-effective AMD treatment processes would mitigate potential environmental damage that could result from decant of AMD water and facilitate the re-use of discharge water. The 2010 Inter-Ministerial Committee on AMD report recognized that ingress prevention and decant control would not limit the production of AMD and that treatment would still be required, and that the variability of water quality between the different basins would necessitate the use of different treatment technologies (Expert Team of the Inter-Ministerial Committee, 2010). Given the high density of coal fields in Mpumalanga, this research aims to facilitate the design of an appropriate

treatment process for the AMD in this region. The aim of this work was to quantify seasonal physico-chemical parameters of AMD produced by a coal operation in Mpumalanga.

3.3 Experimental Procedure

3.3.1 Sampling Procedure

Grab samples were taken from two AMD dams in the Mpumalanga coalfield region at monthly intervals during 2018 and in April 2019. Sample volumes of between 1 – 2.5 L were collected in glass or polypropylene containers. A 50 mL portion of filtered sample, and a 50 mL portion of unfiltered sample were preserved with acid to a pH of less than 2 using 1:1 ultrapure nitric acid, and the remaining sample was stored in a refrigerator at 4 °C. A total of 13 sampling events occurred for Site 1, while six took place for Site 2.

3.3.2 Analytical Methods

A range of physical and chemical parameters were analysed and the instrumentation and methodology used are as follows:

- pH: Ohaus Starter 3100 combined pH and mV meter and a ST310 pH electrode.
- Redox Potential (Eh): Ohaus Starter 3100 combined pH and mV meter and a STORP redox probe and a STREF 2 (saturated calomel) reference electrode. Eh values are reported relative to the standard hydrogen electrode (SHE) (Bednar et al., 2005).
- Electrical Conductivity (EC): Ohaus Starter 3100C conductivity meter and STCON3 electrode.
- Turbidity (NTU): HACH 2100N turbidimeter. Data are reported in Nephelometric Turbidity Units.
- Total dissolved solids (TDS): Gravimetric determination after filtration using a glass fibre (GF) filter, followed by drying of the filtrate to constant mass at 180 ºC (EPA Method 160.1).
- Total suspended solids (TSS): Gravimetric determination after filtration through a GF filter and drying of the retained solids to constant mass at 103–105 ºC (EPA Method 160.2).
- Total acidity (TA): Potentiometric titration to pH 8.3 using 1.0 M NaOH.
- Major cations, sulfur and dissolved metals: Inductively coupled plasma–optical emission spectrometry (ICP–OES) and inductively coupled plasma-mass spectrometry (ICP–MS).
- Sulfate concentrations calculated from sulfur (S), assuming that all S was present as sulfate, and total ion (TI) concentrations were calculated by summing the individual cation and sulfate concentrations. Calcium and magnesium hardness were calculated by converting the elemental calcium and magnesium concentrations to the carbonate form.

3.3.3 Results and Discussion

3.3.3.1 Physical and Chemical Characteristics

The data for the physical parameters, as measured between 2018 and April 2019 for AMD Sites 1 and 2 in Mpumalanga are presented in Tables 3.1 and 3.2, respectively. These data were compared against the general discharge limits specified by the Department of Water Affairs and Forestry (DWAF, 2013). The general discharge limits indicated an acceptable pH range between pH 5.5-9.5, an EC of 70 mS/m above the intake to a maximum EC of 150 mS/m, and a maximum TSS concentration of 25 mg/L. The remaining parameters are not controlled.

Table 3.1 Physical and chemical parameters as measured for Site 1 in Mpumalanga

Date	pH at 25 °C	Eh mV SHE at 25 °C	EC mS/m at 25 °C	NTU	TDS mg/L at 180 °C	TSS mg/L at 180 °C	TA mg/L $CaCO_3$ at pH 8.3	Total Ions mg/L
SITE 1								
2018-02-01	2.94	642	3 460	19	19 640	63	10 500	18 575
2018-02-26	2.87	620	3 685	24	21 130	86	11 200	30 700
2018-03-26	2.57	682	2 335	3	12 015	29	5 760	9 720
2018-05-02	2.16	887	3 750	11	21 340	1	12 600	22 845
2018-05-31	2.87	632	3 725	241	23 180	321	10 700	20 895
2018-06-25	2.90	626	3 780	201	23 920	58	11 100	21 410
2018-08-02	2.49	689	3 940	123	23 950	55	11 700	18 900
2018-08-14	2.86	611	3 865	95	25 150	60	11 800	19 135
2018-09-04	2.99	621	3 985	413	19 575	100	11 900	19 515
2018-10-17	2.73	688	2 650	161	12 850	250	6 050	9 765
2018-11-22	2.84	628	3 790	29	23 830	21	11 100	17 250
2018-12-13	2.69	622	3 990	337	23 565	109	11 000	17 570
2019-04-04	2.64	640	3 705	241	26 635	110	11 100	17 200

Table 3.2 Physical and Chemical parameters as measured for Site 2 in Mpumalanga

Date	pH at 25 °C	Eh mV SHE at 25 °C	EC mS/m at 25 °C	NTU	TDS mg/L at 180 °C	TSS mg/L at 180 °C	TA mg/L $CaCO_3$ at pH 8.3	Total Ions mg/L
SITE 2								
2018-02-01	2.92	752	1090	20	5 820	62	1 480	6 028
2018-02-26	2.87	795	1465	408	9 175	199	2 160	7 346
2018-05-10	2.85	821	1055	205	6 680	80	1 260	6 035
2018-05-31	2.72	816	1720	99	9 900	52	3 440	8 462
2018-08-02	2.54	850	1935	248	10 700	170	3 673	7 646
2019-04-04	7.02	349	727	389	4 525	92	—	3 248

With the exception of the April 2019 sample from Site 2, pH values were acidic and reported pH values ranged between 2 – 3 which fell outside of the pH 5.5 DWAF lower general limit for discharge of wastewater into a water resource (DWAF, 2013). Although similar pH values were recorded for both sites, TA concentrations for Site 1 were an order of magnitude higher than those for Site 2. The acidity of water is defined as its capacity to neutralise a strong base to a predetermined pH and comprises the free protons and undissociated acids, *i.e.,* strong, and weak acids as well as hydrolysable salts in a solution (Cook et al., 2000, Larson and Henley, 1955, Loftus, 2003). The higher TA concentrations for Site 1 would be indicative of the presence of increased concentrations of hydrolysable salts which was corroborated by the elevated EC measurements for Site 1 samples compared with those of Site 2. EC is a measure of the ability of water to conduct electric current and is dependent on the concentration of free ions in the water. All conductivities were significantly in excess of DWAF maximum general wastewater limit of 150 mS/m. The majority of TSS concentrations were in excess of the 25 mg/L DWAF general limit for discharge (DWAF, 2013). The pH and Eh values generally showed an inverse relationship and a lower average Eh of 661 mV was recorded for Site 1 compared with a more electropositive average of 801 mV for Site 2. The different Eh values could be as a result of differing concentrations of oxygen, pyrite, other metals and organic matter present in the rock (Johnson et al., 2012, Tutu et al., 2008). Gravimetrically determined TDS concentrations compared well against calculated TDS values, which were determined by multiplying the EC readings by 6.5, returning Pearson's correlations of 0.88 and 0.98 for Sites 1 and 2, respectively, at a 95 % confidence level (Rusydi, Wolkersdorfer and Hubert, 2015). This indicated a statistically significant relationship and analytical robustness between the TDS and EC data. The stronger correlation achieved between EC and TDS for Site 2 is probably due to the lower ion concentrations present in this AMD water. The gravimetrically determined TDS, the sum of the total ions and the calculated TDS from EC data generally followed similar trends for the duration of the sampling period. For most sampling events, significantly larger variations were noted between the calculated TDS and total ion concentrations compared with the differences between the calculated TDS and the gravimetrically determined TDS for both sites. This could have been as a result of the complex chemistry of AMD waters and

possible removal of contributory ions from solution by adsorption and precipitation resulting in under reporting of the contributary ion concentrations.

3.3.3.2 Major Cations and Anions

The cations calcium (Ca^{2+}), magnesium (Mg^{2+}), sodium (Na^{+}), potassium (K^{+}) and anion sulfur (S) data are presented in Table 3.3. Where specified, the Target Water Quality Range (TWQR) concentrations advised by the Department of Water Affairs (DWAF), and the South African National Drinking Water Standard (SANS 241:2015) regulatory limits are given (DWAF, 1996, SABS, 2015a).

Table 3.3 Site 1 and 2 data – major cations and anions

Date	Ca^{2+} mg/L	Ca Hardness mg/L as $CaCO_3$	Mg^{2+} mg/L	Mg Hardness mg/L as $CaCO_3$	Total Ca & Mg Hardness mg/L as $CaCO_3$	Na^{+} mg/L	K^{+} mg/L	S mg/L
Site 1								
2018-02-01	398	993	375	1 545	2 535	34	6.5	4345
2018-02-26	752	1 880	725	2 990	4 865	<1	18	6845
2018-03-26	310	775	201	827	1 600	20	4.0	2350
2018-05-02	462	1 155	428	1 760	2 915	36	10	5345
2018-05-31	440	1 100	410	1 690	2 790	39	10	4850
2018-06-25	439	1 095	405	1 670	2 765	44	11	4940
2018-08-02	446	1 115	396	1 630	2 745	58	3.2	4515
2018-08-14	433	1 080	349	1 440	2 520	58	13	4455
2018-09-04	437	1 090	365	1 505	2 595	58	14	4545
2018-10-17	324	809	209	860	1 670	35	3.3	2385
2018-11-22	409	1 020	338	1 395	2 415	71	12	4075
2018-12-13	418	1 045	348	1 435	2 475	76	15	4140
2019-04-04	429	1 070	314	1 290	2 365	56	12	4060
Site 2								
2018-02-01	655	1 635	375	1 545	3 180	34	5.6	1 525
2018-02-26	811	2 024	397	1 635	3 660	0.63	6.3	1 840
2018-05-10	633	1 581	333	1 370	2 950	39	13	1 545
2018-05-31	568	1 417	286	1 175	2 595	58	2.9	2 135
2018-08-02	447	1 117	315	1 295	2 415	58	3.9	1 980
2019-04-04	448	1 119	239	985	2 105	42	17	824
DWAF 1996 TWQR	32	—	30	—	—	100	50	—
SANS 241:2015	—	—	—	—	—	200	—	167

The hardness of water is a measure of its capacity to react with soap. Water is classified as “very hard” if the total hardness exceeds 180 mg/L (Kamble, 2014, WHO, 2009); thus, as the Ca and Mg hardness contributions to total hardness are in excess of this concentration, the AMD waters from both sites are classified as very hard. Site 1 had a higher Mg hardness contribution (58 % average) than Ca hardness contribution to total hardness, while Site 2 showed a marginally higher Ca hardness contribution to total hardness (52 % average). The World Health Organisation Guidelines for drinking water indicate the probability of scum and calcium carbonate scale formation in waters with hardness values greater than 200 mg/L, while waters with a hardness values below 100 mg/L could cause corrosion of water pipes owing to decreased buffering capacity (WHO, 2017). Ca^{2+} and Mg^{+} concentrations were in excess of the target water quality range (TWQR) specified in the 1996 DWAF Water Quality Guidelines for Domestic use, while Na^{+} and K^{+} concentrations were below the specified TWQR (DWAF, 1996). The SANS: 241:2015 regulatory acute health limits for sulfate are given as 500 mg/L, which equates to 167 mg/L as S. Assuming all S is in the form of sulfate, the high concentrations reported would render that these waters are in excess of standard limits (SABS, 2015b).

3.3.3.3 Metals

A total of 60 elements were analysed for the first sampling event to determine which were present in significant concentration. For the purposes of this paper, the discussion is limited to the dissolved metals results for the following elements: Fe, as a major metal contributor to AMD; arsenic (As), mercury (Hg), molybdenum (Mo), selenium (Se), and nickel (Ni) because of their noted presence in Witbank Coalfield 4 seam (Bergh, 2009); Mn, Zn, and cadmium (Cd), owing to the difficulty in removing these elements by adsorption; copper (Cu), tin (Sn), lead (Pb), and Al, because of the amphoteric nature of their hydroxides (Gazea et al., 1996, Fu and Wang, 2011). Data are presented in Table 3.4, together with the respective DWAF general discharge limits set for Sections 21 (f) and (h) and South African National Standard (SANS) 241:2015 regulatory limits (DWAF, 2013, SABS, 2015b). Mo, As and Se data were not included as these elements were not detected, and Hg was also omitted as all concentrations were below the 0.005 mg/L legislated limit. Where analysed, most Cd concentrations exceeded legislative limits and all except for two samples from Site 2 exceeded discharge limits; three of the six Pb concentrations for Site 2 were below limits, while all Site 1 concentrations, except for one sample, were at the 0.01 mg/L limit or higher. All Cu, Ni, Mn, and Site 1, Zn concentrations were in excess of legislated concentration limits, with Mn followed by Zn present in noticeably higher concentrations. Fe was significantly in excess of legislated limits. No general discharge limits are available for Al and Ni, and these data were compared against the SANS 241:2015 regulatory limits, where they were found to be in excess of prescribed limits (SABS, 2015b). Al was present in significant concentrations. No guidelines were available for Sn, which, when detected, was present only in very low concentrations.

Table 3.4 Dissolved Metals Concentrations

Date	Al mg/L	Cd mg/L	Cu mg/L	Fe mg/L	Mn mg/L	Ni mg/L	Pb mg/L	Sn mg/L	Zn mg/L
Site 1									
2018-02-01	365	0.02	0.07	4210	97	1.1	0.02	0.001	7.8
2018-02-26	518	—	—	7950	133	1.3	0.43	—	13
2018-03-26	222	—	—	1825	50	0.79	0.07	—	7.4
2018-05-02	354	0.02	0.34	5390	86	0.85	0.02	0.001	9.3
2018-05-31	371	0.02	0.26	4950	78	0.89	0.03	0.003	8.5
2018-06-25	373	0.01	0.09	5185	82	0.83	0.003	0.001	9.0
2018-08-02	442	—	0.08	3770	153	1.6	0.01	0.001	9.2
2018-08-14	300	—	0.02	4475	84	0.90	0.02	0.001	8.3
2018-09-04	259	—	0.02	4600	88	0.80	0.02	<0.0001	7.7
2018-10-17	191	—	0.06	1735	71	0.66	0.006	<0.0001	4.5
2018-11-22	206	—	0.02	3860	76	0.65	0.01	<0.0001	6.4
2018-12-13	193	—	0.02	3975	78	0.62	0.01	<0.0001	6.3
2019-04-04	213	—	0.04	3875	68	0.57	0.01	<0.0001	5.0
Site 2									
2018-02-01	157	0.010	0.10	160	44	1.3	0.02	0.005	3.1
2018-02-26	162	< 0.003	0.08	376	51	1.1	0.12	—	3.6
2018-05-10	126	0.007	0.13	199	35	1.2	0.005	0.004	2.5
2018-05-31	230	0.010	0.15	828	52	0.90	0.03	0.006	4.1
2018-08-02	144	0.004	0.09	646	58	0.92	0.006	0.001	3.3
2019-04-04	0.04	0.003	0.04	4.2	17	0.31	0.005	0.0002	0.44
DWAF 2013 general discharge limit	—	0.005	0.01	0.3	0.1	—	0.01	—	0.1
SANS 241:2015	<0.3	<0.003	—	<2	<0.1	<0.07	<0.01	—	<5

- = not determined

3.3.3.4 Significant Trends

Total acidity, EC, and dissolved Al, Fe and S concentrations showed similar trends over the time, while rainfall volumes showed an inverse trend. As shown in Figure 3.3, increased concentrations for the geochemical parameters measured at Site 1 were observed for the February sampling event which might have resulted from the reduced rainfall volumes from the previous month. The significant decrease in the concentrations observed for the March 2018 sampling event could be as a result of dilution effects caused by substantial

rainfall that occurred immediately prior to this sampling event. Monthly rainfall data for the area, indicated a substantial increase in rainfall volume compared with the previous month (WorldWeatherOnline, 2019). Similarly, lower concentrations recorded for the October 2018 sampling event coincided with a significant increase in recorded rainfall volume. Lower rainfall was recorded for November 2018 and the concentrations increased to approach previously recorded levels. Site 1 showed no reduction in geochemical parameter concentrations in December 2018 despite the significant rainfall recorded for that month, this is probably because the rainfall only occurred in the latter half of the month, after sampling had taken place. High rainfall was recorded for January and February 2019, but rainfall volumes decreased significantly in March, which might explain why the concentrations for Site 1 samples did not reflect any significant dilution effect from the concentrations recorded in December.

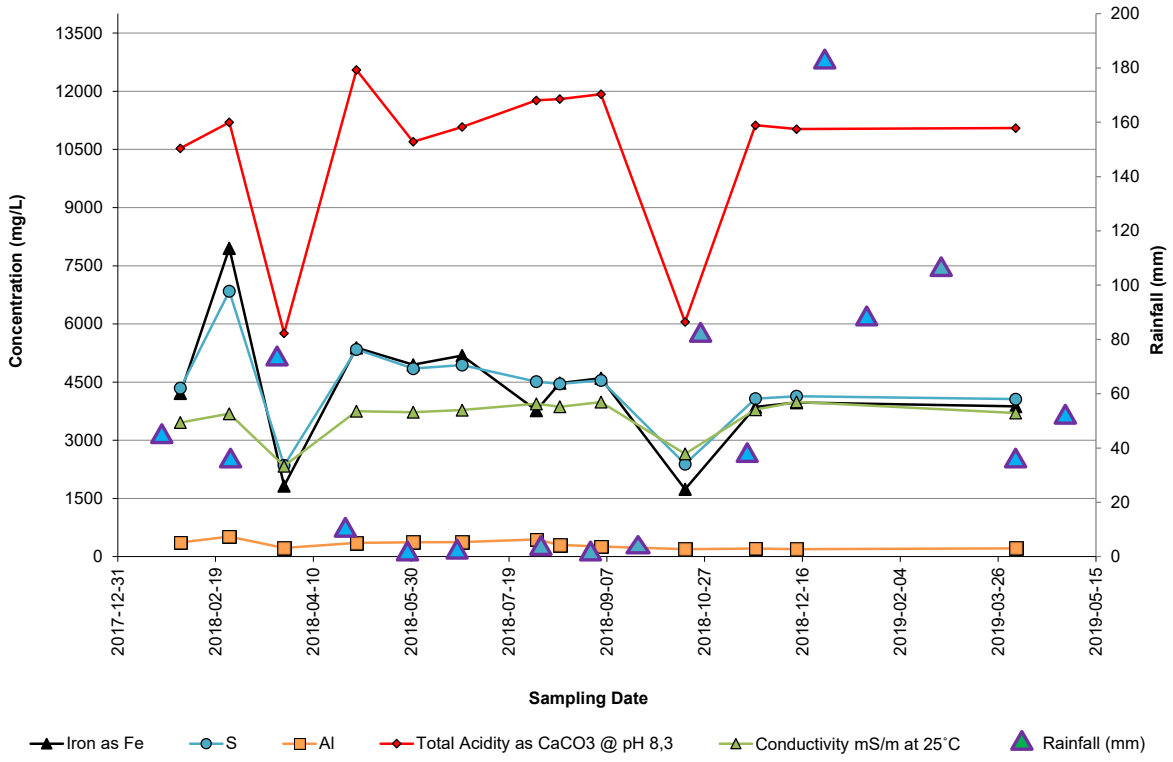


Figure 3.1 Variation in rainfall and total acidity, electrical conductivity, and dissolved aluminium (Al), iron (Fe), and sulfur (S) concentrations for Site 1 over the sampling period.

Site 2 sample concentrations showed an increase in February, which could be as a result of reduced rainfall levels from the previous sampling period. This was followed by a decrease in concentrations in April, probably as a result of the increased rainfall volumes over that period. Concentrations showed a significant increase at the end of May, which could be caused by net evaporation and dry climatic conditions during that time. Significantly reduced concentrations were recorded for the March 2019 sampling event, and the sample was no longer acidic. The increased rainfall recorded from October 2018 to March 2019 could have provided sufficient dilution for natural remediation given the lower ion concentrations present in the Site 2 AMD,

although remediation could also have been as a result of the effectiveness of ongoing remediation processes that were implemented at this site. These trends are shown in Figure 3.2.

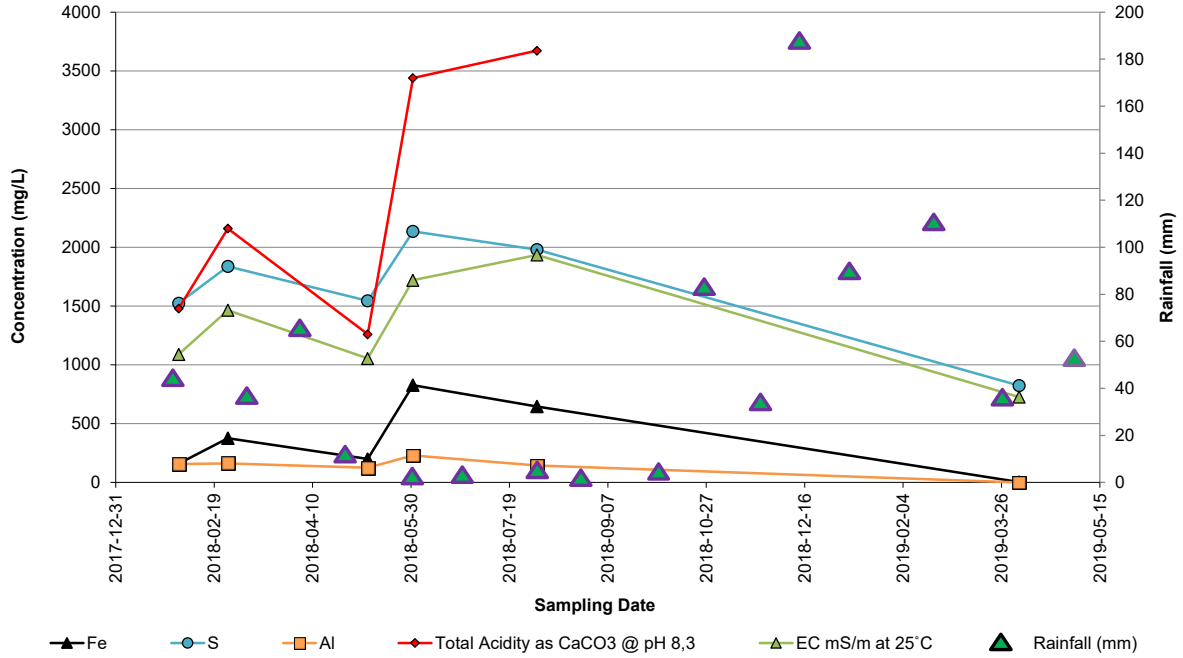


Figure 3.2 Variation in rainfall and total acidity, electrical conductivity, and dissolved aluminium (Al), iron (Fe), and sulfur (S) concentrations for Site 2 over the sampling period

3.4 Conclusions

Characterisation of Mpumalanga coalfield AMD showed that there was significant variation in the physical and chemical parameters of these waters. Total acidity, dissolved Fe and TDS concentrations varied by an order of magnitude between sites, and concentrations differed between sampling events. Reduced rainfall volumes were recorded in the winter months which coincided with increased concentrations, thus confirming the seasonal variability of AMD, which could, in turn, upset passive system dynamics. Pb, Cu, Mn, Zn, Al, S, Fe, Ni, and some Cd concentrations were in excess of legislative limits with Fe, and S present in very high, and Al, Mn, and Zn present in significant concentrations. Removal of Mn and Zn would not support passive treatment systems owing to their difficulty of removal by adsorption, whilst high concentrations of Al, given the amphoteric nature of aluminium hydroxides, would limit the effectiveness of active treatment systems. These factors should be accounted for when designing a suitable treatment system. More importantly, if a treatment process were required to switch between different AMD streams, cognizance must be taken of the extent of variability and should be built into the design. A strong correlation was observed between electrical conductivity and total dissolved solids, indicating analytical robustness between these parameters. Since total acidity, dissolved aluminium, iron, and sulfur showed similar trends over time, potential correlations that might exist between these parameters should be investigated.

3.5 References

Bergh, J. 2009. Trace Element partitioning in the Witbank Coalfield 4 seam. Paper: Fossil Fuel Foundation Indaba, 11-12.

Cook, F. J., Hicks, W., Gardner, E. A., Carlin, G. D. & Froggatt, D. W. 2000. Export of Acidity in Drainage Water from Acid Sulphate Soils. Marine Pollution Bulletin, 41(7-12), pp.319-326.

DMR. 2017. Operating Mines in Mpumalanga [Online]. Department of Mineral Resources of South Africa https://www.dmr.gov.za/mineral-policy-promotion/operating-mines/mpumalanga [Accessed 6 January 2020].

DWAF 1996. Department of Water Affairs and Forestry, 1996. South African Water Quality Guidelines (second edition). Volume 1: Domestic Use.

DWAF 2013. Department of Water Affairs and Forestry, Government Notice 665 in Government Gazette 36820, REVISION OF GENERAL AUTHORISATIONS IN TERMS OF SECTION 39 OF THE NATIONAL WATER ACT, 1998 (ACT NO. 36 OF 1998), DWAF general discharge limits set for Sections 21 (f) and (h).

Expert Team of the Inter-Ministerial Committee, D. 2010. Mine water management in the Witwatersrand Gold Fields with special emphasis on acid mine drainage. Report to the Inter-Ministerial Committee on Acid Mine Drainage. Pretoria: Department of Water Affairs.

Fu, F. & Wang, Q. 2011. Removal of heavy metal ions from wastewaters: a review. Journal of environmental management, 92, 407-418.

Gazea, B., Adam, K. & Kontopoulos, A. 1996. A review of passive systems for the treatment of acid mine drainage. Minerals engineering, 9, 23-42.

Johnson, D. B., Kanao, T. & Hedrich, S. 2012. Redox transformations of iron at extremely low pH: fundamental and applied aspects. Frontiers in microbiology, 3, pp.96.

Kamble, R. 2014. Eccentric observation of total hardness in Lohara village, Chandrapur district, central India. International Journal of Environment, 3, pp.134-140.

Larson, T. E. & Henley, L. 1955. Determination of Low Alkalinity or Acidity in Water. Analytical Chemistry, 27, pp.851-852.

Loftus, T. 2003. An Informational Resource for Operators of Lagoon Systems, Acidity and Alkalinity

[Online]. Maine Lagoon Systems http://www.lagoonsonline.com/laboratory-articles/acid.htm

[Accessed 6 December 2019].

McCarthy, T. S. 2011. The impact of acid mine drainage in South Africa. South African Journal of Science, 107, pp.01-07.

Rusydi, A. F. 2018. Correlation between conductivity and total dissolved solid in various type of water: A review. IOP Conf Ser: Earth Environ Sci 118:012019.

SABS 2015a. South African National Drinking Water Standard (SANS) 241-1: 2015 Second ed.

SABS 2015b. South African National Drinking Water Standard (SANS) 241: 2015.

Tutu, H., McCarthy, T. & Cukrowska, E. 2008. The chemical characteristics of acid mine drainage with particular reference to sources, distribution and remediation: The Witwatersrand Basin, South Africa as a case study. Applied Geochemistry, 23, pp.3666-3684.

WHO 2009. Calcium and magnesium in drinking-water: public health significance, World Health Organization.

WHO 2017. Guidelines for drinking-water quality: fourth edition incorporating the first addendum. Geneva: World Health Organization; 2017. Licence: CC BY-NC-SA 3.0 IGO.

Wolkersdorfer, C. & Hubert, E. 2015. Establishing a Total Dissolved Solids: Electrical Conductivity Ratio for Mine Waters. Agreeing on solutions for more sustainable mine water management, pp.1-8.

WorldWeatherOnline. 2019. Witbank Monthly Climate Averages, Mpumalanga, ZA [Online]. World Weather Online. Available: https://www.worldweatheronline.com/witbank-weather-averages/mpumalanga/za.aspx [Accessed 21 August 2019].

CHAPTER 4.

4 Critical evaluation of the chemical composition of acid mine drainage for the development of statistical correlations linking electrical conductivity with acid mine drainage concentrations

(Published in Environmental Advances, 2022)
Smith, J., Sheridan, C.M., van Dyk, L.D., Harding, K.G., 2022. Critical evaluation of the chemical composition of acid mine drainage for the development of statistical correlations linking electrical conductivity with acid mine drainage concentrations, Environmental Advances, 8, p. 100241.
doi.org/10.1016/j.envadv.2022.100241

This chapter addresses the second component of objective (a): To characterise and critically evaluate the physical and chemical composition of Acid Mine Drainage (AMD) sourced from coal mining operations in the Mpumalanga region, South Africa and determine geographical and temporal variability.

This work details an investigation of the significant correlations observed between certain parameters in AMD samples sourced from the Mpumalanga coalfields region, South Africa. A statistical evaluation of these data showing strong correlations between electrical conductivity (EC), total dissolved solids (TDS), total acidity (TA), dissolved iron (Fe), and dissolved sulfur (S) concentrations is presented. The chapter demonstrates that EC may be useful as a correlative tool for predicting these parameters. Additionally, the results indicate that the measurement of EC of AMD may potentially be used as a rapid screening proxy to test for compliance, prior to submission of samples for a more complete analysis allowing for rapid decision-making at sites with impacted water bodies.

CRediTs: Janet Smith: Conceptualization, Methodology, Project Management, Investigation, Formal analysis, Data Curation, Visualisation, Writing-Original Draft; Craig Sheridan: Conceptualization, Supervision, Funding, Writing – Review and editing; Lizelle van Dyk: Supervision, Writing – Review and Editing; Kevin Harding: Supervision, Writing – Review and Editing

AKNOWLEDGEMENTS
The authors would like to thank to Sasha Naidu and Sean Rossouw for their help with the water sampling, Dr Ansuyah Magan for her insight and technical contribution to the statistical analysis, Professor Kathryn Sole and Mr Stephen Batchelor for document review, technical, and language editing, and Stephen Smith for his assistance with the document format editing.

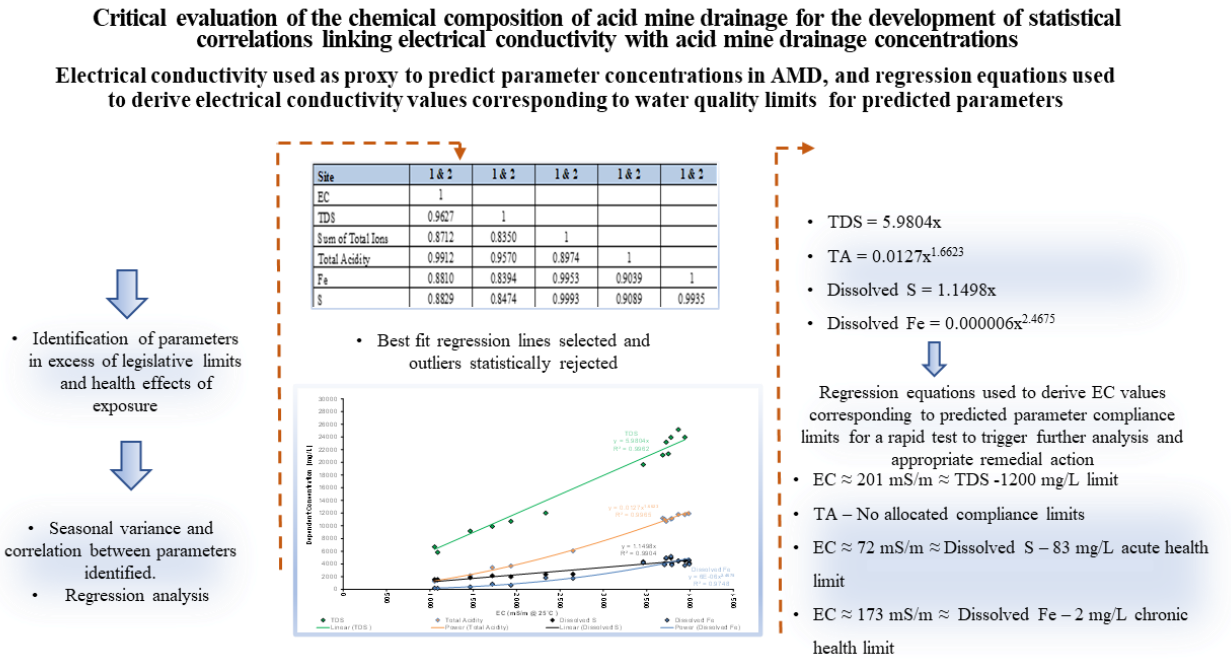


Figure 4.1 Visual Abstract: Critical evaluation of the chemical composition of acid mine drainage for the development of statistical correlations linking electrical conductivity with acid mine drainage concentrations

4.1 Abstract

The design an effective treatment processes for the remediation of acid mine drainage (AMD), requires an understanding of the composition of the AMD water. The pH and elemental composition of AMD waters are site specific and are dependent on the regional geology, and environmental factors. To establish the chemical and physical characteristics of two AMD sites located in the Mpumalanga coal mining region, South Africa, samples were taken between February 2018 to April 2019. These data were compared against regulatory legislation, and the potential health effects of exposure indicated. Strong correlations were noted between parameters and statistical evaluation demonstrated that electrical conductivity (EC) could be a useful correlative for prediction of total acidity, dissolved iron and sulfur concentrations in acidic AMD waters. From these findings, empirical correlations were used to derive regression equations which were used to derive the EC values corresponding to the respective water quality limits for TDS, dissolved iron and sulfur to provide a rapid method for testing compliance. Given the site specificity of AMD composition, this approach is intended as a proof of concept for the development of a methodology for adaption at other AMD sites. The regression equations should not be considered as universal to all AMD sites and EC should also not be used as a replacement for more complete chemical analysis.

Keywords: Physio-chemical composition, electrical conductivity, correlation, regression equations

4.2 Introduction

The uncontrolled decant of acid mine drainage (AMD) is one of the most pressing global environmental challenges facing gold and coal mining operations (Gazea et al., 1996, Geosciences, 2016, Simate and Ndlovu, 2014). Exposure of sulfide-bearing ores to oxygen and water results in the formation of AMD, which is characterised by low pH and comprises significantly elevated concentrations of iron and sulfate. The low pH promotes secondary reactions which could cause the dissolution of other trace metals in the AMD depending on the regional geology, temperature, pH, availability of micro-organisms, the presence of acid neutralising chemicals and oxygen and water availability. The overall reaction for the weathering of pyrite to form AMD is given in Equation 4.1 (Akcil and Koldas, 2006, Banks et al., 1997, Nordstrom et al., 2015, Simate and Ndlovu, 2014).

$$4FeS_2 + 15O_2 + 14H_2O \rightarrow 4Fe(OH)_3 \downarrow + 8SO_4^{2-} + 16H^+ \qquad \textit{Equation 4.1}$$

The pollution loads in surface waters, streams and rivers draining the Witwatersrand gold mining region were previously assessed and the impact of the spatial distribution, seasonality, and chemical processes of these AMD waters are well understood (Davidson, 2003, Marsden, 1986, Tutu et al., 2008). The South African Department of Minerals and Energy (DMR) website lists a total of 126 operating coal mines in the Mpumalanga region (DMR, 2017) (Figure 4.2).

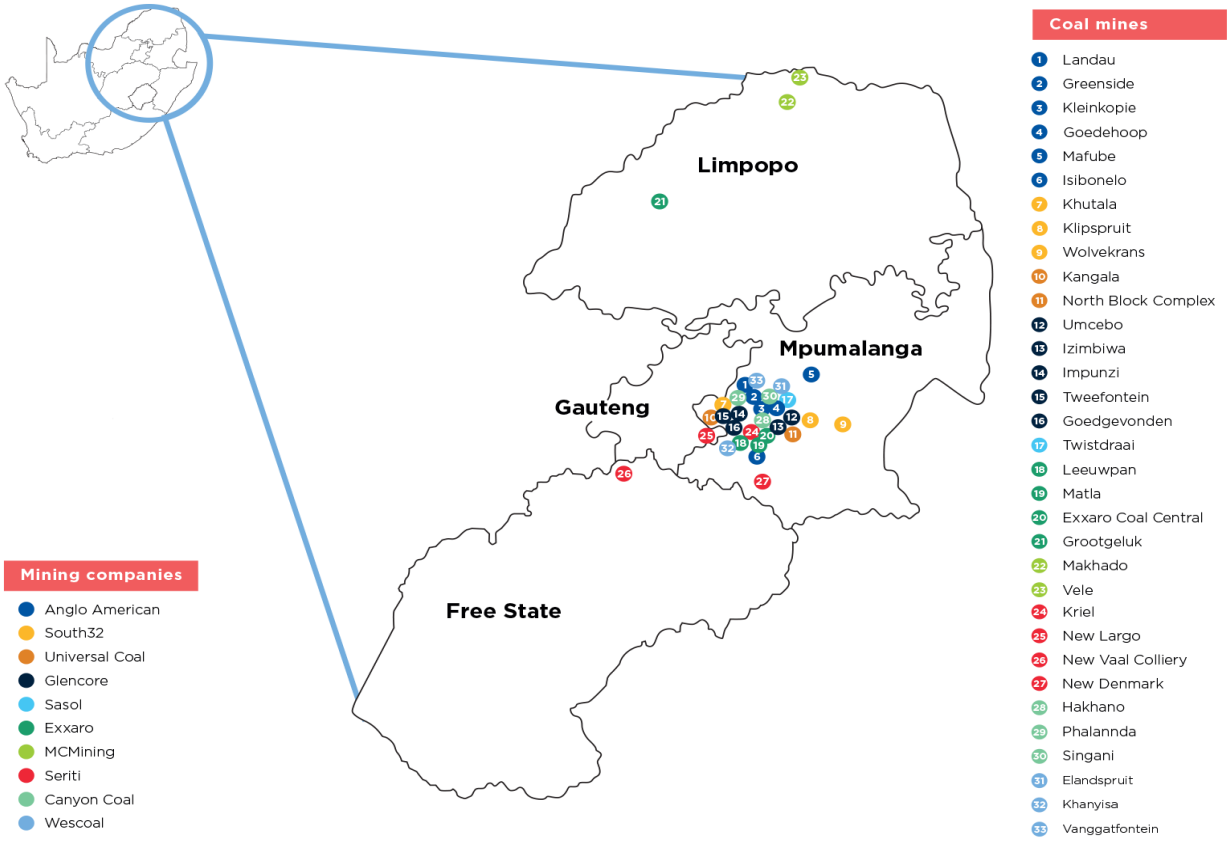


Figure 4.2 Location of coal mines in South Africa (MineralscouncilSouthAfrica, 2019)

The Witbank coalfield extends from Springs to Belfast in the upper Olifants catchment which is shown as Figure A1 in Appendix I-A of the supplementary material for Chapter 4. The Water Research Commission, (WRC) has considered the entire Olifants River Water Management area as highly stressed with limited opportunity for further water resource development (WRC, 2015). Decant from coal mining sites in the Witbank Middelburg area flows into tributaries of the Olifants River causing significant increases in the salinity and sulfate levels of nearby dams thus deleteriously affecting the quality of local watercourses (McCarthy, 2011). Furthermore, the coalfields in this area are classified as posing a significant AMD risk, which results in a medium to high mineralogical risk depending on the local surface water neutralisation capacity (WRC, 2015). Adding to these risks are the poor mine decommissioning efforts, which in the past, were characterised by insufficient closure planning and the underestimation of potential post-closure environmental liability.

Treatment of AMD would avert further pollution of local watercourses and also address historic liability issues. The re-use of AMD was an option proposed by the Honourable Nomvula Mokonyane for “Improving the water mix” in her budget vote speech in May 2015 (DWS, 2017). Design of adequate, robust remediation facilities requires an understanding of the chemical characteristics of the AMD waters and the extent to which

seasonal variation affects contaminants, and the re-use of remediated AMD for mining processes, crop irrigation, or domestic use would be dependent on the quality of water achieved.

With this in mind, two AMD sites in the Mpumalanga region were monitored to quantify seasonal physio-chemical parameters during 2018/2019. Smith et al. (2021) noted that increased rainfall volumes coincided with decreased parameter concentration thus confirming seasonal variability. As expected, total dissolved solids (TDS), and electrical conductivity (EC), ant total ion values were correlated (Smith et al., 2021). The focus of this present paper was to extend the comparison to include a correlation matrix for all parameters analysed and to apply statistical evaluation to evaluate the extent of the relationships between the variables.

4.3 Method

4.3.1 Sampling and Preservation

Approximately monthly sampling from two AMD dams between February 2018 and December 2018, with an additional sample taken in April 2019, resulted in a total of thirteen samples collected from Site 1, a receiving dam for AMD waste from local coal mines, and six samples from Site 2, a dam constructed to collect immediate operational runoff, in the Mpumalanga coalfields region, South Africa. Restricted access to site 2, limited more frequent sampling from this AMD dam. Surface water grab samples were collected in glass or polypropylene (PP) containers and transported back to the School of Chemical and Metallurgical Engineering at the University of the Witwatersrand, Johannesburg. As per the requirements of the American Public Health Association (APHA) Standard Methods for the Examination of Water and Wastewater, a 50 mL portion of each sample was filtered through a 0.45 µm filter and preserved with ultrapure nitric acid to achieve a pH of less than 2 for dissolved metals analysis (APHA, 2005). This, and the remaining samples, were stored at 4 °C. Except for inductively coupled plasma (ICP) analysis, all analyses were conducted at the School facilities. ICP analysis was subcontracted to various laboratories which included: The University of the Witwatersrand School of Chemistry (Wits Chem), De Bruyn Spectroscopic (DBS) and University of Johannesburg analytical department (UJ).

4.3.2 Analytical Methods

The analytical methods used, and the instrumentation models are given in Table 4.1.

Table 4.1 Methodology and/or instrumentation used for sample analysis

Parameter	Instrumentation
pH	Ohaus ST3-100 combined pH and mV meter and ST310 pH electrode with an integrated temperature probe.
Conductivity (EC)	Ohaus ST3-100C conductivity meter and STCON3 electrode.

Parameter	Instrumentation
Redox Potential (Eh)	Ohaus ST3-100 combined pH and mV meter using a STORP1 redox probe and STREF 2 saturated calomel reference probe. Eh values were reported relative to the standard hydrogen electrode (SHE).
Total dissolved solids (TDS)	Gravimetric determination with filtration using GF filter paper followed by drying of filtrate in a Memmert drying oven at 180 ºC to constant mass.
Total suspended solids (TSS)	Gravimetric determination with filtration using GF filter paper followed by drying in a Labotec EcoTherm drying oven at 105 ºC to constant weight.
Turbidity (NTU)	HACH-2100N Turbidimeter.
Alkalinity/acidity (TA)	Potentiometric titration to pH 8.3 for acidity and pH 4.5 for alkalinity, using 1.0 M NaOH and 0.02 M H_2SO_4 for acidity & alkalinity, respectively. Acidity titrations were preceded by the addition of hydrogen peroxide oxidation and heating to oxidise any metals present in the samples.
Anions (S)	Sulfur determined using ICP-OES and sulfate concentration calculated assuming all S present as SO_4^{2-} ion.
Metal(loid)s	Inductively Coupled Plasma Optical Emission Spectroscopy (ICP-OES) - Spectro Genesis, model Genesis Fee - Wits Chem; ICP-OES - Spectro Arcos (SOP) – UJ, and SPECTRO CIROS CCD Vacuum ICP-OES – DBS.

4.3.3 Calibration and data quality control

The pH electrode was calibrated using three buffer solutions at pH 4, 7 and 10. Measurement of a pH 4 control sample was within 0.05 pH units. The conductivity electrode was checked against 1413 µS/cm and 12.88 mS/cm reference solutions before use, the Eh electrode was checked against Eh 475 mV standard buffer solution before measurement and the turbidimeter meter was checked against standard solutions before use. In all instances, readings were within 5 % of the standard value. An error of 1.2 % was shown from repeat analyses of an acidity control sample. Inductively Coupled Plasma Optical Emission Spectroscopy (ICP) standards were prepared using certified standards and all solutions were prepared using deionized, Milli-Q, 18 MΩ water. Analytical-grade nitric acid was used for sample dilutions and a matrix-matched sample blank was determined to quantify any background contaminants that might exist. As a quality control check, TDS, EC, and the sum of the total ions were compared for agreement and cation/anion balances were calculated to confirm the electrical neutrality of the samples. Six of the samples analysed reported cation/anion balances of less than 5 %. Ten samples reported cation/anion balances between 5 and 9 %, and the remaining 3 samples recorded cation/anion balances above 10 %. In most instances, a negative value was reported indicating a possible under-reporting of cations or an over-reporting of anions. The higher cation/anion balances observed for Site 1 coincided with significantly increased rainfall events in March, October, and November, where dilution effects might have resulted in the under-reporting of cations. The higher cation/anion balances observed for Site 2 coincide with high acidity values observed in May and

August. The reduced pHs and increased Fe concentrations reported during this time, would indicate increased AMD formation, which, with the reduced Ca concentrations observed, would have upset the buffering capacity of the water and as such impacted the chemical balance.

4.3.4 Comparison of data with legislative and advisory guides

Data for the dissolved metals analysis were compared against legislative and advisory guides for drinking water, which included: the South African National Standard - SANS 241-1:2015 Drinking Water Specification (SABS, 2015); SANS 241:2006 (Ed.6) Drinking Water Quality Requirements (SABS, 2006); the United States Environmental Protection Agency (EPA) 2018 Edition of the Drinking Water Standards Health Advisories Maximum Contaminant Level (MCL) and Drinking Water Equivalent Level (DWEL) (EPA, 2018); and the Department of Water Affairs (DWAF) 1996 Water Quality Guidelines for Domestic Use Target Water Quality Range (TWQR) (DWAF, 1996).

4.4 Results and Discussion

4.4.1 Analytical Data

All data for the physical and chemical parameters as well as the dissolved metals ICP analysis data are reported in the supplementary material for Chapter 4, Appendix I-B, Tables B.1-B.9. Parameters found in excess of prescribed legislative limits are given in Table C.1-C.4 in Appendix I-C of the supplementary material for Chapter 4.

Acidic pH values of less than pH 3 were reported for all sampling events, and except for the April 2019 site 2 sample, where a pH of 7 was recorded. TA concentrations are comprised of free protons, and hydrolysable metals such as iron (Fe), manganese (Mn), and aluminium (Al) (Cravotta III and Kirby, 2004). The variation in TA concentration between the two sites is attributed to differing concentrations of metals present in the respective AMD waters. TA is not subject to legislative control, but can contribute significantly to the corrosiveness of water, and the hydrolysable salt contribution to the TA concentration, also constitutes a serious pollution problem (Cravotta III and Kirby, 2004, Larson and Henley, 1955). EC, TDS, Fe, and sulfur (S) concentrations were all in excess of legislative limits and recorded significantly higher concentrations for site 1. Calcium (Ca), magnesium (Mg), manganese (Mn), and nickel (Ni) reported concentrations in excess of legislative limits, but with smaller concentration differences between site 1 and 2. With the exception of the April sample for site 2, Al, beryllium (Be), cadmium (Cd), and lead (Pb) concentrations reported concentrations in excess of legislative limits. For site 1 and site 2, chromium (Cr), Uranium (U), and vanadium (V) reported some samples within, and some in excess of legislative limits. All boron (B) and zinc (Zn) concentrations for site 2 were below the required legislative limits. With the exception of one sample, all Zn concentrations from site 1were in excess of legislative limits, and 4 of the 11 samples analysed for B, were outside of legislative limits.

4.4.2 Potential Health Effects

While some metals such as Ca, Co, Cr, Cu, Fe, Mg, Mn, molybdenum (Mo), Ni, and Zn are essential to human and plant health, long-term exposure to concentrations of certain elements over regulatory or advisory levels, or deficiencies in some, could lead to potential health and/or environmental effects (Kyerematen, 2013, Smith, 2007).

Low pH levels result in increased dissolution of metals and metalloids from the surrounding geology and the increased mobility of these potential contaminants into the environment (Smith, 2007). Hydrolysis of metals such as Fe, Mn and Al contribute to elevated TA concentrations, which can have significant environmental and corrosive effects owing to increased TDS concentrations and the toxicity of its contributory ions (Cravotta III and Kirby, 2004). Infiltration of this acidic run-off into watercourses, could cause harm to aquatic systems, negatively impact surrounding vegetation, and, if ingested, cause health issues in humans and animals (DWAF, 1996). High sulfate concentrations could affect health, contribute to corrosion, and could also cause increased sediment levels in water bodies as a result of pH and chemistry changes resulting in precipitation (DWAF, 1996). The potential health effects of elements present in excess of legislative control concentrations, are summarised in Supplementary data for Chapter 4, Appendix I-D, Tables D.1-D.2 (EPA, 2018, DWAF, 1996).

4.4.3 Seasonal Variability

Smith et al. (2021) confirmed that AMD sites were subject to seasonal variability, based on the reduction in TDS, and other parameter concentrations that coincided with increased rainfall volumes. Strong correlations were noted between EC, the calculated sum of the total ions, and the gravimetrically determined TDS concentrations (Smith et al., 2021). Smith et al. (2021) also noted that other parameters followed similar trends to the TDS concentrations over time. This work explores the extent of these relationships.

4.4.4 Correlation Analysis

The Microsoft Excel correlation analysis tool was used to extend the correlation matrix to include all chemical and physical parameters analysed for the two AMD sites. The correlation matrix was then narrowed to include only correlated parameters that were greater than ± 0.5 and common to both sites. Because of the ease of measuring EC, the correlation was further reduced to include only parameters that correlated with EC. These correlations were then exploited for development of a statistical correlation, for use as a screening tool that would link EC with major AMD concentrations. Regression coefficients were established to describe the mathematical equation of the regression line.

Dissolved K was excluded from further statistical analysis as this parameter presented positive and negative correlations for site 1, and site 2 respectively, and reported significantly lower concentrations compared with

other parameters. Remediation efforts at Site 2, resulted in the April 2019 sample presenting a neutral pH which was not representative of the original physio-chemical make-up of this AMD site and hence its omission from further statistical analysis.

Stronger correlations were observed for Site 2, and could be attributed to the lower ion concentration present in this AMD site, and/or because of the small sample size available for evaluation for this site, compared with the 13 data sets available for Site 1 (Smith et al., 2021). As both sites were located in close proximity, and as such, shared regional geology, both data sets were combined to broaden the correlation and give a statistically more robust sample. A pooled correlation was performed using the extended Excel data analysis tool at a 95 % confidence level. The individual and the pooled correlation coefficients are shown in Table 4.2.

Table 4.2 Separate and pooled correlations between electrical conductivity, calculated total dissolved solids, total dissolved solids, total acidity, dissolved iron and dissolved sulfur concentrations

Correlation	**r**									
Parameter	**EC**		**TDS**		**Sum of Total Ions**		**Total Acidity**		**Dissolved Fe**	
Site	**1**	**2**	**1**	**2**	**1**	**2**	**1**	**2**	**1**	**2**
EC	1									
TDS	0.88	0.97	1							
Sum of Total Ions	0.67	0.88	0.55	0.91	1					
TA	0.96	0.98	0.85	0.93	0.75	0.91	1			
Dissolved Fe	0.63	0.90	0.51	0.88	0.99	0.97	0.70	0.95	1	
Dissolved S	0.70	0.92	0.57	0.93	1.00	1.00	0.77	0.94	0.99	0.98
Site	**1 & 2**		**1 & 2**		**1 & 2**		**1 & 2**		**1 & 2**	
EC	1									
TDS	0.9627		1							
Sum of Total Ions	0.8712		0.8350		1					
Total Acidity	0.9912		0.9570		0.8974		1			
Dissolved Fe	0.8810		0.8394		0.9953		0.9039		1	
Dissolved S	0.8829		0.8474		0.9993		0.9089		0.9935	

As indicated by the correlation coefficient "*r*" approaching +1, the combined correlation data indicated strong positive correlations between all selected parameters (Hannigan and Lynch, 2013).

4.4.5 Regression Analysis

To exploit the correlations observed between EC, TDS, TA, dissolved Fe and S, regression analyses were performed at a 95 % confidence level, using the Excel data analysis tool with EC as the independent variable (*x*-value), and TDS, TA, Fe and S as the dependent variables (*y*- values). These data provided a measure of the extent to which the calculated regression analysis fits the source data (Cheusheva, 2019). The regression analysis output included regression statistics, an analysis of variance (ANOVA), and regression coefficients. These data are given in Supplementary data for Chapter 4, Table E.1 of Appendix I-E.

The ANOVA output, tests the significance of the correlation between the dependent and independent variables, and provides information on the regression model (Aydin, 2015). An *F*-critical value of 4.49 was calculated at a 95 % confidence level using *Equation 4.2*.

$$F\,Critical = F.INV.RT(0.05, 1, 16) \qquad \textit{Equation 4.2}$$

The ANOVA output data are reported in Table 4.3, in the format; $[F(x, y) = a, p = b]$; where:
x = degrees of freedom of the independent variable
y = degrees of freedom of the dependent variable
a = the F- statistic
b = the *Significance F* or *P*-value of *F*

Table 4.3 Summary of ANOVA test results at a 95 % confidence level

Dependent Variable	Independent Variable	ANOVA Test Results
TDS	EC	$[\mathrm{F}(1,16) = 203, p = 1.67E^{-10}]$
TA	EC	$[\mathrm{F}(1,16) = 894, p = 1.18E^{-15}]$
Fe	EC	$[\mathrm{F}(1,16) = 56, p = 1.37E^{-06}]$
S	EC	$[\mathrm{F}(1,16) = 57, p = 1.23E^{-06}]$

The statistical output showed that significance *F*, or the *p*-value of *F*, for all dependent variables, were less than 0.05 indicating that there is a linear relationship between the independent variable EC and each of the dependent variables tested. In all instances, the *F*-statistic was greater than the calculated critical value, indicating that the observed relationship between the dependent and independent variables did not occur by chance. Thus the change in EC value, the independent variable, was statistically confirmed to describe the variation in the dependent variables; TDS, TA, dissolved Fe and dissolved S respectively (Mursau, nd).

The regression coefficients output is shown in Supplementary data for Chapter 4, Table E.2 of Appendix I-E. The regression coefficients, describe the mathematical equation for the regression line, y =mx+b, and were calculated using the least-squares method, which calculates the slope (m) and intercept values (b) that

achieve the smallest sum of the squares of the vertical variations of the determined concentrations from the predicted values in the regression line (Tripepi et al., 2008). The intercept value explains the theoretical concentration of the dependent (*y*) variable when the independent (*x*) variable is equal to zero (Tripepi et al., 2008, Yan and Su, 2009). The regression equation is used to calculate the probable concentration of the dependent (*y*) variable from the given value of the independent (*x*) variable (Tripepi et al., 2008, Yan and Su, 2009). A *t*-Critical value of 2.12 was calculated using *Equation 4.3* (Mursau, nd).

$$T\,Critical = T.INV.2T(0.05, 1{,}16) \qquad \textit{Equation 4.3}$$

The *t*-Statistic was greater than the *t*-Critical value for all parameters, confirming the overall significance of the model and the calculated *P*-value was less than 0.05 for all parameters, indicating that the relationship between the dependent and independent variables was significant. The upper and lower confidence intervals, which describe the upper and lower boundaries of the regression line, did not include zero within their range. Regression analysis confirmed that a linear relationship did exist between the dependent and independent variables. Thus, EC could be used as a proxy to predict TDS, TA, dissolved S, and dissolved Fe concentrations in these AMD waters, provided a sufficiently large database was used to underlie the correlation. The linear regression *Equations 4.4–4.7*, were derived using the slope and intercept values, and may be used to estimate the concentrations of the dependent variables, namely; TDS, total acidity, dissolved Fe and dissolved S from the EC value. (Cheusheva, 2019, Tripepi et al., 2008). The units for the x-variable units are expressed in mS/m, and in mg/L for the y-variable.

$$TDS = 6.2384\,x - 963.45 \qquad \textit{Equation 4.4}$$

$$TA = 3.7910\,x - 3103.27 \qquad \textit{Equation 4.5}$$

$$Dissolved\ S = 1.2429\,x - 63.8190 \qquad \textit{Equation 4.6}$$

$$Dissolved\ Fe = 1.7878\,x - 2133.15 \qquad \textit{Equation 4.7}$$

The large intercept value observed in these regression equations would however limit the use of these equations for predictive purposes over a broad concentration range. To remedy this, the trendline intercepts were set to zero and a scatter plot of these data with their regression equations is shown in Figure 4.3. The revised regression equations are given in *Equations 4.8–4.11*.

$$TDS = 5.9524\,x \qquad \textit{Equation 4.8}$$

$$TA = 2.8703\,x \qquad \textit{Equation 4.9}$$

$$Dissolved\ S = 1.2239\,x \qquad \textit{Equation 4.10}$$

$$Dissolved\ Fe = 1.1549\,x \qquad \textit{Equation 4.11}$$

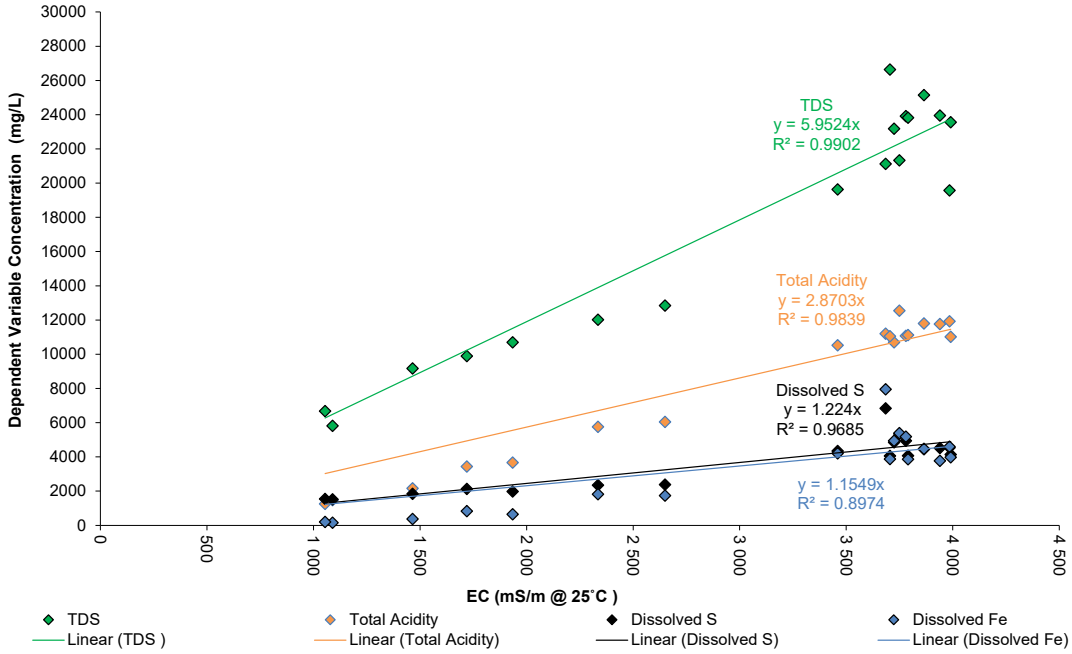


Figure 4.3 Linear regression equations with the intercept set to zero for total dissolved solids, total acidity, dissolved iron and sulfur as a function of electrical conductivity

Setting the intercept to zero improved the R squared value, however, as seen in Figure 4.3, the regression lines for the TA and dissolved Fe data no longer fit the lower concentration data points, requiring the use of different regression options for these parameters. While a linear regression remained the best fit for the TDS and dissolved S data, a power regression provided the best fit for TA and dissolved Fe data. Although the calculated R-squared values for the non-linear equations more closely approach 1, R is not an appropriate indication of goodness-of-fit for non-linear curves. This is better described by the standard error of regression, or residual standard error (S). A comparison of the R- square values achieved for the various mathematical regression equations are given in Table 4.4, and scatter plots showing the amended power regression lines are shown in Figure 4.4.

Table 4.4 A comparison of the R-squared values achieved for each parameter using the different regression options and after rejection of outliers

Parameter	Linear Regression R-Square value	Linear Regression with zero intercept R-Square value	Power Regression R-Square value	Linear/Power Regression R-Square value – after rejection of outliers
Total Dissolved Solids	0.9268	**0.9902**	0.9576	**0.9968**
Total Acidity	0.9824	0.9839	0.9920	0.9965
Dissolved S	0.7794	**0.9685**	0.8732	**0.9904**
Dissolved Fe	0.7764	0.8974	0.9597	0.9748

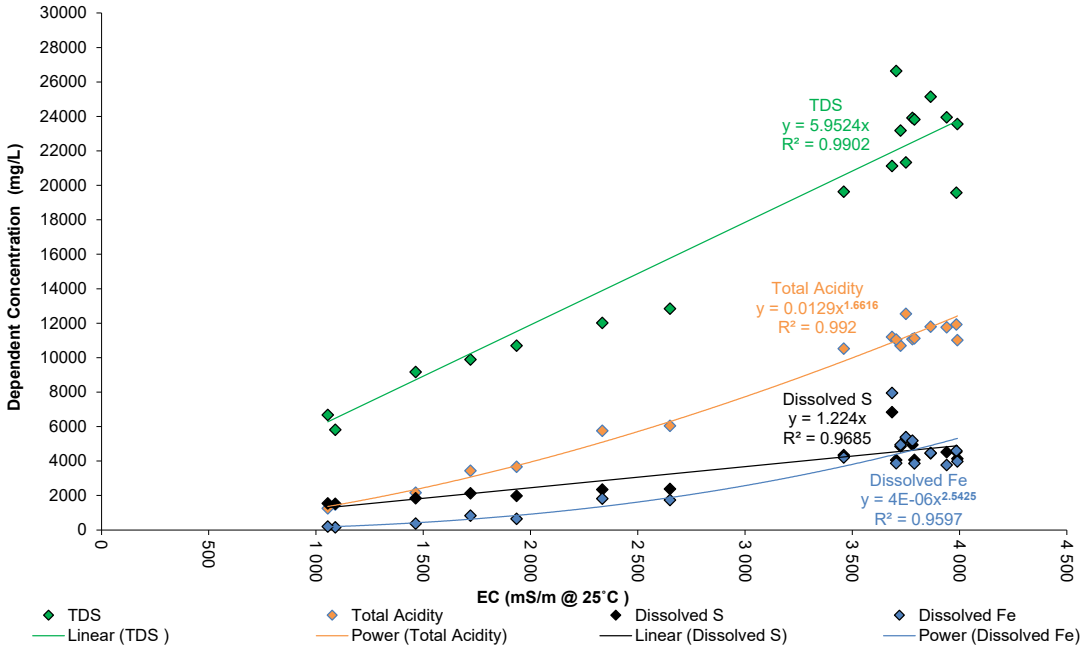


Figure 4.4 Linear regression with the intercept set to zero, and power regression equations used for total dissolved solids total acidity, dissolved iron and sulfur as a function of electrical conductivity.

A visual inspection of the scatter plots indicated the presence of some outlying data points, and further regression analysis was performed, where linear and power residual values were normalized to confirm the rejection of outliers. An iterative process was followed until all outliers were rejected. The output of the statistical analyses are shown in the supplementary data information (Supplementary data for Chapter 4, Appendix I-F1 –F4). The rejection of outliers resulted in an improvement in R- square value for all parameters, and these and the revised linear/power regression lines shown in Figure 4.5.

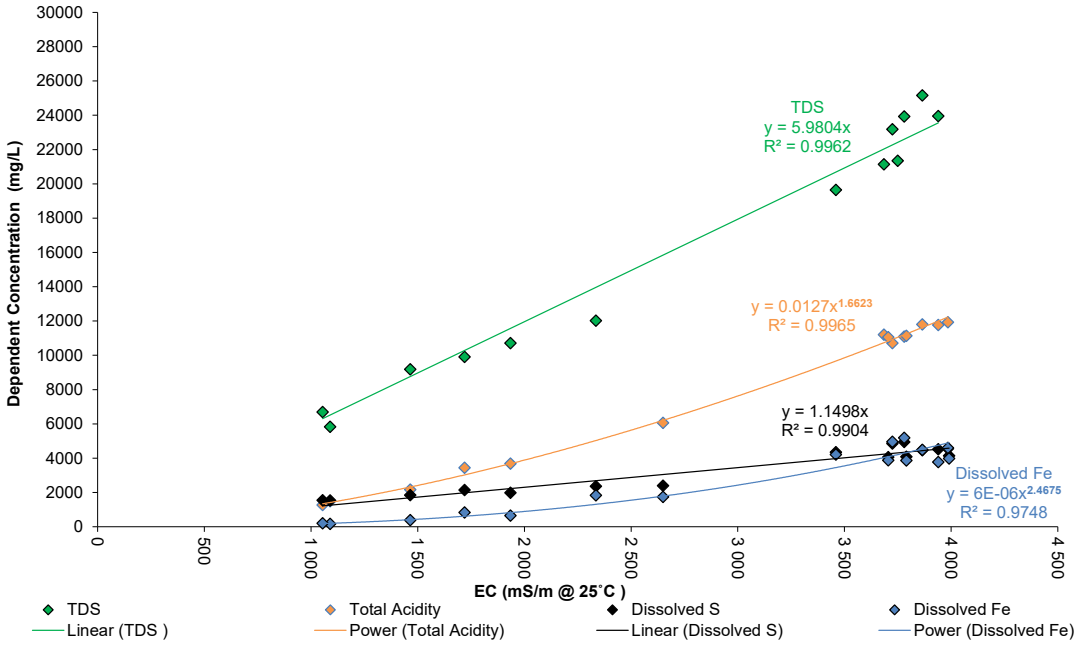


Figure 4.5 Total dissolved solids total acidity, dissolved iron and sulfur as a function of electrical conductivity: Linear regression with the intercept set to zero, and power regression equations after rejection of outliers

Given the significance of the relationship between EC and the selected parameters, and using EC as a proxy, *Equations 4.12–4.15* could be used for prediction of TDS, TA, dissolved S, and dissolved Fe concentrations for the specified sites.

$$TDS = 5.9804\,x \qquad \textit{Equation 4.12}$$

$$TA = 0.0127x^{1.6623} \qquad \textit{Equation 4.13}$$

$$Dissolved\ S = 1.1498\,x \qquad \textit{Equation 4.14}$$

$$Dissolved\ Fe = 0.000006x^{2.4675} \qquad \textit{Equation 4.15}$$

The regression equations were also be used to derive the EC values corresponding to water quality limits for TDS, dissolved Fe and S. This could be useful as a rapid test for compliance, which would then trigger further analysis and appropriate remedial action. The EC values corresponding to the water quality limits for TDS, dissolved S and Fe are as follows:

- EC ≈ 201 mS/m ≈ TDS water quality compliance limit of 1200 mg/L
- EC ≈ 72/145 mS/m Dissolved S – 167/83 mg/L acute health/aesthetic water quality compliance limits
- EC ≈ 173 mS/m ≈ Dissolved Fe – 2 mg/L chronic health water quality compliance limit
- TA – water quality compliance limits not allocated

4.5 Conclusion

Comparison of data from two AMD sites in the Mpumalanga coal mining region, against drinking water legislation values, showed that a range of physical and chemical parameters exceeded regulatory limits and could negatively affect certain chemical and biological processes in the surrounding environment, which, in turn would impact, the health of plant, human and aquatic life.

Strong correlations were observed between the major contributing parameters to these AMD waters. Regression analysis confirmed the linear relationship between the dependent and independent variables, and as such, electrical conductivity could be used as a proxy to predict specific parameter concentrations in AMD waters using the mathematical equations describing the regression lines.

The regression equations could also be used to calculate the electrical conductivity value corresponding to the water quality limits for total dissolved solids, dissolved iron, and sulfur.

The significance of these relationships lies in the relative ease of electrical conductivity determination and the possibility to predict the concentration of the major contributing elements of a specified acid mine drainage body. Derivation of the electrical conductivity value corresponding to the water quality limits for selected parameters would provide a rapid test for compliance, where exceedance of the calculated threshold electrical conductivity values, would trigger a response for further analysis and appropriate remedial action to be taken.

4.6 Acknowledgements

Thank you to Sasha Naidu and Sean Rossouw for their help with the water sampling, Dr Ansuyah Magan for her insight and technical contribution to the statistical analysis, Professor Kathryn Sole and Mr Stephen Batchelor for document review, technical, and language editing, and Stephen Smith for his assistance with the document format editing.

4.7 Recommendations

Acid mine drainage composition is dependent on the geology and environmental conditions which are unique to a particular region, and, as such, the correlations observed for the acid mine drainage sites in this study should not be considered universal. This work is intended as a proof of concept for adaptation at other acid mine drainage sites and individual acid mine drainage sites should be evaluated independently to characterise and establish relationships that might exist between their various parameters.

These relationships should not be viewed as a replacement to continuous monitoring which is required for conformance to respective water use licence conditions, but as a tool that could prove invaluable for a rapid

test of compliance, and during disaster events, where the quick turnaround of analysis data would facilitate a faster response time to expedite remedial action necessary to prevent potential environmental damage caused by unintended release of these waters.

Statistical relevance increases as the data pool increases, and continuous monitoring is essential to increase the data pool, and also to identify any significant changes that might occur as a result of chemical changes in an AMD body over time. This should be accompanied by a periodic re-evaluation of the statistical relationships. The availability of a larger pool of data could also facilitate the identification of relationships between other parameters present in specific AMD waters.

4.8 References

Akcil, A. & Koldas, S. 2006. Acid Mine Drainage (AMD): causes, treatment and case studies. Journal of cleaner production, 14, 1139-1145.

APHA, A., WEF 2005. Standard Methods for the Examination of Water and Wastewater.

ATSDR, A. f. T. S. a. D. R. 2005. Public Health Statement, Nickel. DEPARTMENT of HEALTH AND HUMAN SERVICES.

ATSDR, A. f. T. S. a. D. R. 2010. Toxicological Profile for Boron.

Aydin, G. Ö. K. H. A. N. 2015. Forecasting natural gas production using various regression models. Petroleum Science and Technology, 33, 1486-1492.

Banks, D., Younger, P. L., Arnesen, R.-T., Iversen, E. R. & Banks, S. B. 1997. Mine-water chemistry: the good, the bad and the ugly. Environmental Geology, 32, 157-174.

Cheusheva, S. 2019. Linear Regression analysis in Excel [Online]. Available: https://www.ablebits.com/office-addins-blog/2018/08/01/linear-regression-analysis-excel/ [Accessed 5 November 2019].

Cravotta III, C. A. & Kirby, C. S. Acidity and alkalinity in mine drainage--practical considerations. 2004 National Meeting of the American Society of Mining and Reclamation and the 25th West Virginia Surface Mine Drainage Task Force, April 18-24, 2004. 334-365.

Davidson, C. 2003. Catchment diagnostic framework for the Klip River catchment, Vaal barrage, October 1998-September 1999.

DMR. 2017. Operating Mines in Mpumalanga [Online]. Department of Mineral Resources of South Africa https://www.dmr.gov.za/mineral-policy-promotion/operating-mines/mpumalanga [Accessed 6 January 2020].

DWAF 1996. Department of Water Affairs and Forestry, 1996. South African Water Quality Guidelines (second edition). Volume 1: Domestic Use.

DWS 2017. National Water Act (36/1998) National Norms and Standards for Domestic Water and Sanitation Services V 3 - Final ed.: Department of Water and Sanitation.

EPA 2018. 2018 Edition of the Drinking Water Standards and Health Advisories, EPA 822-F-18-001, Office of Water, U.S. Environmental Protection Agency, Washington, DC.

EPA 2022. National Primary Drinking Water Regulations. US Environmental Protection Agency.

Gazea, B., Adam, K. & Kontopoulos, A. 1996. A review of passive systems for the treatment of acid mine drainage. Minerals engineering, 9, 23-42.

Geosciences, C. f. 2016. Downloadable Maps, Documents, Files [Online]. Available: http://www.geoscience.org.za/index.php/component/content/article?id=386:downloadable-maps-documents-and-files [Accessed 19 January 2016].

Hannigan, A. & Lynch, C. D. 2013. Statistical methodology in oral and dental research: pitfalls and recommendations. Journal of Dentistry, 41, 385-392.

Hobbs, P., Oelofse, S. H. & Rascher, J. 2008. Management of environmental impacts from coal mining in the upper Olifants River catchment as a function of age and scale. Water Resources Development, 24, 417-431.

Kyeremateng, T. K. 2013. Heavy metal pollution in sediments and water from streams within the Damang Mine Concession.

Larson, T. E. & Henley, L. 1955. Determination of Low Alkalinity or Acidity in Water. Analytical Chemistry, 27, pp.851-852.

Marsden, D. 1986. The current limited impact of Witwatersrand gold-mine residues on water pollution in the Vaal River system. Journal of the Southern African Institute of Mining and Metallurgy, 86, 481-504.

McCarthy, T. S. 2011. The impact of acid mine drainage in South Africa. South African Journal of Science, 107, 01-07.

Minerals Council South Africa 2019. Where coal is mined in South Africa - Mining for Schools. Minerals Council South Africa.

Mursau, A. nd. Regression analysis: Evaluate predicted linear equation, R-squared, F-Test, T-Test, p-Value etc. [Online]. Available: http://cameron.econ.ucdavis.edu/excel/ex61multipleregression.html [Accessed 20 November 2019].

Nordstrom, D. K., Blowes, D. W. & Ptacek, C. J. 2015. Hydrogeochemistry and microbiology of mine drainage: an update. Applied Geochemistry, 57, 3-16.

SABS 2006. South African National Standards, Drinking Water 2006, SANS 241:2006 (Ed. 6), ISBN 0-626-18876-8.

SABS 2015. South African National Drinking Water Standard (SANS) 241-1: 2015 Second ed.

Simate, G. S. & Ndlovu, S. 2014. Acid mine drainage: Challenges and opportunities. Journal of Environmental Chemical Engineering, 2, 1785-1803.

Smith, J., Sheridan, C. M., van Dyk, L. D. & Harding, K. G. 2021. Seasonal characterisation of acid mine drainage in Mpumalanga coalfields region. South African Chemical Engineering Congress 2021, 20-22 September 2021 Virtual. Johannesburg.

Smith, K. S. 2007. Strategies to predict metal mobility in surficial mining environments. Reviews in engineering geology, 25-45.

Tripepi, G., Jager, K., Dekker, F. & Zoccali, C. 2008. Linear and logistic regression analysis. Kidney international, 73, 806-810.

Tutu, H., McCarthy, T. & Cukrowska, E. 2008. The chemical characteristics of acid mine drainage with particular reference to sources, distribution and remediation: The Witwatersrand Basin, South Africa as a case study. Applied Geochemistry, 23, pp.3666-3684.

Van Niekerk, H., Silberbauer, M. & Maluleke, M. 2014. Geographical differences in the relationship between total dissolved solids and electrical conductivity in South African rivers. Water Sa, 40, 133-138.

WRC 2015. South African Mine Water Atlas. The Water Research Commission.

Yan, X. & Su, X. 2009. Linear regression analysis: theory and computing, World Scientific.

CHAPTER 5.

5 Classification of grasses in the Mpumalanga coalfields region and assessment of their suitability to increase the pH of acid mine drainage, for potential use in passive acid mine drainage remediation systems

(Published in Ecological Engineering, 2024)
Smith, J., Sheridan, C.M., van Dyk, L.D., Harding, K.G., 2022. Critical evaluation of the chemical composition of acid mine drainage for the development of statistical correlations linking electrical conductivity with acid mine drainage concentrations, Environmental Advances, 8, p. 100241.
doi.org/10.1016/j.envadv.2022.100241

This chapter addresses objective (b): To identify and characterise various commonly occurring grass types that are readily available and co-located with AMD sites and compare these for use in AMD bioremediation.

The identification and characterisation of grass for use in acid mine drainage (AMD) bioremediation is described. This chapter then details the investigation of the physical (cellulose, hemicellulose, and lignin composition) and chemical (carbon, hydrogen, nitrogen, sulfur, and oxygen) composition of various grass types collected from roadside areas that were co-located with coal mining operations in the Mpumalanga coalfields region, South Africa. The experimental exploration of the capability of these grasses to increase the pH of contacted synthetically prepared, and environmentally sampled AMD solutions is described. An investigation of the effect of renewing the organic substrate, to establish if the extent of pH increase improved with regular replenishment of grass is also presented. This work explored the mechanism controlling the pH increase of AMD in the presence of grass within passive remediation systems. The exchange reactions between H^+ ions in the AMD and inorganic cations in the grasses were identified as potentially being the main mechanism for increasing the pH of synthetically prepared AMD.

CRediTs: Janet Smith: Conceptualization, Methodology, Investigation, Validation, Formal analysis, writing-Original Draft; Craig Sheridan: Funding acquisition, Conceptualization, Resources, Supervision, Writing – Review and editing; Lizelle van Dyk: Conceptualization, Supervision, Writing – Review and Editing; Kevin Harding: Conceptualization, Supervision, Writing – Review and Editing

AKNOWLEDGEMENTS
The authors would like to thank Dr Renee Reddy the C.E. Moss Herbarium manager, for her guidance and assistance with the classification of the grass types.

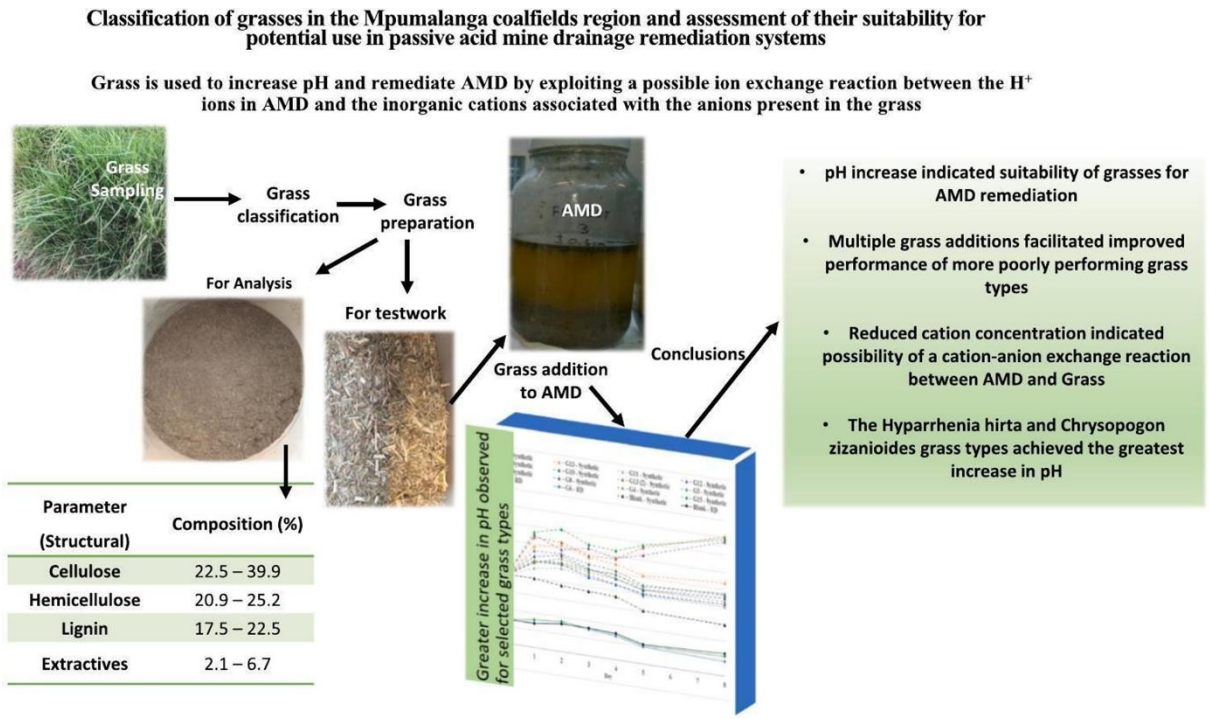


Figure 5.1 Graphical Abstract: Classification of grasses in the Mpumalanga coalfields region and assessment of their suitability for potential use in passive acid mine drainage remediation systems.

5.1 Abstract

Grass samples collected from various locations in the Mpumalanga coalfields region, (South Africa), were classified and characterised using various analytical techniques to determine their physical and chemical composition. The suitability of the grasses for use in acid mine drainage (AMD) remediation was evaluated by adding a defined portion of these grasses to both synthetically prepared and real AMD collected from an AMD received dam (RD) source in the Mpumalanga coalfields region, (South Africa). This was to establish whether the grass addition was able to achieve an increase in pH, and if the effect was more notable for a particular grass type. Results showed that grass addition to AMD resulted in an increase in pH (or decrease in the hydrogen ion (H^+) concentration of synthetically prepared AMD. The addition of different grass types produced varying results, and the *Hyparrhenia hirta* (G12 and G13) and *Chrysopogon zizanioides* (G15) formally known as *Vetiveria zinanioldes* grass types produced a greater overall percentage decrease in H^+ concentration. Multiple grass additions sustained the overall high percentage decrease in H^+ concentration for the best-performing grass types and improved the overall percentage decrease in H^+ concentration of the more poorly performing *Eragrostis curvula* (G6), and *Hyparrhenia filipendula* (G5) grass types tested in synthetic AMD. The notable changes observed in cation and anion concentrations of the grass samples after contact with AMD would suggest that a cation-anion exchange reaction did occur. An exchange of the H^+ ions in the AMD and the inorganic cations (M^+) associated with anions present in the grass, could be responsible for the increase in pH observed in synthetic AMD after grass addition. The addition of grass to the RD AMD did not achieve any significant or sustained decrease in H^+ concentration, which could be attributed to the

more complex matrix and higher mineral acidity of the RD AMD which would require alternate experimental conditions to achieve a decrease in H^+ concentration. Variances in structural and physical composition between the different grass types were not consistent, and it was not possible to attribute the decrease in H^+ concentration in AMD to any compositional parameter. Using locally sourced lignocellulosic materials in passive remediation systems is vital to the successful design of a cost-effective and sustainable, remediation system. This work is important as it explores the suitability of grass types that are readily available from the immediate vicinity of the Mpumalanga coalfields, South Africa to increase the pH of contacted AMD at ambient temperature.

Keywords: Acid Mine Drainage, Grass, Hydrogen ion concentration, Ion-exchange reaction, Lignocellulosic material, pH neutralisation, Remediation.

5.2 Introduction

5.2.1 Acid mine Drainage and Remediation

Acid mine drainage (AMD) occurs when sulfide-bearing ores are exposed to oxygen and water resulting in the formation of sulfate, dissolved metals, and acidity. Secondary reactions then occur when the acidic water dissolves other metals that are present in the surrounding ore bodies resulting in an acidic run-off that is contaminated with a range of heavy metals (Gazea, Adam and Kontopoulos, 1996; McCarthy, 2011a; Simate and Ndlovu, 2014). Gold and coal mining activities have led to the generation of large quantities of AMD in the Witwatersrand goldfields and Mpumalanga coalfields which has negatively impacted the surrounding environment (Gazea, Adam and Kontopoulos, 1996; Tutu, McCarthy and Cukrowska, 2008; Simate and Ndlovu, 2014; Ighalo *et al.*, 2022).

Treatment of AMD seeks to achieve water of neutral pH with the removal of sulfates (SO_4^{2-}), iron (Fe), and other metal(oid)s. Conventional AMD treatment typically comprises acid neutralisation using alkaline materials such as limestone, lime, sodium hydroxide or sodium carbonate. The increase in pH results in the subsequent precipitation of dissolved metal(oid)s present in the AMD. These processes generally have high operating costs as well as prohibitive waste disposal costs (Johnson and Hallberg, 2002, 2005,).

The use of bio-remediation technologies in AMD treatment processes may include several chemical and biological treatment mechanisms, such as microbially mediated redox reactions, chemical and enzymatic hydrolysis; phytoextraction, and biosorption (Gazea, Adam and Kontopoulos, 1996). A key biological AMD remediation process is the reduction of sulfates to sulfide using sulfate-reducing bacteria (SRB). These bacteria obtain energy by anaerobic respiration using sulfate as an electron acceptor and organic carbon, or hydrogen as an electron donor in a process called dissimilatory sulfate reduction (DSR) (Ayala-Parra et al., 2016).

$$SO_4^{2-} + 2CH_2O + 2H^+ \rightarrow H_2S + 2CO_2 + 2H_2O \qquad \textit{Equation 5.1}$$

Equation 5.2 shows the reaction between the soluble sulfides formed in *Equation 5.1*, with cationic metals (Me^{2+}) present in AMD to precipitate as the metal sulfide (Ayala-Parra, Sierra-Alvarez and Field, 2016).

$$Me^{2+} + S^{2-} + 2H^+ \rightarrow MeS \downarrow \qquad \textit{Equation 5.2}$$

For a DSR system to be cost-effective, an inexpensive and sustainable carbon source is required.

5.2.2 Lignocellulose biomass

Lignocellulosic biomass is an abundant, renewable resource that can be derived from agricultural and forestry residues, pulp, garden, municipal wastes, as well as roadside vegetation (Demirbaş, 2001; Petrova and Ivanova, 2010; Koppram et al., 2014; Westensee et al., 2018). Ramla and Sheridan (2015) demonstrated that grass could be used as an electron donor source for DSR in the remediation of AMD and as a resource for biofuel production provided a suitable pre-treatment is developed to break down lignin and increase the cellulose surface area and render it amenable to enzymatic hydrolysis (Ramla and Sheridan, 2015; Rezania et al., 2020; Li et al., 2022).

Lignocellulosic materials are primarily composed of cellulose, hemicellulose, and lignin. The cellulose and hemicellulose materials could provide a source of monomeric sugars that could be used in the DSR process and/or to produce biofuels. These sugars can only be accessed once a pre-treatment process is performed to remove the lignin and disrupt the lignocellulosic structure (Lakaniemi, Tuovinen and Puhakka, 2013; Burman, Harding, et al., 2018). Cellulose and hemicellulose are the most abundant polymers in lignocellulosic biomass with expected concentrations of between 40–50% and 20–30% respectively. Lignin content is expected at between 10–25% (Shahzadi et al., 2014).

Springer and Harris (1985), state that the addition of lignocellulosic material to a mineral acid solution results in a decrease in hydronium ion (H^+) concentration of the mineral acid. This decrease is attributed to an ion-exchange reaction where the H^+ ions in the acid solution are exchanged with the inorganic cations (M^+) that are associated with the anions present in the lignocellulosic material (Springer and Harris, 1985). The simplified reaction for the bound anions using wood to denote the lignocellulosic material is shown in *Equation 5.3*.

$$wood - COO^-M^+ + H^+ \rightarrow wood - COO^-H^+ + M^+ \qquad \textit{Equation 5.3}$$

The main inorganic cations found in wood include: calcium (Ca^{2+}), magnesium (Mg^{2+}), sodium (Na^{+}), and potassium (K^{+}) and the main inorganic anions include: sulfates (SO_4^{2-}), phosphates (PO_4^{3-}), and chlorides (Cl^{-}) (Springer and Harris, 1985).

This work investigated the physical and chemical composition of different grass types from the eastern Mpumalanga Coalfield region in South Africa to (a) establish the suitability of these grasses to support an increase in pH of AMD for potential use in AMD remediation processes; and (b) establish whether there was sufficient inorganic cation content in grass to support a similar ion-exchange reaction as observed in wood when added to AMD.

5.3 Methodology for grass classification

5.3.1 Sampling and classification of grass

A total of fourteen grass samples were collected from roadside areas close to coal operations, extending across the Witbank coal region from Springs to Belfast (Pone *et al.*, 2007). The "Springs," G16 grass was purchased from an unspecified agricultural supplier in Springs and provided a sample from far western reaches of the Witbank coal region. The G15 Vetiver grass *(Chrysopgon zizanioides)* was sourced from Mhlalanyoni, a farm just outside of White River in Mpumalanga and was included in this study because of previously reported success in phytoremediation of soils contaminated with heavy metals (Kiiskila et al., 2019; Daraz et al., 2023). The grass samples were marked as G1–G16, and grass types were classified into types by comparison with catalogued specimens at the Moss Herbarium, at the University of the Witwatersrand. Grass sampling locations were selected to include a representative spread across the Witbank coal region in Mpumalanga, (South Africa). Grass identification and sampling locations were superimposed on a map of the Mpumalanga region using the Microsoft Power BI package (Figure 5.2).

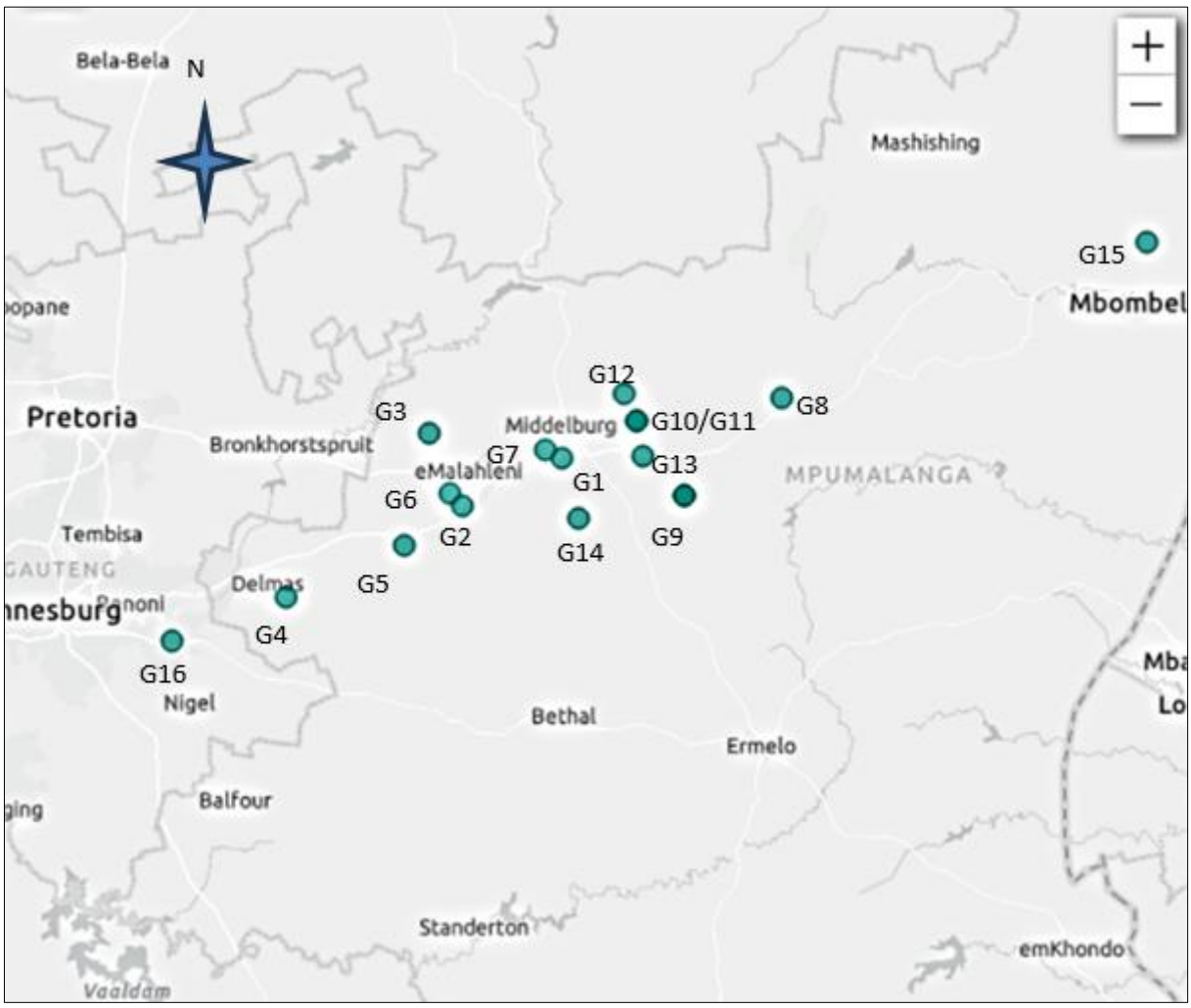


Figure 5.2 The location of the grass samples collected in the Mpumalanga coalfields region of South Africa (Scale 1:2 200 000 cm).

5.3.2 Determination of the structural and chemical composition of grasses

The physical and chemical composition of the grasses were determined using various chemical and instrumental analytical techniques. Compositional and structural analysis of the grasses was conducted at the University of the Witwatersrand, Johannesburg's Schools of Chemical and Metallurgical Engineering, and Chemistry laboratory facilities.

5.3.3 Determination of extractives, structural carbohydrates, and lignin

Lignocellulosic biomass is primarily composed of cellulose, hemicellulose, and lignin. The relative proportion of each of these components was determined using the National Renewable Energy Laboratory (NREL) method (Sluiter *et al.*, 2012). The removal of extractives or non-structural carbohydrates before compositional analysis was achieved using a single-stage Soxhlet extraction using acetone (Ayeni *et al.*, 2015). The extractive-free grass was subjected to a two-stage hydrolysis process, requiring the addition of

concentrated sulfuric acid with incubation at 30°C for 1 h, followed by dilution and autoclaving at 121°C for 1 h. The leached grass solids were separated from the solution using vacuum filtration. The acid-soluble lignin content was determined using a diluted portion of the filtrate solution and determining the absorbance spectrometrically at a wavelength of 320 nm, in a time-critical measurement that had to be made within 6 hours of hydrolysis. Carbohydrates were determined by neutralising a portion of the filtrate solution to a pH range of between pH 5-6 with calcium carbonate and analysing the settled supernatant liquor after filtration through an 0.25 µm filter on an Agilent G1314B high-performance liquid chromatography (HPLC) instrument, with a 1200 series wavelength detector, using a Bio-Rad Animex HPX - 87H column coupled to a G1362A refractive index detector. Calibration standards for the carbohydrate determination were prepared using the same hydrolysis process as the samples. Acid-insoluble lignan was determined gravimetrically from the filter residue after washing with deionised water and drying to constant mass at 105°C.

5.3.4 Ultimate composition analysis

Carbon, hydrogen, nitrogen, and sulphur (CHNS) composition were determined using an Elementar, Vario EL cube CHNS analyser. Catalytic combustion was carried out at 1150°C, and the evolved gas mixture components were separated using purge and trap chromatography, and measurements made by a thermal conductivity detector (TCD). The elemental concentrations were calculated by the instrument software and the oxygen content was determined by difference (Elementar Analysensysteme GmbH, 2023).

5.3.5 Proximate analysis

A thermo-gravimetric technique was used for the determination of moisture, volatile matter, fixed carbon, and ash content. The mass loss resulting from heating the sample to predefined temperatures under set conditions is proportional to the respective parameter, and the ash content was calculated by difference. For comparison, grass samples were analysed using two different programs, using an ALS SDT Q 600 TA instrument (TGA). The first method as described by Moyo, (2013) required a heating rate of 30°C/min in a nitrogen atmosphere of 40 mL/min to a temperature of 110°C to determine the moisture content, and then to 700°C to determine the volatiles content, before changing to an oxygen atmosphere, at the same flow rate and heating to 900°C, to determine the carbon content (Moyo, 2013) In the second method described by Ayeni et al. (2018), the samples were held at 25°C for 4 minutes in a nitrogen atmosphere, at a flow rate of 45 mL/min, the sample was then heated to 110°C at a rate of 85°C/min and held constant at this temperature for 5 minutes. The devolution step required heating to 950°C at a rate of 80°C/min, where the temperature was held constant for 5 minutes before changing to an oxygen atmosphere and maintaining these conditions for 7 minutes to achieve combustion of the remaining char. The ash content was calculated by subtraction of the percentage moisture, volatile matter, and fixed carbon content from 100% (Moyo, 2013; Ayeni *et al.*, 2015).

5.3.6 Calorific value analysis

The calorific value (CV) is a measure of the heat liberated when the grass is completely combusted in oxygen. An Energy Instrumentation, Supercal Modular Calorimeter was used for this determination, and the total heat energy released is reported in megajoules per kilogram (MJ/kg).

5.3.7 Determination of pH, oxidation-reduction potential (ORP), and dissolved oxygen (DO)

pH was measured using an Ohaus ST3-100 combined pH and mV meter and ST310 pH electrode with an integrated temperature probe. ORP measurements were made using an Ohaus ST3-100 combined pH and mV meter using a STORP1 ORP probe with a double junction Ag/AgCl reference. DO was measured using an Aqualitic AL 15 portable meter and oxygen sensor with automatic temperature compensation.

5.4 Methodology for determination of suitability of different grass types from the Mpumalanga coalfields region, (South Africa) to increase the pH of AMD for use in AMD remediation

The suitability of using the grasses collected from the Mpumalanga coalfields region, (South Africa), for AMD remediation was tested by observing whether the addition of these grasses to both synthetic and RD AMD solutions, resulted in significant changes in pH ORP and DO were also measured.

The RD AMD, (pH 2.2) was sourced from a coal mine in the eMalahleni region in Mpumalanga, (South Africa), and comprised ≈3200 mg/L Fe, ≈4800 mg/L total sulfur, 500 mg/L Ca, ≈400 mg/L Al and Mg, ≈80 mg/L Mn, ≈35 mg/L Na and Si, and between 1 and 10 mg/L of Co, Ni, and Zn (Smith *et al.*, 2021). The synthetic AMD solution was prepared using Merck, analytical grade sulfuric acid and ferrous sulfate, to give a final concentration of 2500 mg/L of Fe and 5000 mg/L of sulfate. The solution pH was adjusted to ≈pH 4 using sodium hydroxide (NaOH) and made up to volume using deionised water (DI), Analytical grade reagents provide guaranteed purity, and as such, no other metal(oid)s were expected to be present in the synthetically prepared AMD. The metal(oid) and sulfate concentrations were not re-evaluated in this experimental work, as the purpose of this study was to assess the suitability of different grass types to increase the pH of AMD, for potential use in passive remediation systems.

5.4.1 Single grass addition experiment – Procedure for sample and reactor preparation

Grasses were fed through a commercial garden shredder and then further reduced to size fractions of between 2 and 5 cm using a kitchen blender. The grasses were washed by rinsing 5 times with distilled water and dried over 3 days in a Labcon drying oven at 60°C. Individual reactors were prepared using 750 mL Consol bottles. A 30 g/L grass:AMD ratio was achieved by weighing 15 g portions of grass into separate reactors and

adding 500 mL of synthetic AMD. A further two reactors were prepared using RD AMD to test if these grass types reacted differently in different AMD media, and two control reactors were prepared using synthetic and RD AMD without grass addition. Only two grass types, G6 and G15 were contacted with RD AMD to preserve the limited quantities of RD AMD available for subsequent experimental work. The solutions were swirled to wet the grass completely and the bottles were sealed. pH, ORP and DO measurements were taken and recorded over eight days.

5.5 Testwork to establish the effects of multiple additions of fresh grass to AMD on solution pH, ORP, and DO

Six grass types were selected for further test work to establish if multiple additions of fresh grass to AMD, resulted in an incremental increase in pH Three grasses from the previous, single grass addition experiment that demonstrated the highest increase in pH, and three different grass types were randomly selected to include for verification of previous data and comparison.

5.5.1 Multiple grass addition experiment - Sample and reactor preparation

Samples were prepared in the same way as for the previous experiment. Duplicate portions of each grass sample were weighed into separate Consol bottles. RD AMD was added to the first grass portion and synthetic AMD was added to the second grass portion. A 30 g/L solid-to-liquid ratio was maintained throughout this experimental work, which was terminated after 10 days. Blank samples were included using RD water and synthetic AMD solutions. Immediately after reactor preparation and mixing, pH, ORP and DO were measured. These parameters were measured on day three and immediately after the grass was removed from the reactor solutions by filtration, and a second portion of fresh grass was added on day four. The same parameters were measured on the seventh day before removing the spent grass, and immediately after the addition of the third portion of fresh grass. The third portion of grass was removed on the ninth day and final measurements were taken on day 10 when the experiment was terminated. All spent grass was dried at 60°C for 60 hours, pulverized and passed through an 80 µm-mesh screen where the -80 µm fraction was retained for chemical analysis.

5.5.2 Chemical analysis of grass samples before and after contact with AMD

The grass samples retained from the second experiment were prepared for analysis by digesting in an Anton Paar Multiwave GO - Microwave digestion system, using a rapid digestion procedure described by Huang et al. (2004). The samples were made up to volume in a 1% ultrapure nitric acid solution from which a ten-times dilution was made in the same 1% ultrapure nitric acid before submitting to the School of Chemistry at the University of Johannesburg for chemical analysis. An inductively coupled plasma–optical emission spectrometry (ICP–OES) - Spectro Arcos (SOP) was used to analyse sodium (Na), magnesium (Mg), potassium

(K), calcium (Ca), phosphorus (P), and all sulfur-containing compounds as (S), while an inductively coupled plasma-mass spectrometry (ICP–MS), Perkin Elmer NexION 300D B was used to analyse aluminium (Al), manganese (Mn), cobalt (Co), copper (Cu), zinc (Zn), and lead (Pb) (Havlin and Soltanpour, 1980; Huang *et al.*, 2004). Quality control samples for these analyses included analysis of a reagent blank, a Tea Leaves certified reference material (CRM) and a duplicate analysis of the G15 (Vetiveria) grass sample. All sample and CRM data are presented in Supplementary data for Chapter 5, Appendix II-D, Table D.1, where averaged values of duplicate samples are reported with their standard deviations. Duplicate samples returned excellent precision, and duplicate G15, T2, and the Tea Leaves CRM samples reported relative standard deviations (RSD)s of less than 5% for all elements. The G15, T0 duplicate samples, returned more varied RSDs, which could have resulted from digestion or instrumental inconsistencies; Na, Mg, K, Ca, S, B, and Zn returned RSDs of below 5%, Mn and Cu returned RSDs of ≤ 10%, and P, Al, Co and Pb returned RSDs over 14%. The Tea Leave CRM returned concentrations within specified tolerances for most elements except for Na and Co. The elevated recovery for Na in the CRM material can be attributed to the reduced instrumental sensitivity for this element at low concentrations, and Co reported a marginally low biased concentration.

5.6 Results

5.6.1 Grass classification

Grasses were identified by comparing the sampled grasses with specimen grasses catalogued at the Moss Herbarium at the University of the Witwatersrand, Johannesburg facilities. The grass site identification and grass classification are given in Supplementary data for Chapter 5, Appendix II-A, Table A.1.

Hyparrhenia hirta were identified individually at five of the sampling locations and mixed with other grasses at the G10 and G14 locations. *Eragrostis curvula* grass was identified at four locations, and the remaining grass varieties included, *Digitaria eriantha*, *Eragrostis plana*, *Hyparrhenia filipendula*, *Pogonarthria squarrosa*, and *Chrysopogon zizanioides* (Table 5.1).

Table 5.1 Grass name and classification

Grass Type	Grass Site Identification
Hyparrhenia hirta	G2, G8, G9, **G10**, G12, G13, **G14**
Digitaria eriantha	G1
Eragrostis curvula	G4, G6, G7,G16
Chrysopogon zizanioides	G15
Pogonarthria squarrosa	G11
Eragrostis plana	G3
Hyparrhenia filipendula	G5

5.6.2 Composition of grass

The average structural, proximate, CV, and ultimate, ranges were determined for all grass types at all locations are presented in Table 5.2.

Table 5.2 The averaged structural, proximate, ultimate, and calorific value analysis concentration ranges of the collected grass samples

Parameter (Structural)	Composition (%)	Parameter (TGA – Proximate) & (CV)	Composition TGA (%), CV (MJ/kg)	Parameter (Ultimate)	Composition (%)
Cellulose	22.5 – 39.9	Moisture	2.3 – 4.1	T Carbon	32.6 – 47.4
Hemicellulose	20.9 – 25.2	Volatiles	58.9 – 81.3	T Sulfur	0.11 – 0.53
Lignin	17.5 – 22.5	Fixed C	14.8 – 19.1	Nitrogen	0.00 – 1.0
Extractives	2.1 – 6.7	Ash content	0.00 – 22.6	Hydrogen	5.0 – 6.6
		CV	13.7 – 19.3	Oxygen	45.7 – 61.5

Cellulose was the most abundant structural component in the grass samples analysed. An unusually low cellulose content of 22.5% was reported for G14, while the remaining grasses reported cellulose content ranging between 28.6 – 39.9%. The cellulose content reported lower average compositions than the 40 – 50% as stated by Shahzadi et.al., (2014), but within the 25 – 40% range given for grasses by Malherbe and Cloete, (2002). The 17 – 23% lignin content and 21 – 25% hemicellulose content were within the expected concentration range for agricultural biomass (Malherbe and Cloete, 2002; Shahzadi *et al.*, 2014).

Proximate analysis data reported an average moisture content of between 2.3 – 4.1% for all the grass samples. Except for the G14 grass which presented an unusually high ash content, the remaining grass samples presented a percentage ash content similar to the variations for weeping love grass, switchgrass, elephant grass and dwarf Napier grass, as reported by Burman et.al, (2019).

The total carbon, total sulfur, hydrogen, and nitrogen content were analysed using an Elementar, Vario EL cube CHNS analyser, and the oxygen content was calculated by difference.

The averaged data and standard deviations for the individual grasses are given in Supplementary data for Chapter 5, Appendix II-A, Tables A.2, A.3 and A.4, respectively.

5.7 Single grass addition - Determination of the suitability of grass for AMD remediation

This experiment intended to establish the suitability of different grass types collected from the Mpumalanga coalfields, South Africa, to aid AMD remediation by increasing the pH of contacted AMD. pH and ORP were selected as the test parameters to measure the changes in AMD over time. pH measurements would provide information on the H^+ concentration, while ORP readings would provide information on the AMDs' overall reducing or oxidising capacity. pH, ORP and DO data are used as control measurements in wastewater treatment systems, and ORP values provide a quick measurement of possible biological (oxidation-reduction) reactions occurring in treatment systems (Corominas *et al.*, 2006; Environmental, Y.S.I., 2008). These data were recorded before and after the addition of each grass type to AMD. All grasses were tested using synthetic AMD, and G6 and G15 grass types were also tested using RD AMD. Dissolved oxygen (DO) readings were recorded from the second day of experimental work, and since the initial DO concentrations were not determined before grass addition, these data were not considered conclusive. The changes in pH observed for the synthetic and the RD samples are shown in Figure 5.3. Synthetic sample data are represented as triangles, while the RD data are represented as circles.

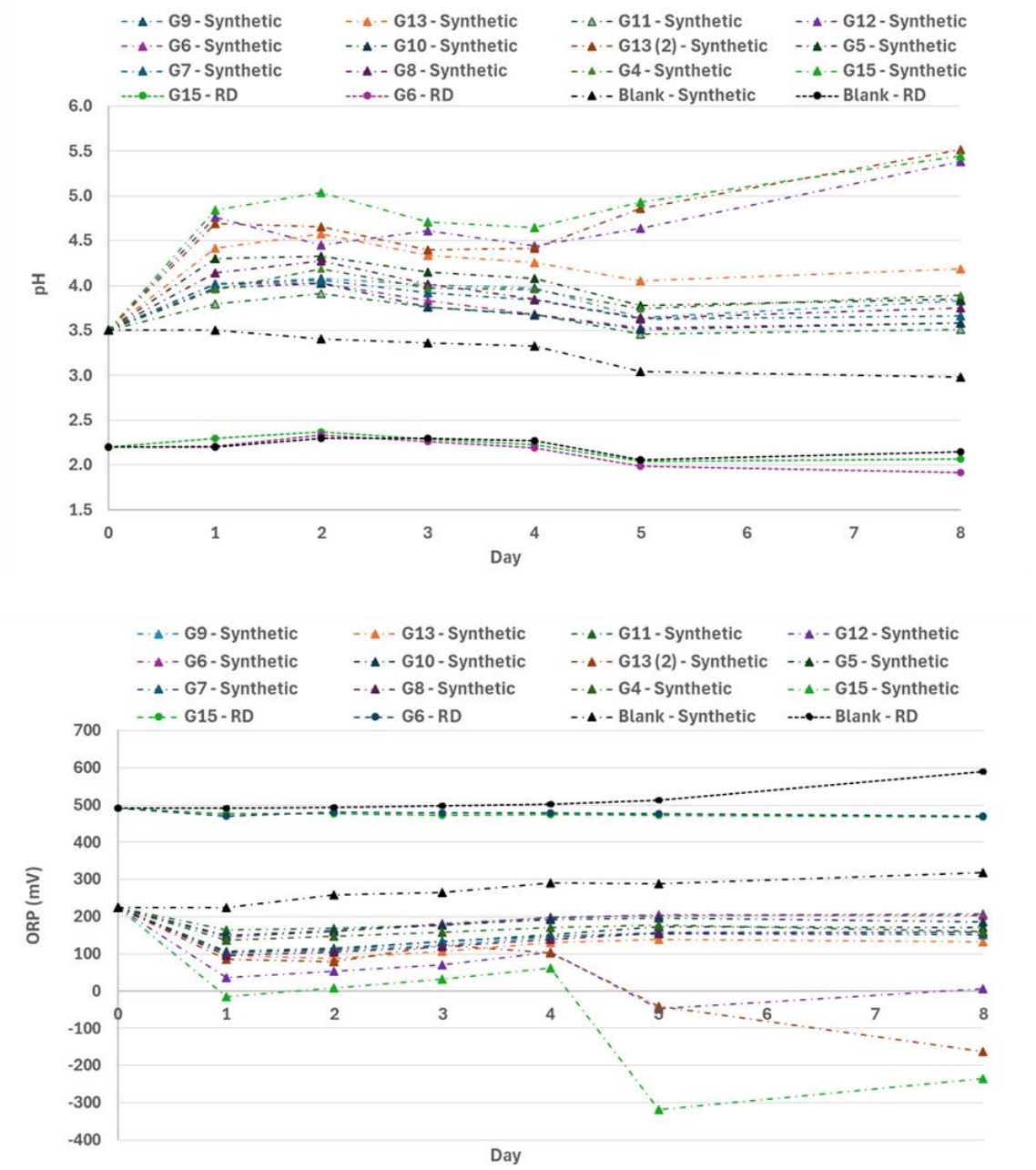


Figure 5.3 pH and ORP data for synthetic and receiving dam (RD) AMD solutions after grass addition

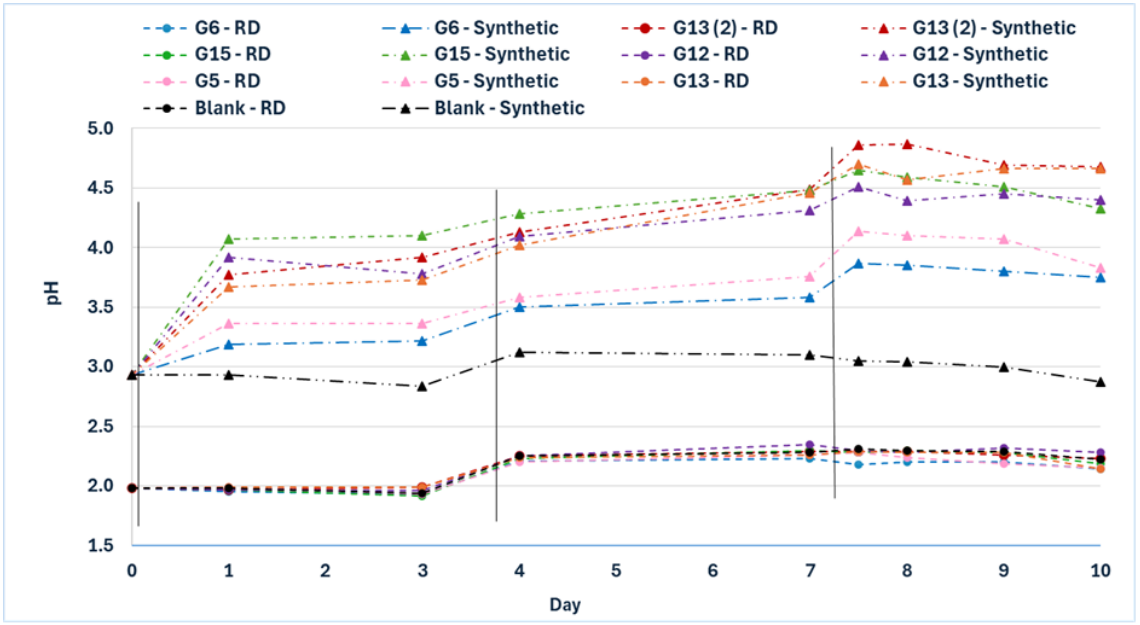
The samples containing the synthetic *Hypermedia hirta* (G12 and (G13 (2)), and *Chrysopogon zizanioides* (G15) grass types presented the greatest initial increase in pH on the first day after grass addition increasing from a pH of 3.5 to an average of pH of 4.8. A significant increase in pH was observed after the fourth day for these samples reporting the highest final average pH of ≈5.5 on the eighth day after the termination of the experiment. The remaining samples containing synthetic AMD reported an increase of between 0.5 and 1.0 pH units on day one after the addition of grass, and marginal to no increase on the second day, followed by a decrease in pH until the termination of the experiment, reporting a final average pH of ≈3.7. The synthetic blank gradually decreased in pH for the duration of the experiment, while marginal changes were observed

for the RD samples and any change observed in the sample H^+ concentration was also observed in the RD blank sample. Both synthetic and RD blank samples reported decreased pHs after the experiment. The drop in pH for the blank samples was expected because of the dissolution of CO_2 from the atmosphere into the AMD solution resulting in the formation of carbonic acid and, the probability of precipitation of ferric hydroxide at pH levels between pH 2.3 and 3.5, which removes ferric iron from solution resulting in the production of further hydrogen (H^+) ions with subsequent reduction of pH levels (Akcil and Koldas, 2006; Bowman, Agrawal and Sharma, 2023).

ORP values for these samples varied throughout the experiment. The RD samples reported initial ORP values of 491 mV, and the synthetic samples reported initial ORP values of 224 mV. ORP changes of between 4 – 4.7%, were observed for the RD samples, compared with the 7.5 – 205% change in ORP for the synthetic samples. The changes in ORP for the synthetic samples and blanks generally inversely followed the trends observed in pH, with G12, G13 (2) and G15 samples showing a significant reduction in ORP between the fourth and fifth days, moving from positive to negative ORP values (Figure 2). The decrease in ORP with the concomitant hydrogen ion (H^+) concentration decrease (pH increase), could be a result of a DSR reaction where electrons are donated from carbohydrates present in the grass resulting in the neutralisation of pH and consumption of H^+ (Bowman, Agrawal and Sharma, 2023). This was however not confirmed experimentally, and the negative ORP readings were used as an indication of a possible biological process occurring (Environmental, Y.S.I., 2008). All pH, ORP, and DO data are presented in Supplementary data for Chapter 5, Appendix II-B, Tables B.1, B.2 and B.3 respectively.

5.8 Multiple grass addition - The effects of multiple additions of fresh grass to AMD on solution pH, ORP, and DO

Initial measurements were recorded on the first day before and after the addition of grass to the AMD samples. Measurements were taken on the fourth day after the removal of the spent grass and the addition of a second portion of fresh grass. Measurements were taken on the seventh day before and immediately after the addition of the third portion of fresh grass. The third portion of grass was removed on the ninth day after measuring parameters, and final measurements were taken on the tenth day before terminating the experiment. The pH and ORP data for the synthetic and RD samples are shown in Figure 5.4. The vertical lines indicate the addition of fresh grass portions.



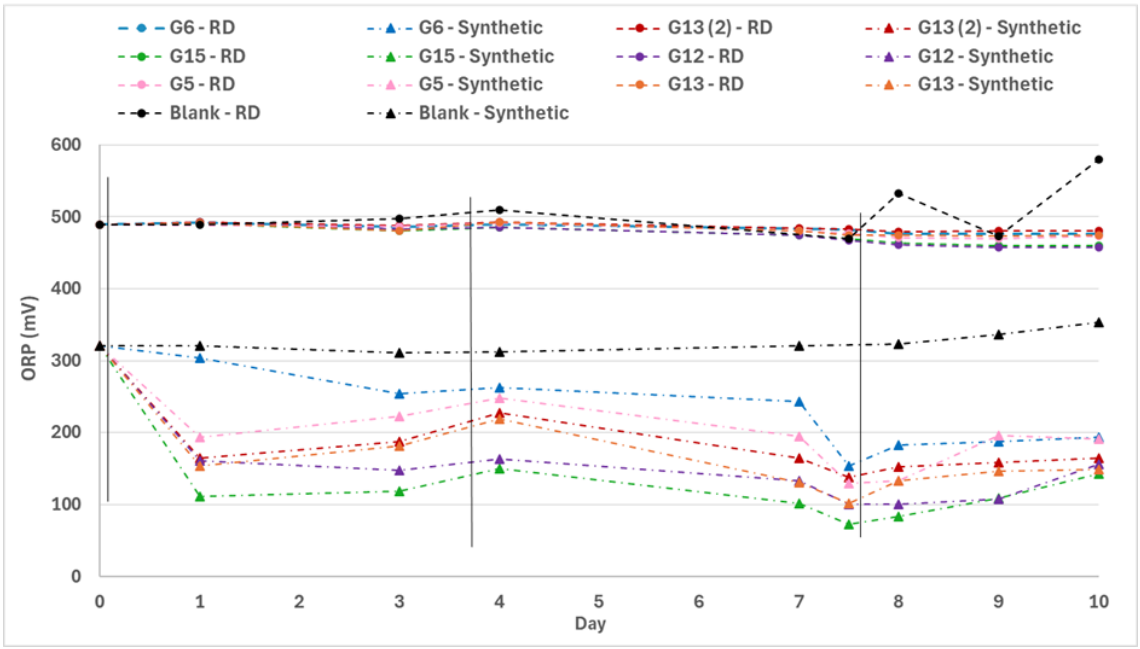


Figure 5.4 pH and Eh data for synthetic and return dam (RD) AMD solutions after subsequent grass addition

An increase in pH was observed for all synthetic samples immediately after each successive grass addition. The synthetic and RD blank samples showed an unexpected increase in pH after the second grass addition, indicating that the pH increase observed after the addition of this grass portion, could be attributed to instrumental error, despite the pH meter being calibrated before analysing the samples. This explanation is supported by the increased rather than the expected decrease in ORP associated with a pH increase (decrease in H^+ concentration). The changes in pH observed for the RD samples followed the trends observed in the RD blank sample, which would suggest that the grass did not achieve any notable change in pH in the

RD samples. This testwork reported similar increases in pH for both G13 and G13 (2) synthetic samples, and the highest overall pH values were achieved for the G12 and G13 and G15 grasses. The replenishment of the fresh grass in the multiple grass addition experiment appeared to maintain the pH increase in the synthetic AMD samples for the duration of the experiment. The decrease in pH of the synthetic blank sample observed after the experiment would support the dissolution of CO_2 from the atmosphere with a concomitant increase in H^+ concentration (Bowman et al., 2023).

The RD samples reported an initial ORP of 489 mV which was similar to the initial ORP value for the single grass addition experiment, while the synthetic samples reported a higher initial ORP value of 321 mV compared with the 224 mV recorded for the single grass experiment. An anomalous reduction in ORP recorded for the RD blank on the seventh day, and an anomalous increase in ORP for the synthetic blank recorded on the eighth day, were probably owing to a sample swap, and these data were omitted from Figure 5.3. The RD and synthetic blank samples demonstrated increased final ORP values, while all samples reported reduced final ORP values. Changes in ORP for the RD samples ranged between ≈1.8 – 6.5%, compared with the ≈39.9 – 53.6% range observed for the synthetic samples. The larger decrease in ORP observed in the synthetic AMD samples would support the more significant increase in pH observed for these samples (Bowman, Agrawal and Sharma, 2023). Synthetic samples reported an initial DO concentration of 73% compared with 29% for the RD samples. Spurious data reported on day four for the synthetic G13, and day ten, for the RD G13 (2) samples could have been as a result of inadvertent analysis duplication of the respective preceding and subsequent samples. Except for the synthetic G15, G13 (2) and G12 samples, the DO concentration for all samples increased after the first grass addition. A negligible change in DO concentration was observed after the second grass addition, and a pronounced increase in DO concentration was noted immediately after the third grass addition. The final DO concentration for synthetic samples reported between ≈4 and ≈13%, and RD samples reported between ≈66 and ≈77%. The depletion of DO concentration observed in the synthetic samples could be aligned with a DSR reaction where electrons are accepted by sulfate for microbial respiration, but this was not confirmed experimentally (Zhou *et al.*, 2022). The behaviour of the blank samples cannot be explained, the synthetic blank sample DO concentration declined, from ≈70% to ≈50%, while the RD blank DO concentration declined from ≈30% to ≈10%, but then increased after the third grass addition, to report a final DO concentration of ≈50%. The data for testwork conducted to determine whether the addition of fresh grass significantly affected the changes observed in pH in AMD samples are presented in Supplementary data for Chapter 5, Appendix II-C, Tables C.1, C.2 and C.3 for pH, ORP and DO, respectively.

5.9 Elemental concentration data for grass samples before and after subsequent addition to AMD

To explore whether the increase in pH could have resulted from an ion-exchange reaction between the hydronium ions in the AMD and the inorganic cations present in the grass (Springer and Harris, 1985), the relevant concentrations of cations and sulfur in the grass were determined before and after grass addition. Analysis was conducted using ICP:OES and ICP:MS after microwave digestion of selected grass samples. The elements present in the highest concentrations included K, S, Ca, Mg, P, Al and Na respectively, which were per the principal cation components in wood described by Springer and Harris (1985). In this instance, all sulfur compounds reported as S. Quality control measures included analysis of a sample blank, duplicate analysis of the original, the first addition of G15 grass samples, and analysis of a Tea Leaves certified reference material (CRM). Except for Na, which was present in low concentrations, the CRM concentrations returned values within the accepted tolerances. All sample and CRM data are presented in Supplementary data for Chapter 5, Appendix II-D Table D.1 where averaged values of duplicated samples were reported with their standard deviations. The poor CRM recovery for Na could be attributed to reduced instrumental sensitivity for Na at low concentrations. However, except for the low Na concentrations observed in the initial *Hyparrhenia filipendula* and *Eragrostis curvula* grass samples, Na reported concentrations in orders of magnitude higher than the given CRM value. At these high concentrations, Na would not be subject to the instrumental error observed at method detection limits. The K, Mg, Ca, P, Na and S concentrations are shown in Figure 5.5 where the first, second and third grass addition samples are denoted as Add 1, Add 2, and Add 3 respectively.

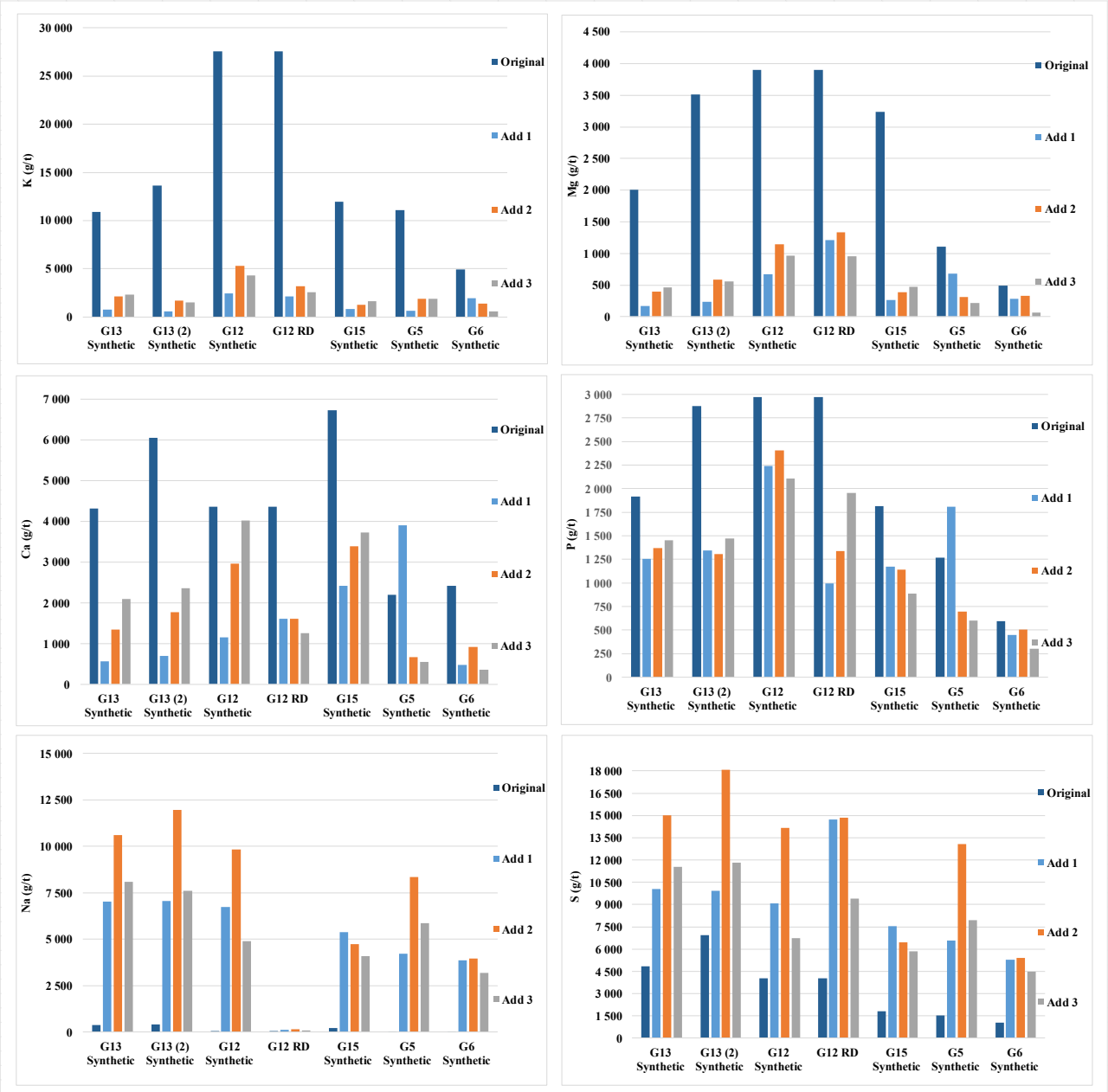


Figure 5.5 K, Mg, Ca, P, Na and S concentrations in grass samples before and after subsequent addition to AMD. Samples 13, 13 (2), and 12 are classified as Hyparrhenia hirta, grass 15 is classified as Chrysopogon zizanioides, G5 as Hyparrhenia filipendula, and G6 as Eragrostis curvula.

The *Hyparrhenia hirta* grass type reported the highest initial K concentrations, followed by *Chrysopogon zizanioides*, *Hyparrhenia filipendula* and *Eragrostis curvula*. Decreased K concentrations were reported in all grass types after the addition of AMD.

The *Hyparrhenia hirta* and *Chrysopogon zizanioides* grass types reported the highest initial Mg concentrations, followed by *Hyparrhenia filipendula* and *Eragrostis curvula* grass types which reported

between 50 – 75% lower Mg concentrations. Decreased Mg concentrations were reported in all grass types after the addition of AMD.

The *Chrysopogon zizanioides* and *Hyparrhenia hirta* grass types reported the highest initial Ca concentrations compared with the *Hyparrhenia filipendula* and *Eragrostis curvula* grass types. All first-addition grasses reported decreased Ca concentrations except for an unexplained increase in Ca concentration that was observed for the first addition *Hyparrhenia filipendula* grass sample. Increased Ca concentrations were reported for the second- and most third-addition grasses. The third addition synthetic AMD *Hyparrhenia filipendula* and *Eragrostis curvula* grass samples, and the *Hyparrhenia hirta* RD AMD grass samples reported decreased Ca concentrations.

The *Hyparrhenia hirta* and *Chrysopogon zizanioides* grass types reported the highest initial P concentrations, followed by *Hyparrhenia filipendula* and *Eragrostis curvula* grass types. All first addition grasses reported decreased P concentrations except for an unexplained increase in P concentration that was observed for the first addition *Hyparrhenia filipendula* grass sample. An increase in P concentration was observed for the third grass addition for most *Hyparrhenia hirta* samples, while the remaining grass types showed decreased P concentrations in the third addition grasses.

All initial grass samples reported between one and two orders of magnitude lower Na concentrations compared with the Na concentrations reported for the first, second and third grass addition samples. Except for the synthetic *Eragrostis curvula*, *Chrysopogon zizanioides*, and the RD *Hyparrhenia hirta* grass, the concentrations of Na in the second grass addition reported between 46% – 97% more than the first addition grasses. Decreased Na concentrations were observed for all third-addition samples, which, in most instances reported similar Na concentrations to the first addition grass concentrations.
Despite initial S concentrations reporting at least one order of magnitude greater than initial Na concentrations, S concentrations followed the same trends observed for Na concentrations.

5.10 Discussion

Conversion of logarithmic pH values to hydrogen ion (H^+) concentrations in mmol/L presented an increase in pH as a decrease in H^+ concentration. The H^+ concentration for the synthetic single and multiple grass experiments decreased while marginal to no decrease in H^+ concentration was observed in the multiple grass experiment. Any decrease in H^+ concentration observed for the RD samples was also observed in the RD blank, indicating that the addition of fresh grass did not achieve any significant reduction in H^+ concentration in these samples. The complex sample matrix and higher mineral acidity present in the RD AMD could explain why little to no reduction in H^+ concentration was observed in these samples (Smith *et al.*, 2022).

The H^+ concentration data were used to calculate the percentage change in H^+ concentration after the initial grass addition, and the overall change in H^+ concentration compared with the initial H^+ concentration after each subsequent grass addition and at the termination of the single and multiple grass experiments. The percentage change in H^+ concentration for the synthetic AMD sample data is presented in Table 5.3.

Table 5.3 Percentage change in hydrogen ion concentration (H^+) from initial H^+ concentration after each successive grass addition to synthetic AMD, and after the experiment.

% Change in H+ from before grass addition - Synthetic samples						
Grass ID	**Single Grass - Day 1**	**Single Grass - Day 8**	**Multiple Grass - ADD 1**	**Multiple Grass - ADD 2**	**Multiple Grass - ADD 3**	**Multiple Grass removed - Day 8**
G13	-88	-79.6	-81.8	-91.9	-98.3	-97.7
G13 (2)	-93.5	-99	-85.5	-93.7	-98.8	-98.9
G12	-94.5	-98.7	-89.8	-93.1	-97.4	-96.5
G15	-95.4	-98.9	-92.8	-95.5	-98.1	-97.8
G6	-69.8	-16.8	-45	-73.1	-88.5	-88.0
G5	-84.2	-55.3	-62.8	-77.6	-93.8	-93.2
Blank	0	231.1	0	-35.4	-24.1	-222.4

The first grass addition for the multiple grass experiment yielded a smaller percentage decrease in H^+ concentration than was observed in the single grass addition experiment. This could be because of the elevated initial synthetic and RD AMD H^+ concentrations reported for the multiple grass experiment. The percentage decrease from initial H^+ concentration was enhanced with each successive grass addition in the multiple grass experiment and an improved overall percentage decrease in H^+ concentration was reported for the synthetic *Hyparrhenia hirta* (G13), *Eragrostis curvula* (G6), and *Hyparrhenia filipendula* (G5) samples. The *Chrysopogon zizanioides* (G15), *Hyparrhenia hirta* (G12 and G13 (2)) samples which performed best in the single grass experiment, reported similar percentage decreases in H^+ concentration after the multiple grass experiment.

A decreased decline in percentage H^+ concentration was noted for the final readings taken one day after the removal of the last portion of grass in the multiple grass experiment and would suggest that grass addition did support the reduction in H^+ concentration. The *Hyparrhenia hirta* (G12 and G13), and *Chrysopogon zizanioides* (G15) grasses achieved the greatest percentage decrease in H^+ concentration and the lowest H^+ concentration (highest pH) in both single and multiple grass experiments. All H^+ data are shown in Supplementary data for Chapter 5, Appendix II-B, Tables 4 – 6 for the single grass experiments, and Appendix II-C, Tables 4 – 6 for the multiple grass experiments.

Except for the *Chrysopogon zizanioides* (G15), and *Hyparrhenia hirta* (G13 (2)) samples, the DO concentrations of the synthetic samples initially increased by between 4% and 13% in the multiple grass experiment. DO concentrations then decreased between 24% and 79% between the second and third days, reporting a final decrease in DO concentration of between 82% – 94% from the starting DO concentration. The RD samples reported a ≥150% increase in DO concentration after the first grass addition. In most instances, a marginal increase in DO concentration was noted after each grass addition, which was generally followed by a reduction in DO concentration. The final increase in RD DO concentrations remained at ≥129% of starting concentrations.

The decreasing DO concentrations observed over time in the synthetic grass samples could indicate the establishment of an anaerobic system over time, which is required to facilitate a dissimilatory reduction (DSR) process. This would be supported by the increased pH values observed and decreased ORP values for the synthetic samples, which could be attributed to the additional alkalinity produced from the reduction of sulfate in the system, which is further supported by the decrease in ORP observed (Ayala-Parra, Sierra-Alvarez and Field, 2016; Bowman, Agrawal and Sharma, 2023). This can however not be confirmed, as the decrease in sulfate and metal(oid) concentration in the AMD was not determined as part of this experimental work.

The correlation between H^+ concentration and ORP was tested for each grass addition using the Excel data analysis tool at a 95 % confidence level. A strong positive correlation was observed after the first grass addition, reporting $r(11) = .85$, $p < .05$ and $r(5) = .92$, $p < .05$ for the synthetic AMD single and multiple grass experiments respectively. The correlation weakened to $r(11) = .65$, $p < .05$ on day eight at the end of the single grass experiment. In the multiple grass experiment, the correlation weakened to $r(5) = .85$, $p < .05$ after the addition of the second grass portion and then strengthened to $r(5) = .99$, $p < .05$ after the addition of the third grass portion on day seven. The correlation observed on day eight of the multiple grass experiment had weakened to $r(5) = .94$, $p < .05$ but remained stronger than the correlation reported on the eighth day for the single grass experiment. The H^+ concentration was positively correlated with the ORP, which confirms the negative correlation observed between pH and ORP (Bowman, Agrawal and Sharma, 2023). A plot of the correlation which included all data for the duration of the single and multiple grass experiments (Figure 5.6), using H^+ concentration as the independent (x) variable and the ORP value as the dependent (y) variable, gave a correlation coefficient (R^2) of 0.89 which was fit to a logarithmic curve for the single grass addition experiment, and a R^2 of 0.91 which was fit to a polynomial curve for the multiple grass experiment. Owing to the limited change in pH and ORP observed in the RD AMD, these samples generally produced poor H^+/ORP correlation.

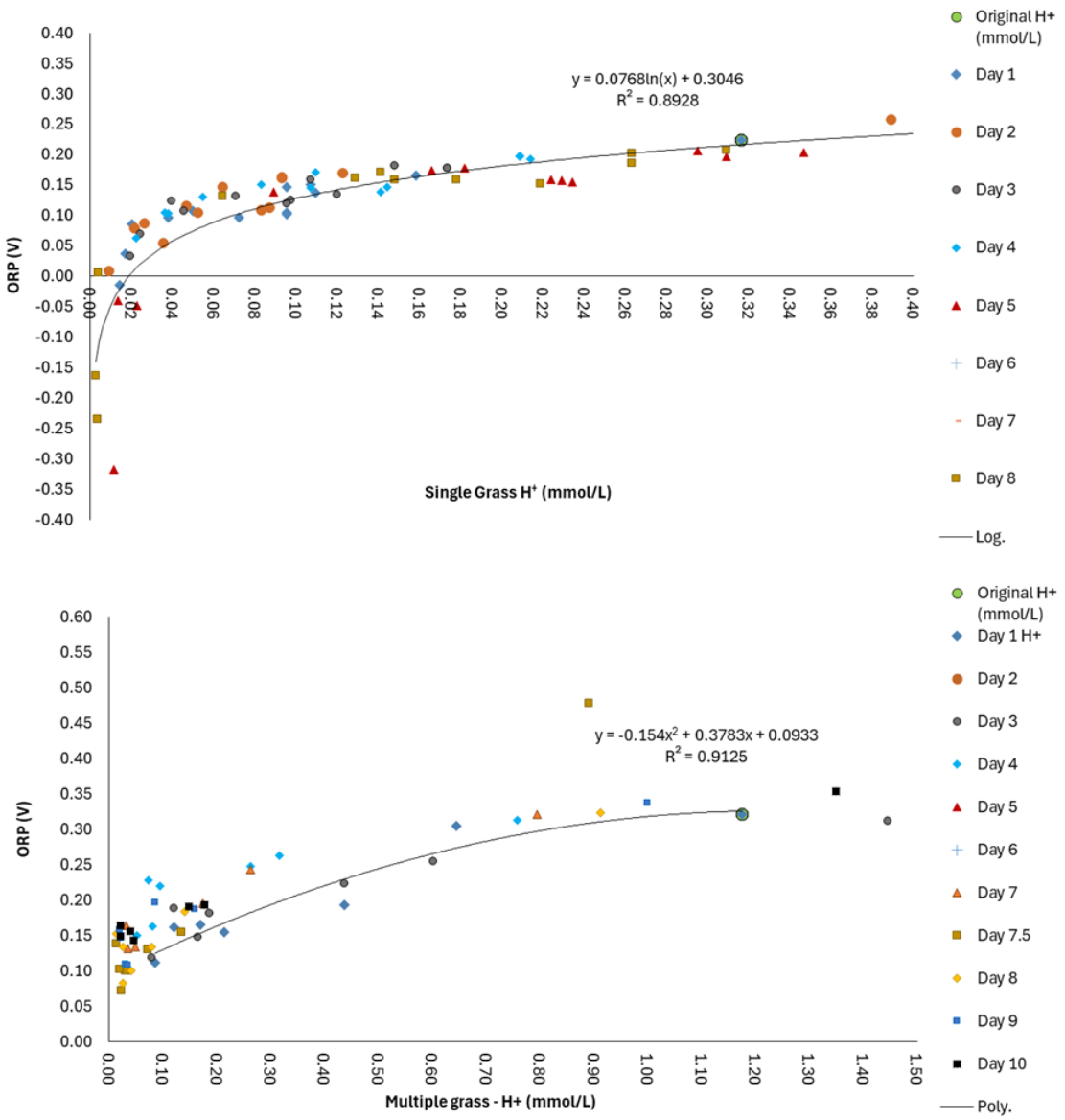


Figure 5.6 Oxidation-reduction potential (ORP) plotted as a function of hydrogen ion concentration (H^+) for single and multiple grass additions

Analysis of the major cations in the grass samples before and after addition to AMD showed the most pronounced decrease in K, Ca, and Mg concentrations observed in the first-addition grass, except for the *Hyparrhenia filipendula* (G5) first-addition grass which increased in Ca concentration. Again, except for the *Hyparrhenia filipendula* (G5), and *Eragrostis curvula* (G6) samples, these elements generally reported increased concentrations for second and third addition grasses. The K, Ca, and Mg concentrations for all grasses' third-addition grasses were lower than the original sample concentration. The decreased cation concentrations reported could be a result of ion exchange reactions occurring between the inorganic anions associated with the cations present in the grasses and the H+ ions in the AMD, in a similar mechanism as suggested by Springer and Harris (1985) (Springer and Harris, 1985). A decrease in H^+ concentration would

result in an increase in pH, which might have caused precipitation of Na_2SO_4 and thus explain the increased Na^+ and S^{2-} concentrations observed in the synthetic first, second and third grass addition samples. The additional sodium in the synthetic AMD samples was probably introduced from the sodium hydroxide (NaOH) used in the preparation of the synthetic AMD solution. No additional NaOH was introduced into the RD AMD sample, and previous analysis of this solution reported Na concentrations of less than 35 mg/L (Smith et al., 2021).

The best-performing grass types *Hyparrhenia hirta* (G12, G13) and *Chrysopogon zizanioides* (G15), reported higher moisture, extractives, total sulfur, oxygen, and lignin content, and the lower volatile, total carbon, Hydrogen, and CV content, than the *Eragrostis curvula* (G6), and *Hyparrhenia filipendula* (G5) samples. Percentage differences between the highest and the average concentration, and lowest and the average concentration for most components ranged between zero and 8.6%. The most notable difference from the average was reported for *Hyparrhenia hirta* (G13) grass type which reported ≈154% more than the average Total S concentration, and the *Hyparrhenia filipendula* (G5) grass type, which reported ≈88% less than the average Total S concentration. The *Hyparrhenia filipendula* (G5) grass type reported 18.9% less than the average moisture concentration. The variances from the average were not consistent for the best and worst performing grass types, making it difficult to assess whether compositional variances had any direct impact on the increase in pH of the synthetic AMD solutions.

5.11 Conclusions

The increase in the pH, or decrease in H^+ concentration, observed in all synthetic AMD solutions would indicate that the grass types tested could be considered suitable for use in AMD remediation. Multiple grass additions to synthetic AMD achieved a sustained and elevated percentage H^+ reduction for the duration of the experiment and facilitated a greater percentage H^+ reduction for the grass types *Eragrostis curvula* (G6), *Hyparrhenia filipendula* (G5) and *Hyparrhenia hirta (G 13)* that performed more poorly in the single grass addition experiment. The varying results achieved by the different grass types would indicate that some grass types would be more suited for AMD remediation. The *Hyparrhenia hirta* (G12, G13 (2)), and *Chrysopogon zizanioides* (G15) grass types achieved the greatest increase in pH in both the single and multiple grass experiments. A decrease in cation concentration of the grass samples from the multiple grass addition experiment could indicate the likelihood of a cation-anion exchange reaction between the H^+ ions in the AMD and the inorganic cations associated with the anions present in the grass. Single and multiple grass additions were, however, not successful in increasing the pH of the RD AMD samples under the given conditions. The varied structural and physical composition of the different grass types did not provide conclusive evidence on whether compositional parameters had any effect on the increase in pH.

5.12 Recommendations

Further test work should be conducted using different grass:AMD ratios and using aerobic and anaerobic conditions to establish if changing experimental parameters could achieve a greater decrease in H^+ concentration in RD AMD. Testwork should include the determination of all metal(oid)s, Fe, and sulfate concentrations to verify that a DSR process is occurring.

5.13 Acknowledgements

The authors thank Dr Renee Reddy the C.E. Moss Herbarium manager, for her guidance and assistance with the classification of the grass types.

5.14 References

Akcil, A., Koldas, S., 2006. Acid Mine Drainage (AMD): causes, treatment and case studies. J. Clean. Prod. 14, 1139–1145. https://doi.org/10.1016/j.jclepro.2004.09.006

Ayala-Parra, P., Sierra-Alvarez, R., Field, J.A., 2016. Algae as an electron donor promoting sulfate reduction for the bioremediation of acid rock drainage. J. Hazard. Mater. 317, 335–343. https://doi.org/10.1016/j.jhazmat.2016.06.011

Ayeni, A.O., Adeeyo, O.A., Oresegun, O.M., Oladimeji, T.E., 2015. Compositional analysis of lignocellulosic materials: Evaluation of an economically viable method suitable for woody and non-woody biomass A. Am. J. Eng. Res. 4, 14–19.

Bowman, S., Agrawal, V., Sharma, S., 2023. Role of pH and Eh in geothermal systems: Thermodynamic examples and impacts on scaling and corrosion. Geothermics 111, 102710. https://doi.org/10.1016/j.geothermics.2023.102710

Burman, N.W., Harding, K.G., Sheridan, C.M., Van Dyk, L., 2018. Evaluation of a combined lignocellulosic / waste water bio-refinery for the simultaneous production of valuable biochemical products and the remediation of acid mine drainage. Biofuels Bioprod. Biorefining 12, 649–664. https://doi.org/10.1002/bbb.1880

Corominas, Ll., Sin, G., Puig, S., Traore, A., Balaguer, M., Colprim, J., Vanrolleghem, P.A., 2006. Model-based evaluation of an on-line control strategy for SBRs based on OUR and ORP measurements. Water Sci. Technol. 53, 161–169. https://doi.org/10.2166/wst.2006.120

Demirbaş, A., 2001. Biomass resource facilities and biomass conversion processing for fuels and chemicals. Energy Convers. Manag. 42, 1357–1378. https://doi.org/10.1016/S0196-8904(00)00137-0

Elementar Analysensysteme GmbH, 2023. Elementar vario EL CUBE, Experience the gold standard.

Environmental, Y.S.I., 2008. ORP Management in Wastewater as an Indicator of Process Efficiency (Application Note No. 1008 A567–01). YSI, Yellow Springs, OH.

Gazea, B., Adam, K., Kontopoulos, A., 1996. A review of passive systems for the treatment of acid mine drainage. Miner. Eng. 9, 23–42. https://doi.org/10.1016/0892-6875(95)00129-8

Havlin, J.L., Soltanpour, P.N., 1980. A nitric acid plant tissue digest method for use with inductively coupled plasma spectrometry. Commun. Soil Sci. Plant Anal. 11, 969–980. https://doi.org/10.1080/00103628009367096

Huang, L., Bell, R.W., Dell, B., Woodward, J., 2004. Rapid Nitric Acid Digestion of Plant Material with an Open-Vessel Microwave System. Commun. Soil Sci. Plant Anal. 35, 427–440. https://doi.org/10.1081/CSS-120029723

Ighalo, J.O., Kurniawan, S.B., Iwuozor, K.O., Aniagor, C.O., Ajala, O.J., Oba, S.N., Iwuchukwu, F.U., Ahmadi, S., Igwegbe, C.A., 2022. A review of treatment technologies for the mitigation of the toxic environmental effects of acid mine drainage (AMD). Process Saf. Environ. Prot. 157, 37–58. https://doi.org/10.1016/j.psep.2021.11.008

Johnson, D.B., Hallberg, K.B., 2005. Acid mine drainage remediation options: a review. Sci. Total Environ. 338, 3–14. https://doi.org/10.1016/j.scitotenv.2004.09.002

Johnson, D.B., Hallberg, K.B., 2002. Pitfalls of passive mine water treatment. Rev. Environ. Sci. Biotechnol. 1, 335–343. https://doi.org/10.1023/A:1023219300286

Koppram, R., Tomás-Pejó, E., Xiros, C., Olsson, L., 2014. Lignocellulosic ethanol production at high gravity: challenges and perspectives. Trends Biotechnol. 32, 46–53. https://doi.org/10.1016/j.tibtech.2013.10.003

Lakaniemi, A.-M., Tuovinen, O.H., Puhakka, J.A., 2013. Anaerobic conversion of microalgal biomass to sustainable energy carriers – A review. Bioresour. Technol. 135, 222–231. https://doi.org/10.1016/j.biortech.2012.08.096

Li, X., Shi, Y., Kong, W., Wei, J., Song, W., Wang, S., 2022. Improving enzymatic hydrolysis of lignocellulosic biomass by bio-coordinated physicochemical pretreatment—A review. Energy Rep. 8, 696–709. https://doi.org/10.1016/j.egyr.2021.12.015

Malherbe, S., Cloete, T.E., 2002. Lignocellulose biodegradation: Fundamentals and applications. Rev. Environ. Sci. Biotechnol. 1, 105–114. https://doi.org/10.1023/A:1020858910646

McCarthy, T.S., 2011. The impact of acid mine drainage in South Africa. South Afr. J. Sci. 107, 01–07.

Moyo, P., 2013. The application of a Distributed Activation Energy based model to the gasification and combustion of coal and biomass char blends (Dissertation). University of the Witwatersrand.

Petrova, P., Ivanova, V., 2010. Perspectives for the Production of Bioethanol from Lignocellulosic Materials. Biotechnol. Biotechnol. Equip. 24, 529–546. https://doi.org/10.1080/13102818.2010.10817894

Pone, J.D.N., Hein, K.A.A., Stracher, G.B., Annegarn, H.J., Finkleman, R.B., Blake, D.R., McCormack, J.K., Schroeder, P., 2007. The spontaneous combustion of coal and its by-products in the Witbank and Sasolburg coalfields of South Africa. Int. J. Coal Geol. 72, 124–140. https://doi.org/10.1016/j.coal.2007.01.001

Ramla, B., Sheridan, C., 2015. The Potential Utilisation of Indigenous South African Grasses for Acid Mine Drainage Remediation. Water SA 41, 247. https://doi.org/10.4314/wsa.v41i2.10

Rezania, S., Oryani, B., Cho, J., Talaiekhozani, A., Sabbagh, F., Hashemi, B., Rupani, P.F., Mohammadi, A.A., 2020. Different pretreatment technologies of lignocellulosic biomass for bioethanol production: An overview. Energy 199, 117457. https://doi.org/10.1016/j.energy.2020.117457

Shahzadi, T., Mehmood, S., Irshad, M., Anwar, Z., Afroz, A., Zeeshan, N., Rashid, U., Sughra, K., 2014. Advances in lignocellulosic biotechnology: A brief review on lignocellulosic biomass and cellulases. Adv. Biosci. Biotechnol. 05, 246–251. https://doi.org/10.4236/abb.2014.53031

Simate, G.S., Ndlovu, S., 2014. Acid mine drainage: Challenges and opportunities. J. Environ. Chem. Eng. 2, 1785–1803. https://doi.org/10.1016/j.jece.2014.07.021

Sluiter, A., Hames, B., Ruiz, R. O, Scarlata, C, Templeton, D, Crocker, C, 2012. Determination of Structural Carbohydrates and Lignin in Biomass Laboratory Analytical Procedure (LAP) (Technical No. NREL/TP-510-42618). NREL.

Smith, J., Sheridan, C., Van Dyk, L., Harding, K.G., 2022. Critical evaluation of the chemical composition of acid mine drainage for the development of statistical correlations linking electrical conductivity with acid mine drainage concentrations. Environ. Adv. 8, 100241. https://doi.org/10.1016/j.envadv.2022.100241

Smith, J., Sheridan, C.M., Van Dyk, L.D., Harding, K.G., 2021. Seasonal characterisation of acid mine drainage in Mpumalanga coalfields region. Presented at the SACEC, SCIENTIFIC COMMITTEE, p. 118.

Springer, E.L., Harris, J.F., 1985. Procedures for determining the neutralizing capacity of wood during hydrolysis with mineral acid solutions. Ind. Eng. Chem. Prod. Res. Dev. 24, 485–489. https://doi.org/10.1021/i300019a030

Tutu, H., McCarthy, T.S., Cukrowska, E., 2008. The chemical characteristics of acid mine drainage with particular reference to sources, distribution and remediation: The Witwatersrand Basin, South Africa as a case study. Appl. Geochem. 23, 3666–3684. https://doi.org/10.1016/j.apgeochem.2008.09.002

Westensee, D.K., Rumbold, K., Harding, K.G., Sheridan, C.M., Van Dyk, L.D., Simate, G.S., Postma, F., 2018. The availability of second-generation feedstocks for the treatment of acid mine drainage and to improve South Africa's bio-based economy. Sci. Total Environ. 637–638, 132–136. https://doi.org/10.1016/j.scitotenv.2018.04.410

CHAPTER 6.

6 Investigation of suitable, readily available, sources of sulfate-reducing bacteria inoculum, and evaluation of sulfate reduction rates achieved at different pHs

(Published in Environmental Microbiology Reports, 2025)
Smith, J., Sheridan, C., van Dyk, L. and Harding, K.G. (2025), Investigation of Suitable, Readily Available, Sources of Sulfate-Reducing Bacteria Inoculum, and Evaluation of Sulfate Reduction Rates Achieved at Different pHs. Environmental Microbiology Reports, 17: e70081. https://doi.org/10.1111/1758-2229.70081

This chapter addresses objective (c): To source naturally occurring sulfate reducing bacteria (SRB) inoculum in different pH environments and compare then in the production of sulfides.

The work presents an investigation into the suitability of naturally occurring sulfate reducing bacteria (SRB) for use in AMD bioremediation, and their activity at different pH values. The inoculum sources assessed included AMD water (AMD), mud (MUD) and reed-bed mud (RM) sourced from an AMD impacted environment, mealworms (MW), cow dung (CD), and raw sewage sludge (RS). The results show that only two of the six sources evaluated; RS, and RM, achieved appreciable reduction of sulfate to sulfide at neutral pH.

CRediTs: Janet Smith: Conceptualization, Methodology, Investigation, Validation, Formal analysis, writing-Original Draft; Craig Sheridan: Funding acquisition, Conceptualization, Resources, Supervision, Writing – Review and editing; Lizelle van Dyk: Conceptualization, Supervision, Writing – Review and Editing; Kevin Harding: Conceptualization, Supervision, Writing – Review and Editing

AKNOWLEDGEMENTS
The authors would like to thank the School of Chemical and Metallurgical Engineering of the University of the Witwatersrand, Johannesburg for the use of their laboratory facilities for this test work.

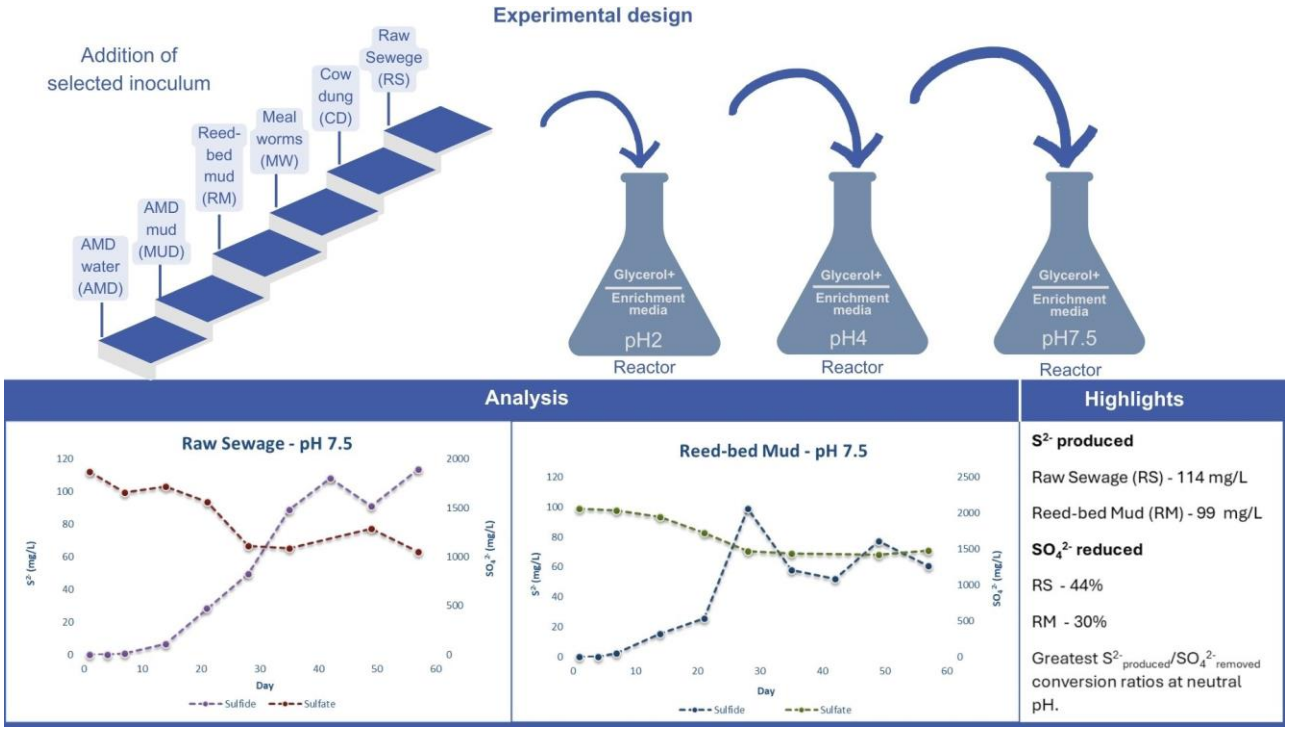


Figure 6.1 Visual abstract: The investigation of suitable, readily available, sources of sulfate-reducing bacteria inoculum, and evaluation of sulfate reduction rates achieved at different pHs

6.1 Abstract

This study investigated the suitability of readily available, and naturally occurring sources of microorganisms (inoculum) to use for the cultivation of sulfate-reducing bacteria (SRB) for acid mine drainage (AMD) remediation. The selected inocula included AMD water (AMD), mud (MUD) and reed-bed mud (RM) from the AMD surrounds, mealworms (MW), cow dung (CD), and raw sewage sludge (RS). The suitability of the different inoculum sources was evaluated by comparing the SO_4^{2-} reduction and sulfide (S^{2-}) production rates at three different pHs. Experimental results showed that the AMD, MW, MUD, and CD inoculum did not produce appreciable reduction of SO_4^{2-} to S^{2-} and were unsuitable sources of SRB inoculum. The inoculum evaluated in pH 2 media did not achieve SO_4^{2-} reduction. Of the inoculum assessed in pH 4 media, only the RM inoculum achieved SO_4^{2-} reduction (40%) with S^{2-} production (36 mg/L). In contrast, a notable S^{2-} production, RS (114 mg/L,) and RM (99 mg/L), accompanied the SO_4^{2-} reduction achieved in the pH 7.5 RS (44%), and RM (30%) samples. The improved S^{2-}produced/SO_4^{2-} removed conversion ratios for samples pH 7.5 RS (0.14) and pH 7.5 RM (0.17) are indicative of increased SRB activity and the suitability of these inoculum as SRB sources.

Keywords: Acid mine drainage (AMD); Circular economy; Dissimilatory sulfate reduction (DSR); Remediation processes; Sustainability

6.2 Introduction

AMD is a highly mineralised, acidic water that forms from exposure of sulfidic rock to oxygen and water during industrial and mining activities. AMD is a global problem and has caused substantial environmental issues, including the degradation of watercourses and surrounding ecosystems (McCarthy, 2011a; Simate and Ndlovu, 2014). Once AMD formation exceeds natural dilution capacity, remediation is necessary to prevent further ecological damage from this contaminated water. Active remediation processes are effective but often rely on the addition of chemicals, require high capital investment and operating costs and produce large quantities of waste sludge that requires disposal (Simate and Ndlovu, 2014; Costa, Verola, *et al.*, 2020; Zhang *et al.*, 2023). Development of a remediation process that uses waste, and/or naturally occurring, renewable materials is vital to ensuring a transition to a circular economy approach that is cost-effective, and sustainable, and uses waste products to produce clean water.

A key biological AMD remediation process is the reduction of SO_4^{2-} to S^{2-} using SRB via a dissimilatory sulfate reduction (DSR) process. This reaction consumes protons (H^+) producing S^{2-} and alkalinity resulting in an increase in pH and the concomitant precipitation of metals out of solution as metal sulfides (Gazea, Adam and Kontopoulos, 1996; Greben *et al.*, 2007; Sánchez-Andrea *et al.*, 2014; Ramla and Sheridan, 2015; Nogueira *et al.*, 2021; Ilin *et al.*, 2022). The theoretical S^{2-} production from SO_4^{2-} reduction is 0.33 (Greben *et al.*, 2007; Gil-Garcia *et al.*, 2023). In the DSR process, the SRB obtain energy for growth and development by anaerobic respiration using SO_4^{2-} as an electron acceptor (reduction) and organic carbon or hydrogen as an electron source (oxidation). In this instance, glycerol ($C_3H_8O_3$) was selected as a non-ionic carbon source owing to its low toxicity to the environment, easy availability, low cost, and the ability of non-ionic substrates to allow SO_4^2 reduction at pH 4 (Sánchez-Andrea *et al.*, 2013). Glycerol has an anticipated high-energy biomass production owing to its high negative Gibbs free energy change (Sánchez-Andrea *et al.*, 2013; Ilin *et al.*, 2022; Novair *et al.*, 2024). The carbon source is oxidized, and SO_4^{2-} is reduced as H^+ ions are consumed, resulting in an increase in pH (Zagury, Kulnieks and Neculita, 2006; Bekmezci *et al.*, 2011; Ilin *et al.*, 2022) (*Equation 6.1*).

$$7SO_4^{2-} + 4\ C_3H_8O_3 + 14H^+ \xrightarrow{SRB} 7H_2S + \ 12CO_2 + 16H_2O \qquad \textit{Equation 6.1}$$

The soluble sulfides (H_2S) that are formed during the DSR process react with the metals present in the AMD and precipitate out as metal sulfides. (Me^{2+}) represents the cationic metal in *Equation 6.2* (Zagury, Kulnieks and Neculita, 2006; Bekmezci *et al.*, 2011; Ayala-Parra, Sierra-Alvarez and Field, 2016; Ilin *et al.*, 2022).

$$Me^{2+} + H_2S \rightarrow MeS\downarrow + 2H^+ \qquad \textit{Equation 6.2}$$

Microorganisms play an essential role in the DSR process, which is influenced by factors such as inoculum, pH, substrate, and reactor design (Sánchez-Andrea *et al.*, 2014). SRB are single-celled microorganisms that

are critical to the DSR process (Ferraz *et al.*, 2021). They occur naturally in different ecosystems and in the gut and oral cavities of humans and animals (Kushkevych, Dordević, *et al.*, 2021; Kushkevych, Kovářová, *et al.*, 2021). Previous studies were able to detect SRB in mine tailings, however, iron and sulfur-oxidizing acidophiles were found to be the most common bacteria found in AMD environments (Johnson and Hallberg, 2003; Mendez-Garcia *et al.*, 2015). Sanchez-Andrea et al. (2013) reported success in achieving stable SRB enrichments from sediment samples at pH 4 with glycerol. Growth and enrichment of these bacteria are necessary to ensure the preservation of a viable, sustainable SRB colony. Cultivation of SRB is dependent on seasonal (temperature) and other physio-chemical variables (Sánchez-Andrea *et al.*, 2014; Kushkevych, Dordević, *et al.*, 2021; Kushkevych, Kovářová, *et al.*, 2021). Physiochemical variables include SRB type, pH, temperature, Oxidation-Reduction Potential (ORP), hydraulic retention time (HRT), electron donor source, chemical oxygen demand (COD)/SO_4^{2-} ratio, carbon (C)/nitrogen (N) ratio, heavy metal(oid) ions, and competing bacterial colonies (Ferraz *et al.*, 2021; Zhang *et al.*, 2022). Previous studies concluded that optimal conditions for the reduction of SO_4^{2-} by SRB included a completely anaerobic system, pHs between 6.5-8.0, and temperatures between 20-35°C (Eloff, E. *et al.*, 2003; Costa, Verola, *et al.*, 2020). Previous work on this topic describes AMD characteristics and the effects of seasonal changes on AMD composition (Smith *et al.*, 2021, 2022). The treatment of AMD using SRB presents an alternate, efficient, cost-effective, and low waste generating remediation technology (Costa, De Castro, *et al.*, 2020). This experimental work seeks to further explore a biological process using SRB to remediate AMD waters by investigating potential naturally occurring, easily accessible, and sustainable sources of SRB inoculum, and to evaluate the SO_4^{2-} reduction rates achieved at different pHs using these inoculum sources.

6.3 Materials and Methods

Potential inoculum sources that were collected included: AMD water sampled from a coal mining operation in Mpumalanga, South Africa, mud sampled from an area close to the Mpumalanga AMD source, mud sampled from surrounding reeds beds, mealworms purchased from a pet shop, cow dung collected from a cattle grazing field in the south of Johannesburg, and raw sewage sludge that was sampled from the Bushkoppies wastewater treatment facility near Soweto. The impact of pH on SO_4^{2-} reduction rates of the various SRB inocula was evaluated by conducting this experimental work at three different pHs: pH 2, pH 4 and pH 7.5.

6.4 Reactor set-up

Reactors were assembled using 1000 mL Schott bottles with modified screw-top fittings as shown in Figure 6.2. The tubing allowed access to the sealed reactors for nitrogen sparging and sampling while maintaining a closed anaerobic system. To prevent biological contamination, all reactor bottles and attachments were autoclaved prior to use.

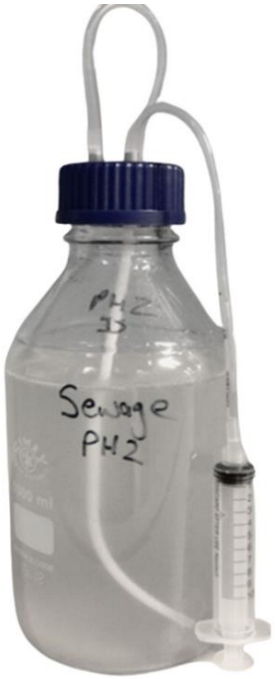


Figure 6.2 Reactor arrangement for experimental work.

A total of 21 Schott bottles were filled to the 700 mL mark with deionised water and Merck, analytical grade, reagents were added to each reactor to create a synthetic sulfate-rich enrichment media with a final sulfate concentration of 2000 mg/L. The growth-media reagents included: potassium hydrogen phosphate (KH_2PO_4), 0.5 g/L (Merck); ammonium chloride, (NH_4Cl) 1 g/L (Merck); yeast extract powder, 1 g/L (Biolab Merck); sodium sulfate (Na_2SO_4), 2.9 g/L (Merck) (Greben *et al.*, 2000; Greben, Tjatji, M and Maree, JP, 2004). In this instance, a 1.15 g/L concentration of glycerol (Merck) was used as the carbon and energy source. The quantity of glycerol added was calculated using the theoretical COD value per unit mass of glycerol (≈1.22 g COD/g glycerol) using reaction stoichiometry, to give a final concentration of 1400 mg/L COD (van Haandel and Van Der Lubbe, no date). This would provide a 0.70 COD/SO_4^{2-} ratio, which is marginally higher than the theoretical 0.67 g of COD required for SRB to reduce 1 g of SO_4^{2-} to hydrogen sulfide (H_2S) (Greben *et al.*, 2000; Greben, Tjatji, M and Maree, JP, 2004; Liu *et al.*, 2018; Ferraz *et al.*, 2021). The reactors were divided into three sets of seven reactors. The enrichment media of the first set of reactors was adjusted to pH 2, the second set to pH 4, and the third set to pH 7.5, using 37% hydrochloric acid and/or 1 M sodium hydroxide. Sufficient deionised water (DI) was prepared in separate containers, at each of the required pHs for dilution of final reactor volumes to 1000 mL. The reactors and DI solution containers were loosely stoppered and autoclaved at 121°C for 20 min to inhibit biological contamination.

After cooling, nitrogen gas was bubbled through each of the reactors and the pH-adjusted DI water containers for 10 minutes to remove oxygen from the solutions. Each reactor set comprised a reactor blank and six reactor samples, each containing a different inoculum source. Table 6.1 shows the experimental set-up with

the selected inoculum sources, and quantity added to each reactor. The blank sample was prepared by replacing the inoculum with 200 mL of DI.

Table 6.1 Reactor conditions.

Inoculum Number	Inoculum source	Inoculum volume (mL)/ mass (g) @ pH 2, 4 and 7.5
1	Blank - Deionised Water (Blk)	200 mL
2	Coal mine AMD (AMD)	200 mL
3	Raw Sewage Sludge (RS)	200 mL
4	Mealworms (MW)	3 g
5	Cow dung (CD)	5 g
6	Coal mine AMD mud (MUD)	5 g
7	Coal mine AMD reed-bed mud (RM)	5 g

After addition of the inoculum, the reactors were made up to a final volume of 1000 mL using the pH adjusted DI water, and the reactor lids were tightly fastened. To create an anaerobic environment, nitrogen gas bubbled through the modified tubing ports for 5 minutes. Immediately after nitrogen sparging, syringes were attached to the end of the reactor port tubing, for drawing off sample aliquots. Reactors were kept at a constant 28°C ±0.5°C temperature in a Labcon shaking incubator and agitated at 100 RPM.

6.5 Parameters evaluated

The parameters measured included pH, COD, S^{2-}, and SO_4^{2-}. A Spectroquant Pharo 300 spectrophotometer was used for the colorimetric determination of S^{2-}, $SO_4^{2-,}$ and COD at wavelengths of 670 nm, 880 nm, and 610 nm respectively. COD was determined after digestion. pH was determined using an Ohaus ST3-combined pH and mV meter using an ST310 pH electrode with an integrated temperature probe. All parameters were measured at the start of the experiment, pH and S^{2-} were measured on the fourth day, and seventh day, and then weekly for the duration of the experiment. To limit analysis costs, COD and SO_4^{2-} analyses were performed less frequently. Test work was terminated for samples when no notable changes in parameter concentrations were observed.

6.6 Results and Discussion

The coal mine AMD, AMD mud, reed-bed mud, raw sewage sludge, and cow-dung inocula were collected as single grab samples and immediately transported to the biochemistry laboratory located in the Chemical and Metallurgical Engineering building, at the University of the Witwatersrand, Johannesburg. The samples were stored at 4°C in a temperature controlled refrigerator under anaerobic conditions until needed.

6.6.1 Results

All test work results are presented in Appendix III, Supplementary data for Chapter 6, Tables S1–S3 and graphical presentation of results for test work performed at pH 2, pH 4, and pH 7.5 are shown in Figures 6.3–6.5. Quality control measures included the analysis of a blank samples containing only enrichment media which were adjusted to each of the three pHs tested. Method quality control samples were prepared from alternate reagent sources and analysed with each calibration. The control sample concentrations with averages and percentage error are included in Appendix III, Supplementary material for Chapter 6, Tables S4–S7. Replicate sulfate analysis were performed for some samples, and the averages and standard deviations are reported in Appendix III, Supplementary material for Chapter 6, Table S8.

6.7 Testwork performed at pH 2

Figure 6.3 shows the results of test work performed at pH 2.

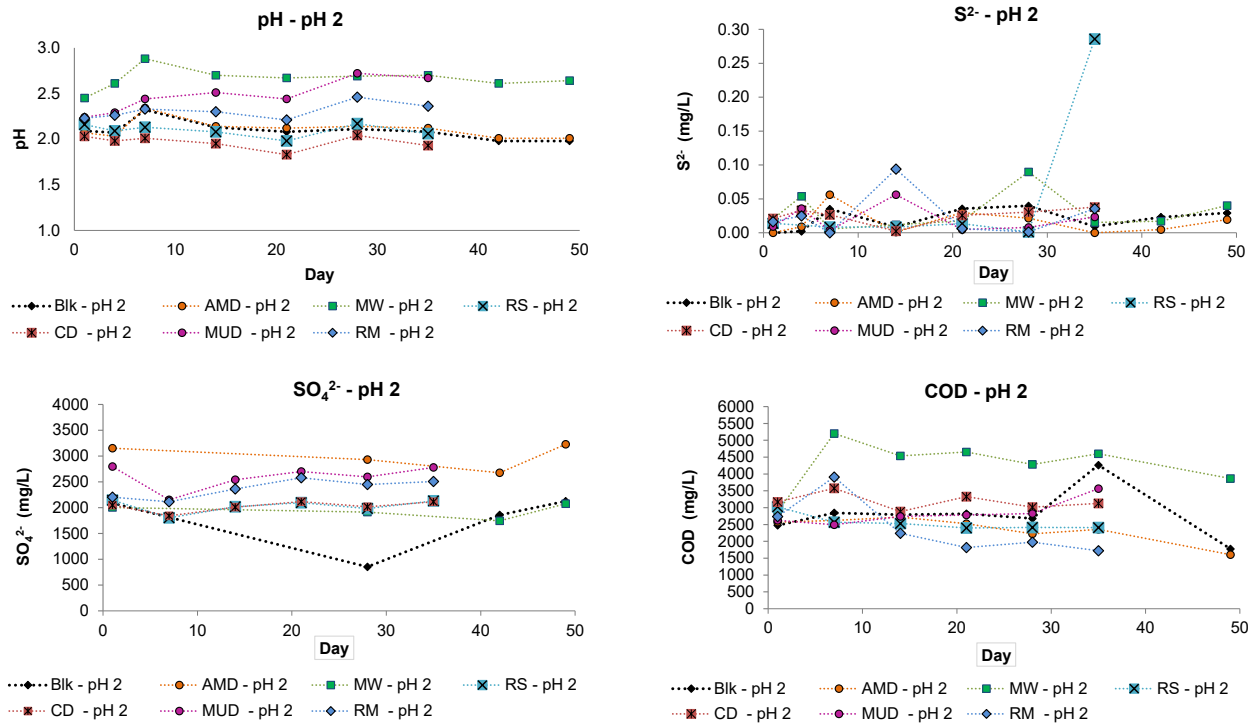


Figure 6.3 Experimental data for test work performed at pH 2 showing the change in pH, S^{2-}, SO_4^{2-}, and COD concentrations over time.

The pH values for the pH 2 samples showed variation over the course of the experiment, but the general trend shown for the Blk, AMD, RS, and CD samples was to decrease in pH, reporting marginally lower, (more acidic), final pH values. The MUD sample, RM, and MW samples increased in pH and reported higher final values.

The RM and MW samples reported S^{2-} concentrations of ≈ 0.1 mg/L on days 14 and 25 respectively, and the RS sample reported ≈ 0.3 mg/L on day 35. S^{2-} concentrations remained low and ranged between 0–0.05 mg/L for most samples.

On day twenty-eight an anomalous decrease in SO_4^{2-} concentration occurred in the blank sample. Given that there was no concomitant change in other measured parameters, and also that SO_4^{2-} concentrations increased significantly for the next sampling interval, the assumption is that this deviation resulted from analytical error. Most samples reported increased SO_4^{2-} concentrations at the end of the experiment.

The COD concentration of the MW sample almost doubled on the seventh day, indicating that, as expected, the meal worms made a significant organic contribution to the reactor media. The MW sample COD concentration then steadily reduced but still reported a final concentration of ≈1000 mg/L more than the initial COD concentration. The MUD sample also reported an ≈1000 mg/L increase in COD concentration at the end of the experimental period. The CD sample reported a 45 mg/L reduction in COD concentration, and the remaining samples reported between 500–1000 mg/L final reduction in COD concentration, which was similar to the reduction observed in the blank sample. The decrease in pH and COD observed could be attributed to various chemical interactions between the inorganic and organic components present in the sulfate-enrichment media.

6.8 Testwork performed at pH 4

Figure 6.4. shows the results of test work performed at pH 4.

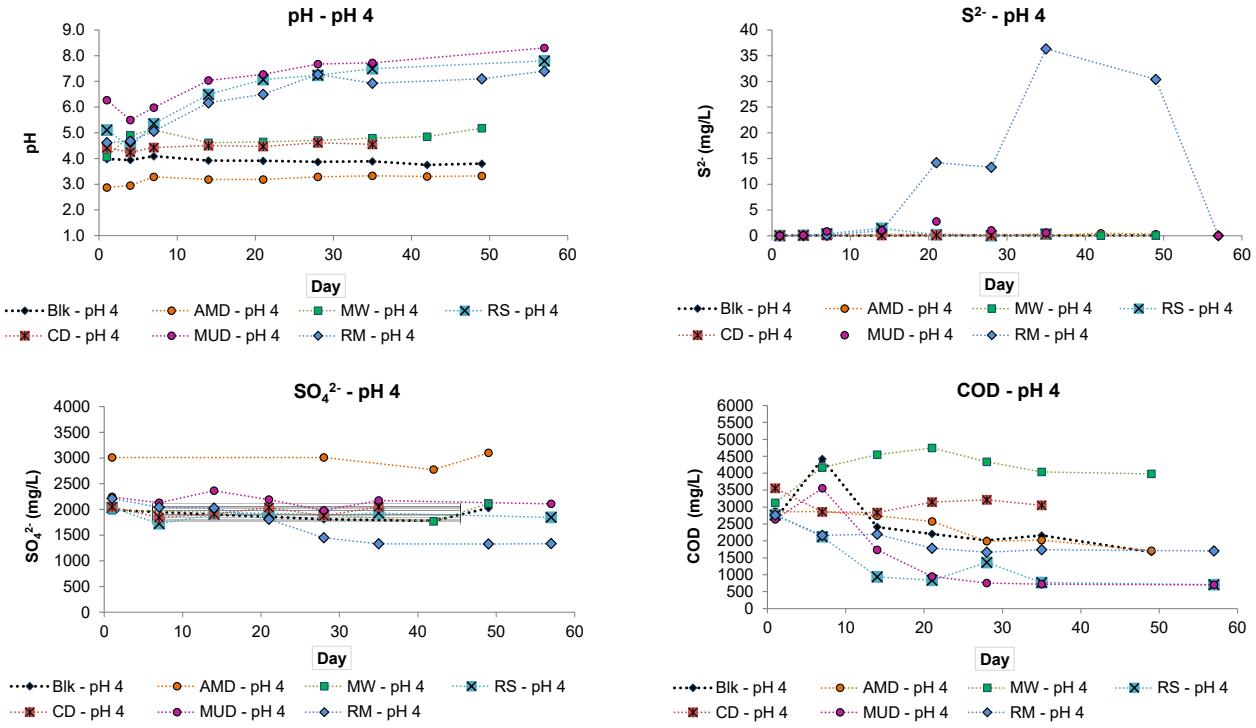


Figure 6.4 Experimental data for test work performed at pH 4 showing the change in pH, S^{2-}, SO_4^{2-}, and COD concentrations over time.

Minor variations in pH occurred in the pH 4 blank sample for the duration of the experiment, reporting lower final pH values on day forty-nine. The addition of the AMD inoculum to the AMD pH 4 sample decreased the initial pH to 2.8. The pH recovered marginally and reported a final value of 3.32. The same initial decrease in pH did not occur when adding the AMD inoculum to the pH 2 sample, indicating that the pH of the added AMD inoculum was around pH 2. The CD sample achieved a marginal overall increase in pH, while the MW sample pH increased by ≈1 pH unit, which could be attributed to the efficiency of the chitin component present in meal worms in removing acidity and producing alkalinity (Zhang *et al.*, 2022). The addition of RM, RS and MUD inoculum to the pH 4 medium resulted in increased starting pHs of 4.6, 5.1 and 6.3 respectively, with these inocula achieving a significant increase in final pH values over the duration of the testwork. The RM sample increased by 2.8 pH units, RS by 2.7 pH units, and MUD by 2.0 pH units. The increased starting pHs for these inoculum could be attributed to nutrients present in these inocula resulting in increased neutralising capacity (Merry, RH and Sabljic, A, 2009).

The pH 4 AMD and MW samples achieved the highest S^{2-} concentrations of ≈0.5 mg/L and ≈0.4 mg/L respectively, while the pH 4 RS sample achieved its highest S^{2-} concentration of 1.4 mg/L. The pH 4 MUD inoculum sample showed a more pronounced increase in S^{2-} concentration, reporting 0.86 mg/L on day seven, 1.0 mg/L on day fourteen, and 2.8 mg/L on day twenty-one, after which S^{2-} concentrations decreased. The most notable increase in S^{2-} concentration occurred in the pH 4 RM inoculum sample, increasing from

1.0 mg/L on day fourteen, to 36 mg/L on day thirty-five. Elevated S^{2-} concentrations remained until day forty-nine when concentrations declined to 30 mg/L.

The most significant decrease in SO_4^{2-} concentration for the pH 4 samples, occurred in the RM inoculum sample (≈880 mg/L). The RS and MUD inoculum samples achieved decreases in SO_4^{2-} concentration of between ≈100–300 mg/L, which remained for the duration of the experiment. The remaining samples reported varying SO_4^{2-} concentrations and reported marginally increased SO_4^{2-} concentrations at the conclusion of the experiment.

The pH 4 MW inoculum sample reported an overall increase in COD concentration. The pH 4 RS and MUD inoculum samples reported an overall decrease in COD concentration of ≈2000 mg/L. The remaining pH 4 samples and blank showed a decrease of between ≈500 – 1000 mg/L in COD concentration during the test work period. The increased COD reduction observed in the RS and MUD inoculum samples could be attributed to an increased utilisation of the available carbon source either from increased SRB activity or from other competing microorganisms, such as fermenting bacteria that might be present in the matrix (Zhang *et al.*, 2022).

6.9 Testwork performed at pH 7.5

Figure 6.5. shows the results of test work performed at pH 7.5.

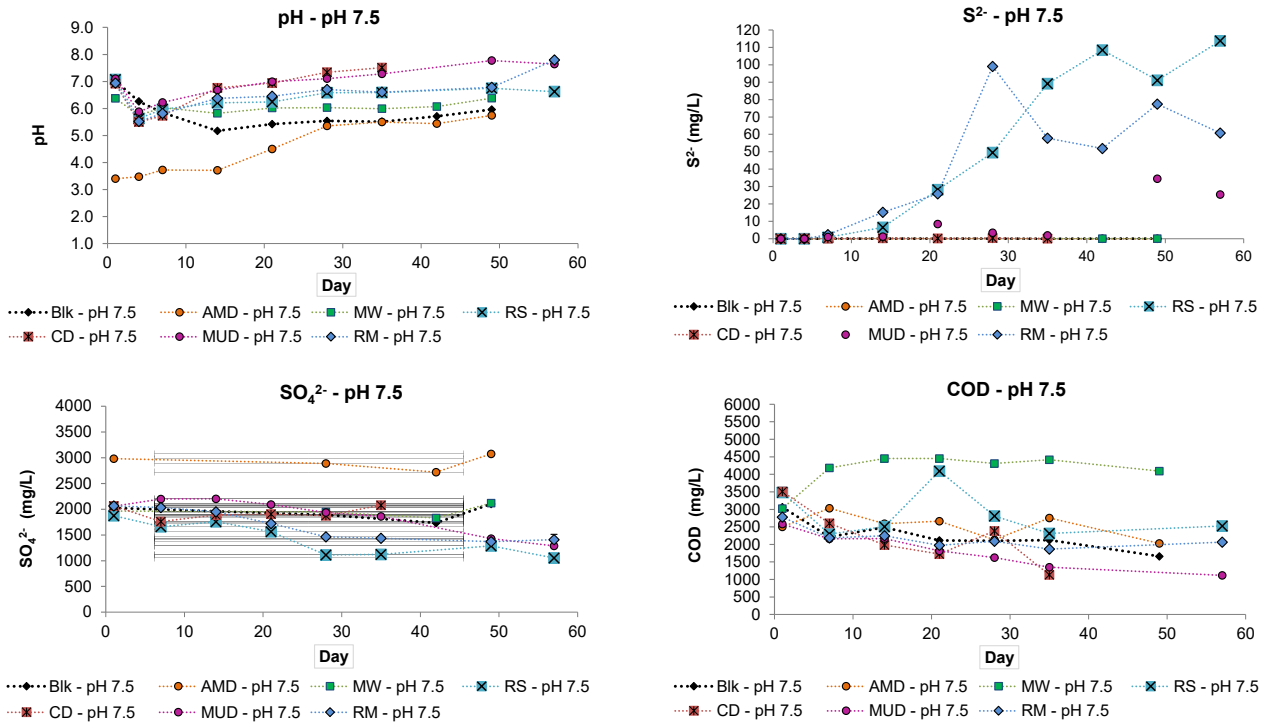


Figure 6.5 Experimental data for test work performed at pH 7.5 showing the change in pH, S^{2-}, SO_4^{2-}, and COD, concentrations over time.

The addition of the AMD inoculum to the growth media provided sufficient acidity to decrease the starting pH of the pH 7.5 AMD sample to pH 3.5. Despite the lower initial pH, this sample achieved an increase of over two pH units over the duration of the experiment. The decreased starting pH (pH 6.4) observed for the MW pH 7.5 sample would indicate that the mealworms had introduced acidity into the system. The same decrease in pH did not occur in the pH 2 and pH 4 mealworm samples. Except for the AMD sample, all samples reported a decreased pH on day four, followed by an increase in pH. The pH of the pH 7.5 blank sample decreased until day fourteen and then increased to report a final pH of six.

The pH 7.5 blank sample reported the highest S^{2-} concentration of all the blank samples, however, these concentrations were negligible (<0.06 mg/L). While small variations in S^{2-} concentration occurred in some samples, the pH 7.5 RS, RM and MUD samples achieved more notable increases in S^{2-} concentration, reporting maximum concentrations of 113 mg/L, 99 mg/L and 36 mg/L, respectively. The pH 7.5 RS, MUD, and RM inoculum samples achieved the largest decrease in SO_4^{2-} concentration decreasing by 822, 770, and 644 mg/L, respectively.

The COD concentration of the pH 7.5 MW inoculum sample increased by over 1000 mg/L between the first and seventh day, and these elevated COD concentrations remained for the duration of the experiment. The general trend of the remaining samples was to decrease in COD concentration. The largest decrease from

the initial COD concentration recorded, was for the pH 7.5 CD (2380 mg/L), and pH 7.5 MUD (1465 mg/L) samples.

6.10 Discussion

The aim of this test work was to investigate the suitability of six types of readily available and naturally occurring sources of inoculum for the enrichment of SRB. The subsequent activity of the SRB in promoting DSR after addition to a synthetic sulfate-rich reaction medium, was evaluated by assessing the changes in pH, SO_4^{2-}, S^{2-} and COD over time. The inoculum were also evaluated for their capacity for direct use at a range of different pHs. Deviations of the starting pH from the expected values, could be due to the addition of the inoculum after the initial pH adjustment of the enrichment media.

Of the inoculum evaluated, the pH 7.5 RS, MUD, and RM inoculum achieved a noticeable decrease in SO_4^{2-} concentration of 44%, 37% and 30% respectively, accompanied by S^{2-} production and COD reduction. The maximum decrease in COD concentration observed in these samples was: pH 7.5 RS (34%), pH 7.5 MUD (57%), and pH 7.5 RM (33%). The reduction of COD could be as a result of the oxidation of glycerol by SRB, but could also be attributed to other processes from competing bacteria that might be present in the matrix (Zhang *et al.*, 2022). The pH 4 RM inoculum sample presented a larger percentage decrease in SO_4^{2-} (40%) and COD (38%) concentration than the pH 7.5 RM inoculum sample, but with lower S^{2-} production (36 mg/L). The decreased S^{2-} production in the pH 4 sample could be a result of the increased hydrogen ions present in a system at low pH, forcing SRB to use up valuable energy to maintain cellular pH homeostasis, and causing inhibition of metabolic activity of SRB, and thereby resulting in lower S^{2-} production. Lower pHs could also have enabled the success of other competing bacteria for the carbon sources (Kaksonen and Puhakka, 2007; Zhang *et al.*, 2022).

Calculation of the ratio of S^{2-} production to SO_4^{2-} reduction ($S^{2-}_{produced}/SO_4^{2-}_{removed}$), showed that the pH 2, pH 4 and pH 7 AMD, MW, MUD, and CD inoculum did not achieve appreciable conversion ratios. The reduced conversion ratios for AMD are in line with anticipated reduced presence of SRB in AMD environments (Johnson and Hallberg, 2003; Mendez-Garcia *et al.*, 2015). Inoculum samples able to realise notable conversion ratios, included the pH 7.5 RS inoculum, which achieved the highest conversion ratio of 0.14 on day forty-nine, and the pH 7.5 RM inoculum which achieved the highest conversion ratio of 0.17 on day twenty-eight These inocula demonstrated notable conversion ratios from day seven onwards. Conversion ratios reporting lower than the theoretical sulfide production from sulfate reduction ratio of 0.33 could be attributed to reduction of SO_4^{2-} to sulfite, thiosulfate and sulfite, or from loss of gaseous H_2S from reactor fittings or during sampling (Greben *et al.*, 2007; Zhang *et al.*, 2022). An increase in pH and a decrease in COD concentration, accompanied the S^{2-} production and SO_4^{2-} reduction observed for the pH 7.5 RS and RM inoculum samples.

The success of the pH 7.5 RS inoculum in SO_4^{2-} to S^{2-} conversion could be attributed to the presence of additional and readily available, sources of nitrogen, phosphorus, and trace elements in the RS inoculum that would enhance SRB growth (Kaksonen and Puhakka, 2007). Similarly, for the RM inoculum, contributions from additional macro and micronutrients, and organic matter present in the soil and from the lignocellulosic ruminants, would provide additional carbon, nitrogen and phosphorus nutrients. The increased nutrient contribution, would provide increased COD/SO_4^{2-} and carbon-to-nitrogen (C/N) ratios in the matrix, resulting in enhanced growth and metabolism of SRB (Zhang *et al.*, 2022). The success of the RM inoculum is in agreement with the observed abundance of SRB in river sediments and soil amendments (Johnson and Hallberg, 2003; Sánchez-Andrea *et al.*, 2013; Ramla and Sheridan, 2015).

Data showed a more notable decrease in COD concentration for the pH 4 and pH 7.5 MUD inoculum compared with the pH 4 and pH 7.5 RM inoculum. Of the inoculum tested at pH 4, the pH 4 RM inoculum reported a significant increase in S^{2-} concentration (36 mg/L), with a maximum SO_4^{2-}/S^{2-} conversion ratio of only 0.041, while the pH 4 MUD inoculum achieved a maximum S^{2-} concentration of ≈ 3 mg/L. The reduced S^{2-} production in the pH 4 MUD sample could be attributed to the inhibitory effects of low pH on SRB combined with the absence of lignocellulosic material, and thus reduced nutrient content available in the MUD sample (Zhang *et al.*, 2022).

6.11 Conclusions

This work sought to assess the suitability of different, readily available, and naturally occurring SRB sources for use in a biologically mediated DSR process for the remediation of AMD. The study evaluated the effectiveness of the SRB cultures to function in different pH environments. The results show that the conversion of SO_4^{2-} to S^2, indicative of the dissimilatory reduction process, did not occur for the AMD water (AMD), mealworms (MW), AMD mud (MUD), and cow dung (CD) inoculum, rendering these unsuitable as natural sources of inoculum for sulfate-reducing bacteria (SRB) cultivation. The raw sewage sludge (RS) and reed-bed mud (RM) were able to achieve notable SO_4^{2-} reduction and S^{2-} production in pH 7.5 media. These inoculum achieved the greatest $S^{2-}_{produced}/SO_4^{2-}_{removed}$ conversion ratios of all the inoculum tested, thus supporting their potential use in biologically mediated DSR remediation processes. This work is important as it contributes to knowledge in the area of sustainable AMD treatment. Using readily available and/or naturally occurring SRB cultures to enhance SRB growth and activity supports the transition to a circular economy model where waste products such as raw sewage sludge is used as a resource in the design of more cost-effective and sustainable biological AMD remediation processes to produce clean water. Further investigation is needed to establish optimal reactor conditions to achieve the best S^{2-}/SO_4^{2-} conversion rates and to limit potential losses of S^{2-}. This work should include the evaluation of using 1.) alternate carbon/electron sources that are more efficient than glycerol, 2.) different COD/SO_4^{2-} ratios, and 3.) varying acclimatation times for SRB at differing pHs.

6.12 Acknowledgements

The authors thank the School of Chemical and Metallurgical Engineering of the University of the Witwatersrand, Johannesburg for the use of their laboratory facilities for this test work.

6.13 References

Ayala-Parra, P., Sierra-Alvarez, R. and Field, J.A. (2016) 'Algae as an electron donor promoting sulfate reduction for the bioremediation of acid rock drainage', Journal of Hazardous Materials, 317, pp. 335–343. Available at: https://doi.org/10.1016/j.jhazmat.2016.06.011

Bagheri Novair, S. et al. (2024) 'The role of sulphate-reducing bacteria (SRB) in bioremediation of sulphate-rich wastewater: Focus on the source of electron donors', Process Safety and Environmental Protection, 184, pp. 190–207. Available at: https://doi.org/10.1016/j.psep.2024.01.103

Bekmezci, O.K. et al. (2011) 'Sulfidogenic biotreatment of synthetic acid mine drainage and sulfide oxidation in anaerobic baffled reactor', Journal of Hazardous Materials, 189(3), pp. 670–676. Available at: https://doi.org/10.1016/j.jhazmat.2011.01.087

Costa, J.M., De Castro, K.C., et al. (2020) 'Anaerobic reactors for the treatment of sulphate and metal-rich wastewater: a review', International Journal of Environmental Analytical Chemistry, 102(4), pp. 923–934. Available at: https://doi.org/10.1080/03067319.2020.1728261

Costa, J.M., Verola, L.M., et al. (2020) 'Biologic removal of sulfate from acid mine drainage in an anaerobic sequencing batch reactor: Temperature and inoculum origin effects on the startup operation', Journal of Water Process Engineering, 36, p. 101349. Available at: https://doi.org/10.1016/j.jwpe.2020.101349

Eloff, E. et al. (2003) 'Biological sulphate removal using hydrogen as the energy source', in Nel, P. J. L.: Mine Water and the Environment. 8th International Mine Water Association Congress, Johannesburg, pp. 99–108, 3 fig., 5 tab. Available at: http://www.mwen.info/docs/imwa_2003/imwa_2003_099-108.pdf (Accessed: 14 March 2024).

Ferraz, R.M. et al. (2021) 'Effects of the inoculum source, electron donor, and immobilization on the microbial community of sulfidogenic bioreactors', Chemical Engineering Journal, 404, p. 126549. Available at: https://doi.org/10.1016/j.cej.2020.126549

Gazea, B., Adam, K. and Kontopoulos, A. (1996) 'A review of passive systems for the treatment of acid mine drainage', Minerals Engineering, 9(1), pp. 23–42. Available at: https://doi.org/10.1016/0892-6875(95)00129-8

Gil-Garcia, C. et al. (2023) 'Recovering the sulfidogenic activity under harsh sulfide-rich fermentative conditions in a thermophilic structured-bed reactor: Performance and microbial aspects', Environmental Technology & Innovation, 30, p. 103080. Available at: https://doi.org/10.1016/j.eti.2023.103080

Greben, H. et al. (2007) 'Improved sulphate removal rates at increased sulphide concentration in the sulphidogenic bioreactor', Water SA, 31(3), pp. 351–358. Available at: https://doi.org/10.4314/wsa.v31i3.5206

Greben, H.A. et al. (2000) 'Biological sulphate removal from acid mine effluent using ethanol as carbon and energy source', Water Science and Technology, 42(3–4), pp. 339–344. Available at: https://doi.org/10.2166/wst.2000.0400

Greben, H.A., Tjatji, M and Maree, JP (2004) 'COD/SO4 ratios using propionate and acetate as the energy source for the biological sulphate removal in Acid Mine Drainage', in. IMWA, Newcastle Upon Tyne.

van Haandel, A.C. van and van Lubbe, J.G.M. van der (2012) Handbook of biological wastewater treatment: design and optimisation of activated sludge systems. 2nd ed. London: IWA publ.

Ilin, A.M. et al. (2022) 'Glycerol amendment enhances biosulfidogenesis in acid mine drainage-affected areas: An incubation column experiment', Frontiers in Bioengineering and Biotechnology, 10, p. 978728. Available at: https://doi.org/10.3389/fbioe.2022.978728

Johnson, D.B. and Hallberg, K.B. (2003) 'The microbiology of acidic mine waters', Research in Microbiology, 154(7), pp. 466–473. Available at: https://doi.org/10.1016/S0923-2508(03)00114-1

Kaksonen, A.H. and Puhakka, J.A. (2007) 'Sulfate Reduction Based Bioprocesses for the Treatment of Acid Mine Drainage and the Recovery of Metals', Engineering in Life Sciences, 7(6), pp. 541–564. Available at: https://doi.org/10.1002/elsc.200720216.

Kushkevych, I., Kovářová, A., et al. (2021) 'Distribution of Sulfate-Reducing Bacteria in the Environment: Cryopreservation Techniques and Their Potential Storage Application', Processes, 9(10), p. 1843. Available at: https://doi.org/10.3390/pr9101843

Kushkevych, I., Dordević, D., et al. (2021) 'Environmental Impact of Sulfate-Reducing Bacteria, Their Role in Intestinal Bowel Diseases, and Possible Control by Bacteriophages', Applied Sciences, 11(2), p. 735. Available at: https://doi.org/10.3390/app11020735

Liu, Z. et al. (2018) 'Removal of sulfate and heavy metals by sulfate-reducing bacteria in an expanded granular sludge bed reactor', Environmental Technology, 39(14), pp. 1814–1822. Available at: https://doi.org/10.1080/09593330.2017.1340347

McCarthy, T.S. (2011) 'The impact of acid mine drainage in South Africa', South African Journal of Science, 107, pp. 01–07.

Mendez-Garcia, C. et al. (2015) 'Microbial diversity and metabolic networks in acid mine drainage habitats', Frontiers in Microbiology, 6. Available at: https://doi.org/10.3389/fmicb.2015.00475

Merry, RH and Sabljic, A (2009) 'Acidity and alkalinity of soils', Environmental and ecological chemistry, 2, pp. 115–131.

Nogueira, E.W. et al. (2021) 'Sulfate and metal removal from acid mine drainage using sugarcane vinasse as electron donor: Performance and microbial community of the down-flow structured-bed bioreactor', Bioresource Technology, 330, p. 124968. Available at: https://doi.org/10.1016/j.biortech.2021.124968

Ramla, B. and Sheridan, C. (2015) 'The Potential Utilisation of Indigenous South African Grasses for Acid Mine Drainage Remediation', Water SA, 41(2), p. 247. Available at: https://doi.org/10.4314/wsa.v41i2.10

Sánchez-Andrea, I. et al. (2013) 'Enrichment and isolation of acidophilic sulfate-reducing bacteria from Tinto River sediments', Environmental Microbiology Reports, 5(5), pp. 672–678. Available at: https://doi.org/10.1111/1758-2229.12066

Sánchez-Andrea, I. et al. (2014) 'Sulfate reduction at low pH to remediate acid mine drainage', Journal of Hazardous Materials, 269, pp. 98–109. Available at: https://doi.org/10.1016/j.jhazmat.2013.12.032

Simate, G.S. and Ndlovu, S. (2014) 'Acid mine drainage: Challenges and opportunities', Journal of Environmental Chemical Engineering, 2(3), pp. 1785–1803. Available at: https://doi.org/10.1016/j.jece.2014.07.021

Smith, J. et al. (2021) 'Seasonal characterisation of acid mine drainage in Mpumalanga coalfields region', in. SACEC, SCIENTIFIC COMMITTEE, p. 118

Smith, J. et al. (2022) 'Critical evaluation of the chemical composition of acid mine drainage for the development of statistical correlations linking electrical conductivity with acid mine drainage concentrations', Environmental Advances, 8, p. 100241. Available at: https://doi.org/10.1016/j.envadv.2022.100241

Zagury, G.J., Kulnieks, V.I. and Neculita, C.M. (2006) 'Characterization and reactivity assessment of organic substrates for sulphate-reducing bacteria in acid mine drainage treatment', Chemosphere, 64(6), pp. 944–954. Available at: https://doi.org/10.1016/j.chemosphere.2006.01.001

Zhang, X. et al. (2023) 'Selective separation of metals from wastewater using sulfide precipitation: A critical review in agents, operational factors and particle aggregation', Journal of Environmental Management, 344, p. 118462. Available at: https://doi.org/10.1016/j.jenvman.2023.118462

Zhang, Zhao et al. (2022) 'A review of sulfate-reducing bacteria: Metabolism, influencing factors and application in wastewater treatment', Journal of Cleaner Production, 376, p. 134109. Available at: https://doi.org/10.1016/j.jclepro.2022.134109

CHAPTER 7.

7 The effects of grass pre-treatment time on acid mine drainage bioremediation potential, and bioconversion of sugars to ethanol

(For journal submission)

The chapter addresses objective (d): To investigate the effects of conducting biological AMD remediation at ambient temperature (with no additional heating), and the effects of grass-AMD contact time, with and without SRB amendment, on the extent of both a bioremediation process using grass as an organic substrate, and on subsequent bioethanol production using the spent grass residue.

The investigation of a dual process is presented, whereby; locally sourced grass from the Mpumalanga coal mining region, South Africa, were used for the biological remediation of AMD, and the "acid" (AMD) pre-treated (hydrolysis) grass residue was subsequently used for bioethanol production. Scanning electron microscope (SEM) analysis images are presented to visually confirm the ability of a synthetically prepared pH 3 AMD solution to disrupt the lignocellulosic structure of the grass at ambient temperature. This was also experimentally demonstrated by an increase in sugars and subsequent VFA concentration in the AMD solution. An evaluation of the extent of AMD bioremediation at different grass-AMD contact times (hydrohalic retention times), with and without SRB addition is given. In this work the pre-treated grasses were subjected to a combined hydrolysis and fermentation process, known as simultaneous saccharification and fermentation (SSF). The extent of bioconversion of sugars to ethanol from the different hydraulic retention time (HRT), pretreated grass residue samples were compared with an untreated grass sample. A suitable HRT of grass-AMD contact to enable optimal AMD remediation and to provide optimal ethanol production was assessed. The results show that the longer hydraulic retention times tested, with SRB amendment, achieved the greatest bioremediation of AMD, and consequent bioethanol production. The data showed that the untreated grass sample was able to produce appreciable bioethanol concentrations.

CRediTs: Janet Smith: Conceptualization, Methodology, Investigation, Validation, Formal analysis, writing-Original Draft; Craig Sheridan: Funding acquisition, Conceptualization, Resources, Supervision, Writing – Review and editing; Lizelle van Dyk: Conceptualization, Supervision, Writing – Review and Editing; Kevin Harding: Conceptualization, Supervision, Writing – Review and Editing

AKNOWLEDGEMENTS

The authors thank Moshibudi Mahlo and Mbengeni Nefale for their assistance with the experimental work, Nicholas Burman for his technical input in the fermentation experimental work, and Archie Corfield for his assistance with SEM analysis interpretation.

7.1 Abstract

Coal mining activity in South Africa had led to the generation of acid mine drainage (AMD) and finding sustainable treatment solutions has become necessary. This work explores the grass acid hydrolysis process at ambient conditions, with and without sulfate-reducing bacteria (SRB) amendment, and the effects of increased grass-AMD contact (hydraulic retention time) for both AMD remediation and for subsequent bioethanol production, as a potential bioremediation process. Scanning electron microscopy (SEM) image analysis confirmed that the synthetically prepared, weak acid AMD solution was suitable to disrupt the grass lignocellulosic structure. The increased glucose and xylose concentrations also supported the hypothesis of breakdown of the grass lignocellulosic structure. The subsequent conversion of sugars to volatile fatty acids provided an accessible and soluble carbon source for SRB to convert sulfates to sulfides, which was indicative of the biologically mediated dissimilatory sulfate reduction (DSR) remediation process. This was shown by increased sulfide concentrations and increased pHs. The greatest increases in ethanol concentration were achieved by the longer hydraulic retention time (HRT), and SRB amended pretreated grass samples. The ethanol concentration for the SRB-amended day thirteen HRT sample increased by 2605 mg/L followed by the same retention time non-amended sample (2274 mg/L). The untreated grass sample produced similar ethanol concentrations (2057 mg/L) to the SRB-amended day eleven pre-treated grass samples (2170 mg/L). Data showed that extended grass-AMD contact times with SRB amendment, improved both the extent of the AMD remediation and bioethanol production. This research is important as it contributes to a circular economy whereby grass cuttings, which are considered a waste material are used to remediate AMD to produce value products namely clean water, and the grass residue from the AMD remediation process is used for subsequent bioethanol production.

Keywords: Acid hydrolysis, Sulfate Reducing Bacteria; pH; Enzymatic hydrolysis; Fermentation

7.2 Introduction

Mining and industrial activities requiring land excavation have resulted in large quantities of fragmented rock. Acid mine drainage (AMD) occurs when sulfide minerals in the pyritic rock, which comprises predominantly iron and sulfide, are exposed to oxygen and water, resulting in oxidation products containing ferrous sulfate and acidity. Further oxidation reactions may occur depending on pH conditions resulting in large quantities of highly mineralised, acidic water. Surface decant, and ingress of AMD into underground fissures can be detrimental to the surrounding environment if quantities exceed natural dilution capacity (Akcil and Koldas, 2006; Simate and Ndlovu, 2014; Skousen et al., 2019; Tutu et al., 2008). Active and obsolete gold mining operations from the Western, Eastern, and Central basins in South Africa generate approximately 360 ML of AMD decant per day, while coal mining-related activities in the Mpumalanga Province, South Africa, account for between 50-62 ML of AMD decant per day (Hobbs et al., 2008; Masindi et al., 2016).

South Africa is a water-scarce country which receives an average of 456 mm of rainfall annually and is ranked as Sub-Saharan Africa's fifth most water-scarce country, and amongst the 20 most water-scarce countries globally (Egoh et al., 2009; The World Bank Group, 2021; Woodford et al., 2006). South Africa's water scarcity, an increasing population, and the anticipated increased average temperature owing to climate change trends, will increase the demand for water and energy for industrial processes, to maintain agricultural crops as well as to provide cooling (The World Bank Group, 2021). This will necessitate the conservation of water to ensure the sustainability of the country's water supply.

Remediating AMD will thus serve a dual purpose of limiting the environmental damage associated with AMD decant and recovering substantial volumes of water for reuse. Active remediation processes require the addition of alkaline chemicals to neutralise the pH and precipitate the metals present in AMD. While these processes are effective, and have a small footprint, they carry high capital, operating, and maintenance costs, which are compounded by the generation of large quantities of waste sludge that require further treatment or disposal at hazardous waste sites (Johnson and Hallberg, 2005).

Biological treatment systems are considered a potential alternative for AMD remediation, whereby a dissimilatory sulfate reduction (DSR) mechanism, which is catalysed by sulfate-reducing bacteria (SRB), reduces sulfates to sulfides. The reaction requires an organic carbon and electron donor source and sulfates take up the electrons for conversion to sulfide (Kaksonen and Puhakka, 2007; Ruehl and Hiibel, 2020). Formaldehyde (CH_2O) is used as a carbon source which is oxidised to produce bicarbonates which then increase the pH of the media, and sulfates are reduced to sulfides under anaerobic conditions (Zagury et al., 2006) (Equation 7.1).

$$SO_4^{2-} + 2CH_2O + 2H^+ \rightarrow H_2S + 2HCO^{3-} \qquad \textit{Equation 7.1}$$

Soluble sulfides are formed which then react with metals (where Me^{2+} represents the cationic metal) present in the AMD to precipitate as the metal sulfide (*Equation 7.2*).

$$Me^{2+} + H_2S + 2H^+ \rightarrow MeS\downarrow + 2H^+ \qquad \textit{Equation 7.2}$$

Lignocellulose has been identified as a suitable carbon source. Magowo et al. (2015) showed that switchgrass was able to increase pH, remove metals from AMD and produce sugars from subsequent enzymatic hydrolysis of the grass residue. Lignocellulose wastes can easily be sourced at low cost (Mandree et al., 2023; Niju et al., 2020), and according to Westensee et al. (2018), the combined availability of agricultural and lignocellulosic residue in South Africa amounts to 21.31 Mt/year. As a second-generation feedstock, using lignocellulosic waste as a raw material for industrial processes such as AMD remediation and biofuel production will not threaten future food security (Cazier et al., 2024; Niju et al., 2020; Westensee et al., 2018). The combined utilisation of AMD as a dilute acid source to facilitate the disruption of the lignocellulosic

structure of the lignocellulosic waste (Burman et al., 2019), addresses a circular economy concept whereby a waste product is used for water treatment and biofuel production, and the products thereof provide clean water and fuel. Environmental benefits are also realised whereby remediation of AMD prevents potential further degradation of the surrounding environment from highly mineralised and acidic water, which would in turn affect freshwater courses, crops and livestock and thus detrimentally impact food production.

Lignocellulose biomass is a complex organic carbon source, which is comprised of cellulose, hemicellulose and lignin, with traces of inorganic elements and extractable compounds (Sun et al., 2021; Wang et al., 2024). An initial pretreatment stage is required to breakdown the ligno-hemicellulosic structure of grass to release monomeric sugars, glucose and xylose, and to enable cellulase enzymes access to cellulose fibrils for subsequent enzymatic hydrolysis and fermentation (Burman et al., 2019; Cazier et al., 2024; Sun et al., 2021; Wang et al., 2024). Cellulose comprises mainly glucose, and the degradation of the hemicellulose from acid pretreatment (hydrolysis) typically results in the formation of sugars such as glucose, mannose, galactose, xylose and arabinose, while products of carbohydrate degradation include furan aldehydes: 5-hydroxymethylfurfural (HMF) and furfural; and aliphatic acids: acetic acid, formic acid and levulinic acid (Jönsson et al., 2013; Niju et al., 2020; Sluiter et al., 2012). Subsequent microbially catalysed acidogenic reactions produce volatile fatty acids (VFAs), such as acetate, propionate, and butyrate which provide the electron donor required by SRB to facilitate the conversion of sulfate to sulfide by DSR (Meegoda et al., 2018; van Hille et al., 2021). A COD/sulfate ratio of 0.67 is required to provide sufficient organic material for the complete conversion of sulfate to sulfide (Chen et al., 2020; Greben et al., 2000). Oxidation of organic compounds in the DSR process releases energy required by SRB for conversion of sulfates to sulfides. A decrease in sugar concentration over time as well as the concomitant increase in sulfide concentration over time, would indicate that the sugars are being consumed for VFA production to provide the carbon source required by SRB for the reduction of sulfates to sulfides (Naidu et al., 2021; Novair et al., 2024).

The production of biofuels from lignocellulosic material can be achieved using a two-step process, separate hydrolysis and fermentation (SSF), where the first stage requires the enzymatic hydrolysis of the cellulose and hemicellulose present in pretreated grass using a buffer/cellulase mixture to release monomeric sugars. This is followed by a fermentation stage whereby the sugars in the hydrolysis filtrate are converted into alcohols, biogas and organic acids using an inoculum solution prepared with added yeast extract and peptone nutrients (Burman et al., 2021, 2018; Ojo, 2023). The process can be combined into a single step, simultaneous saccharification and fermentation (SSF), where the pre-treated grass is added to a combined mixture of buffer/cellulase and inoculum (Burman et al., 2018).

In this work grass from the Mpumalanga coal mining region, South Africa, was used as a carbon source for the biological remediation of a synthetically prepared, pH 3 AMD solution containing 5 g/L of sulfate (SO_4^{2-}), and 300 mg/L of iron (Fe). The AMD was leveraged as a weak sulfuric acid source to facilitate the disruption

of the lignocellulosic structure of the grass and to hydrolyse the grass to release monomeric sugars for remediation by DSR at ambient temperature.

This research sought to experimentally investigate whether a synthetic AMD solution of weak acid concentration was able to sufficiently disrupt the lignocellulosic structure of grass to release sugars to support the reduction of sulfates to sulfides and achieved remediation of AMD at ambient temperatures. The extent of remediation was evaluated at different grass-AMD contact (or hydraulic retention (HRT) times, with and without additional SRB amendment. The opened grass structure will facilitate enzyme access to the remaining sugars in the grass in a subsequent SSF process to produce bioethanol products. This work also investigated the effects of the grass pre-treatment time, and SRB amendment on the production of sugars and bioethanol during a subsequent combined enzymatic hydrolysis and fermentation process, known as simultaneous saccharification and fermentation (SSF). The extent of bioconversion of sugars from the pretreated grass samples to ethanol was compared with that of an untreated grass sample.

7.3 Materials and Methods

7.3.1 Grass collection and preparation

Grass samples previously identified as grass type *Eragrostis curvula*, were collected from the roadside in the Delmas area of the Mpumalanga coal mining region (Smith et al., 2024). The grass was fed through a Ryobi garden shredder, rinsed using deionised water (DI), and dried overnight at 50°C in a Labcon drying oven. Once cooled, a kitchen blender was used to reduce the grass to smaller size fragments of between 2 and 5 cm in length.

7.3.2 Pre-treatment of grass

Grass was contacted with a synthetically prepared, pH 3, acid mine drainage (AMD) solution which was prepared using Merck analytical grade reagents; 18 M sulfuric acid (H_2SO_4), ferrous sulfate ($Fe_2SO_4.7H_2O$) and sodium hydroxide (NaOH) for pH adjustment. The final synthetic AMD solution comprised 5 g/L SO_4^{2-}, and 300 mg/L Fe.

Reactors were prepared using one litre Consol glass bottles that had been cleaned, rinsed with DI water, and sterilised by autoclaving at 121°C for 20 minutes. After cooling, 800 mL of synthetic AMD solution and 24 g of dried, shredded grass were added to each of 20 Consol bottles to give a grass-AMD ratio of 30 g/L. Two additional AMD blank reactors were prepared without grass and containing only 800 mL of the prepared AMD solution. The inoculated samples were prepared by adding 20 mL of sulfate-reducing bacteria (SRB) inoculum solution (24 mL/L), that had been cultivated from previous enrichment testwork (Smith et al., 2025), to ten of the sample reactors and to one AMD blank reactor. No SRB was added to the remaining reactors. The reactor contents were thoroughly mixed before taking an initial sample portion for analysis

(Day 0). The reactors were then sealed and only opened at their allocated retention time. The reactors were kept at ambient temperature (≈20°C) for the duration of the pre-treatment trial. Five different hydraulic retention times (HRT) were evaluated for grass/AMD contact: namely one, four, seven, eleven, and thirteen days. The change in pH, chemical oxygen demand (COD), sulfide (S^{2-}), iron (Fe), and the production of sugars and volatile fatty acids (VFA)s in the AMD were evaluated.

pH measurements were made using an Ohaus ST3-combined pH and mV meter with an ST310 pH electrode and integrated temperature probe. S^{2-} and COD were determined using a Spectroquant Pharo 300 UV-VIS spectrophotometer at 670 nm, and 610 nm, respectively. COD was analysed after digestion at 148°C for 2 hours. The Fe concentration was determined using an Agilent Technologies, 200 Series, atomic absorption (AA) instrument. Sugars and volatile fatty acids (VFAs) were determined using an Agilent High Performance Liquid Chromatography (HPLC) instrument, connected to a refractive index (RID) detector and using a Bio-Rad 125-0098 column. Scanning electron microscopy (SEM) analysis of untreated and pre-treated grass samples was conducted in-house at the School of Chemical and Metallurgical Engineering at the University of the Witwatersrand, Johannesburg using an FEI Quanta 200 ESEM instrument. Sample preparation for SEM analysis included coating the grass samples with two carbon and one gold-palladium layer to render the samples conductive for subsequent SEM analysis. An Energy Dispersive Spectrometer (EDS) was used in conjunction with the SEM, to perform X-ray microanalysis of the grass samples to identify and quantify elements present in the samples.

Two samples with SRB amendment, and two samples without SRB amendment, were allocated to each of the preselected retention times. The blank non-amended sample (AMD Blank) and the blank SRB-amended sample (AMD Blank SRB) were analysed at each sampling event. The filtrates were retained for analysis on each respective grass sampling day and on Day 27. The removed grass was washed using DI, dried at room temperature, and retained for further simultaneous hydrolysis and fermentation (SSF) experimental work.

7.3.3 Simultaneous hydrolysis and fermentation of pre-treated grass

A combined enzymatic hydrolysis and fermentation, or simultaneous saccharification and fermentation (SSF) reactor configuration was used in this experiment (Burman et al., 2019). Testwork investigated if pre-treatment time, and/or SRB amendment influenced the extent of bioconversion of sugars to ethanol.

A 0.05 M sodium citrate buffer was prepared using AR-grade reagents sourced from Merck. Sodium citrate dihydrate and citric acid were added to 2400 mL of DI water, and the pH was adjusted to pH 4.5 using sodium hydroxide (NaOH). The solution was then made up to 3000 mL with DI water.

A commercially available home distillers' yeast, Alcotech Turbo-yeast 48, was used for fermentation (Burman et al., 2019). Yeast inoculum solution was prepared in a 1 L conical flask and comprised yeast extract (10 g/L), peptone (20 g/L) and dextrose (glucose) (5 g/L), and made up to 500 mL with DI. The flask was covered with

foil and autoclaved for 20 minutes at 121°C. The solution was cooled to 36°C in a laminar flow cabinet and a small portion of the sample was transferred to a 16 mm Spectroquant vial, to use as a spectrophotometric blank.

A sterile sample loop was used to add the fermentation yeast *Saccharomyces cerevisiae* to the inoculum solution before closing the culture and incubating at 30°C (Burman et al., 2021). The spectrophotometric blank sample was used to zero the UV-visible spectrometer, and the optical density (OD) was rechecked every 10 hours until the required OD600 of between 0.5 and 0.6 was obtained (Dowe and McMillan, 2008).

The enzymatic hydrolysis buffer solution was then prepared by adding 100 g of 1.5 L celluclast cellulase enzyme from Novozymes (16.5 FPU/gram) to 2.5 L of the prepared sodium citrate buffer solution. Additional yeast nutrients, yeast extract (50 g), and peptone (100 g) were added before making the solution up to 5000 mL using deionized water (Burman et al., 2021).

The simultaneous enzymatic hydrolysis and fermentation reactors were then prepared by adding 20 g of grass sample, 180 mL of enzymatic hydrolysis buffer, and 20 mL of yeast inoculum solution into pre-sterilised, 250 mL Erlenmeyer flasks (20 wt.% solids loading). A total of 22 reactors were prepared, four grass samples (two with, and two without SRB amendment), were allocated to each of the five retention times selected for the pre-treatment experiment. An untreated grass sample, and a blank sample containing only the hydrolysis and fermentation mixture were included in the batch. The samples were swirled to ensure adequate contact between the grass with the SSF mixture. The reactors were immediately sampled for sugars and VFA analysis (Day 0), before covering the flask openings with foil. The samples were agitated at 100 RPM at a temperature of 37°C ±0.5°C in a Labcon shaking incubator. Sample aliquots were taken and analysed on days one, two, four, six, eight, and twelve.

7.4 Results and discussion

7.4.1 Acid mine drainage grass pre-treatment results

During the initial acid hydrolysis process, grass was contacted with synthetically prepared AMD solution, (representative of real AMD), to test if the AMD solution could disrupt the lignocellulosic structure of grass. The release of monomeric sugars, glucose and xylose, from the grass into the contaminated water would confirm the disruption of the grass lignocellulosic structure. These sugars are then converted into VFAs in an microbially catalysed acidogenesis process which provides an electron donor source for SRB to use for the conversion of sulfates to sulfides in a DSR process. The production of VFAs (acetate and propionate) from glucose and xylose, provided an evaluation of subsequent acidogenic reactions. The extent of AMD remediation was evaluated by monitoring the changes in pH, COD, sulfide and Fe concentration, for each of the five HRT samples. Tests were conducted in duplicate and average concentrations and standard deviations for each retention time data for both non-inoculated and SRB-inoculated samples are reported in Appendix

IV - Supplementary data for Chapter 7 - Tables S1.1 – S1.16. These results are discussed in the following sections.

7.4.1.1 Extent of disruption of the grass lignocellulosic structure

The grass residues from the AMD acid hydrolyses stage were rinsed and dried, and untreated, and pre-treated grass samples were submitted for SEM analysis. SEM images of the grass samples were obtained at a magnification of 2000x. The Figure 7.1(i) shows a secondary electron image of the grass before acid pre-treatment, while Figure 7.1(ii) shows the grass without SRB amendment, and Figure 7.1(iii) shows the SRB amended grass. Images (ii) and (iii) show the disruption of the uniform cell structure of the untreated grass sample (i), after contact with AMD, thus demonstrating that the AMD solution was able to break down the cellulosic structure of the grass at a grass-AMD ratio of 30 g/L, at ambient temperature (Oktaviani et al., 2019).

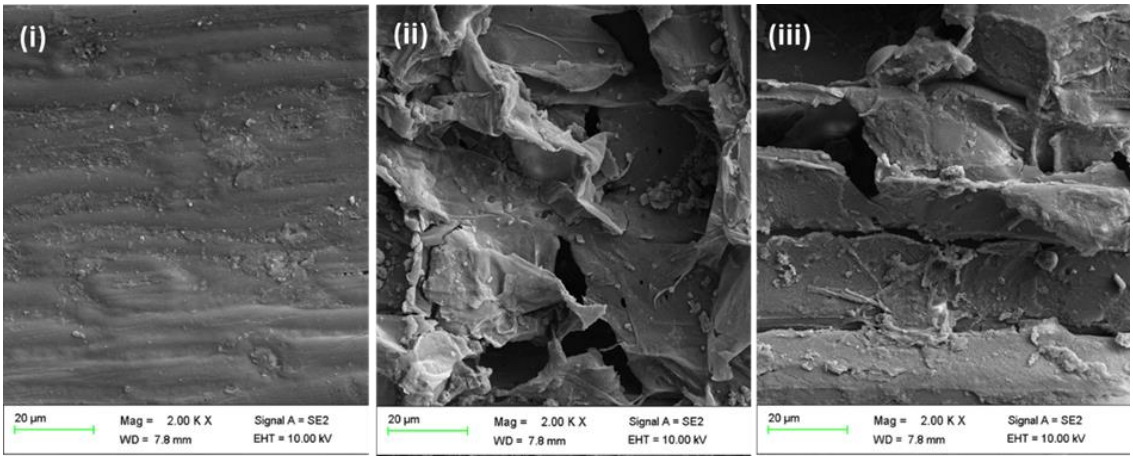


Figure 7.1 SEM secondary electron images of (i) grass before pre-treatment; (ii) grass pre-treated without SRB amendment; and (iii) grass pretreated with SRB amendment.

7.4.1.2 Extent of release of monomeric sugars from the grass

A disruption of the lignocellulosic structure of the grass should result in an increase in available sugars dissolved in the AMD. The average concentration, with standard deviation, of the monomeric sugars, glucose and xylose, liberated into solution at each allocated grass-AMD contact HRT, are shown in Figures 7.2. Average glucose data are presented in Appendix IV, Supplementary data for Chapter 7 - Table S1.1, and xylose data are presented in Appendix IV, Supplementary data for Chapter 7 - Table S1.3. The SRB-amended samples are identified in the graphs as “AMD Grass SRB”, and non-amended samples are identified as “AMD Grass”.

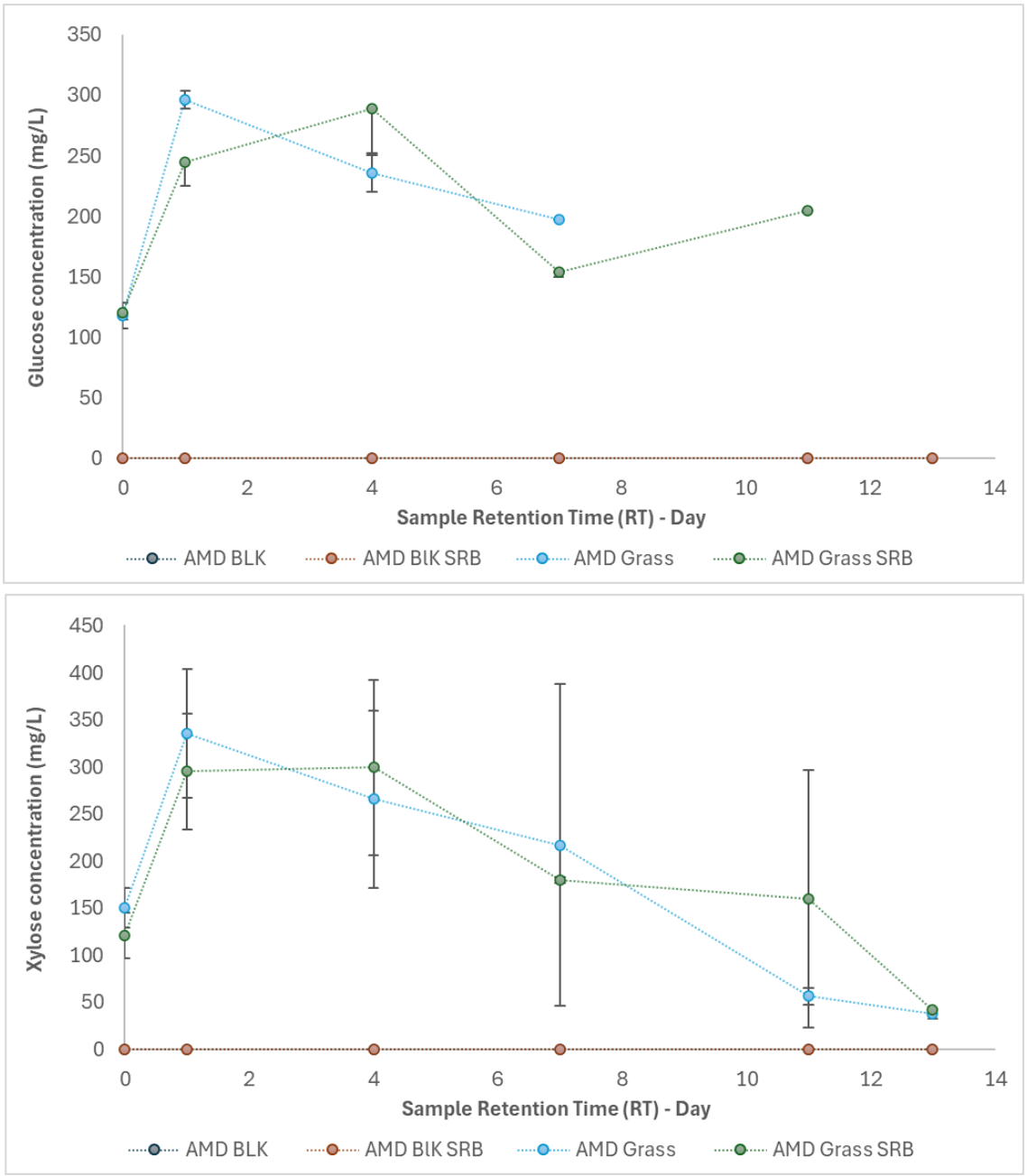


Figure 7.2 Glucose and xylose concentrations produced for non- and SRB-amended samples, at each grass-AMD contact hydraulic retention time (HRT), using a 30 g/L grass-AMD ratio. Error bars represent the standard deviation of duplicate analyses.

An increase in glucose concentration was observed for all samples immediately after the addition of grass to the AMD solution and reported an average increase of 118 mg/L for the non-amended samples and 123 mg/L for the SRB-amended sample. A further increase in glucose concentration occurred on the first day for samples with and without SRB amendment, and on the fourth day for SRB amended sample. The glucose concentration for both samples decreased on day seven. A small increase in glucose concentration was observed in the SRB-amended sample on day eleven. Glucose concentrations for filtrate samples with and

without SRB amendment were depleted over time. The glucose filtrate analyses data are available in Appendix IV, Supplementary data for Chapter 7 - Table S1.2.

Immediately after grass contact with AMD, the xylose concentrations increased by an average of 151 mg/L for the non-amended samples and 121 mg/L for the SRB-amended samples. The initial increase in concentration of both glucose a xylose is in line with the release of soluble monomeric sugars resulting from acid hydrolysis and disintegration of the grass lignocellulosic structure by the acidic AMD. Although duplicate sample analyses reported high standard deviations, the general trend showed a decrease in xylose concentration with extended AMD-grass contact HRT. The decrease in concentration of glucose and xylose with extended retention time are likely because of acidogenesis where monomeric sugars are converted to volatile fatty acids (VFA)s such as acetate and propionate which will provide a carbon source for SRB to support the conversion of sulfates to sulfides (Chen et al., 2020).

Analysis of the filtrate samples also showed a decrease in xylose concentrations for both non- and SRB-amended samples over time. This can be attributed to supporting SRB processes, where VFAs are consumed in the reduction of sulfate and the production of sulfides in the filtrate solutions (see section 7.4.1.3) (Chen et al., 2020). The xylose filtrate analyses data are available in Appendix IV, Supplementary data for Chapter 7 - Table S1.4.

7.4.1.3 Extent of conversion of monomeric sugars to volatile fatty acids (VFA)s

The formation of VFAs were shown by the increasing concentrations of acetate and propionate during the pre-treatment stage of grass-AMD contact which are shown in Figure 7.3. The average acetate concentrations with standard deviations are presented in Appendix IV, Supplementary data for Chapter 7 - Table S1.5, and average propionate data with standard deviations are presented in Appendix IV, Supplementary data for Chapter 7 - Table S1.7.

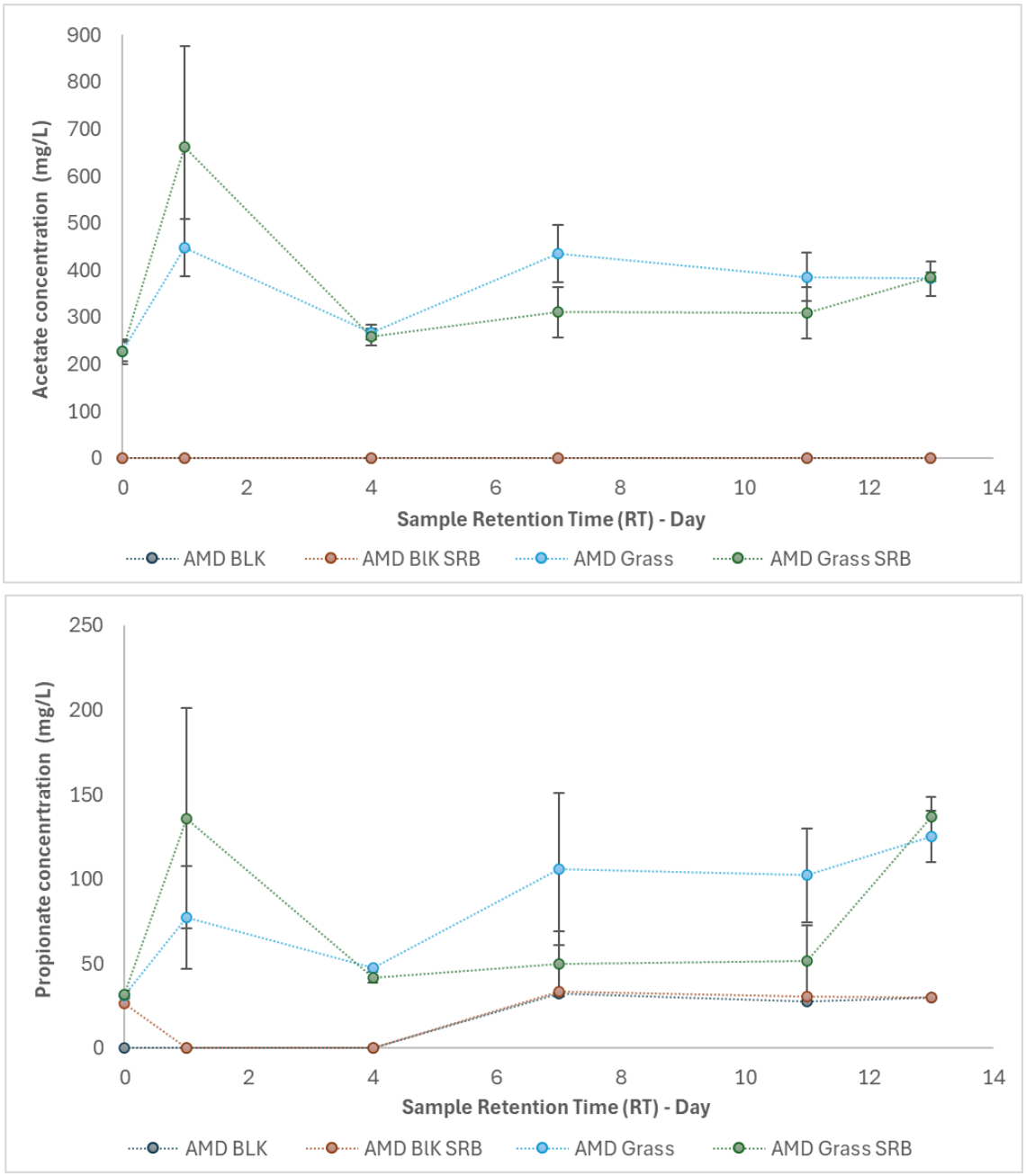


Figure 7.3 Acetate and propionate concentrations produced for non- and SRB-amended samples, at each grass-AMD contact hydraulic retention time (HRT), using a 30 g/L grass-AMD ratio. Error bars represent the standard deviation of duplicate analyses.

The non-amended and SRB-amended samples reported an average increase in acetate concentration of 227 mg/L immediately after grass was contacted with AMD. The highest acetate concentrations were reported for day one samples, which reported 449 mg/L for the non-amended and 662 mg/L for the SRB-amended sample. Acetate concentrations decreased significantly on day four and then increased on day seven. The day 13 non and SRB-amended samples reported similar final concentrations (average 384 mg/L). The increase in VFA concentrations, are in line with the decrease in glucose and xylose concentrations

observed. This is indicative of an acidogenesis process, whereby monomeric sugars are converted to VFAs (Chen et al., 2020).

Varied acetate concentrations were observed in the filtrate samples, but the general trend was for acetate concentrations to decrease as the time after grass removal increased. The final acetate concentrations for the day one, four, and seven filtrate samples reported approximately 200 mg/L (with, and without SRB amendment). The non-amended day eleven and thirteen filtrate samples reported marginal increases from an averaged 384 mg/L to an averaged 423 mg/L final acetate concentration. The SRB-amended day eleven and thirteen samples decreased marginally reporting a final average acetate concentration of 330 mg/L. The acetate data with standard deviations are available in Appendix IV, Supplementary data for Chapter 7 - Table S1.6.

Propionate concentrations for both amended and non-amended samples increased by an average of 31.6 mg/L immediately after grass was contacted with AMD. Propionate concentrations decreased on day four and then increased as grass-AMD HRT increased. The greatest propionate concentrations were reported for the day thirteen samples, 125 mg/L for non-amended, and 137 mg/L for the SRB-amended samples.

After the grass was removed, the day eleven and thirteen non-amended filtrate samples increased marginally and reported final concentrations of 130 and 155 mg/L respectively. The remaining filtrate samples generally decreased in concentration over time. The non-amended day one, four, and seven filtrate samples reported an average of 42 mg/L, while all SRB-amended samples reported an average of 36 mg/L. The propionate filtrate data, with standard deviations are available in Appendix IV, Supplementary data for Chapter 7 - Table S1.8.

The decrease in both acetate and propionate concentrations in the SRB-amended filtrate samples would imply that the SRB amendment improved the utilisation of the available VFAs in the reduction of sulfates to sulfides. This observation is supported by the decreased sulfide concentrations noted in the non-amended filtrate samples, compared with the substantially increased sulfide concentrations in the SRB-amended samples, as discussed in section 7.4.1.6.

7.4.1.4 Evaluation of the extent of AMD remediation through pH

As AMD remediation seeks to increase pH, the extent of the increase in pH achieved can be used as a measure of the success of a remediation process. Figure 7.4 shows the blank and average sample pH values for the non- and SRB-amended samples, with standard deviations for the different retention times tested. The data are provided in Appendix IV, Supplementary data for Chapter 7 - Table S1.9.

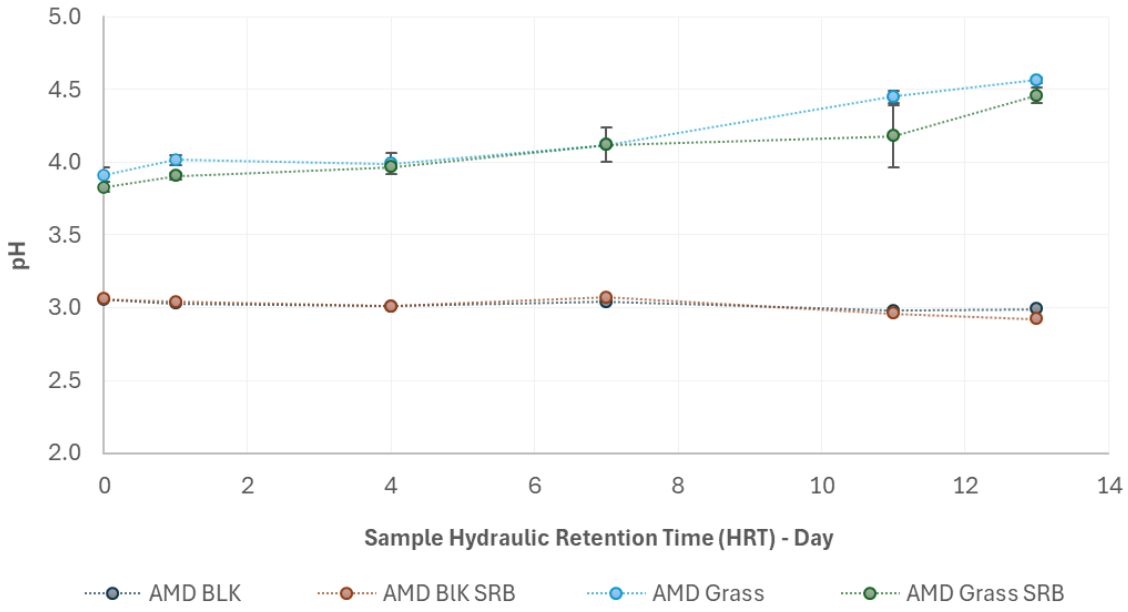


Figure 7.4 pH values for AMD blanks and for non- and SRB-amended samples, for each of the selected grass-AMD hydraulic retention times (HRT), using a 30 g/L grass-AMD ratio, and 24 mL/L of SRB. Error bars represent the standard deviation of duplicate analyses.

The pH of the blank samples remained largely unchanged for the duration of the experiment. The slight decrease in pH observed on days eleven and thirteen could have resulted from the introduction of CO_2 during sampling which would chemically react with the AMD to form carbonic acid causing the observed decrease in pH (Akcil and Koldas, 2006; Bowman et al., 2023). The pH of the non and SRB-amended samples increased by an average of 0.86 and 0.77 pH units respectively after initial contact of grass with AMD. A small increase in pH was observed for the day one and four samples, but more notable increases were observed for subsequent retention time samples. The greatest increase in pH from the initial grass contact was achieved for the day thirteen samples, increasing by 0.66 pH units for the non-amended, and 0.63 for the SRB-amended samples.

The pH continued to increase in the filtrate samples after the grass was removed (figure 7.5), and the non-amended samples achieved a final average pH of 4.8, and the SRB-amended samples a final pH of 5.0 on day twenty seven. The increase in pH indicates that the remediation in the AMD continued in the filtrate sample after the grass was removed. Figure 7.5(a) presents a plot of the increase in the pH of the non-amended filtrate samples against the number of days after grass removal, while Figure 7.5(b) presents a plot of the pH of the SRB-amended filtrate sample against the number of days after grass removal. The filtrate data shows a greater increase in pH in the SRB-amended samples, indicating that SRB amendment improved the extent of AMD remediation. Filtrate sample pH data are presented in Appendix IV, Supplementary data for Chapter 7 - Table S1.10.

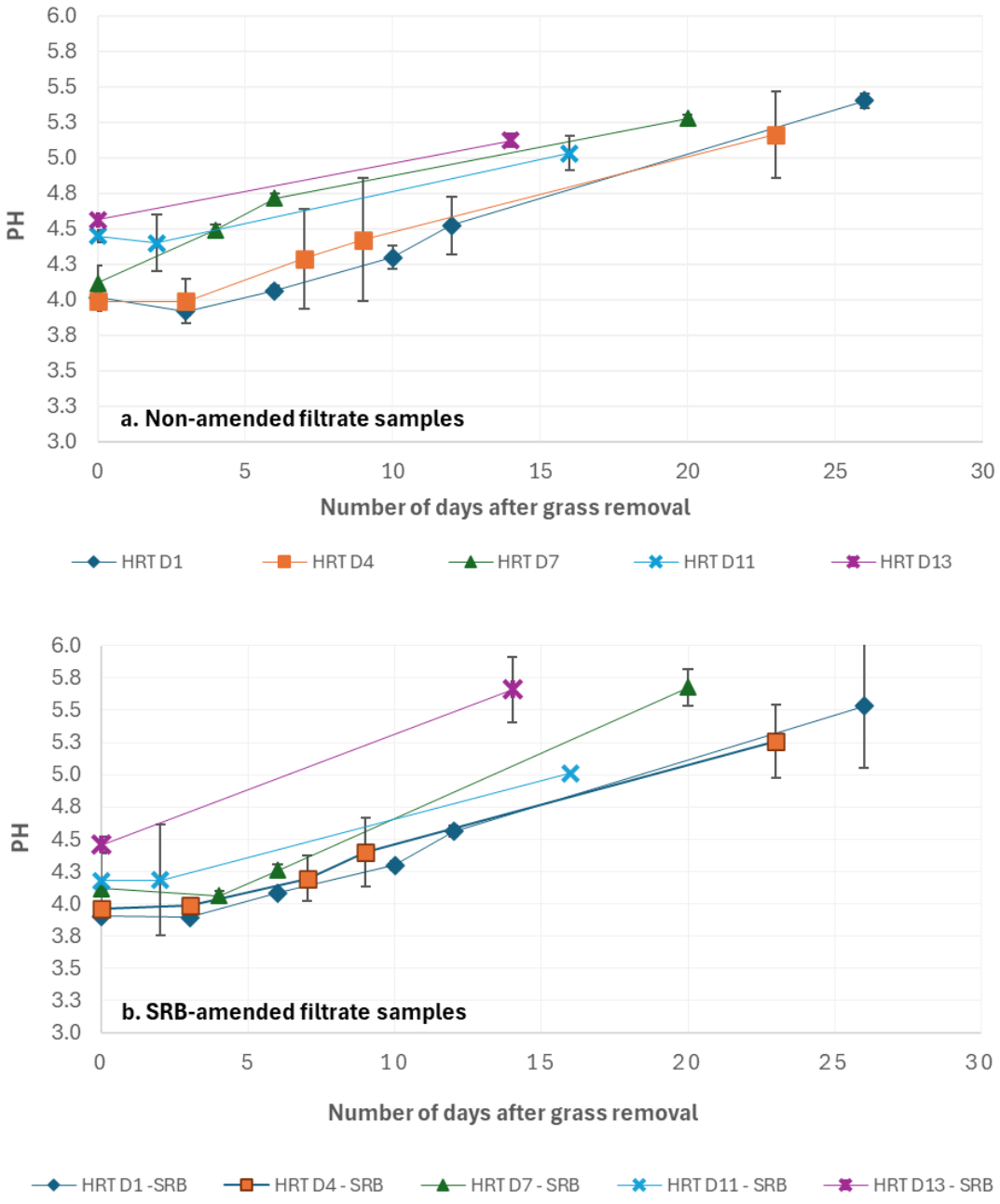


Figure 7.5 pH values for (a) non-amended filtrate samples and (b) SRB-amended filtrate samples vs the number of days after grass removal for initial grass hydraulic retention times (HRT). Error bars represent the standard deviation of duplicate analyses.

7.4.1.5 Evaluation of oxidizable material provided by the grass

Chemical oxygen demand (COD) determination provides a measure of the organic content and oxidizable material present in a system (Luis, 2018; Meegoda et al., 2018). As described in *Equation 7.1*, during the DSR remediation of AMD, carbon material (from the grass) is oxidised, and electrons are lost. The electrons are accepted by sulfates present in the AMD, which are reduced to sulfides (Kaksonen and Puhakka, 2007; Reyes-

Alvarado et al., 2018). Figure 7.6 shows the average COD concentration with standard deviations for each retention time sample, and the sample blanks for both non-and SRB-amended samples. These data are presented in Appendix IV, Supplementary data for Chapter 7 - Table S1.11.

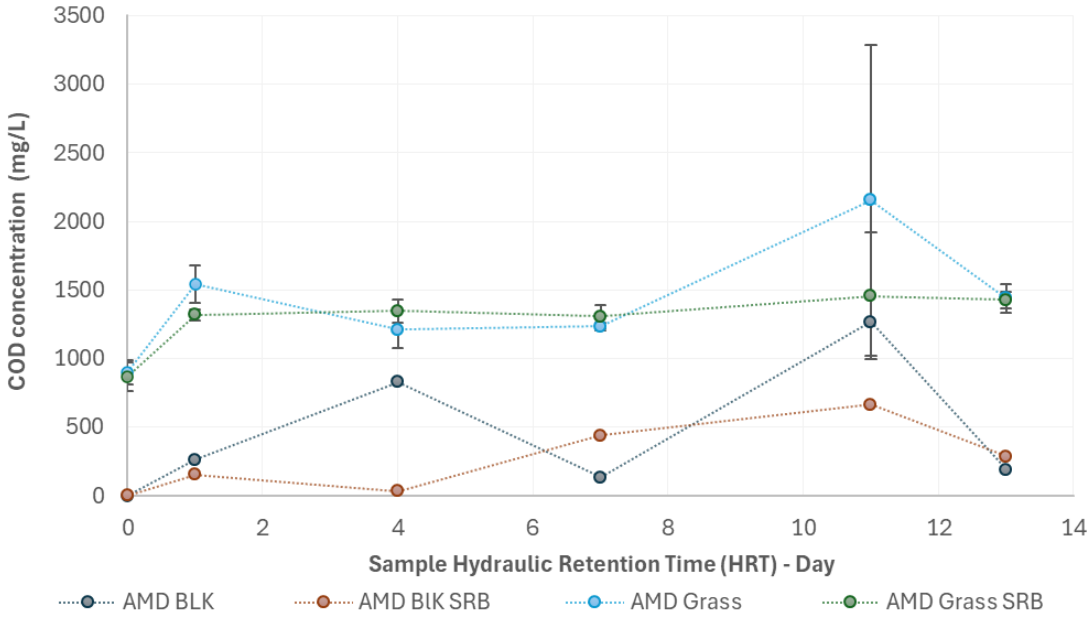


Figure 7.6 Average COD concentrations with standard deviations for non- and SRB-amended samples and AMD blank samples for each selected grass-AMD hydraulic retention times (HRT), using a 30 g/L grass-AMD ratio. Error bars represent the standard deviation of duplicate analyses.

After initial grass contract with AMD, the average COD concentration of the AMD samples increased by an average of 901 mg/L for the non-amended sample and 865 mg/L for the SRB-amended sample. The initial increase in COD is expected, owing to the organic carbon contribution from the grass (Matshusa-Masithi et al., 2012; Naidu et al., 2021). A further increase in COD concentration of 643 mg/L occurred on day one for the AMD Grass sample and 454 mg/L and for the Grass SRB sample. The increase in COD can be attributed to the breakdown of the grass lignocellulosic structure by acid hydrolysis and the release of soluble monomeric sugars in the AMD media (Greenway, 2019; Sluiter et al., 2012; van Hille et al., 2021). The COD concentration of the non-amended sample decreased on day four, while the SRB-amended sample initially increased marginally, and thereafter, similar concentrations were maintained until day thirteen. The high COD concentration observed for the non-amended sample on day eleven was accompanied by an elevated blank concentration. A high standard deviation was reported for replicate sample analysis, and as such, these data are considered anomalous and likely caused by contamination or analytical error. The elevated COD concentration reported for the day four blank sample was not accompanied by elevated COD concentration in the samples and could have resulted from possible contamination of the blank during analysis. After removing the anomalous day eleven non-amended value, similar average COD concentrations were observed

for both the non-amended and SRB-amended samples indicating that SRB addition did not affect the extent to which soluble COD was produced.

Figure 7.7 presents plots of the COD concentration of the non-amended (a), and SRB-amended (b) filtrate samples against the number of days after grass was removed. Results showed that the COD concentrations in the filtrate samples generally decreased after grass was removed and a final average COD concentration of 1163 mg/L was reported for the non-amended filtrate samples, and 1022 mg/L for the SRB-amended filtrate samples. The decreased COD concentrations in the filtrate samples could be attributed to the removal of the grass with concomitant cessation of release of further monomeric sugars, and the continued conversion of the monomeric sugars present in the filtrate samples to VFAs (Chen et al., 2020; Greenway, 2019). The COD data with standard deviations are reported in Appendix IV, Supplementary data for Chapter 7 - Table S1.12.

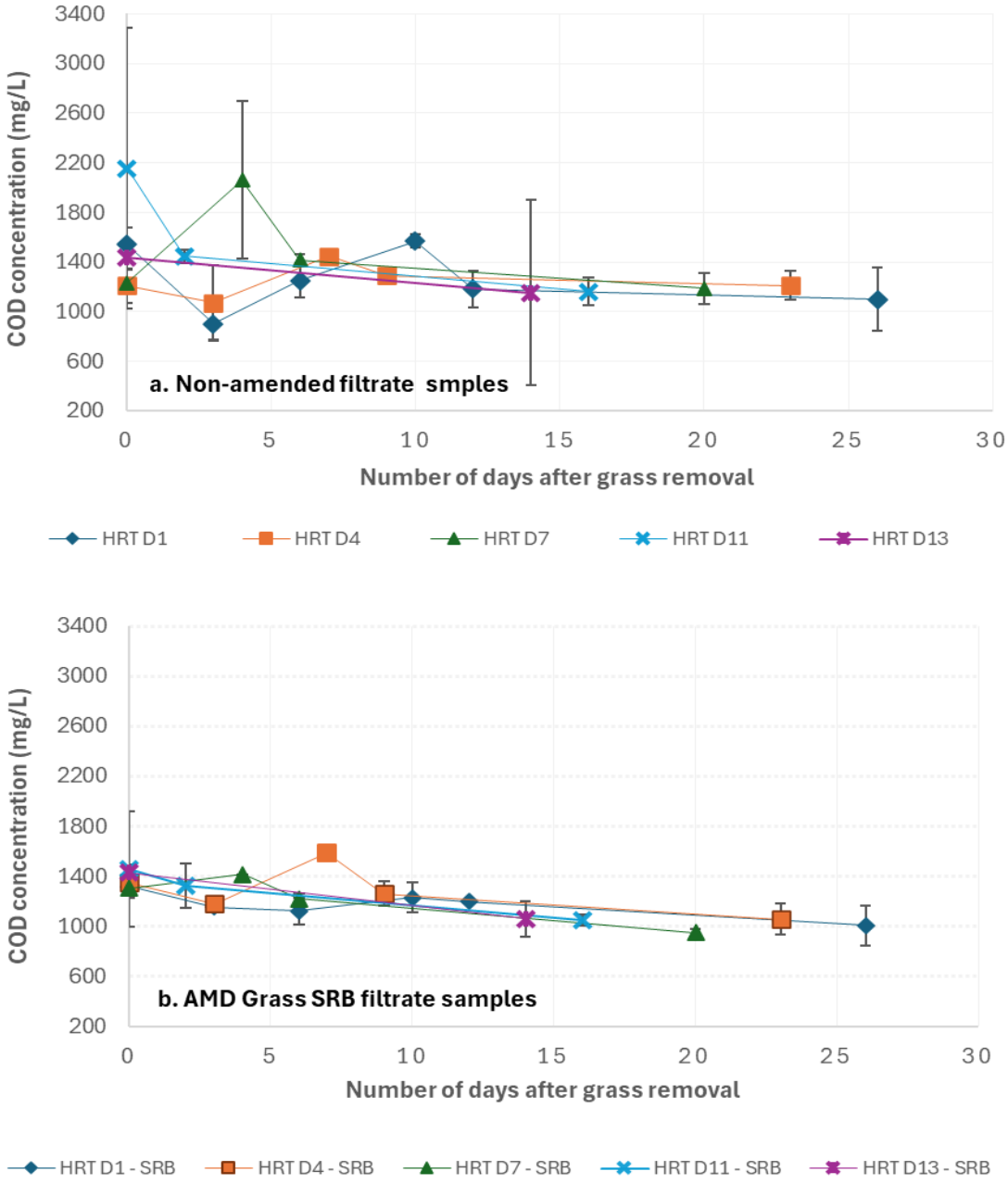


Figure 7.7 COD concentrations for (a) non-amended filtrate samples and (b) SRB-amended filtrate samples plotted against the number of days after grass removal. Error bars represent the standard deviation of duplicate analyses.

7.4.1.6 Evaluation of the conversion sulfate to sulfide

Sulfate is reduced to sulfide in the DSR process, and in this research, an increase in sulfide concentration was used as an indication of the effectiveness of the DSR reaction. The blank and average sample sulfide concentrations, including standard deviations for the different retention times, are shown in Figure 7.8 for the non- and SRB-amended samples. The sulfide data with standard deviations are reported in Appendix IV, Supplementary data for Chapter 7 - Table S1.13.

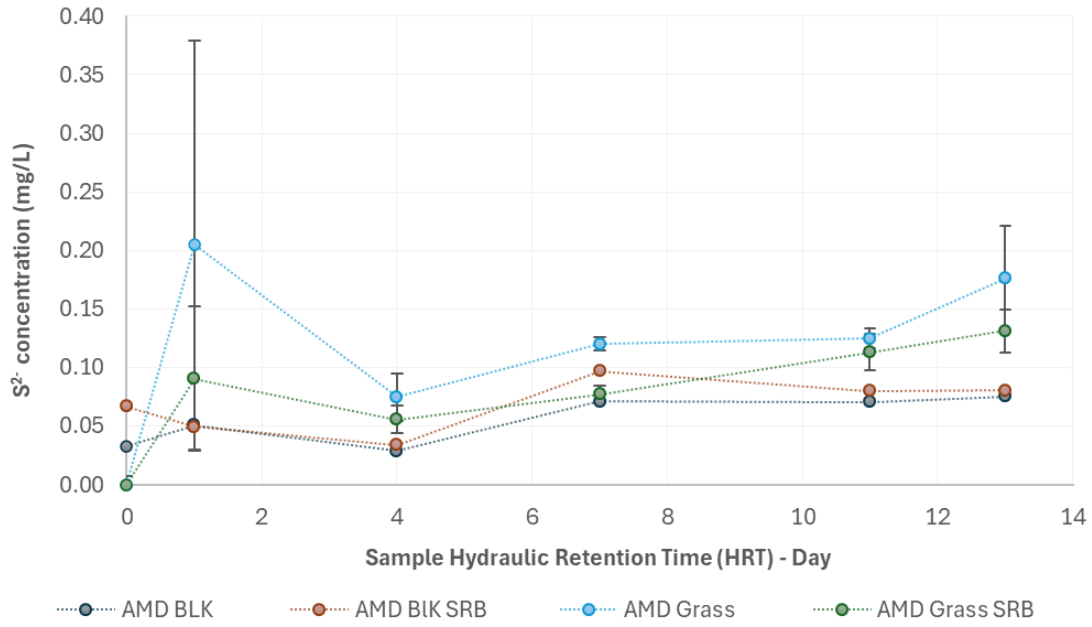


Figure 7.8 Sulfide concentrations for AMD blanks and for non- and SRB-amended samples, for each for the selected grass-AMD hydraulic retention times (HRT), using a 30 g/L grass-AMD ratio. Error bars represent the standard deviation of duplicate analyses.

The initial blank and all non-amended and SRB-amended samples reported sulfide concentrations of less than 0.1 mg/L. While some variations occurred, the sulfide concentrations of the blank samples remained below 0.1 mg/L for the test duration. The highest sulfide concentration was reported on the first day for the non-amended grass sample (0.21 mg/L), however the high standard deviation reported for replicate analysis casts doubt on the validity of this result. The steady increase in sulfide concentrations reported from the fourth day onwards are more likely owing to an anticipated lag time required for SRB acclimatise to low pH conditions (Dong et al., 2023; Naidu et al., 2021). The improved sulfide production with increased grass-AMD HRT were supported by increased pH (Zagury et al., 2006). The greater increase in sulfide concentration observed in the non-amended samples was unexpected, as the anticipation was for the SRB amended reactors to enhance the DSR reaction.

The change in sulfide concentration observed in the filtrate solutions after grass removal are shown in Figure 7.9(a) for the non-amended sample and in 7.9(b) for the SRB-amended sample.

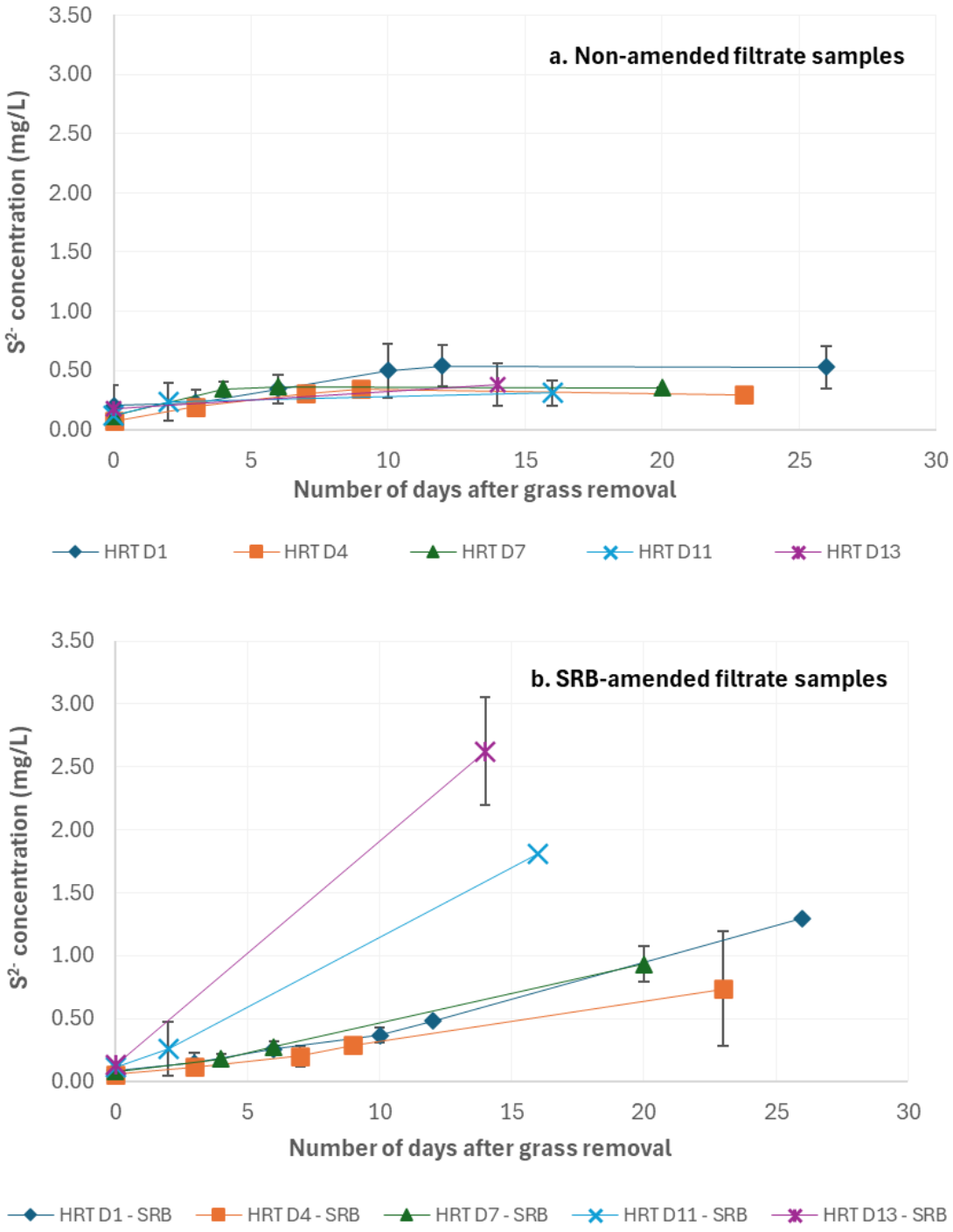


Figure 7.9 Sulfide concentrations for (a) non-amended filtrate samples and (b) SRB-amended filtrate samples plotted against the number of days after grass removal. Error bars represent the standard deviation of duplicate analyses.

In this instance, a larger increase in sulfide concentration occurred in the SRB-amended filtrate solutions than in the non-amended filtrate solutions. An exponential increase in sulfide concentration was noted for the day eleven and thirteen HRT SRB-amended filtrate solutions, and these samples reported an order of magnitude higher final sulfide concentration than the same retention time non-amended filtrate samples. The increase

in sulfide concentration with concomitant increase in pH, would imply sustained DSR activity after the grass was removed from the reactor. Greater decreases in COD and VFA concentration, were observed in SRB-amended day eleven and thirteen samples. This observation, combined with significantly increased sulfide concentrations reported for these samples would indicate that longer grass-AMD HRT, with SRB amendment, promoted an improved conversion of sulfate to sulfide. However, for complete conversion of the initial 5000 mg/L of sulfate to sulfide, a final sulfide concentration of 1667 mg/L is needed. To achieve complete conversion of all the sulfates to sulfides, sufficient available organic material is required to provide a 0.67 COD/sulfate ratio (Chen et al., 2020; Greben et al., 2000). An approximate COD/sulfate ratio of 0.27 was calculated for these samples using the initial sulfate concentration and the averaged COD concentration achieved during acid hydrolysis. Thus, indicating that the available organic carbon content was insufficient to support complete conversion of sulfate to sulfide. An increased solids loading would be required to achieve the necessary COD/sulfate ratio (van Hille et al., 2021). All sulfide data are reported in Appendix IV, Supplementary data for Chapter 7 - Table S1.14.

7.4.1.7 Evaluation of iron (Fe) decrease as a measure of metals decrease during the AMD remediation process

The change in iron (Fe) concentration was monitored over time and the average Fe concentrations for the blank, non-amened and SRB-amended samples, with standard deviations are shown in Figure 7.10. It is expected that an increase in pH would result in the precipitation of metals, and the solution metals concentrations would decrease (Naidu et al., 2020; Skousen et al., 2017). Significantly increased Fe concentrations were observed for all day eleven blanks and samples, however, the high standard deviation reported for the SRB-amended replicate analyses which could indicate the possibility of either dilution or instrumental error for this sampling point. As such, day eleven data were omitted from Figure 7.10, but are provided in Appendix IV, Supplementary data for Chapter 7 - Table S1.15.

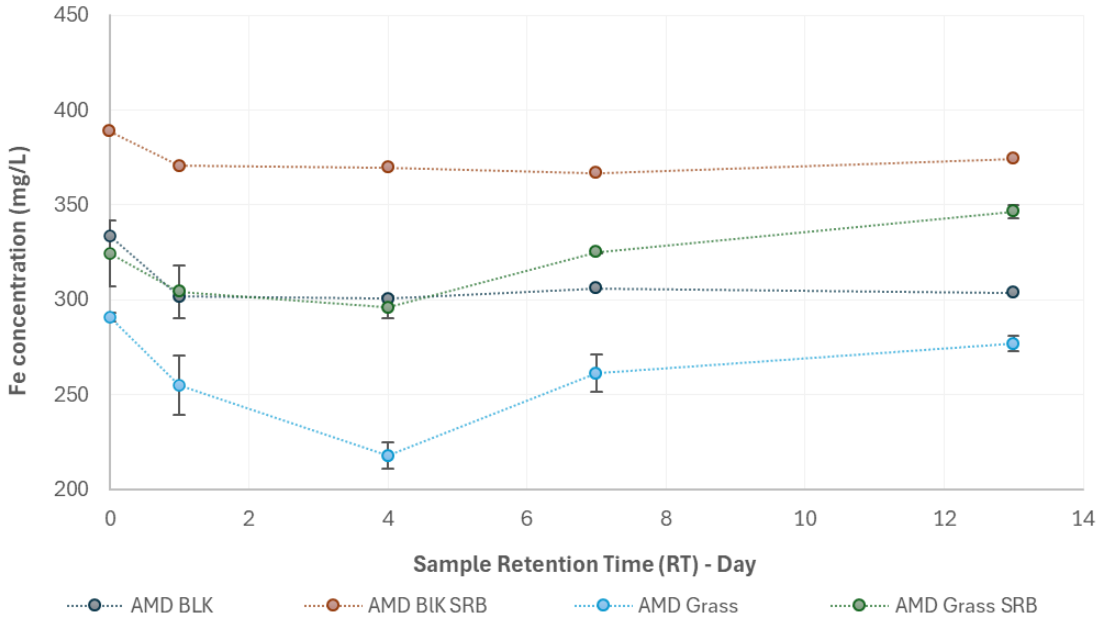


Figure 7.10 Fe concentrations for blanks and for non- and SRB-amended samples, for each of the selected grass-AMD hydraulic retention times (HRT), using a 30 g/L grass-AMD ratio. Error bars represent the standard deviation of duplicate analyses.

An initial Fe concentration of 296 mg/L was reported for the non-amended sample and 327 mg/L for the SRB-amended sample. The SRB-amended blank sample also reported higher Fe concentrations, indicating that Fe might have been introduced from the SRB inoculum enrichment source which comprised reed bed mud collected from AMD surrounds in the Mpumalanga coal fields (Smith et al., 2025). A decrease in Fe concentration was observed immediately after the addition of grass to AMD for both non-and SRB-amended samples, and also in the blank samples. A possible explanation for the decrease in Fe concentration could be that the Fe was oxidised when the reactors were first opened for sampling, resulting in precipitation of Fe hydroxide. No further decrease was noted in either of the blank samples, however a further decrease in Fe concentration was observed in the grass samples, and the non-amended samples decreased more than the SRB-amended samples (37 mg/L vs 8 mg/L) on day four. This decrease could probably be attributed to the expected precipitation of the Fe from solution as the pH of the AMD increased (Naidu et al., 2021, 2020; Skousen et al., 2017). Both samples then reported increased Fe concentrations on day seven and on day thirteen. The non-amended sample reported a final decrease in concentration of 14 mg/L from starting concentration, while the SRB-amended sample increased by 22 mg/L in Fe concentration. The increase and decrease in Fe concentration may be as a result of precipitation and redissolution of Fe hydroxides because of low pH values.

The Fe concentrations in the filtrate samples are shown in Figures 7.11(a) for the non-amended samples and 7.11(b) for SRB-amended samples, and the data are reported in Appendix IV, Supplementary data for Chapter 7 - Table S1.16.

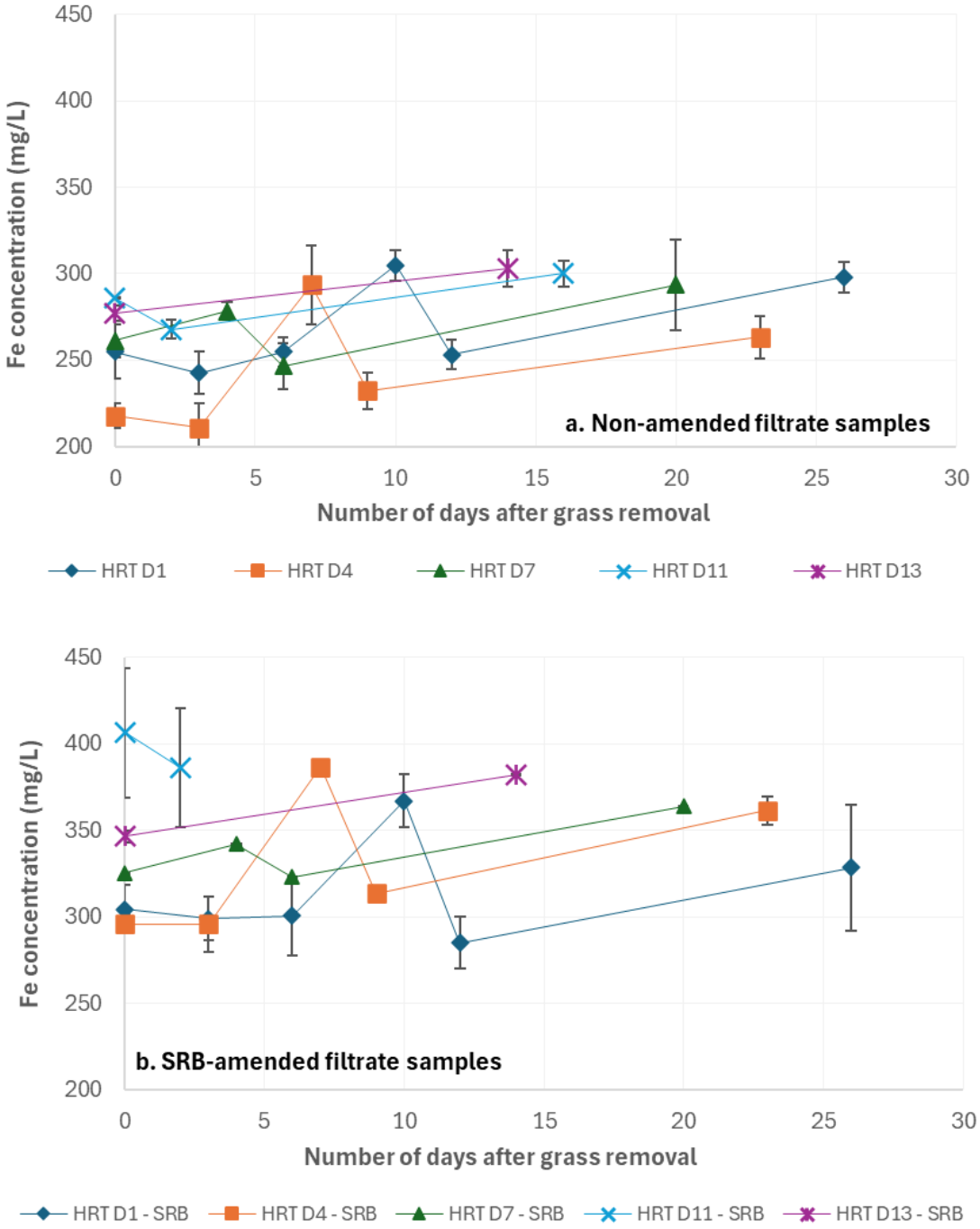


Figure 7.11 Fe concentrations for (a) non-amended filtrate samples and (b) SRB-amended filtrate samples plotted against the number of days after grass removal. Error bars represent the standard deviation of duplicate analyses.

An increase in Fe concentration was observed in the filtrate samples, and in most instances, Fe concentrations continued to increase with time. Higher Fe concentrations were reported for the longer grass-AMD retention time day 11 and 13 samples. This increase was not expected, but it could possibly be because some of the Fe hydroxide precipitated particles were so small that they passed through the filter paper into

the filtrate solution, resulting in a similar dynamic precipitation/redissolution of these particles, that were affected by pH.

7.4.2 Enzymatic hydrolysis and fermentation data

The results of experimental work to investigate the effect of SSF on pre-treated and untreated grass samples are presented here. Samples were analysed immediately after contacting the grass with the SSF mixture to determine sugars: (glucose, xylose), lactate, VFAs: (acetate, propionate, isovalerate, and valerate), and ethanol concentrations. Samples were maintained at 37°C ± 0.5°C in a Labcon shaking incubator and re-analysed on days one, two, four, six, eight, and twelve. An untreated grass sample, and a sample blank containing only SSF reagents were included in the study. These data are presented in Appendix IV, Supplementary data for Chapter 7 - Table S2.1 – S2.9. Glucose concentrations over time are shown in Figure 7.12 (Supplementary material Table S2.1).

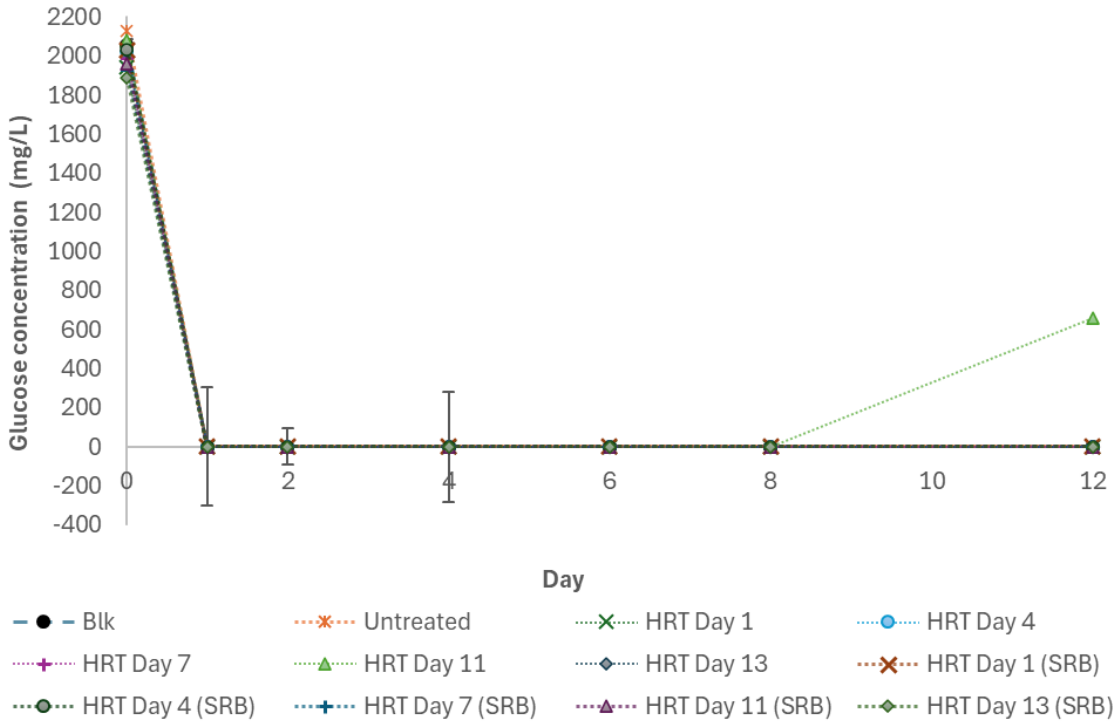


Figure 7.12 Glucose concentrations produced during SSF hydrolysis of untreated and pre-treated grass samples, for non- and SRB-amended samples. Error bars represent the standard deviation of duplicate analyses.

Immediately after grass was contacted with the SSF mixture, the glucose concentration in the untreated grass sample reported 2126 mg/L, and the average glucose concentration for the pre-treated grass samples reported 2012 mg/L. These concentrations were similar to the blank sample concentration of 2059 mg/L. Except for one of the non-amended day eleven samples, which reported an increased glucose concentration

of 660 mg/L on day twelve of SSF, no further glucose peaks were detected. A possible explanation for this could be that the initial glucose present was immediately used up in the production of ethanol as demonstrated by Burman et al. (2019). A further explanation could be attributed to a peak overlap from an unidentified peak at retention time (RT) 3.68 min, immediately preceding the glucose peak at RT 4.00 min. This is shown in chromatogram peaks in Figure 7.13(a) and 7.13(b). In Figure 7.13(a), the glucose peak is clearly separated from the unidentified RT 3.68 min peak. In Figure 3.13(b), the unidentified peak extends past the 4 minute retention time where the glucose peak was previously seen, thus indicating a possible peak overlap. As 5 g/L (5000 mg/L) dextrose was used in the preparation of the SSF mixture, it is assumed that the unidentified peak is attributed to a glucose isomer, possibly D-glucose. Dextrose and glucose are used interchangeably, and dextrose is referred to as D-glucose sugar (Bryant, 1934; Galadima and Muraza, 2019; Sun et al., 2010). The peak overlap occurred one day after the addition of the hydrolysed grass residue to the SSF mixture and is likely caused by chemical reactions between reaction products from the grass and the SSF mixture.

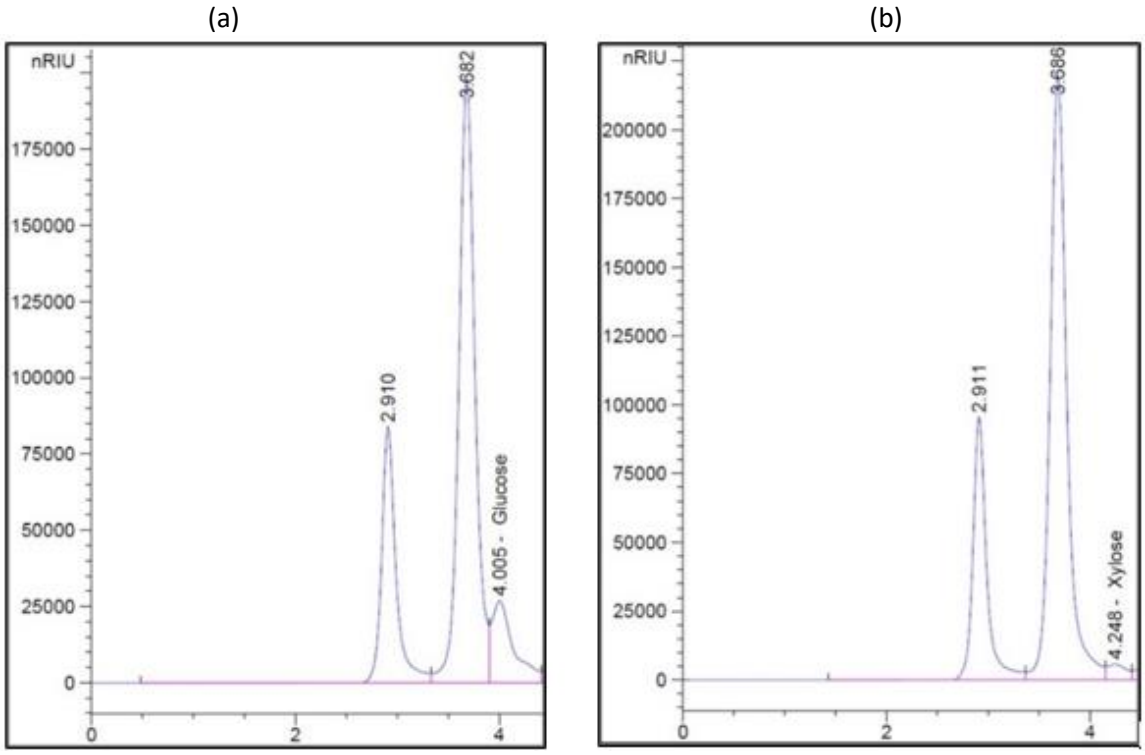


Figure 7.13 HPLC chromatograms showing (a), the assumed glucose isomer peak at RT 3.68, and a separate glucose peak at RT 4.00 and (b), a possible glucose isomer peak overlapping glucose peak

The initial glucose peak concentration was determined to be ≈2000 mg/L, and since 5000 mg/L of dextrose was added to the SSF mixture, an assumption was made that the initial concentration of the glucose isomer peak (RT 3.68) was 3000 mg/L. By equating this concentration to the initial peak height of the isomer peak, the concentrations of the remaining glucose isomer peaks were calculated. Figure 7.14 shows that for most samples, an initial increase in glucose isomer concentration occurred, presumably from the peak overlap on day one. A further increase in concentration was noted for the non- and SRB-amended day thirteen samples

on the second day of SSF, which could be attributed to increased glucose concentration resulting from enzymatic hydrolysis of the grass. After which, the glucose-isomer/glucose concentrations decreased, which was in line with the increase observed in the ethanol concentration (Figure 7.21). The glucose-isomer/glucose data are shown in Appendix IV, Supplementary data for Chapter 7 - Table S2.2.

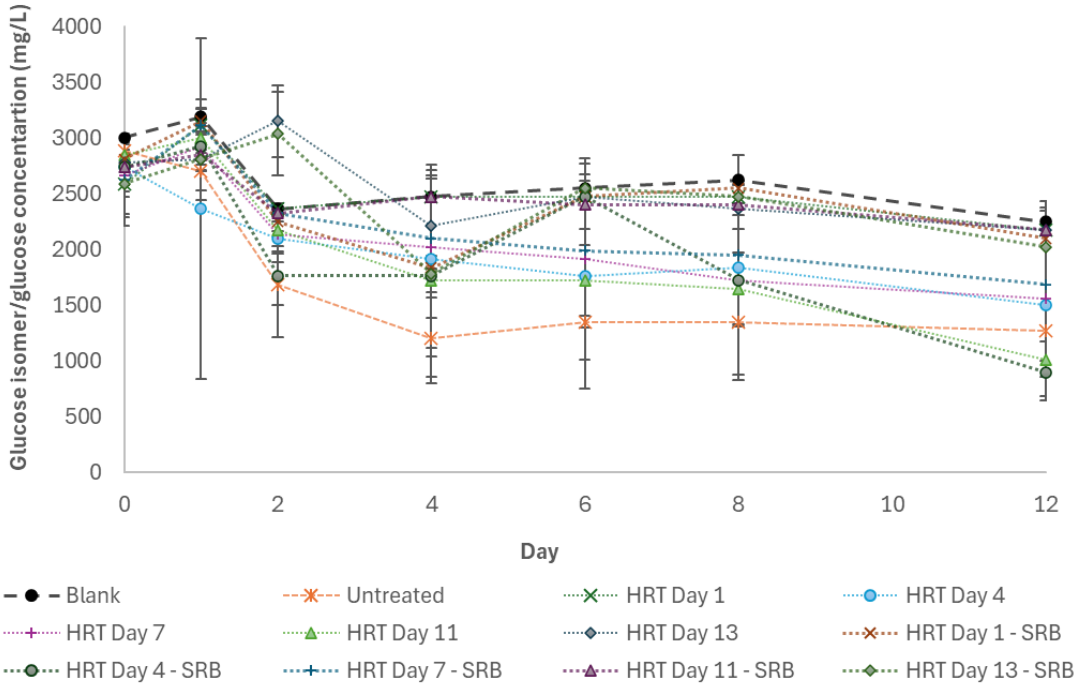


Figure 7.14 The glucose-isomer/glucose peak showing an initial increase in concentration, followed by a decrease in concentration over time for non- and SRB-amended samples. Error bars represent the standard deviation of duplicate analyses.

The changes in xylose concentrations achieved during SSF are shown in Figure 7.15 and data are provided in Appendix IV, Supplementary data for Chapter 7 - Table S2.3.

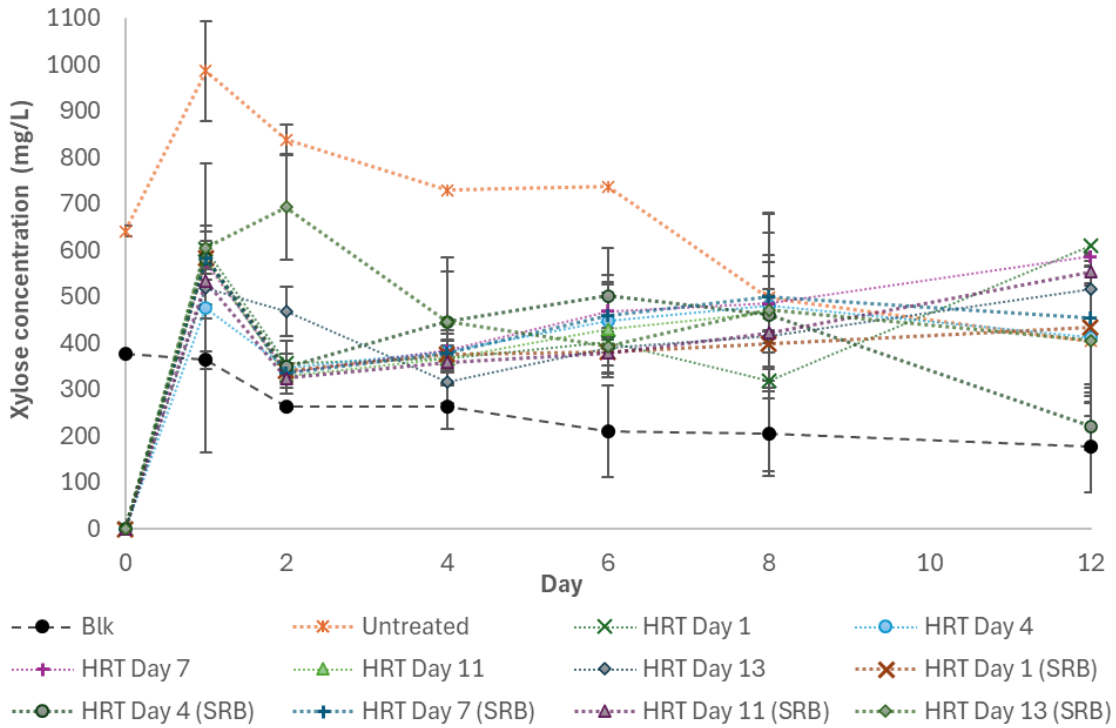


Figure 7.15 Xylose concentrations produced during SSF hydrolysis of untreated and pre-treated grass samples, for non- and SRB-amended samples. Error bars represent the standard deviation of duplicate analyses.

The blank (378 mg/L) and the untreated grass sample (642 mg/L) were the only samples to show an increase in xylose concentrations immediately after contacting the grass samples with the SSF mixture. All samples increased in xylose concentrations on day one. The untreated grass sample reported the highest xylose concentration from day one (987 mg/L) until day six (738 mg/L). Of the pre-treated samples, the SRB-amended day thirteen sample presented the second highest concentration on the second (693 mg/L) to the fourth day (446 mg/L). After an initial decrease of ≈100 mg/L between days one and two, and then ≈54 mg/L between days four and six, the blank maintained an average xylose concentration of ≈197 mg/L the until day twelve when the experiment was terminated. All xylose concentrations reported higher concentrations than the blank sample, indicating that xylose was released from the grass during the SSF process. It was expected that the treated grass samples would report lower xylose concentrations during SSF, owing to the prior release of xylose during acid hydrolysis, which was utilised in the AMD bioremediation phase.

The changes in Lactate concentrations achieved during SSF are shown in Figure 7.16 and data are provided in Appendix IV, Supplementary data for Chapter 7 - Table S2.4.

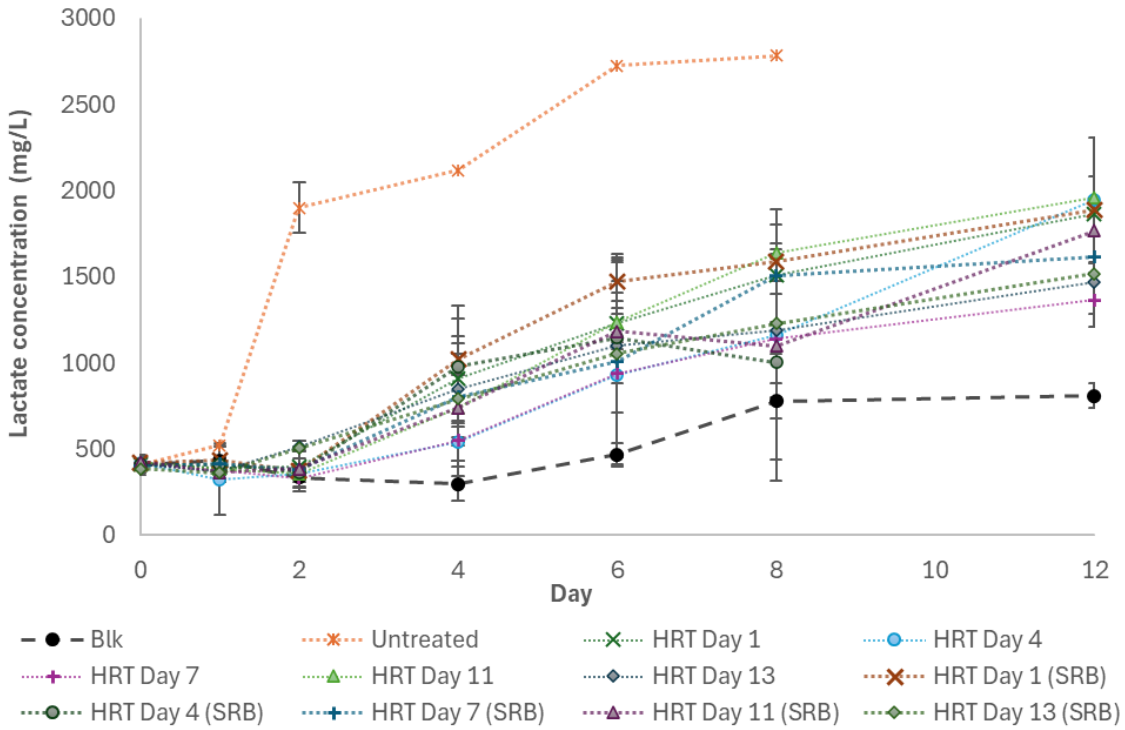


Figure 7.16. Lactate concentrations produced during SSF hydrolysis of untreated and pre-treated grass samples, for non- and SRB-amended samples. Error bars represent the standard deviation of duplicate analyses.

Lactate concentrations increased over time for all samples. The average increase in lactate concentration of the non-amended pretreated samples taken from the starting concentration was 1305 mg/L. The SRB-amended pretreated samples increased by a marginally smaller average of 1151 mg/L. The untreated grass sample increase by 2380 mg/L between day zero and day eight which was significantly more than the increase observed in the pretreated samples. No results was available for day twelve for the untreated sample. The blank sample doubled in xylose concentration on day eight and maintained a similar concentration on day twelve when the experiment was stopped. The increase in blank concentration was not anticipated and cannot be explained.

The increase in concentration of short-chain volatile fatty acid (VFA) fermentation products is shown in Figures 7.17 for acetate and 7.18 for propionate, and these data are provided in Appendix IV, Supplementary data for Chapter 7 - Tables S2.5 and S2.6.

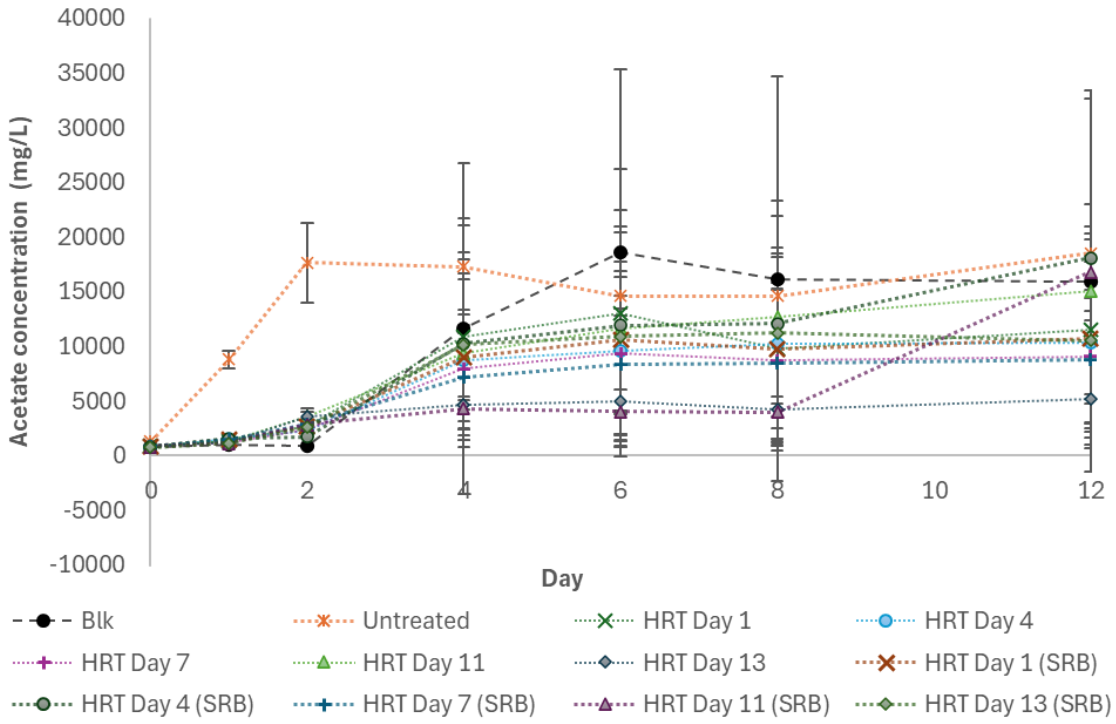


Figure 7.17 Acetate concentrations produced during fermentation of untreated, and pre-treated grass samples, for non- and SRB-amended samples. Error bars represent the standard deviation of duplicate analyses.

Most sample concentrations increased to maximum acetate concentration between day two and day six, after which, concentrations increased only slightly or remained the same until the end of the experiment. Exceptions were for the untreated sample, the non- and SRB-amended day four and eleven samples, which reported more notable increases in acetate concentration on day twelve. However, the high standard deviations encountered after day four, render these results unreliable, and further investigation will be required to establish the cause of the high standard deviations observed.

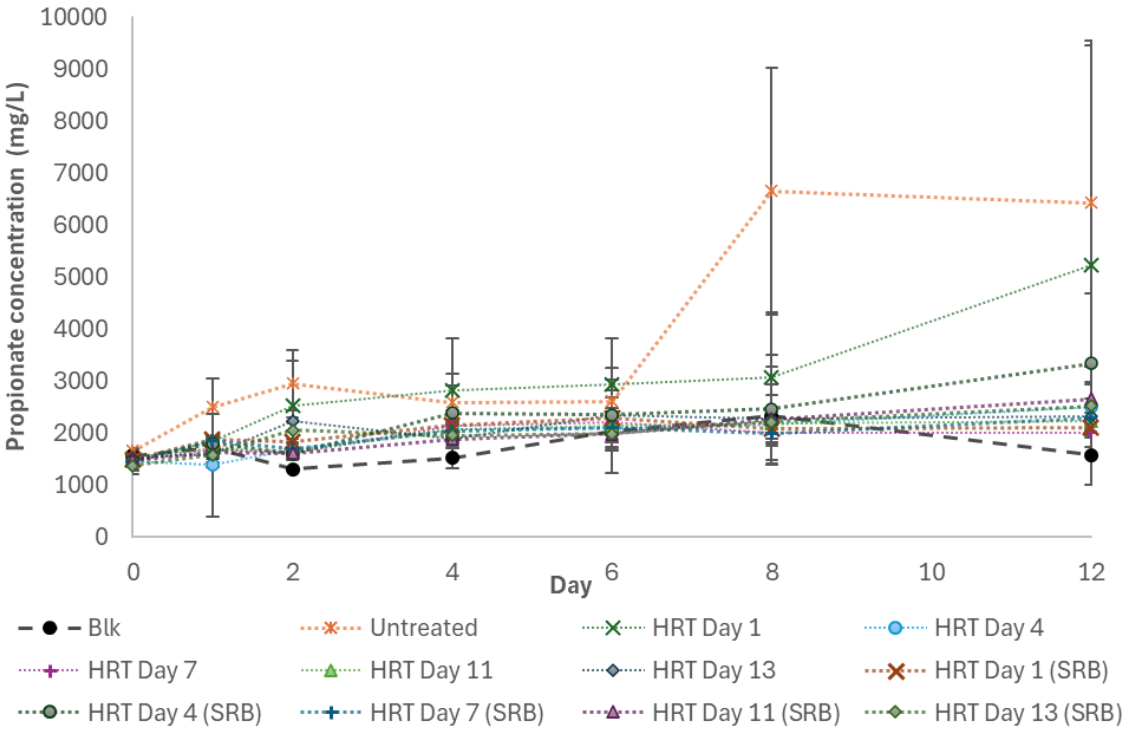


Figure 7.18 Propionate concentrations produced during fermentation of untreated, and pre-treated grass samples, for non- and SRB-amended samples. Error bars represent the standard deviation of duplicate analyses.

Propionate concentrations increased marginally over time, however, the untreated, and the HRT day one sample showed more pronounced increase, particularly between day eight and day twelve. High standard deviations were also reported on these days, which would cast doubt on the actual extent of the increase observed.

Valerate and iso-valerate are products of the fermentation of organic matter and have slightly longer chain lengths than acetate and propionate. These results are shown in Figures 7.19 and 7.20 respectively and the data provided in Appendix IV - Supplementary data for Chapter 7, Tables S2.7 and S2.8.

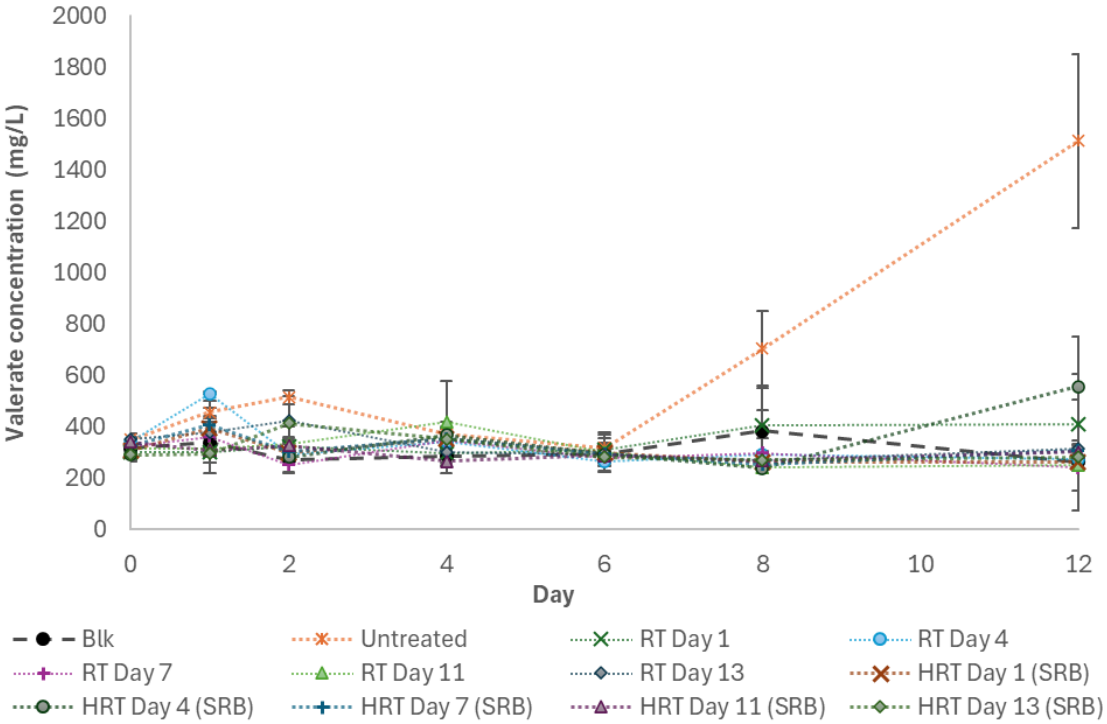


Figure 7.19 Valerate concentrations produced during fermentation of untreated, and pre-treated grass samples, for non- and SRB-amended samples. Error bars represent the standard deviation of duplicate analyses.

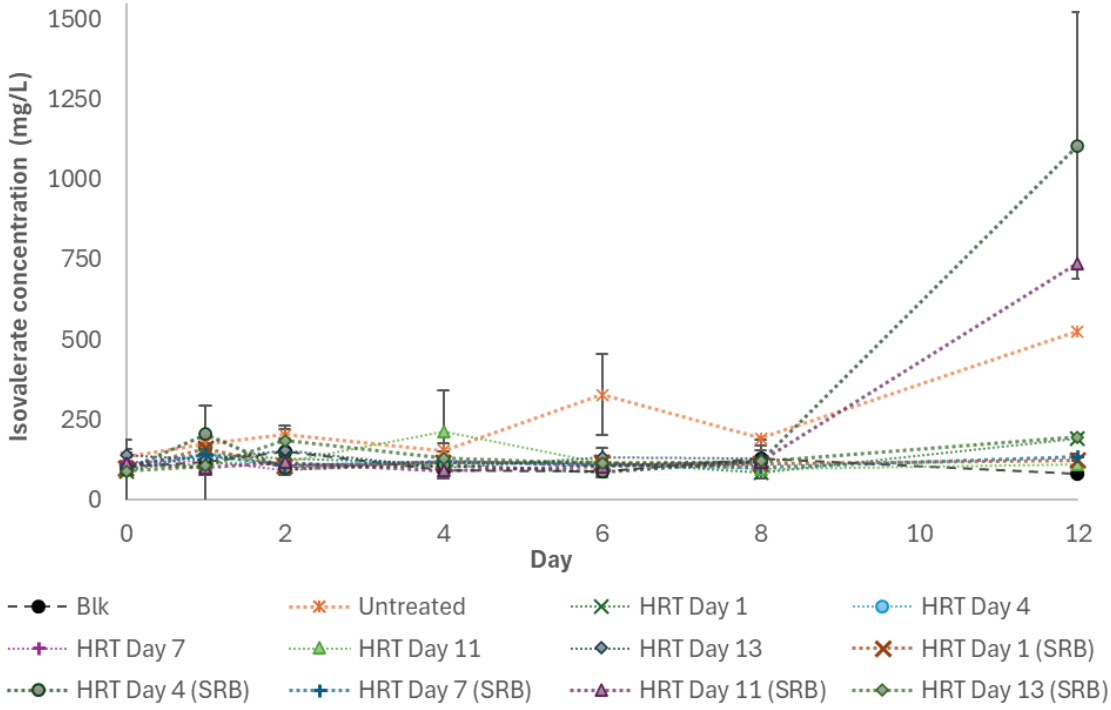


Figure 7.20 Isovalerate concentrations produced during fermentation of untreated, and pre-treated grass samples, for non- and SRB-amended samples. Error bars represent the standard deviation of duplicate analyses.

Valerate and iso-valerate concentrations remained mostly low for the duration of the SSF experiment. The average valerate concentration for both the non and SRB-amended samples was 320 mg/L. The untreated grass sample increased in concentration from 319 mg/L to 1514 mg/L between days six and twelve. Similarly, for isovalerate, the concentrations remained low and reported an average of 123 mg/L for the non-amended samples, and 460 mg/L for the SRB-amended samples. The isovalerate concentration of the SRB-amended day four sample increased tenfold between days eight and twelve (119 – 1106 mg/L). The SRB-amended day eleven sample increased from 118 – 739 mg/L during the same period, and the untreated sample increased from 191 – 526 mg/L.

VFAs such as acetic, propionic, valeric and iso-valeric acids are produced from the bioconversion of organic matter and can be used to produce high value products (Agnihotri et al., 2022). Optimisation of these processes did not form part of this study.

Ethanol concentrations produced during SSF are presented in Figure 7.21 and data are provided in Appendix IV, Supplementary data for Chapter 7 - Tables S2.9.

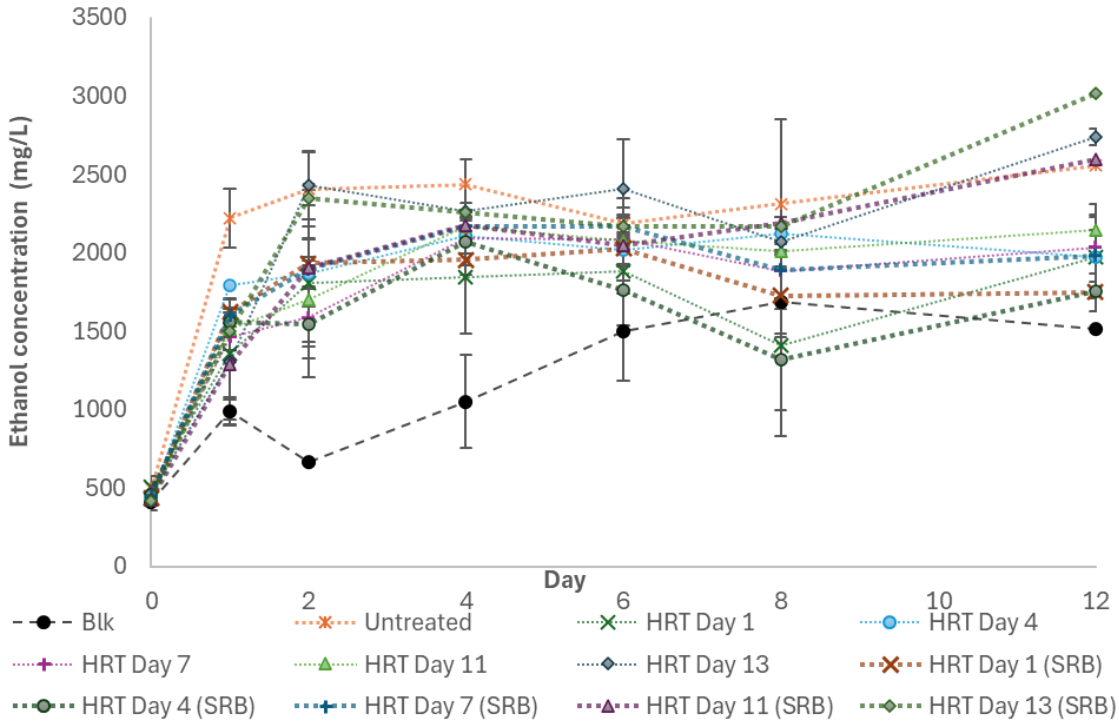


Figure 7.21 Ethanol concentrations produced during fermentation of untreated and pre-treated grass samples, for non- and SRB-amended samples. Error bars represent the standard deviation of duplicate analyses.

An initial average ethanol concentration of 447 mg/L was reported for all samples including the blank sample immediately after grass was contacted with the SSF medium. Some ethanol was expected in the blank

sample, owing the addition of dextrose to the SSF hydrolysis and fermentation mixture. Ethanol concentrations generally increased as SSF retention times increased. The greatest increase from the starting ethanol concentration was achieved on day twelve of SSF for the SRB-amended grass sample that had been acid-hydrolysed for thirteen days. The increase in ethanol concentration taken from the initial ethanol concentration immediately after the hydrolysed grass was added to the SSF mixture and the last day twelve of the SSF experiment is shown in Table 7.1.

Table 7.1 The Increase in ethanol concentration produced during SSF

Non-amended Sample	**Blank**	**Untreated**	**HRT Day 1**	**HRT Day 4**	**HRT Day 7**	**HRT Day 11**	**HRT Day 13**
Increase in ethanol concentration from day 0 to day 12 (in mg/L)	1107	2057	1464	1537	1564	1718	2274
SRB-amended Sample	**Blank**	**Untreated**	**HRT Day 1 (SRB)**	**HRT Day 4 (SRB)**	**HRT Day 7 (SRB)**	**HRT Day 11 (SRB)**	**HRT Day 13 (SRB)**
Increase in ethanol concentration from day 0 to day 12 (in mg/L)	1107	2057	1314	1296	1532	2170	2605

The results show that all samples achieved greater increases in ethanol concentration than were measured in the blank sample where no grass was added. This indicated that the addition of grass to the SSF reactors did contribute to increased ethanol concentrations. The SRB-amended HRT day thirteen sample showed an increase in concentration of 2605 mg/L from the initial ethanol concentration at day 0. This was followed by the non-amended HRT day thirteen sample with an increase of 2274 mg/L. The HRT day eleven SRB-amended sample achieved an increase in concentration of 2170 mg/L followed by the untreated sample (2057 mg/L), and the non-amended day eleven sample (1745 mg/L). These data demonstrated that the samples that had the longest pretreatment HRT, and the untreated grass sample achieved the greatest increase in ethanol concentration. The day eleven and thirteen SRB-amended samples achieved a greater increase in ethanol concentration than the non-amended samples. The percentage relative standard deviations (% RSDs) of replicate ethanol concentrations were calculated to relate the standard deviation to the mean ethanol concentration for each sample. These values are included in Appendix IV, Supplementary data for Chapter 7 - Table S2.9. The % RSDs varied across samples, with 63% of the uninoculated samples, and 75% of the inoculated samples achieving % RSDs of below 10%. Although RSDs greater than 10% reduce confidence in the data shown in Table 7.1, the overall trends observed support an increase in ethanol concentration.

Using the initial average glucose concentration of 2012 mg/L to calculate the theoretical glucose conversion to ethanol, an ethanol concentration of 1029 mg/L was possible. In most instances the ethanol

concentrations produced were significantly higher, and the day eleven and thirteen samples produced double to two and a half times the expected concentration. This would equate to the theoretical contribution from the proposed glucose isomer peak and to any glucose released from the grass samples.

7.5 Conclusions

SEM analysis confirmed the disruption of the complex polymeric lignocellusic structure of the grass sample tested using a weak-acid AMD solution at ambient temperature. Increased glucose and xylose concentrations showed that monomeric sugars were released from the disrupted lignocellulosic structure. The subsequent decrease in the monomeric sugars concentration was accompanied by increased acetate and propionate concentrations indicating the successful acidogenesis conversion of sugars to volatile fatty acid compounds. pH and sulfide concentrations increased indicating the success of the dissimilatory reduction of sulfate (DSR) process. The incomplete conversion of sulfates to sulfides suggested a lack of available organic material to sustain the sulfate reduction process (calculated experimental COD/sulfate ratio of 0.27 vs required 0.67 COD/sulfate ratio). It implies that an increased solids loading would be required to achieve the necessary reduction of sulfates to sulfides. Even though pH increased, only a small reduction in iron concentration was observed during the AMD pre-treatment experimental work. The AMD remediation processes continued in the filtrate samples after the grass had been removed, and an improved remediation of AMD was achieved with the addition of SRB and with extended grass-AMD retention times.

The combined hydrolysis and fermentation (SSF) of the pre-treated grass samples showed that the grass samples with the longest pre-treatment hydraulic retention times (HRT), and SRB-amendment produced greater bioethanol concentrations than the non-amended samples. The untreated grass sample that had not been exposed to prior acid hydrolysis, produced an increase in ethanol concentration that was similar to the best performing pre-treated grass samples. This would indicate that the physical pre-treatment to reduce the grass size fraction was sufficient to allow adequate conversion of glucose to ethanol. The conversion could however be improved by employing an extended acid hydrolysis pre-treatment step and by the amendment of the acid hydrolysis stage with sulfate reducing bacteria (SRB). Thus, extended grass-AMD hydraulic retention times, with SRB amendment, improved both the extent of the AMD remediation and bioethanol production.

High standard deviation or anomalous data points may reduce confidence in the interpretation of the data points in question. To address this, follow up investigations should consider strategies such as sterilisation of the grass to limit variability potential originating from microbes on the grass. Also, increasing the number of replicates would improve the statistical significance of the data.

7.6 Acknowledgements

The authors thank Moshibudi Mahlo and Mbengeni Nefale for their assistance with the experimental work, Nicholas Burman for his technical input in the fermentation experimental work, and Archie Corfield for his assistance with SEM analysis interpretation and document review.

7.7 References

Agnihotri, S., Yin, D.-M., Mahboubi, A., Sapmaz, T., Varjani, S., Qiao, W., Koseoglu-Imer, D.Y., Taherzadeh, M.J., 2022. A Glimpse of the World of Volatile Fatty Acids Production and Application: A review. Bioengineered 13, 1249–1275. https://doi.org/10.1080/21655979.2021.1996044

Akcil, A., Koldas, S., 2006. Acid Mine Drainage (AMD): causes, treatment and case studies. J. Clean. Prod. 14, 1139–1145. https://doi.org/10.1016/j.jclepro.2004.09.006

Bowman, S., Agrawal, V., Sharma, S., 2023. Role of pH and Eh in geothermal systems: Thermodynamic examples and impacts on scaling and corrosion. Geothermics 111, 102710. https://doi.org/10.1016/j.geothermics.2023.102710

Bryant, A.P., 1934. The Terminology of Sugars. Ind. Eng. Chem. 26, 231–231. https://doi.org/10.1021/ie50290a024

Burman, N.W., Harding, K.G., Sheridan, C.M., 2021. Evaluation of two different reactor configurations for the simultaneous remediation AMD and pretreatment of lignocellulosic biomass. Presented at the South African Chemical Engineering Congress (SACEC), At: Virtual.

Burman, N.W., Sheridan, C., Van Dyk, L., Harding, K.G., 2018. Modelling of low temperature dilute sulfuric acid pre-treatment of South African grass. Bioresour. Technol. Rep. 4, 21–28. https://doi.org/10.1016/j.biteb.2018.08.014

Burman, N.W., Sheridan, C.M., Harding, K.G., 2019. Lignocellulosic bioethanol production from grasses pre-treated with acid mine drainage: Modelling and comparison of SHF and SSF. Bioresour. Technol. Rep. 7, 100299. https://doi.org/10.1016/j.biteb.2019.100299

Cazier, E.A., Pham, T.-N., Cossus, L., Abla, M., Ilc, T., Lawrence, P., 2024. Exploring industrial lignocellulosic waste: Sources, types, and potential as high-value molecules. Waste Manag. 188, 11–38. https://doi.org/10.1016/j.wasman.2024.07.029

Chen, G., Ekama, G.A., Van Loosdrecht, M.C.M., Brdjanovic, D. (Eds.), 2020. Anaerobic wastewater treatment, in: Biological Wastewater Treatment: Principles, Modelling and Design. IWA Publishing, pp. 701–756. https://doi.org/10.2166/9781789060362_0701

Dong, Y., Gao, Z., Di, J., Wang, D., Yang, Z., Wang, Y., Xie, Z., 2023. Study on the Effectiveness of Sulfate Reducing Bacteria to Remove Heavy Metals (Fe, Mn, Cu, Cr) in Acid Mine Drainage. Sustainability 15, 5486. https://doi.org/10.3390/su15065486

Dowe, N., McMillan, J., 2008. SSF Experimental Protocols — Lignocellulosic Biomass Hydrolysis and Fermentation (Laboratory Analytical Procedure (LAP) No. NREL/TP-510-42630). NREL, Golden, Colorado.

Egoh, B., Reyers, B., Rouget, M., Bode, M., Richardson, D.M., 2009. Spatial congruence between biodiversity and ecosystem services in South Africa. Biol. Conserv. 142, 553–562. https://doi.org/10.1016/j.biocon.2008.11.009

Eskom, 2021. COAL IN SOUTH AFRICA: Fact Sheet.

Galadima, A., Muraza, O., 2019. Zeolite catalyst design for the conversion of glucose to furans and other renewable fuels. Fuel 258, 115851. https://doi.org/10.1016/j.fuel.2019.115851

Greben, H.A., Maree, J.P., Singmin, Y., Mnqanqeni, S., 2000. Biological sulphate removal from acid mine effluent using ethanol as carbon and energy source. Water Sci. Technol. 42, 339–344. https://doi.org/10.2166/wst.2000.0400

Greenway, N., 2019. The bioremediation of acid mine drainage utilising Indigenous South African grass as the organic carbon source of dissimilatory sulphate reduction (MSc. Dissertation). University of the Witwatersrand, Johannesburg.

Hobbs, P., Oelofse, S.H.H., Rascher, J., 2008. Management of Environmental Impacts from Coal Mining in the Upper Olifants River Catchment as a Function of Age and Scale. Int. J. Water Resour. Dev. 24, 417–431. https://doi.org/10.1080/07900620802127366

Johnson, D.B., Hallberg, K.B., 2005. Acid mine drainage remediation options: a review. Sci. Total Environ. 338, 3–14. https://doi.org/10.1016/j.scitotenv.2004.09.002

Jönsson, L.J., Alriksson, B., Nilvebrant, N.-O., 2013. Bioconversion of lignocellulose: inhibitors and detoxification. Biotechnol. Biofuels 6, 16. https://doi.org/10.1186/1754-6834-6-16

Kaksonen, A.H., Puhakka, J.A., 2007. Sulfate Reduction Based Bioprocesses for the Treatment of Acid Mine Drainage and the Recovery of Metals. Eng. Life Sci. 7, 541–564. https://doi.org/10.1002/elsc.200720216

Luis, P. (Ed.), 2018. Fundamental modelling of membrane systems: membrane and process performance. Elsevier, Amsterdam Kidlington Cambridge, Mass.

Magowo, E., Rumbold, K., Sheridan, C., 2015. The Utilization of Cellulosic Biomass in treating AMD and the Subsequent Generation of Fermentable Sugars. Presented at the 10th International Conference on Acid Mine Drainage & IMWA Annual Conference, Santiago, Chile.

Mandree, P., Thopil, G.A., Ramchuran, S., 2023. Potential Opportunities to Convert Waste to Bio-Based Chemicals at an Industrial Scale in South Africa. Fermentation 9, 908. https://doi.org/10.3390/fermentation9100908

Masindi, V., Gitari, M.W., Tutu, H., De Beer, M., 2016. Fate of inorganic contaminants post treatment of acid mine drainage by cryptocrystalline magnesite: Complimenting experimental results with a geochemical model. J. Environ. Chem. Eng. 4, 4846–4856. https://doi.org/10.1016/j.jece.2016.03.020

Matshusa-Masithi, M., Ogola, J., Chimuka, L., 2012. Use of compost bacteria to degrade cellulose from grass cuttings in biological removal of sulphate from acid mine drainage. Water SA 35. https://doi.org/10.4314/wsa.v35i1.76647

Meegoda, J.N., Li, B., Patel, K., Wang, L.B., 2018. A Review of the Processes, Parameters, and Optimization of Anaerobic Digestion. Int. J. Environ. Res. Public. Health 15, 2224. https://doi.org/10.3390/ijerph15102224

Naidu, T., Sheridan, C., Van Dyk, L., 2021. Design of Acid Mine Drainage Remediation Plant - Report to the Water Research Commission (No. WRC Report No. 2757/1/21).

Naidu, T.S., Sheridan, C.M., Van Dyk, L.D., 2020. Basic oxygen furnace slag: Review of current and potential uses. Miner. Eng. 149, 106234. https://doi.org/10.1016/j.mineng.2020.106234

Niju, S., Swathika, M., Balajii, M., 2020. Pretreatment of lignocellulosic sugarcane leaves and tops for bioethanol production, in: Lignocellulosic Biomass to Liquid Biofuels. Elsevier, pp. 301–324. https://doi.org/10.1016/B978-0-12-815936-1.00010-1

Novair, S.B., Biglari Quchan Atigh, Z., Asgari Lajayer, B., Shu, W., Price, G.W., 2024. The role of sulphate-reducing bacteria (SRB) in bioremediation of sulphate-rich wastewater: Focus on the source of electron donors. Process Saf. Environ. Prot. 184, 190–207. https://doi.org/10.1016/j.psep.2024.01.103

Ojo, A., 2023. An Overview of Lignocellulose and Its Biotechnological Importance in High-Value Product Production. Fermentation 9, 990. https://doi.org/10.3390/fermentation9110990

Oktaviani, M., Hermiati, E., Thontowi, A., Laksana, R.P.B., Kholida, L.N., Andriani, A., Yopi, Mangunwardoyo, W., 2019. Production of xylose, glucose, and other products from tropical lignocellulose biomass by using maleic acid pretreatment. IOP Conf. Ser. Earth Environ. Sci. 251, 012013. https://doi.org/10.1088/1755-1315/251/1/012013

Reyes-Alvarado, L.C., Camarillo-Gamboa, Á., Rustrian, E., Rene, E.R., Esposito, G., Lens, P.N.L., Houbron, E., 2018. Lignocellulosic biowastes as carrier material and slow release electron donor for sulphidogenesis of wastewater in an inverse fluidized bed bioreactor. Environ. Sci. Pollut. Res. 25, 5115–5128. https://doi.org/10.1007/s11356-017-9334-5

Ruehl, M.D., Hiibel, S.R., 2020. Evaluation of organic carbon and microbial inoculum for bioremediation of acid mine drainage. Miner. Eng. 157, 106554. https://doi.org/10.1016/j.mineng.2020.106554

Simate, G.S., Ndlovu, S., 2014. Acid mine drainage: Challenges and opportunities. J. Environ. Chem. Eng. 2, 1785–1803. https://doi.org/10.1016/j.jece.2014.07.021

Skousen, J., Zipper, C.E., Rose, A., Ziemkiewicz, P.F., Nairn, R., McDonald, L.M., Kleinmann, R.L., 2017. Review of Passive Systems for Acid Mine Drainage Treatment. Mine Water Environ. 36, 133–153. https://doi.org/10.1007/s10230-016-0417-1

Skousen, J.G., Ziemkiewicz, P.F., McDonald, L.M., 2019. Acid mine drainage formation, control and treatment: Approaches and strategies. Extr. Ind. Soc. 6, 241–249. https://doi.org/10.1016/j.exis.2018.09.008

Sluiter, A., Hames, B., Ruiz, R. O, Scarlata, C, Templeton, D, Crocker, C, 2012. Determination of Structural Carbohydrates and Lignin in Biomass Laboratory Analytical Procedure (LAP) (Technical No. NREL/TP-510-42618). NREL.

Smith, J., Sheridan, C., Van Dyk, L., Harding, K., 2024. Classification of grasses in the Mpumalanga coalfields region and assessment of their suitability to increase the pH of acid mine drainage, for potential use in passive acid mine drainage remediation systems. Ecol. Eng. 209, 107424. https://doi.org/10.1016/j.ecoleng.2024.107424

Smith, J., Sheridan, C., Van Dyk, L., Harding, K.G., 2025. Investigation of Suitable, Readily Available, Sources of Sulfate-Reducing Bacteria Inoculum, and Evaluation of Sulfate Reduction Rates Achieved at Different pHs. Environ. Microbiol. Rep. 17, e70081. https://doi.org/10.1111/1758-2229.70081

Sun, J., Zhang, L., Loh, K.-C., 2021. Review and perspectives of enhanced volatile fatty acids production from acidogenic fermentation of lignocellulosic biomass wastes. Bioresour. Bioprocess. 8, 68. https://doi.org/10.1186/s40643-021-00420-3

Sun, J., Zhao, R., Zeng, J., Li, G., Li, X., 2010. Characterization of Destrins with Different Dextrose Equivalents. Molecules 15, 5162–5173. https://doi.org/10.3390/molecules15085162

The World Bank Group, 2021. Climate Risk Profile: South Africa.

Tutu, H., McCarthy, T.S., Cukrowska, E., 2008. The chemical characteristics of acid mine drainage with particular reference to sources, distribution and remediation: The Witwatersrand Basin, South Africa as a case study. Appl. Geochem. 23, 3666–3684. https://doi.org/10.1016/j.apgeochem.2008.09.002

van Hille, R., Naidoo, N., Rossouw, S., Horn, E., 2021. Report to the Water Research Commission: PILOT-SCALE SEMI-PASSIVE TREATMENT OF ARD – EVALUATION OF TREATMENT PRODUCTS FOR DOWNSTREAM USE (No. WRC Report No. 2762/1/21). Pretoria.

Wang, Y., Zhang, Y., Cui, Q., Feng, Y., Xuan, J., 2024. Composition of Lignocellulose Hydrolysate in Different Biorefinery Strategies: Nutrients and Inhibitors. Molecules 29, 2275. https://doi.org/10.3390/molecules29102275

Westensee, D.K., Rumbold, K., Harding, K.G., Sheridan, C.M., Van Dyk, L.D., Simate, G.S., Postma, F., 2018. The availability of second generation feedstocks for the treatment of acid mine drainage and to improve South Africa's bio-based economy. Sci. Total Environ. 637–638, 132–136. https://doi.org/10.1016/j.scitotenv.2018.04.410

Woodford, A., Rosewarne, P., Girman, J., 2006. "How much groundwater does South Africa have?" Internal discussion document.

Zagury, G.J., Kulnieks, V.I., Neculita, C.M., 2006. Characterization and reactivity assessment of organic substrates for sulphate-reducing bacteria in acid mine drainage treatment. Chemosphere 64, 944–954. https://doi.org/10.1016/j.chemosphere.2006.01.001

CHAPTER 8.

8 Discussion and Concluding remarks

This chapter presents an overview of the thesis findings and connects them to the research objectives from in Chapter 1, which are listed here. Each of these are discussed separately. The research objectives were:

a. To characterise and critically evaluate the physical and chemical composition of Acid Mine Drainage (AMD) sourced from coal mining operations in the Mpumalanga region, South Africa and determine geographical and temporal variability.

b. To identify and characterise various commonly occurring grass types that are readily available and co-located with AMD sites and compare these for use in AMD bioremediation.

c. To source naturally occurring sulfate reducing bacteria (SRB) inoculum in different pH environments and compare then in the production of sulfides.

d. To investigate the effects of conducting biological AMD remediation at ambient temperature (with no additional heating), and the effects of grass-AMD contact time, with and without SRB amendment, on the extent of both a bioremediation process using grass as an organic substrate, and on subsequent bioethanol production using the spent grass residue.

8.1 Discussion of objectives

8.1.1 Objective a: Characterisation of acid mine drainage (AMD)

The first objective of this research was to characterise AMD in the Mpumalanga coalfields region, South Africa. The results of this study are presented in Chapters three and four. The concentrations of total acidity, total dissolved solids, and dissolved iron concentrations differed by orders of magnitude between the two sites, thus confirming AMD composition to be site specific. As example, while similar pH values were reported for both sites, the average acidity of the first site was ≈ 10 500 mg/L as $CaCO_3$, and the average acidity of the second site was ≈ 2400 mg/L as $CaCO_3$. These differences were attributed to mineral contribution to acidity from the different metal concentrations present in the AMD from the two sites. This work highlights the individuality of each AMD source, and by extension, it confirms that it is not necessarily possible to apply the same remediation process to AMD found at different sites. The variability in composition of the AMD sources was also assessed by evaluating the changes in chemical and physical composition of two AMD sites over a twelve month period. Increased metals and acidity concentrations were reported during the winter months, which coincided with reduced rainfall volumes, thus affirming the seasonal variability of the AMD sites. Iron concentrations for AMD Site 1 ranged between 1735 and 7950 mg/L, while lower iron concentrations of

between 4 and 828 mg/L were reported for AMD site 2. An understanding of the variability in AMD composition is essential to build into a remediation process design and ensure a sufficiently dynamic process which accommodates the anticipated compositional changes. An evaluation of the compliance of selected parameters to South African discharge water legislation, showed that Pb, Cu, Mn, Zn, Al, S, Fe, Ni, and some Cd concentrations exceeded legislative limits. This must also be factored into the selection of appropriate remediation systems. In so far as designing a process to reduce these limits to below acceptable discharge limits, it was found that, (i) Passive adsorption treatment systems would not support the removal of manganese and zinc owing to their slow removal by adsorption at low pH.; (ii) Active treatment systems where hydroxides are precipitated would not be suited to accommodate high concentrations of aluminium because of the amphoteric nature of aluminium hydroxide.

Chapter four showed the statistical correlations between electrical conductivity (EC) and the principal components present in AMD, viz. total acidity, dissolved iron and sulfate. This correlation implies that changes in the principal AMD components can be directly related to EC. Thus, obtaining an EC measurement using a portable EC meter and probe would allow one to correlate EC with these specific AMD parameter concentrations. This is useful for mines because it obviates the need for a first pass assessment of AMD quality and variability using expensive equipment and facilitates a sense of how AMD variability plays out as a function of electrical conductivity. This does not replace the need for more sophisticated chemical and physical analysis, which is required to gain an in-depth understanding of the complete compositional make-up and variances of individual AMD sources. These data can be used to establish similar site-specific statistical correlations. A novel use of these correlations is to calculate of electrical conductivity values corresponding to water quality limits for the predicted parameters to use as a simple rapid method for testing environmental compliance. This will assist in expediting remedial efforts to prevent soil and groundwater contamination, and the maintenance of water quality and security. This may also be used for the implementation of control systems to manage remediation processes.

Although the data are specific to the two sites previously mentioned, this methodology can be followed to characterise other AMD sources, to inform the selection of an appropriate remediation process that is best suited to specific requirements.

8.1.2 Objective b: Characterisation of grasses

The second objective of this research was to characterise commonly found grass types that were co-located with AMD sites in the Mpumalanga region. Furthermore, it sought to establish the suitability of these grass types as a substrate and carbon source for AMD bioremediation. The different grass types were classified, and their physical and chemical composition determined. The capability of these grasses to increase pH when contacted with a synthetically prepared AMD solution and/or real AMD was experimentally investigated; an increase in pH was observed which indicated the suitability of the grass for raising pH. This work also tested the effects on the pH of adding fresh grass after a specific period. Grass types that had previously shown a

lower efficacy to increase pH, benefited from the addition of renewed grass. This is an important finding, as it broadens the range of grass types that may be used for effective AMD remediation. Vetiver (Vetiveria zizanioides) and *Hyparrhenia hirta* grasses were shown to affect the greatest increase in pH; (pH 3.5–pH 5.45 and pH 3.5–pH 5.38). These results suggest that a potential ion-exchange mechanism between the inorganic cations associated with the anions present in the grass and the hydrogen ions (H^+) in the AMD was found which may be controlling the pH increase. Real AMD from the environment is a complex mixture with many conjugate acids and bases, which had an effect on the pH change. The change in pH was consequently less than was expected, and treatment with grass was not as effective as that observed with an artificial AMD. A strong correlation between H^+ and oxidation and reduction potential (ORP) was however found. The single grass addition experiment achieved a correlation coefficient (R2) of 0.89 and the multiple grass addition experiment achieved a R2 of 0.91 at a 95% confidence interval. This affirms that there was a pH-ORP relationship. This relationship is useful for process control of water treatment processes by providing an indirect means of identifying the occurrence of biochemical events such as sulfate reduction (Holman, 2004).

This work successfully demonstrates the ability of the grasses used to increase the pH of AMD, with the extent of the pH increase being dependent on the composition of the AMD. As such, each remediation system will need to be optimised based on the relative physical and chemical composition of the specific AMD source. The process can further be optimised by assessing how many times organic substrate needs to be renewed before the system reaches steady state. Other aspects to consider would include assessment of optimal grass size fraction, and if changing the solid/liquid ratio and grass/AMD contact time could further improve the increase in pH.

8.1.3 Objective c: Naturally occurring sources of sulfate reducing bacteria (SRB) inoculum

The third objective experimentally investigated the suitability of using naturally occurring microbial communities, to support the growth and activity of sulfate-reducing bacteria by assessing the sulfide production and sulfate reduction ($S^{2-}{}_{produced}/SO_4^{2-}{}_{removed}$) ratios at different pH conditions. The results indicated that natural sources of SRB are limited for these sorts of environments. Amongst the sources of AMD investigated, the AMD water, meal worms, acid mine drainage mud, and cow dung did not achieve appreciable reduction in sulfates and were thus not considered suitable sources of SRB inoculum.

The greatest sulfide produced/sulfate removed conversion ratios were achieved at pH 7.5 for the raw sewage sludge (0.19) and AMD reed-bed mud (0.17). The AMD reed-bed inoculum achieved a 40% reduction in sulfate concentration and produced 36 mg/L of sulfide in pH 4 media, however, the sulfide produced/sulfate conversion ratio was low with a reported value of 0.041. The ability of the AMD reed-bed mud to achieve some degree of conversion at lower pH shows that the most effective natural SRB were located where there had been evolutionary pressures leading to the evolution of SRB in order to function under very hostile AMD environments. The SRB found in the raw sewage sludge were only effective in high pH environments and would need long term adaptation to perform effectively in a low pH environment. The addition of grass to

the AMD (Chapter six), successfully achieved an increase in pH. If the pH could be increased by adding grass to the AMD, the SRB from the AMD reed-mud would achieve better conversion ratios, and the SRB from the raw sewage could potentially be used as is.

8.1.4 Objective d: Grass pre-treatment time and SRB addition for acid mine drainage remediation and bioconversion of sugars to ethanol

The final objective in the experimental work investigated the effect of grass/AMD contact time for AMD bioremediation and for subsequent bioethanol production using the partially hydrolysed grass residue. This work considered three objectives:

i. The suitability of a weak acid AMD solution to disrupt the lignocellulosic structure of grass
ii. The effect of grass/AMD contact time (hydraulic retention time) on the extent of AMD remediation achieved
iii. The suitability of the pre-treated grass residue from the AMD remediation, for bioconversion to ethanol.

Experiments for objectives i and ii were conducted with and without the addition of sulfate reducing bacteria (SRB) inoculum. Scanning electron microscopy image analysis confirmed that the weak AMD acid had disrupted the lignocellulosic structure of the grass at ambient temperature. The disruption of the grass facilitated the release of glucose (average maximum 293 mg/L) and xylose (average maximum 318 mg/L), from the grass which was used by SRB for AMD bioremediation. Increased pH and sulfide concentrations were shown whilst the grass was still contacted with AMD. However, the benefits of longer hydraulic retention time were more pronounced in the filtrate samples, after the grass was removed from the reactor. The non-amended, day thirteen sample, increased from pH 4.57 on the last day of grass AMD contact to pH 5.13 in the filtrate solution fourteen days after the grass was removed. The same hydraulic retention time SRB-amended sample increased from pH 4.46 on the last day of grass AMD contact to pH 5.66 in the filtrate solution fourteen days after the grass was removed. These results are important in that they provide some flexibility for optimisation of hydraulic retention time of grass pre-treatment, to facilitate continued remediation of AMD while still maintaining sufficient concentrations of glucose and xylose in the grass residue to allow effective bioconversion of these sugars to bioethanol and other bioproducts. The benefits of SRB addition are also shown by the increased sulfide concentrations in the filtrate solutions. Here, sulfide concentrations increased by orders of magnitude in the SRB amended reactors; from 0.13 on the thirteenth day of grass/AMD contact to 2.62 mg/L fourteen days after grass was removed. Thus, the SRB amendment did improve the extent of bioremediation achieved, particularly at longer hydraulic retention times. Objective iii compared the extent of bioethanol production of the pre-treated grass residue with an untreated grass sample. The greatest increase in bioethanol concentration were achieved for the grass residue samples that had been subjected to the longest pre-treatment hydraulic retention times. The longest hydraulic retention time samples, days eleven and thirteen, SRB-amended samples achieved greater increases in bioethanol

concentration than their respective non-amended samples. This showed that the addition of SRB in the pretreatment stage, enhanced both AMD remediation and subsequent bioethanol production. The untreated grass sample that had not been subjected to prior acid hydrolysis, achieved a marginally lower increase in bioethanol concentration (2057 mg/L) than the SRB-amended day eleven HRT grass residue sample (2170 mg/L) and a greater increase than the same non-amended day eleven grass residue sample (1745 mg/L). Thus, the pre-treatment of the grass for thirteen days with SRB amendment, prior to fermentation and hydrolysis gave best increase in bioethanol concentration (2605 mg/L), but appreciable bioethanol concentrations were achieved without prior acid hydrolysis of grass.

8.2 Concluding remarks

As a water-scarce country, South Africa's limited water resources are further reduced by AMD pollution of freshwater sources. AMD has affected the health and livelihoods of communities that are without the means or resources to deal with the ramifications of AMD pollution. This calls for the implementation of low-cost and sustainable AMD treatments processes. Bioremediation offers a sustainable alternative to chemical remediation processes, but there is still a need to reduce costs associated with bioremediation systems. This study addresses these challenges by showing that it is possible to use grasses that are co-located with AMD sites in the Mpumalanga Coalfields region in a bioremediation process. Using a naturally occurring carbon source in bioremediation systems will provide significant cost reduction compared with the addition of commercially available carbon sources, such as ethanol and glycerol. Also, the immediacy of a locally available carbon source will reduce transportation costs. This work also showed that the grass can act as a pH modifier allowing remediation at higher pH values. This work also demonstrates that naturally occurring sources of sulfate reducing bacteria (SRB), such as mud from reed-beds co-located with AMD sites, or waste products such as raw sewage can be used as SRB amendment in bioremediation systems. These findings promote further process sustainability and cost reduction. These findings support the ideas around circular economy whereby waste products such as cut grass, and sewage can be used to produce clean water from AMD.

Despite the increasing urgency of climate impact and the need for just transition away from coal intensive use in electricity and industry, South Africa is still heavily dependent on coal for energy provision. Recent struggles to meet electricity needs in South Africa as a result of ill maintained and ageing power facilities, has necessitated seeking alternative options of fuel production. Using grass and other lignocellulosic waste rather than primary crops as alternative secondary sources for biofuels production, presents a combined opportunity to reduce waste and produce energy without affecting food production. This study included the assessment of a combined AMD remediation, and bioethanol process using grass. AMD was successfully remediated at ambient temperature, and the grass residue from the AMD remediation process was effectively used for subsequent bioethanol production. This study also highlighted the need for additional SRB amendment to improve process outcomes. Additionally, this study demonstrated the successful bioconversion of untreated grass into bioethanol. The successful conversion to bioethanol without additional

heating in the pre-treatment stage, reduces energy requirements associated with heating in bioethanol processes. The findings of these investigations should be used to optimise a combined remediation process that leverages optimal remediation of AMD with optimal bioconversion to bioethanol.

The establishment of low-cost and sustainable remediation processes could also provide potential employment opportunities, whereby the local community members that were previously employed at mining operations, could take over the running of these facilities post mine closure. This would ensure the production of acceptable quality water for consumption and prevention of environmental pollution, while providing a means of livelihood for the local community. This is in line with the principles of a just transition.

8.3 Recommendations

Future research should include an evaluation of the use of the correlated parameters observed in these specific AMD sites for process control of a bioremediation system. This work should experimentally evaluate the compositional changes in the AMD that are associated with changes in electrical conductivity and also changes in oxidation reduction potential. These data can then be used to design a process model, whereby the final conductivity and oxidation reduction potential can be used to predict the extent of remediation achieved.

The bioremediation of AMD using grass can be expanded further by varying grass/AMD ratios, with differing AMD compositions, to explore improved remediation of more complex AMD matrices.

Data from the investigation of natural sources of SRB can be used to inform further research to optimise reactor conditions and achieve improved sulfate to sulfide conversion rates. These conditions may include the use of grass in the reactors to increase the pH of the AMD, and an assessment of different acclimatation times for SRB in different pH conditions. Chemical oxygen demand/sulfate ratios should be optimised and all microbial communities associated with the different microbial sources characterised.

Further studies should experimentally establish the reaction kinetics of a process that maximises AMD bioremediation, using the sewage sludge and reed-bed mud SRB inoculum sources in the process. Once optimal kinetics are established, the data can be used to perform an economic assessment of the process viability.

Although not included as part of this study, alternative uses of the grass residue from AMD bioremediation process should be explored. These can include drying and burning the grass to produce an iron rich ash that could be used in industrial processes such as steel mills.

The recovery of metals as metal sulfides, from the bioremediation process; and other byproducts from biofuel production presents further opportunity to derive additional direct economic value from waste.

Future research should explore alternative strategies towards deriving value from AMD such as the extraction of value metals, and the recovery of rare earth elements from the AMD. The sale of these byproducts could potentially be used to offset remediation costs. Based on the characterisation work in this research, Co, Ni, Cu, Zn are identified as critical metals based on their limited availability and importance in clean energy transition technologies.

Appendix I - Supplementary data for Chapter 4

(with Figures and Tables in sub-Appendices A – F from the original published paper)

Appendix I-A: Olifants River management and catchment area

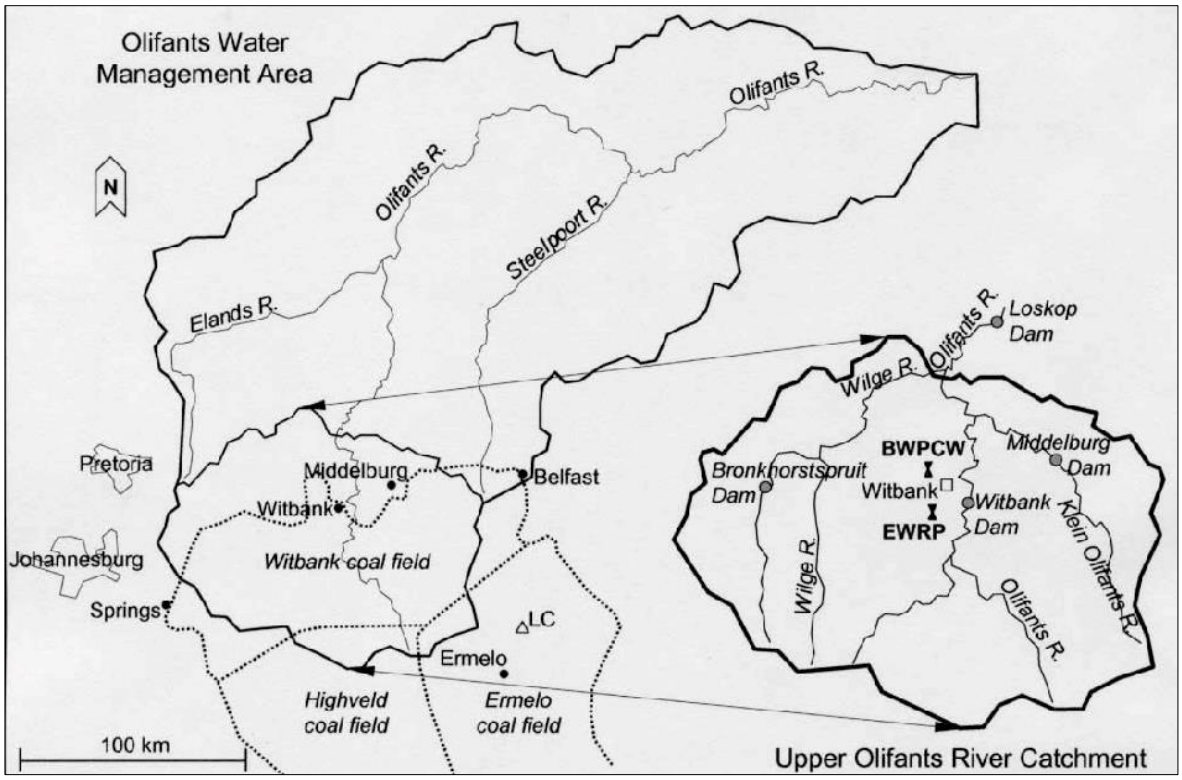


Figure A1 Olifants River management and catchment area (Hobbs et al., 2008)

Appendix I-B - Chemical and Physical Data

Table B.1. Chemical and physical data

SITE 1									
Data point	Date	pH at 25˚C	REDOX mV SHE at 25 °C	EC mS/m at 25˚C	Turbidity NTU	TDS mg/L at 180˚C	Total Ions	EC * 6,5	TSS mg/L at 105˚C
1	2018-02-01	2.94	642	3 460	19	19 640	18 575	22 490	63
2	2018-02-26	2.87	620	3 685	24	21 130	30 700	23 953	86
3	2018-03-26	2.57	682	2 335	3	12 015	9 720	15 178	29
4	2018-05-02	2.16	887	3 750	11	21 340	22 845	24 375	1
5	2018-05-31	2.87	632	3 725	241	23 180	20 895	24 213	321
6	2018-06-25	2.90	626	3 780	201	23 920	21 410	24 570	58
7	2018-08-02	2.49	689	3 940	123	23 950	18 900	25 610	55
8	2018-08-14	2.86	611	3 865	95	25 150	19 135	25 123	60
9	2018-09-04	2.99	621	3 985	413	19 575	19 515	25 903	100
10	2018-10-17	2.73	688	2 650	161	12 850	9 765	17 225	250
11	2018-11-22	2.84	628	3 790	29	23 830	17 250	24 635	21
12	2018-12-13	2.69	622	3 990	337	23 565	17 570	25 935	109
13	2019-04-04	2.64	640	3 705	241	26 635	17 200	24 083	110
SITE 2									
Data point	Date	pH at 25˚C	REDOX mV SHE at 25 °C	EC mS/m at 25˚C	Turbidity NTU	TDS mg/L at 180˚C	Total Ions	EC * 6,5	TSS mg/L at 105˚C
14	2018-02-01	2.92	752	1 090	20	5 820	6 028	7 085	62
15	2018-02-26	2.87	795	1 465	408	9 175	7 346	9 523	199
16	2018-05-08	2.85	821	1 055	205	6 680	6 035	6 858	80
17	2018-05-31	2.72	816	1 720	99	9 900	8 462	11 180	52
18	2018-08-02	2.54	850	1 935	248	10 700	7 646	12 578	170
19	2019-04-04	7.02	349	727	389	4 525	3 248	4 726	92

Table B.2. Chemical, physical and Dissolved metals data

SITE 1				mg/L					
Data point	Date	Partial Acidity mg/L $CaCO_3$ at pH 4,5	Total Acidity mg/L $CaCO_3$ at pH 8,3	Ag	Al	As	B	Ba	Be
1	2018-02-01		10 530		365	<0.002	2.0	0.06	0.09
2	2018-02-26		11 200		518	<0.002		0.00	0.06
3	2018-03-26		5 760	<0.001	222	<0.002		0.01	
4	2018-05-02	9 275	12 550	0.008	354	<0.002	2.5	0.05	0.06
5	2018-05-31		10 700	0.018	371	<0.002	2.5	0.03	0.07
6	2018-06-25		11 080	0.008	373	<0.002	2.5	0.07	0.06
7	2018-08-02		11 765	<0.001	442		< 0.01	0.008	0.11
8	2018-08-14		11 800	<0.001	300		< 0.01	0.01	0.06
9	2018-09-04	9 275	11 925	<0.001	259		< 0.01	0.01	0.05
10	2018-10-17	4 750	6 050	<0.001	191		< 0.01	0.005	0.04
11	2018-11-22	8 675	11 125	<0.001	206		< 0.01	0.008	0.05
12	2018-12-13	8 588	11 025	<0.001	193		< 0.01	0.03	0.04
13	2019-04-04	8 650	11 050	<0.001	213		< 0.01	0.007	0.04
SITE 2				mg/L					
Data point	Date	Partial Acidity mg/L $CaCO_3$ at pH 4,5	Total Acidity mg/L $CaCO_3$ at pH 8,3	Ag	Al	As	B	Ba	Be
14	2018-02-01		1 480	0.011	157	<0.002	0.16	0.05	0.05
15	2018-02-26		2 160		162	<0.002	< 0.01	0.01	0.04
16	2018-05-08		1 260	0.012	126	<0.002	0.17	0.08	0.02
17	2018-05-31		3 440	0.0092	230	<0.002	0.48	0.03	0.07
18	2018-08-02		3 673	<0.001	144		< 0.01	0.02	0.03
19	2019-04-04			<0.001	0.040		< 0.01	0.03	< 0.001

Table B.3. Dissolved metals data

SITE 1		mg/L							
Data point	Date	Bi	Ca	Cd	Ce	Co	Cr	Cs	Cu
1	2018-02-01		398	0.02	8.6	1.8	0.09	0.03	0.07
2	2018-02-26		752			1.3			
3	2018-03-26		310			0.9	0.08		
4	2018-05-02	<0.002	462	0.02	6.1	0.5	0.08	0.03	0.34
5	2018-05-31	<0.002	440	0.02	5.9	2.7	0.09	0.04	0.26
6	2018-06-25	<0.002	439	0.01	5.8	1.4	0.05	0.03	0.09
7	2018-08-02		446		14	2.7	0.09	0.02	0.08
8	2018-08-14		433		4.4	0.8	0.03	0.02	0.02
9	2018-09-04		437		4.1	0.7	0.02	0.02	0.02
10	2018-10-17		324		4.8	1.0	0.08	0.01	0.06
11	2018-11-22		409		3.5	0.6	0.02	0.02	0.02
12	2018-12-13		418		3.3	0.6	0.02	0.02	0.02
13	2019-04-04		429		2.7	0.5	0.03	0.01	0.04
SITE 2		mg/L							
Data point	Date	Bi	Ca	Cd	Ce	Co	Cr	Cs	Cu
14	2018-02-01	<0.002	655	0.01	2.3	1.3	0.07	0.02	0.10
15	2018-02-26		811	<0.003		1.3	0.05		0.08
16	2018-05-08	<0.002	633	0.01	1.4	1.05	0.08	0.01	0.13
17	2018-05-31	<0.002	568	0.01	2.8	1.9	0.07	0.02	0.15
18	2018-08-02		447	0.004	2.2	0.9	0.02	0.01	0.09
19	2019-04-04		448	0.003	0.02	0.26	0.01	0.003	0.04

Table B.4. Dissolved metals data

SITE 1		mg/L							
Data point	Date	Dy	Er	Eu	Fe	Ga	Gd	Ge	Hf
1	2018-02-01	0.35	0.20	0.07	4 210	<0.002	0.7	<0.005	0.01
2	2018-02-26				7 950		3.0		
3	2018-03-26				1 825		0.74		
4	2018-05-02	0.37	0.20	0.07	5 390	<0.002	0.56	<0.005	0.007
5	2018-05-31	0.34	0.19	0.07	4 950	<0.002	0.54	<0.005	0.007
6	2018-06-25	0.34	0.19	0.07	5 185	<0.002	0.55	<0.005	0.007
7	2018-08-02	0.48	0.26	0.10	3 770		0.54	0.02	0.001
8	2018-08-14	0.32	0.18	0.06	4 475		0.34	0.01	0.001
9	2018-09-04	0.29	0.16	0.05	4 600		0.30	0.01	0.001
10	2018-10-17	0.19	0.10	0.04	1 735		0.22	0.01	0.001
11	2018-11-22	0.24	0.13	0.04	3 860		0.25	0.01	0.001
12	2018-12-13	0.22	0.12	0.04	3 975		0.23	0.01	0.001
13	2019-04-04	0.21	0.11	0.04	3 875		0.22	0.01	0.001
SITE 2		mg/L							
Data point	Date	Dy	Er	Eu	Fe	Ga	Gd	Ge	Hf
14	2018-02-01	0.16	0.09	0.04	160	<0.002	0.29	<0.005	0.003
15	2018-02-26				376		0.43		
16	2018-05-08	0.11	0.06	0.03	199	<0.002	0.17	<0.005	0.003
17	2018-05-31	0.20	0.12	0.05	828	<0.002	0.35	<0.005	0.004
18	2018-08-02	0.16	0.09	0.03	646	0.17		0.01	0.001
19	2019-04-04	0.0004	0.0003	0.0001	4.2	0.001		<0.005	<0.001

Table B.5. Dissolved metals data

SITE 1		mg/L							
Data point	Date	Hg	Ho	In	Mg	Mn	Mo	Na	Nb
1	2018-02-01	<0.005	0.07	<0.002	375	97	<0.01	34	0.02
2	2018-02-26	<0.005			725	133		<1	
3	2018-03-26	<0.005			201	50	<0.01	20	
4	2018-05-02	<0.005	0.07	<0.002	428	86	<0.01	36	0.02
5	2018-05-31	<0.005	0.06	<0.002	410	78	<0.01	39	0.02
6	2018-06-25	<0.005	0.06	<0.002	405	82	<0.01	44	0.02
7	2018-08-02	<0.005	0.10		396	153		58	<0.0001
8	2018-08-14	<0.005	0.07		349	84		58	<0.0001
9	2018-09-04	<0.005	0.06		365	88		58	<0.0001
10	2018-10-17	<0.005	0.04		209	71		35	<0.0001
11	2018-11-22	<0.005	0.05		338	76		71	<0.0001
12	2018-12-13	<0.005	0.05		348	78		76	<0.0001
13	2019-04-04	<0.005	0.04		314	68		56	<0.0001
SITE 2		mg/L							
Data point	Date	Hg	Ho	In	Mg	Mn	Mo	Na	Nb
14	2018-02-01	<0.005	0.03	<0.002	375	44	<0.01	34	<0,001
15	2018-02-26	<0.005			397	51		0.63	
16	2018-05-08	<0.005	0.02	<0.002	333	35	<0.01	39	0.02
17	2018-05-31	<0.005	0.04	<0.002	286	52	<0.01	58	0.02
18	2018-08-02	<0.005	0.03		315	58		58	<0.0001
19	2019-04-04	<0.005	0.0002		239	17		42	<0.0001

Table B.6. Dissolved metals data

SITE 1		mg/L							
Data point	Date	Nd	Ni	K	La	Li	Lu	P	Pb
1	2018-02-01	1.3	1.1	6.5	0.82	0.36	0.02	<2	0.02
2	2018-02-26		1.3	18		0.92		2.1	0.43
3	2018-03-26		0.79	4.0		0.28		<2	0.07
4	2018-05-02	1.2	0.85	10	0.60	0.44	0.02	<2	0.02
5	2018-05-31	1.1	0.89	10	0.52	0.40	0.02	<2	0.03
6	2018-06-25	1.1	0.83	11	0.50	0.38	0.02	<2	0.003
7	2018-08-02	2.2	1.6	3.2	1.5	0.47	0.03		0.01
8	2018-08-14	1.1	0.90	13	0.48	0.38	0.02		0.02
9	2018-09-04	1.0	0.80	14	0.42	0.34	0.02		0.02
10	2018-10-17	0.89	0.66	3.3	0.56	0.16	0.01		0.01
11	2018-11-22	0.80	0.65	12	0.35	0.26	0.01		0.01
12	2018-12-13	0.76	0.62	15	0.32	0.24	0.01		0.01
13	2019-04-04	0.74	0.57	12	0.33	0.23	0.01		0.01
SITE 2		mg/L							
Data point	Date	Nd	Ni	K	La	Li	Lu	P	Pb
14	2018-02-01	0.64	1.3	5.6	0.51	0.22	0.01	<2	0.02
15	2018-02-26		1.1	6.3		0.50		<2	0.12
16	2018-05-08	0.40	1.2	13	0.31	0.30	0.01	<2	0.01
17	2018-05-31	0.81	0.90	2.9	0.60	0.31	0.01	<2	0.03
18	2018-08-02	0.65	0.92	3.9	0.43	0.16	0.01		0.01
19	2019-04-04	0.004	0.31	17	0.01	0.08	0.0001		0.005

Table B.7. Dissolved metals data

SITE 1		mg/L							
Data point	Date	Pr	Rb	S	Sb	Sc	Se	Si	Sm
1	2018-02-01	0.30	0.15	4 345	0.002	<0.002	<0.005	25	0.34
2	2018-02-26			6 845				49	
3	2018-03-26			2 350	<0.004		<0.005	24	
4	2018-05-02	0.27	0.19	5 345	0.004	<0.002	<0.005	18	0.32
5	2018-05-31	0.24	0.19	4 850	0.004	<0.002	<0.005	17	0.29
6	2018-06-25	0.23	0.20	4 940	0.002	<0.002	<0.005	23	0.29
7	2018-08-02	0.49	0.07	4 515		0.0002		53	0.47
8	2018-08-14	0.22	0.16	4 455		0.0001		36	0.26
9	2018-09-04	0.19	0.15	4 545		<0.0001		37	0.23
10	2018-10-17	0.20	0.05	2 385		<0.0001		22	0.19
11	2018-11-22	0.16	0.13	4 075		0.0001		38	0.19
12	2018-12-13	0.15	0.12	4 140		<0.0001		38	0.18
13	2019-04-04	0.15	0.10	4 060		0.0001		39	0.18
SITE 2		mg/L							
Data point	Date	Pr	Rb	S	Sb	Sc	Se	Si	Sm
14	2018-02-01	0.16	0.07	1 525	0.004	<0.002	<0.005	11	0.16
15	2018-02-26			1 840	0.75		<0.005	19	
16	2018-05-08	0.10	0.13	1 545	0.003	<0.002	<0.005	6.1	0.10
17	2018-05-31	0.20	0.08	2 135	0.003	<0.002	<0.005	15	0.20
18	2018-08-02	0.15	0.05	1 980	<0.1			22	0.14
19	2019-04-04	0.001	0.04	824	0.18			5.0	0.0005

Table B.8. Dissolved metals data

SITE 1		mg/L							
Data point	Date	Sn	Sr	Ta	Tb	Te	Th	Ti	Tl
1	2018-02-01	0.001	0.89	<0.002	0.07	0.003	0.04	0.83	<0.002
2	2018-02-26		1.4					0.10	
3	2018-03-26		0.68					<0.0001	
4	2018-05-02	0.001	1.1	<0.002	0.07	0.003	0.01	3.2	<0.002
5	2018-05-31	0.003	1.1	<0.002	0.06	0.003	0.01	3.5	<0.002
6	2018-06-25	0.001	1.0	<0.002	0.06	0.004	0.09	0.22	<0.002
7	2018-08-02	0.001	0.89		0.09	<0.0001	0.05	<0.0001	
8	2018-08-14	0.001	0.93		0.06	<0.0001	0.01	<0.0001	
9	2018-09-04	<0.0001	0.85		0.05	<0.0001	0.004	<0.0001	
10	2018-10-17	<0.0001	0.41		0.03	<0.0001	0.03	<0.0001	
11	2018-11-22	<0.0001	0.69		0.04	<0.0001	0.01	<0.0001	
12	2018-12-13	<0.0001	0.66		0.04	<0.0001	0.00	<0.0001	
13	2019-04-04	<0.0001	0.71		0.04	<0.0001	0.01	<0.0001	
SITE 2		mg/L							
Data point	Date	Sn	Sr	Ta	Tb	Te	Th	Ti	Tl
14	2018-02-01	0.01	1.5	<0.002	0.03	0.002	0.02	0.04	<0.002
15	2018-02-26		1.9					< 0.006	
16	2018-05-08	0.004	1.8	<0.002	0.02	0.002	0.01	3.22	<0.002
17	2018-05-31	0.01	1.4	<0.002	0.04	0.003	0.03	0.16	<0.002
18	2018-08-02	0.001	0.8		0.03	<0.0001	0.01	<0.0001	
19	2019-04-04	0.0002	1.3		0.0002	<0.0001	0.0001	<0.0001	

Table B.9. Dissolved metals data and cation/anion balance

SITE 1		mg/L								% Diff.
Data point	Date	Tm	U	V	W	Y	Yb	Zn	Zr	Cation / Anion Balance
1	2018-02-01	0.02	0.03	0.62	0.007	2.0	0.14	7.8	0.15	-4.76
2	2018-02-26			0.17				13		1.85
3	2018-03-26			< 0.004				7.4	< 0.001	-8.33
4	2018-05-02	0.02	0.02	0.73	0.008	2.0	0.14	9.3	0.01	-6.13
5	2018-05-31	0.02	0.01	0.73	0.008	2.0	0.13	8.5	0.01	-4.15
6	2018-06-25	0.02	0.01	0.76	0.008	2.0	0.13	9.0	0.02	-3.58
7	2018-08-02	0.03	0.06	0.13	0.001	2.4	0.19	9.2	< 0.001	-6.81
8	2018-08-14	0.02	0.01	0.13	0.002	1.7	0.12	8.3	< 0.001	-5.52
9	2018-09-04	0.02	0.01	0.12	0.001	1.6	0.11	7.7	< 0.001	-6.21
10	2018-10-17	0.01	0.02	0.04	0.001	1.0	0.07	4.5	< 0.001	-10.61
11	2018-11-22	0.02	0.01	0.10	0.001	1.3	0.09	6.4	< 0.001	-8.52
12	2018-12-13	0.02	0.01	0.09	0.002	1.3	0.08	6.3	< 0.001	5.93
13	2019-04-04	0.01	0.01	0.08	0.001	1.1	0.08	5.0	< 0.001	5.67
SITE 2		mg/L								% Diff.
Data point	Date	Tm	Uranium as U	Vanadium as V	Tungston as W	Yttrium as Y	Yb	Zinc as Zn	Zirconium as Zr	Cation / Anion Balance
14	2018-02-01	0.01	0.03	0.04	0.007	0.88	0.06	3.1	0.02	-2.99
15	2018-02-26			< 0.001				3.6	< 0.001	-3.86
16	2018-05-08	0.01	0.02	0.01	0.007	0.61	0.04	2.5	0.01	-7.29
17	2018-05-31	0.01	0.03	0.08	0.007	1.20	0.08	4.1	0.02	-9.03
18	2018-08-02	0.01	0.01	< 0.001	0.001	0.93	0.07	3.3	< 0.001	-14.87
19	2019-04-04	0.0001	0.0004	< 0.001	0.0004	0.01	0.0001	0.44	< 0.001	-12.28

Appendix I-C – Analytical Data

Table C.1. Legislative limits and concentration ranges for physical and dissolved chemical parameters for acid mine drainage Sites 1 and 2

Parameter	**Maximum Concentration Level/ Recommended Level**	**Legislative/ Advisory Source**	**Site 1 Concentration/value range**	**Site 2 Concentration/value range**
pH	≥ 5 to ≤ 8.5	SANS 241–1:2015	< 3 for all samples	< 3 for all 2018 samples April 2019 – pH 7
Total acidity (TA) (mg/L as $CaCO_3$)	Not classified	Not classified	5760 – 12 550	2018: 1260 – 3673 April 2019 – total alkalinity 304
Electrical Conductivity (EC) (mS/m)	≤ 170	SANS 241–1:2015	2335 – 3 990	727 – 1935
Total Dissolved Solids @ 180 ˚C (TDS) (mg/L)	≤ 1 200	SANS 241–1:2015	12 015 – 26 635	4525 – 10 700
Turbidity (NTU)	≤ 1 (Operational) ≤ 5 (Aesthetic)	SANS 241–1:2015	3 – 413	20 – 408
Sulfur (S) / Sulfate (SO_4^{2-}) (mg/L)	≤ 500 as SO_4^{2-} (Acute health) ≤ 167 as S (Aesthetic) ≤ 250 as SO_4^{2-} ≤ 83 as S	SANS 241–1:2015	(S): 2350 – 6845 converted to (SO_4^{2-}): 7050 – 20 535	(S): 824 – 2135 converted to (SO_4^{2-}) 2472 – 6405

Table C.2. Legislative limits and concentration ranges for dissolved chemical parameters for acid mine drainage Sites 1 and 2 continued

Parameter	Maximum Concentration Level/ Recommended Level	Legislative/ Advisory Source	Site 1 Concentration/value range	Site 2 Concentration/value range
Aluminium (Al) (mg/L)	≤ 0.3	SANS 241–1:2015	191 – 518	2018: 126 – 230 April 2019 – 0.04
Boron (B) (mg/L)	≤ 2.4	SANS 241–1:2015	Three samples reported 2.5 Where analysed, remaining samples, within limits	All samples, within limits
Beryllium as (Be) (mg/L)	0.004	EPA – 2018 MCL	0.04 – 0.11	2018: 0.02 – 0.07 April 2019 – <0.001
Calcium (Ca) (mg/L)	< 150	SANS 241:2006 (Ed. 6) - Class 1 recommend operational limit.	310 – 752	447 – 811
Cadmium (Cd) (mg/L)	≤ 0.003	SANS 241–1:2015	Where tested, 0.01 – 0.02	2018: 0.003 – 0.01 Feb 2019 – <0.003
Chromium (Cr) (mg/L)	≤ 0.05	SANS 241–1:2015	8 samples between 0.05 – 009 5 samples below recommended limits	Four samples between 0.05 – 0.08 August 2018, April 2019 – below recommended limits

Table C.3 Legislative limits and concentration ranges for dissolved chemical parameters for acid mine drainage Sites 1 and 2 continued

Parameter	Maximum Concentration Level/ Recommended Level	Legislative/Advisory Source	Site 1 Concentration/ value range	Site 2 Concentration/ value range
Iron (Fe) (mg/L)	≤ 2 (Chronic Health) ≤ 0.3 (Aesthetic)	SANS 241– 1:2015	1735 – 7950	4 – 828
Manganese (Mn) (mg/L)	≤ 0.4 (Chronic Health) ≤ 0.1 (Aesthetic)	SANS 241– 1:2015	50 – 153	17 – 58
Magnesium (Mg) (mg/L)	< 70	SANS 241:2006 (Ed. 6) - Class 1 recommended operational limit	201 – 725	239 – 397
Nickel (Ni) (mg/L)	≤ 0.07	SANS 241– 1:2015	0.57 – 1.6	0.31 – 1.3
Lead (Pb) (mg/L)	≤ 0.01	SANS 241– 1:2015	0.01 – 0.43 25/6/18 sample – 0.003	0.01 – 0.12 April 2019 – 0.005
Uranium (U) (mg/L)	≤ 0.03	SANS 241– 1:2015	2/8/18 sample reported 0.06 Remaining samples below limits	31/5/18 sample reported 0.03 Remaining samples below limits

Table C.4. Legislative limits and concentration ranges for dissolved chemical parameters for acid mine drainage Sites 1 and 2 continued

Parameter	Maximum Concentration Level/ Recommended Level	Legislative/Advisory Source	Site 1 Concentration/ value range	Site 2 Concentration/ value range
Vanadium (V) (mg/L)	0 – 0.1	DWAF 1996 TWQR	0.04 – 0.76 26/3/18 sample reported <0.004	3 samples reported 0.01-0.08 Remaining 3 samples below limits
Zinc (Zn) (mg/L)	≤ 5	SANS 241– 1:2015	5.0 – 13 17/10/18: 4.5	All concentrations below required limits.

Appendix I-D – Potential Health Effects

Table D.1. Potential health and /or environmental effects from long-term exposure to parameters found in excess of regulatory or advisory concentration levels

Parameter	**Potential health effects from long-term exposure above maximum concentration level (MCL) (unless specified as short-term)**
pH	pH can affect the degree of solubility/corrosion of metals as well as treatment efficiency; thus, any effect on health is likely to be indirect and due to increased ingestion of metals or inadequate disinfection (DWAF, 1996).
Total Dissolved Solids @ 180 ˚C (TDS)	High TDS affects the taste and appearance of water, can cause corrosion or scaling and consumption can disrupt the body salt balance (DWAF, 1996).
Electrical Conductivity	Indicates mineralization in water. Because EC can be used as an approximation of the TDS value, health effects as described for TDS are relevant to this parameter. The conversion factor used to approximate TDS concentration should be specific to the water system being measured (DWAF, 1996, Van Niekerk et al., 2014)
Turbidity	Aesthetic impacts as water appears dirty, high levels could indicate increased concentrations of disease-causing microorganisms; ingestion could cause nausea, cramps, diarrhoea, and headaches (EPA, 2022).
Sulfate	Ingestion of high concentrations can lead to diarrhoea and dehydration. Imparts a salty or bitter taste to water in elevated concentrations (DWAF, 1996)
Aluminium as Al	Excessive quantities could impart undesirable colour and turbidity to water. Possible link to neurological disorders, such as dementia, and Alzheimer's disease (DWAF, 1996).
Boron as B	Can affect stomach, intestines, liver, kidney and brain. May lead to death (ATSDR, 2010)
Beryllium as Be	Intestinal lesions (EPA, 2022).
Calcium as Ca	Dietary requirement for all organisms to maintain teeth and bones (DWAF, 1996).
Cadmium as Cd	Possible kidney damage (DWAF, 1996, EPA, 2022)
Chromium as Cr	Allergic skin rashes (EPA, 2022)

Table D.2. Potential health and /or environmental effects from long-term exposure to parameters found in excess of regulatory or advisory concentration levels continued

Parameter	Potential health effects from long-term exposure above maximum concentration level (MCL) (unless specified as short-term)
Iron as Fe	Predominantly aesthetic effects. Chronic and acute health effects from iron poisoning if present in high concentration. Iron poisoning is more common from overdose of iron supplement tablets rather than water (DWAF, 1996)
Magnesium as Mg	Essential nutrient. High concentrations impart a bitter taste to water and may cause diarrhoea (DWAF, 1996)
Manganese as Mn	Essential to humans and animals but toxic in excessive quantities. Aesthetic effects in water, unpleasant taste and neurotoxic effects in high concentrations (DWAF, 1996)
Nickel as Ni	Allergic skin reactions increased red blood cells and protein in urine. More serious health effects from exposure to dust (ATSDR, 2005)
Lead as Pb	Developmental delays in children. Kidney problems and elevated blood pressure in adults (EPA, 2022).
Uranium as U	Chemical toxicity and increasing cancer and renal damage risk as concentrations increase (DWAF, 1996).
Vanadium as V	Has metabolic effects and toxicity symptoms included eye, nose and throat irritation. Excessive concentrations can cause chronic bronchitis (DWAF, 1996).
Zinc as Zn	Essential nutritional trace element for plants and animals. High concentrations have aesthetic effects and imparts a bitter taste to water. Health effects include possible gastrointestinal irritation, nausea and vomiting, electrolyte disturbances and renal damage (DWAF, 1996).

Appendix I-E – Summary of Regression Statistics and Coefficients

Table E.1. Summary output regression statistics at a 95 % confidence level

Independent Variable	**Dependent Variable**			
EC	TDS	TA	Fe	S
Multiple R	0.9627	0.9912	0.8810	0.8829
R Square	0.9268	0.9824	0.7764	0.7795
Adjusted R Square	0.9223	0.9813	0.7622	0.7658
Standard Error	1969.45	569.97	1078.61	742.66
Observations	18	18	18	18

Table E.2. Summary of regression coefficients at a 95 % confidence level

Regression of TDS on EC	**Coefficients**	**Standard Error**	**t Stat**	**P-value**	**Lower 95%**	**Upper 95%**
Intercept	-963.45	1392.27	-0.6920	0.4989	-3914.93	1988.04
TDS	6.2384	0.4381	14.2382	1.6652E-10	5.3096	7.1672
Regression of TA on EC	**Coefficients**	**Standard Error**	**t Stat**	**P-value**	**Lower 95%**	**Upper 95%**
Intercept	-3103.27	402.93	-7.7018	9.0454E-07	-3957.43	-2249.10
TA	3.7910	0.1268	29.8977	1.8098E-15	3.5222	4.0598
Regression of Fe on EC	**Coefficients**	**Standard Error**	**t Stat**	**P-value**	**Lower 95%**	**Upper 95%**
Intercept	-2133.15	762.26	-2.7985	0.0129	-3749.07	-517.23
Fe	1.7878	0.2399	7.4527	1.3732E-06	1.2792	2.2963
Regression of S on EC	**Coefficients**	**Standard Error**	**t Stat**	**P-value**	**Lower 95%**	**Upper 95%**
Intercept	-63.8190	525.32	-0.1215	0.9048	-1177.45	1049.82
S	1.2429	0.1653	7.5184	1.2293E-06	0.8925	1.5934

Appendix I-F – Statistical Data

F1.1 Total Dissolved Solids (TDS) vs Electrical Conductivity (EC)

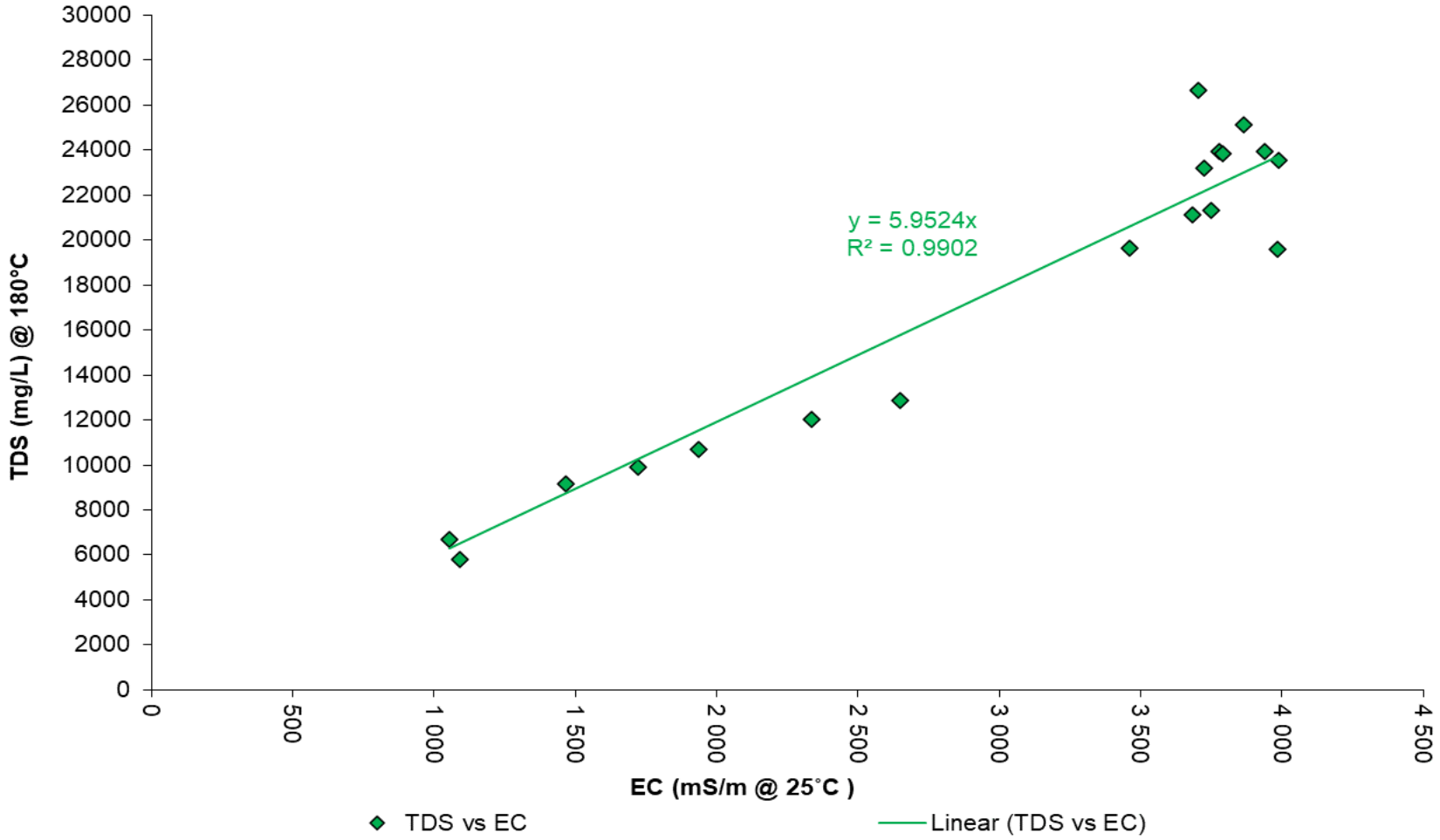


Figure F1.1 Total Dissolved Solids (TDS) vs Electrical Conductivity (EC) - Graphs - All Data

Table F1.1 All Data

Regression analysis
TDS vs EC
SUMMARY OUTPUT

Regression Statistics	
Multiple R	0.962730116
R Square	0.926849276
Adjusted R Square	0.922277356
Standard Error	1969.454167
Observations	18

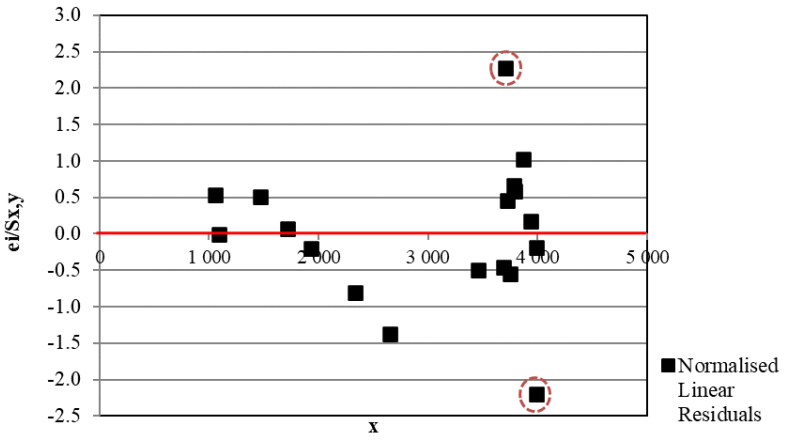
F critical value	F.INV.RT(0,05,1,16)	4.49	*Significance F*	
	F-statistic	203	1.67E-10	
R^2 Correlation is significant		F value > F - critical	Significance F < 0,05	
T critical value	T.INV.2T(0.05,16)	2.12	*P-value*	*Lower 95%*	*Upper 95%*
	t Stat	14.24	1.67E-10	5.31	7.17
Regression model is significant		t Stat > t-critical	P-value < 0,05	Does not pass through zero	

ANOVA

	df	*SS*	*MS*	*F*	*Significance F*
Regression	1	786325262.6	786325262.6	202.7264764	1.66516E-10
Residual	16	62059995.45	3878749.716		
Total	17	848385258			

	Coefficients	*Standard Error*	*t Stat*	*P-value*	*Lower 95%*	*Upper 95%*
Intercept	-963.446116	1392.270547	-0.691996335	0.498859615	-3914.927826	1988.035594
EC	6.23837608	0.438143443	14.23820481	1.66516E-10	5.309553473	7.167198686

		RESIDUAL OUTPUT	Y	$e_i = Y_i - y_i$	$e_i/S_{x,y}$
			Linear	Linear	*Normalised*
EC	TDS	*Observation*	*Predicted TDS*	*Residuals*	*Normalised Linear Residuals*
3 460	19 640	1	20621.33512	-981.3351191	-0.4983
3 685	21 130	2	22024.96974	-894.969737	-0.4544
2 335	12 014	3	13603.16203	-1589.16203	-0.8069
3 750	21 338	4	22430.46418	-1092.064182	-0.5545
3 725	23 178	5	22274.50478	903.4952198	0.4588
3 780	23 922	6	22617.61546	1304.384535	0.6623
3 940	23 952	7	23615.75564	336.2443627	0.1707
3 865	25 152	8	23147.87743	2004.122569	1.0176
3 985	19 576	9	23896.48256	-4320.482561	-2.1937
2 650	12 852	10	15568.25049	-2716.250495	-1.3792
3 790	23 832	11	22679.99923	1152.000775	0.5849
3 990	23 566	12	23927.67444	-361.6744413	-0.1836
3 705	26 635	13	22149.73726	4485.262741	2.2774
1 090	5 820	14	5836.383811	-16.38381065	-0.0083
1 465	9 175	15	8175.77484	999.2251595	0.5074
1 055	6 680	16	5618.040648	1061.959352	0.5392
1 720	9 900	17	9766.560741	133.4392592	0.0678
1 935	10 700	18	11107.8116	-407.8115979	-0.2071



The normalized linear residuals $e_i/Sx,y$ for data points 9 & 13 > 2 and the standard residuals are not consistent with neighbours – Reject data pt. 9 & 13

F 1.2 Total Dissolved Solids (TDS) vs Electrical Conductivity (EC) - Data point 9 & 13 rejected

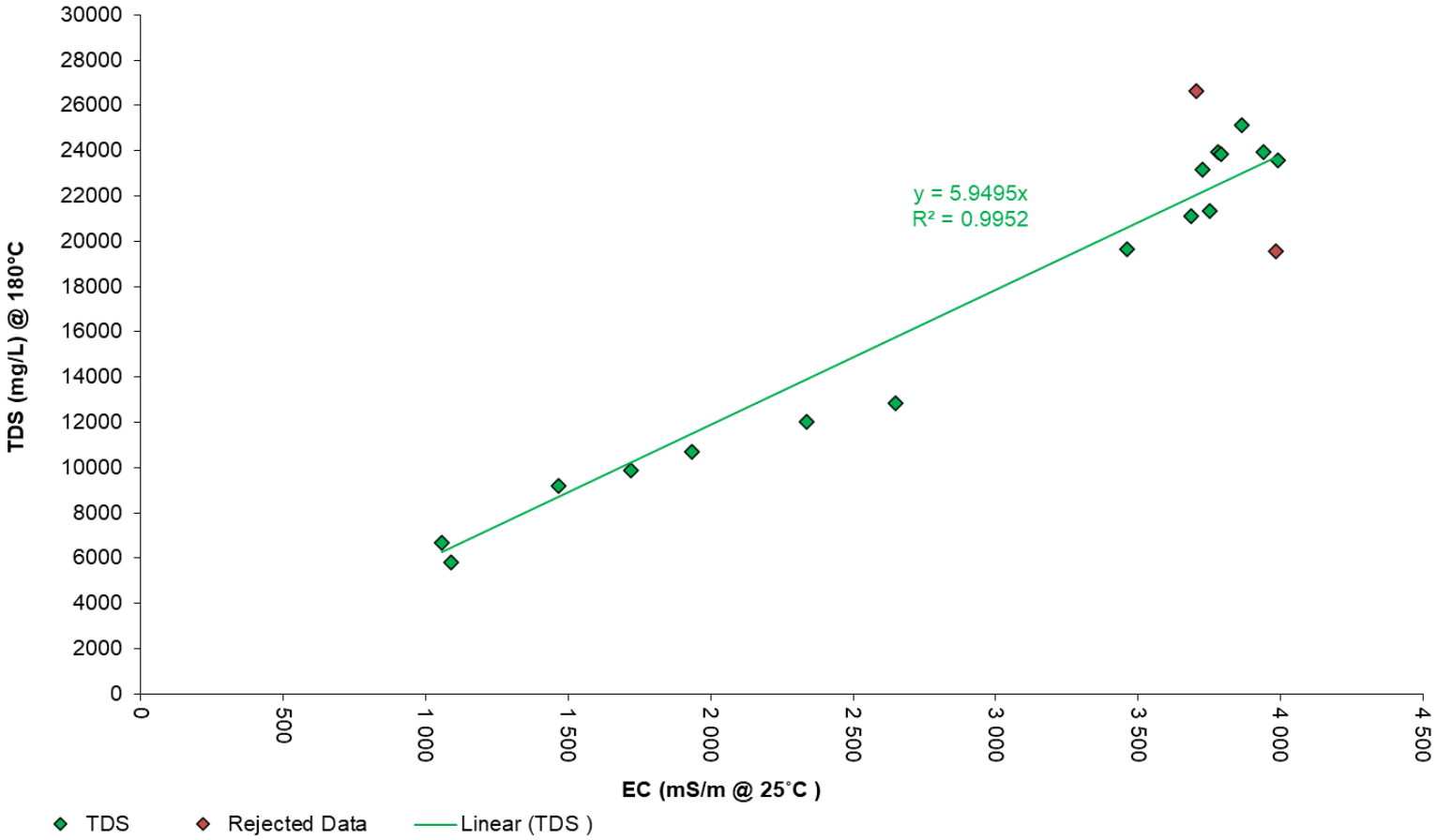
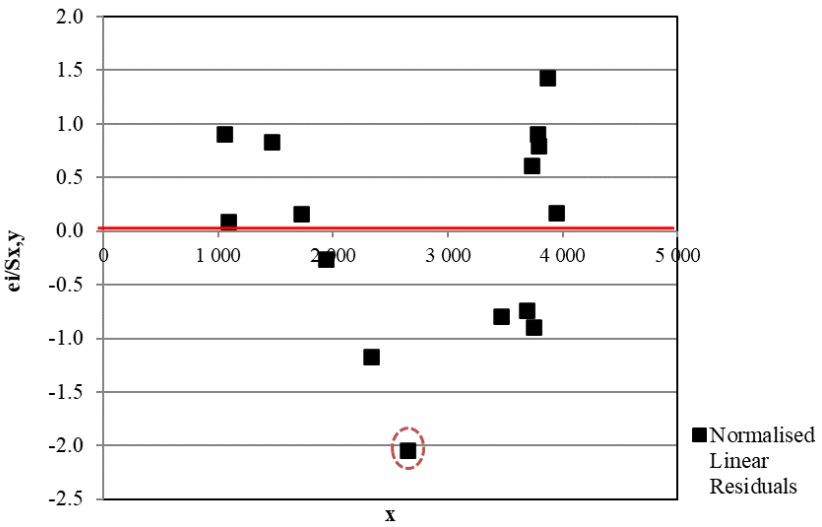


Figure F1.2. Total Dissolved Solids (TDS) vs Electrical Conductivity (EC) - Data pt. 9 & 13 rejected

Table F1.2. Total Dissolved Solids (TDS) vs Electrical Conductivity (EC) - Data point 9 & 13 rejected

		TDS vs EC								
		SUMMARY OUTPUT								
		Regression Statistics			F critical value	F.INV.RT(0,05,1,14)	4.60	*Significance F*		
		Multiple R	0.983731108			F-statistic	390	4.47E-11		
		R Square	0.967726894		**R^2 Correlation is significant**		F value > F - critical	Significance F < 0,05		
		Adjusted R Square	0.965244347		T critical value	T.INV.2T(0.05,14)	2.14	*P-value*	*Lower 95%*	*Upper 95%*
		Standard Error	1330.533341			*t Stat*	19.74	4.47E-11	5.63	7.02
		Observations	15		**Regression model is significant**		t Stat > t-critical	P-value < 0,05	Does not pass through zero	
		ANOVA								
			df	*SS*	*MS*	*F*	*Significance F*			
		Regression	1	690091882.7	690091882.7	389.8121718	4.46943E-11			
		Residual	13	23014146.62	1770318.971					
		Total	14	713106029.3						
			Coefficients	*Standard Error*	*t Stat*	*P-value*	*Lower 95%*	*Upper 95%*		
		Intercept	-1193.196422	965.3702112	-1.2359988	0.238327188	-3278.751968	892.3591239		
		EC	6.324614661	0.32033646	19.74366156	4.46943E-11	5.632569812	7.016659509		

		RESIDUAL OUTPUT	Y	$e_i = Y_i - y_i$	$e_i/S_{x,y}$
			Linear	Linear	*Normalised*
EC	TDS	*Observation*	*Predicted TDS*	*Residuals*	*Normalised Linear Residuals*
3 460	19 640	1	20689.97	-1049.97	-0.7891
3 685	21 130	2	22113.01	-983.01	-0.7388
2 335	12 014	3	13574.78	-1560.78	-1.1730
3 750	21 338	4	22524.11	-1185.71	-0.8912
3 725	23 178	5	22365.99	812.01	0.6103
3 780	23 922	6	22713.85	1208.15	0.9080
3 940	23 952	7	23725.79	226.21	0.1700
3 865	25 152	8	23251.44	1900.56	1.4284
2 650	12 852	9	15567.03	-2715.03	-2.0406
3 790	23 832	10	22777.09	1054.91	0.7928
1 090	5 820	11	5700.63	119.37	0.0897
1 465	9 175	12	8072.36	1102.64	0.8287
1 055	6 680	13	5479.27	1200.73	0.9024
1 720	9 900	14	9685.14	214.86	0.1615
1 935	10 700	15	11044.93	-344.93	-0.2592



The normalized linear residual $e_i/Sx,y$ for data point 10 > 2 and the standard residual is not consistent with neighbours – Reject data pt.10

F1.3 Total Dissolved Solids (TDS) vs Electrical Conductivity (EC) - Data point 9, 10 & 13 rejected

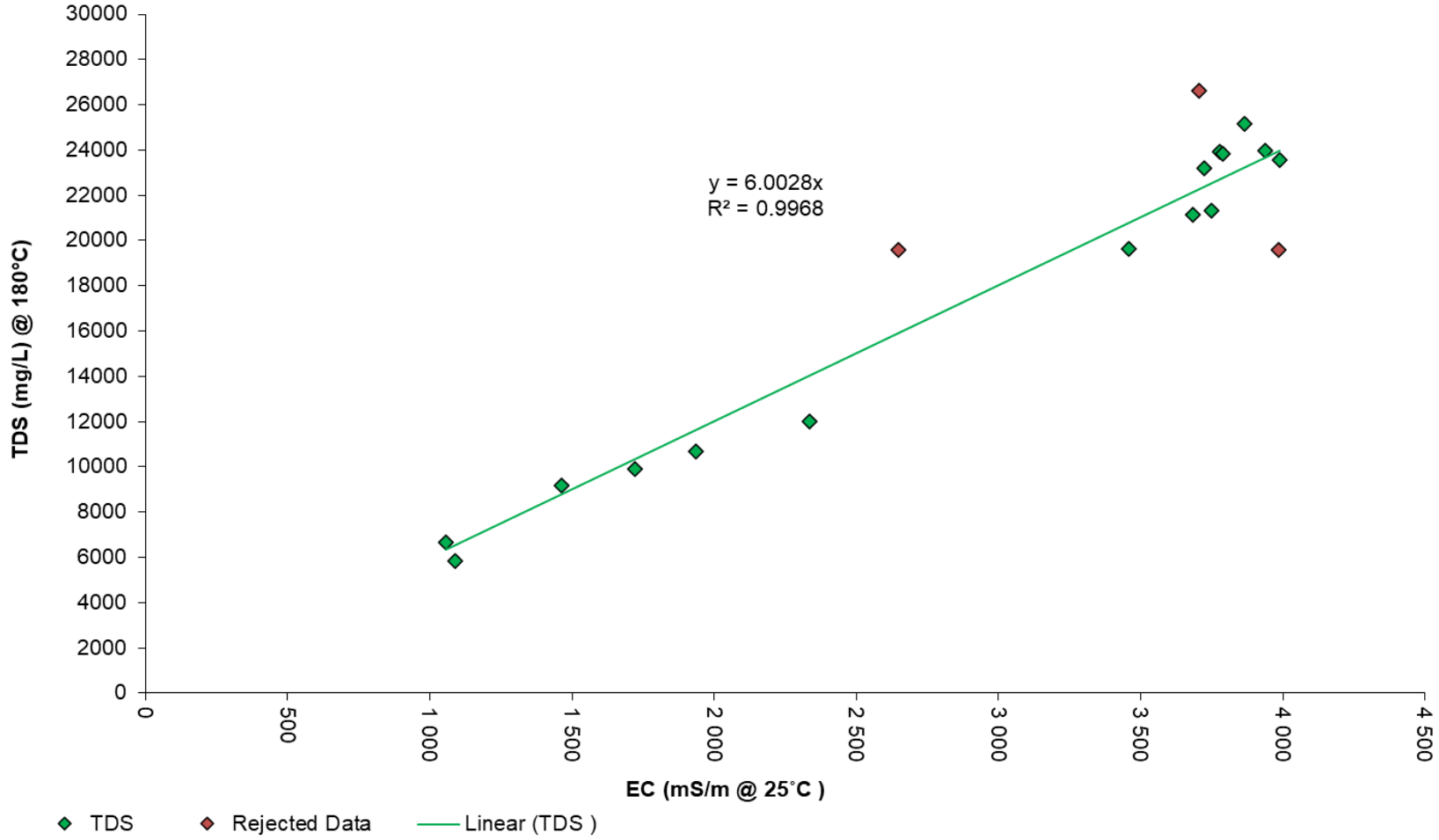
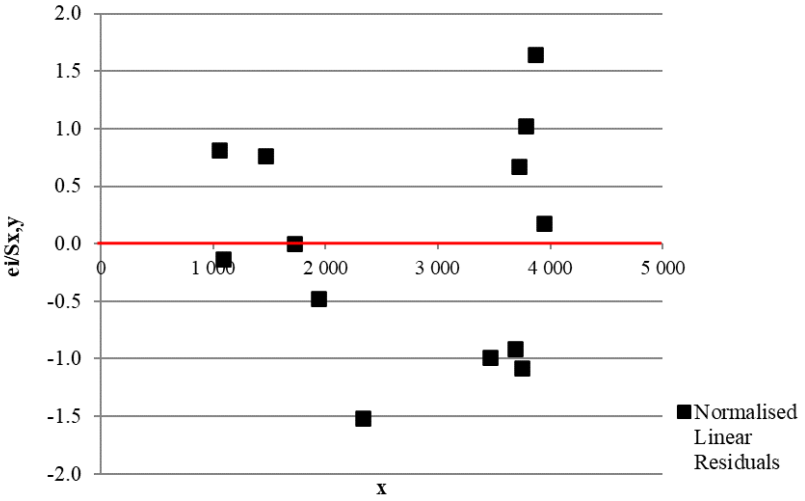


Figure F1.3. Total Dissolved Solids (TDS) vs Electrical Conductivity (EC) - Data pt. 9, 10 & 13 rejected

Table F1.3. Data points 9, 10 & 13 rejected

		SUMMARY OUTPUT								
		TDS vs EC								
		Regression Statistics			F critical value	F.INV.RT(0,05,1,13)	4.67	*Significance F*		
		Multiple R	0.988946778			F-statistic	489	1.81E-10		
		R Square	0.97801573		**R^2 Correlation is significant**		F value > F - critical	Significance F < 0,05		
		Adjusted R Square	0.97601716		T critical value	T.INV.2T(0.05,13)	2.16	*P-value*	*Lower 95%*	*Upper 95%*
		Standard Error	1136.23348			*t Stat*	22.12	1.81E-10	5.62	6.86
		Observations	13		**Regression model is significant**		t Stat > t-critical	P-value < 0,05	Does not pass through zero	
		ANOVA								
			df	*SS*	*MS*	*F*	*Significance F*			
		Regression	1	631773836.6	631773836.6	489.3577522	1.80752E-10			
		Residual	11	14201291.74	1291026.521					
		Total	12	645975128.3						
			Coefficients	*Standard Error*	*t Stat*	*P-value*	*Lower 95%*	*Upper 95%*		
		Intercept	-831.9945662	838.3733361	-0.992391492	0.342334977	-2677.241838	1013.252705		
		EC	6.239836039	0.282071977	22.12143197	1.80752E-10	5.618999804	6.860672273		

		RESIDUAL OUTPUT	Y	$e_i = Y_i - y_i$	$e_i/S_{x,y}$
			Linear	Linear	*Normalised*
EC	TDS	*Observation*	*Predicted TDS*	*Residuals*	*Normalised Linear Residuals*
3 460	19 640	1	20757.84	-1117.84	-0.9838
3 685	21 130	2	22161.80	-1031.80	-0.9081
2 335	12 014	3	13738.02	-1724.02	-1.5173
3 750	21 338	4	22567.39	-1228.99	-1.0816
3 725	23 178	5	22411.39	766.61	0.6747
3 780	23 922	6	22754.59	1167.41	1.0274
3 940	23 952	7	23752.96	199.04	0.1752
3 865	25 152	8	23284.97	1867.03	1.6432
1 090	5 820	9	5969.43	-149.43	-0.1315
1 465	9 175	10	8309.37	865.63	0.7618
1 055	6 680	11	5751.03	928.97	0.8176
1 720	9 900	12	9900.52	-0.52	-0.0005
1 935	10 700	13	11242.09	-542.09	-0.4771



All normalized linear residuals $e_i/Sx,y$ for all data are < 2 and standard residuals are consistent with neighbours – No further points to reject

F2. Total Acidity (TA) vs Electrical Conductivity (EC)

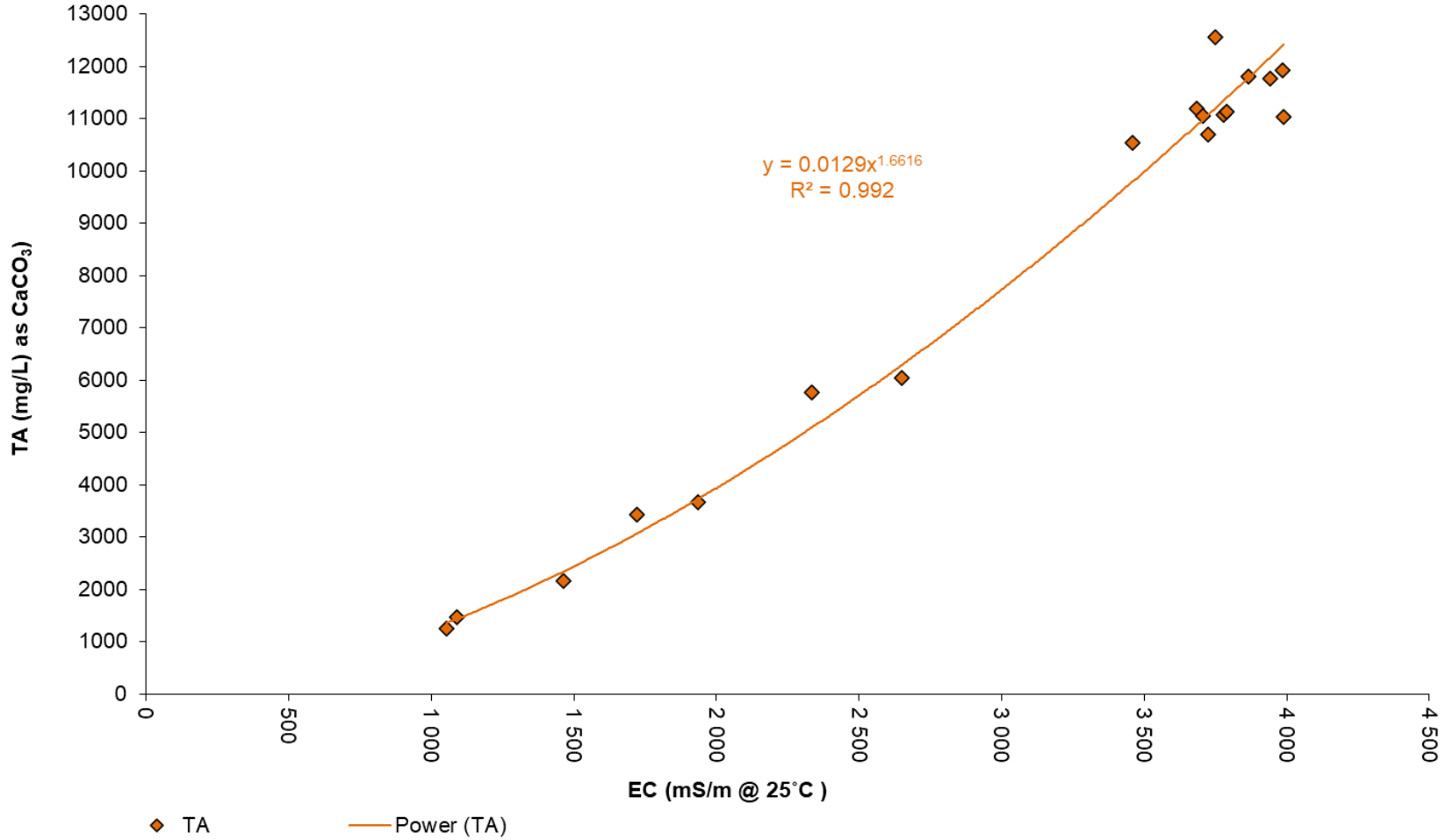
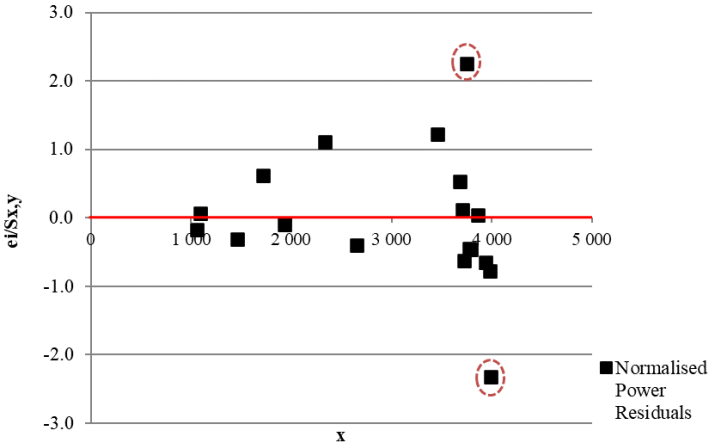


Figure F2.1. Total Acidity (TA) vs Electrical Conductivity (EC) – All Data

Table F2.1. All Data

		SUMMARY OUTPUT									
		TA vs EC									
		Regression Statistics			F critical value	F.INV.RT(0,05,1,16)	4.49	*Significance F*			
		Multiple R	0.991168568			F-statistic	894	1.81E-15			
		R Square	0.98241513		**R^2 Correlation is significant**		F value > F - critical	Significance F < 0,05			
		Adjusted R Square	0.981316076		T critical value	T.INV.2T(0.05,16)	2.12	*P-value*	*Lower 95%*	*Upper 95%*	
		Standard Error	569.9659144			*t Stat*	29.90	1.81E-15	3.52	4.06	
		Observations	18		**Regression model is significant**		t Stat > t-critical	P-value < 0,05	Does not pass through zero		
		ANOVA									
			df	*SS*	*MS*	*F*	*Significance F*				
		Regression	1	290384635.9	290384635.9	893.8730952	1.80981E-15				
		Residual	16	5197778.298	324861.1436						
		Total	17	295582414.2							
			Coefficients	*Standard Error*	*t Stat*	*P-value*	*Lower 95%*	*Upper 95%*			
		Intercept	-3103.26716	402.927252	-7.70180509	9.04541E-07	-3957.434777	-2249.099544			
		EC	3.791030299	0.12680002	29.89771053	1.80981E-15	3.522226264	4.059834334			

		RESIDUAL OUTPUT	$y = 0.0129x^{1.6616}$	$e_i = Y_i - y_i$	e_i^2	$e_i/S_{x,y}$
			Power	*Power*	*Power*	*Power*
EC	TA	*Observation*	*Predicted TA*	*Residuals*	*Residuals*	*Normalised Power Residuals*
3 460	10 530	1	9797.57	732.43	536447.72	1.2219
3 685	11 200	2	10878.83	321.17	103149.25	0.5358
2 335	5 760	3	5097.24	662.76	439249.02	1.1057
3 750	12 550	4	11199.54	1350.46	1823750.60	2.2529
3 725	10 700	5	11075.75	-375.75	141187.83	-0.6269
3 780	11 080	6	11348.80	-268.80	72255.44	-0.4484
3 940	11 765	7	12158.11	-393.11	154539.09	-0.6558
3 865	11 800	8	11775.99	24.01	576.63	0.0401
3 985	11 925	9	12389.72	-464.72	215962.68	-0.7753
2 650	6 050	10	6290.06	-240.06	57630.66	-0.4005
3 790	11 125	11	11398.73	-273.73	74930.34	-0.4567
3 990	11 025	12	12415.56	-1390.56	1933653.99	-2.3198
3 705	11 050	13	10977.11	72.89	5312.26	0.1216
1 090	1 480	14	1437.40	42.60	1814.78	0.0711
1 465	2 160	15	2349.34	-189.34	35848.89	-0.3159
1 055	1 260	16	1361.53	-101.53	10307.57	-0.1694
1 720	3 440	17	3067.21	372.79	138970.98	0.6219
1 935	3 673	18	3730.26	-57.76	3335.93	-0.0964
			For Power Normalised Residuals Sum e_i^2		**359308**	
			$S_{y,x}$ =SQURT[$(e_i)^2$/(n-2)]		**599**	



The normalized power residual $e_i/Sx,y$ for data point 4 *& 12* > 2 and the standard power residuals are not consistent with neighbours – Reject data *pt.4* & 12

F2.2 Total Acidity (TA) vs Electrical Conductivity (EC) - Data point 4 & 12 rejected

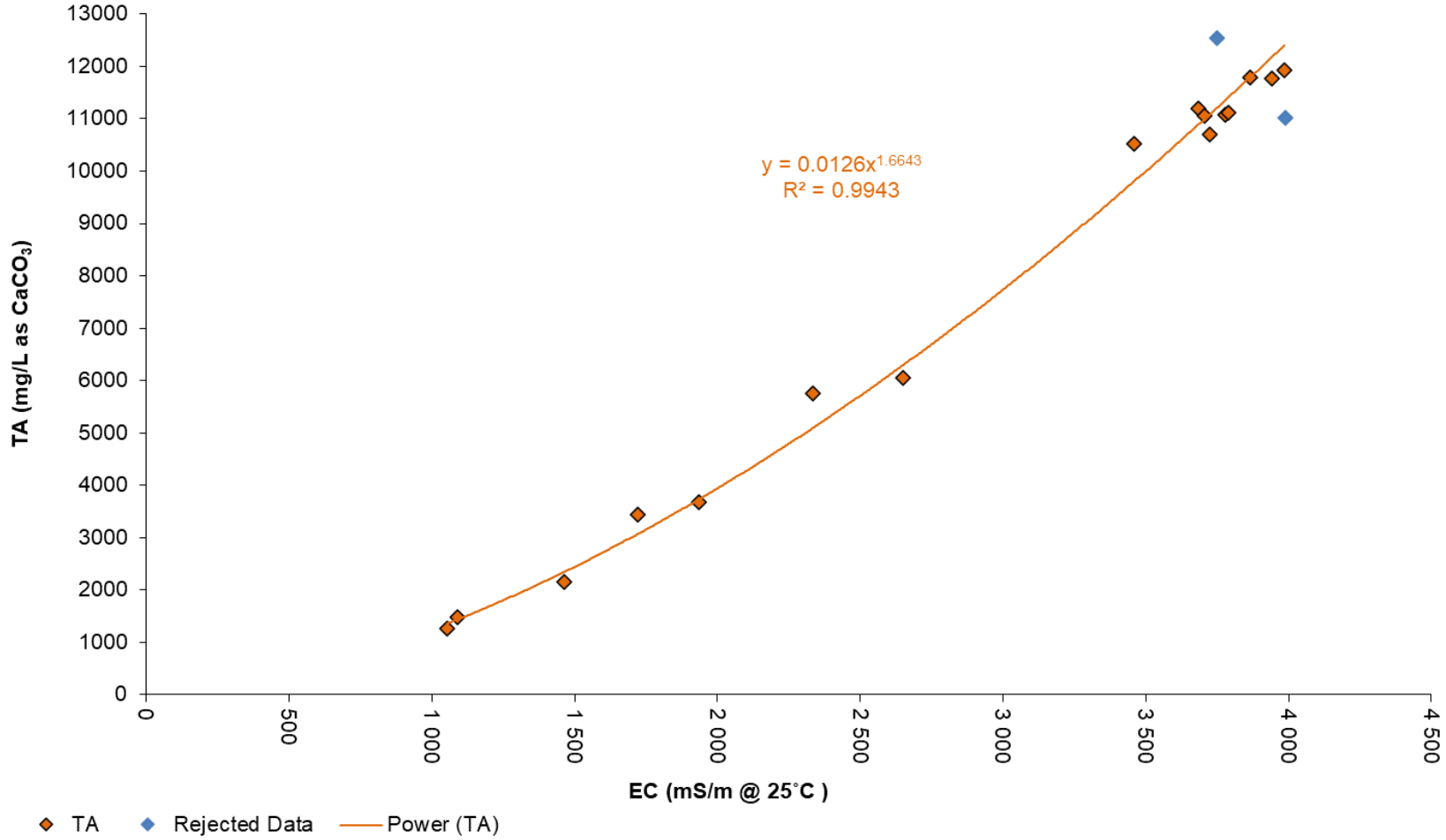
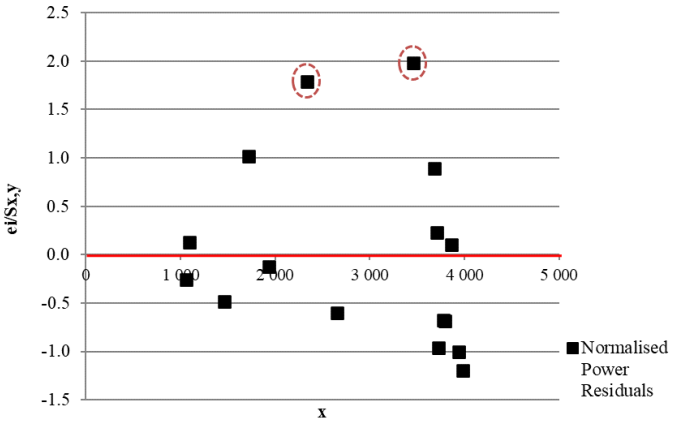


Figure F2.2. Total Acidity (TA) vs Electrical Conductivity (EC) – Data points 4 and 12 rejected

Table F2.2. All Data

		SUMMARY OUTPUT								
		TA vs EC								
		Regression Statistics			F critical value	F.INV.RT(0,05,1,14)	4.60	*Significance F*		
		Multiple R	0.996004261			F-statistic	1741	4.31E-16		
		R Square	0.992024487		**R^2 Correlation is significant**		F value > F - critical	Significance F < 0,05		
		Adjusted R Square	0.991454808		T critical value	T.INV.2T(0.05,14)	2.14	*P-value*	*Lower 95%*	*Upper 95%*
		Standard Error	389.5141189			*t Stat*	41.73	4.31E-16	3.59	3.98
		Observations	16		**Regression model is significant**		t Stat > t-critical	P-value < 0,05	Does not pass through zero	
		ANOVA								
			df	*SS*	*MS*	*F*	*Significance F*			
		Regression	1	264203295.9	264203295.9	1741.373064	4.31478E-16			
		Residual	14	2124097.483	151721.2488					
		Total	15	266327393.4						
			Coefficients	*Standard Error*	*t Stat*	*P-value*	*Lower 95%*	*Upper 95%*		
		Intercept	-3108.883774	279.2424585	-11.13327748	2.43328E-08	-3707.799281	-2509.968266		
		EC	3.783471698	0.090666026	41.72976233	4.31478E-16	3.589012413	3.977930983		

		RESIDUAL OUTPUT	$y = 0.0126x^{1.6643}$	$e_i = Y_i - y_i$	e_i^2	$e_i/S_{x,y}$
			Power	*Power*	*Power*	*Power*
EC	TA	*Observation*	*Predicted TA*	*Residuals*	*Residuals*	*Normalised Power Residuals*
3 460	10 530	1	9782.61	747.39	558586.55	1.9823
3 685	11 200	2	10864.07	335.93	112850.51	0.8910
2 335	5 760	3	5084.06	675.94	456898.99	1.7928
3 725	10 700	4	11061.04	-361.04	130350.71	-0.9576
3 780	11 080	5	11334.18	-254.18	64608.03	-0.6742
3 940	11 765	6	12143.81	-378.81	143495.82	-1.0047
3 865	11 800	7	11761.52	38.48	1480.70	0.1021
3 985	11 925	8	12375.52	-450.52	202967.02	-1.1949
2 650	6 050	9	6275.94	-225.94	51048.04	-0.5993
3 790	11 125	10	11384.13	-259.13	67147.48	-0.6873
3 705	11 050	11	10962.38	87.62	7677.64	0.2324
1 090	1 480	12	1430.74	49.26	2426.95	0.1307
1 465	2 160	13	2340.31	-180.31	32513.09	-0.4782
1 055	1 260	14	1355.09	-95.09	9042.98	-0.2522
1 720	3 440	15	3056.75	383.25	146877.23	1.0165
1935	3673	16	3718.72	-46.22	2136.45	-0.1226
			For Power Normalised Residuals Sum e_i^2		**142151**	
			Sy,x =SQURT[$(e_i)^2$/(n-2)]		**377**	



The normalized power residual $e_i/Sx,y$ for all data points < 2, however the standard power residual points 1 & 3 are not consistent with neighbours – Reject points 1 & 3.

F2.3 Total Acidity (TA) vs Electrical Conductivity (EC) - Data points 1, 3, 4 & 12 rejected

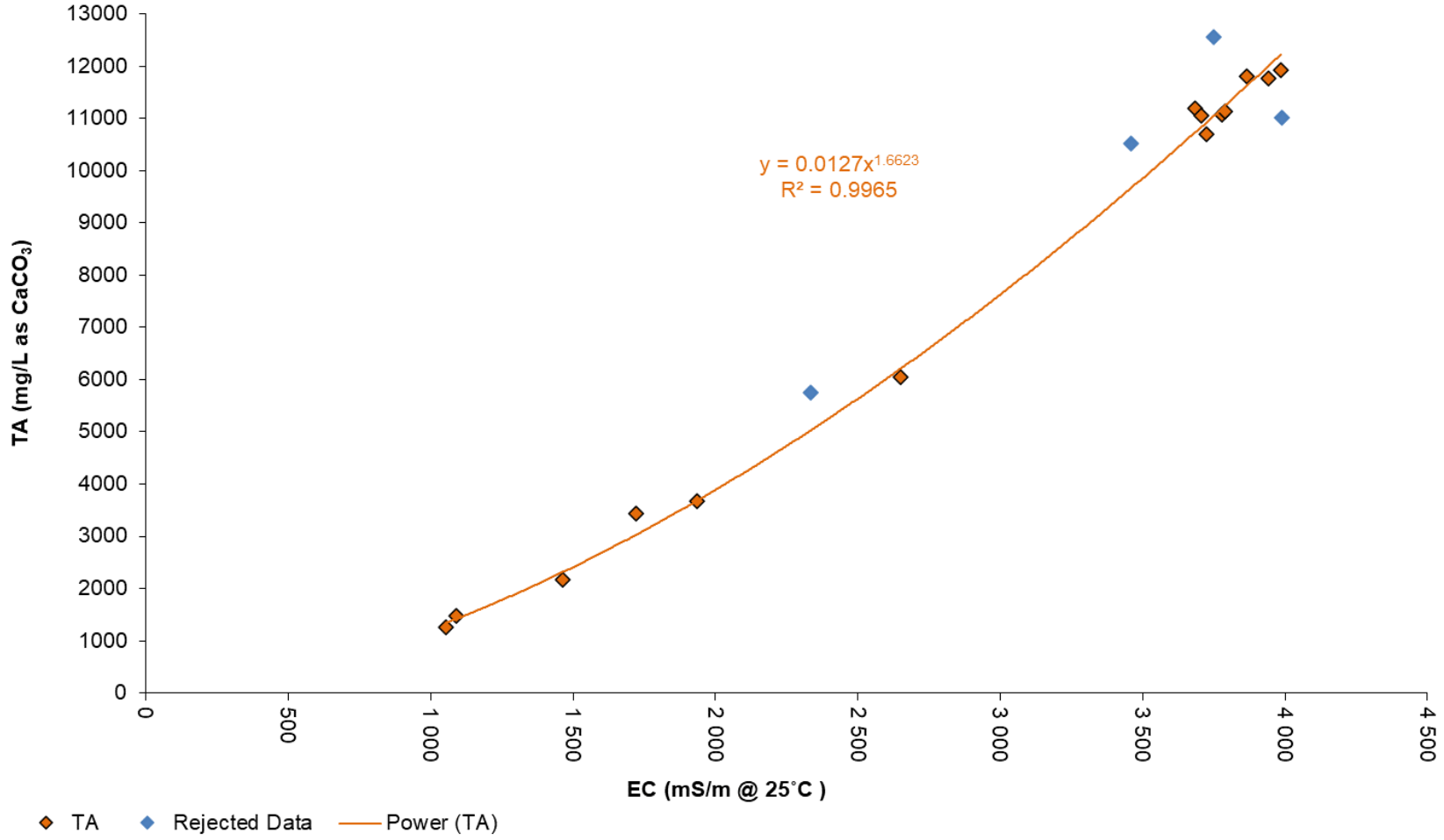


Figure F2.3. Total Acidity (TA) vs Electrical Conductivity (EC) – Data points 1, 3, 4 and 12 rejected

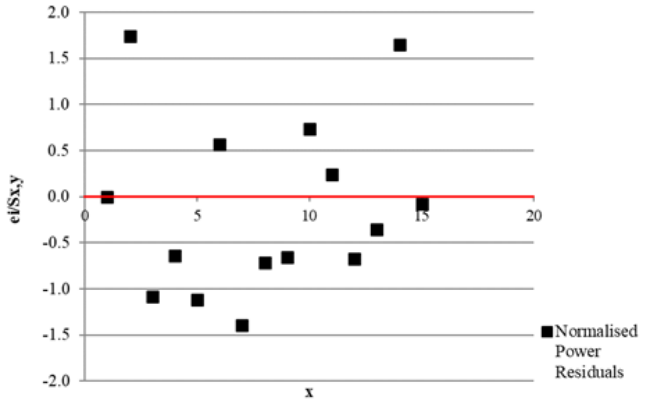
Table F2.3. Total Acidity (TA) vs Electrical Conductivity (EC) - Data points 1,3, 4 & 12 rejected

SUMMARY OUTPUT								
ECvs TA								
Regression Statistics			F critical value	F.INV.RT(0,05,1,14)	4.60	*Significance F*		
Multiple R	0.996473211			F-statistic	1692	2.76E-14		
R Square	0.99295886		**R^2 Correlation is significant**		F value > F - critical	Significance F < 0,05		
Adjusted R Square	0.992372098		T critical value	T.INV.2T(0.05,14)	2.14	*P-value*	*Lower 95%*	*Upper 95%*
Standard Error	386.5837922			*t Stat*	41.14	2.76E-14	3.57	3.97
Observations	14		**Regression model is significant**		t Stat > t-critical	P-value < 0,05	Does not pass through zero	

ANOVA								
	df	*SS*	*MS*	*F*	*Significance F*			
Regression	1	252904641.5	252904641.5	1692.269456	2.7573E-14			
Residual	12	1793364.341	149447.0284					
Total	13	254698005.8						

	Coefficients	*Standard Error*	*t Stat*	*P-value*	*Lower 95%*	*Upper 95%*		
Intercept	-3102.554145	283.6593743	-10.93760484	1.34877E-07	-3720.594829	-2484.513461		
EC	3.766854618	0.091568079	41.13720283	2.7573E-14	3.567344914	3.966364322		

		RESIDUAL OUTPUT	$y = 0.0127x^{1.6623}$	$e_i = Y_i - y_i$	e_i^2	$e_i/S_{x,y}$
			Power	*Power*	*Power*	*Power*
EC	TA	*Observation*	*Predicted TA*	*Residuals*	*Residuals*	*Normalised Power Residuals*
3 685	11 200	1	10771.91	428.09	183260.03	1.7429
3 725	10 700	2	10966.98	-266.98	71276.70	-1.0870
3 780	11 080	3	11237.46	-157.46	24795.13	-0.6411
3 940	11 765	4	12039.19	-274.19	75177.45	-1.1163
3 865	11 800	5	11660.64	139.36	19421.63	0.5674
3 985	11 925	6	12268.62	-343.62	118074.93	-1.3990
2 650	6 050	7	6226.81	-176.81	31260.37	-0.7198
3 790	11 125	8	11286.93	-161.93	26220.05	-0.6593
3 705	11 050	9	10869.27	180.73	32663.43	0.7358
1 090	1 480	10	1422.06	57.94	3357.09	0.2359
1 465	2 160	11	2324.75	-164.75	27141.41	-0.6707
1 055	1 260	12	1346.96	-86.96	7562.90	-0.3541
1 720	3 440	13	3035.45	404.55	163663.11	1.6471
1 935	3 673	14	3691.93	-19.43	377.54	-0.0791
			For Power Normalised Residuals Sum ei2		**60327**	
			Sy,x =SQURT[(ei)2/(n-2)]		**246**	



The normalized power residual $e_i/Sx,y$ for all data points < 2, and all standard power residual points are consistent with neighbours – No further rejection

F3. Dissolved S (S) vs Electrical Conductivity (EC)

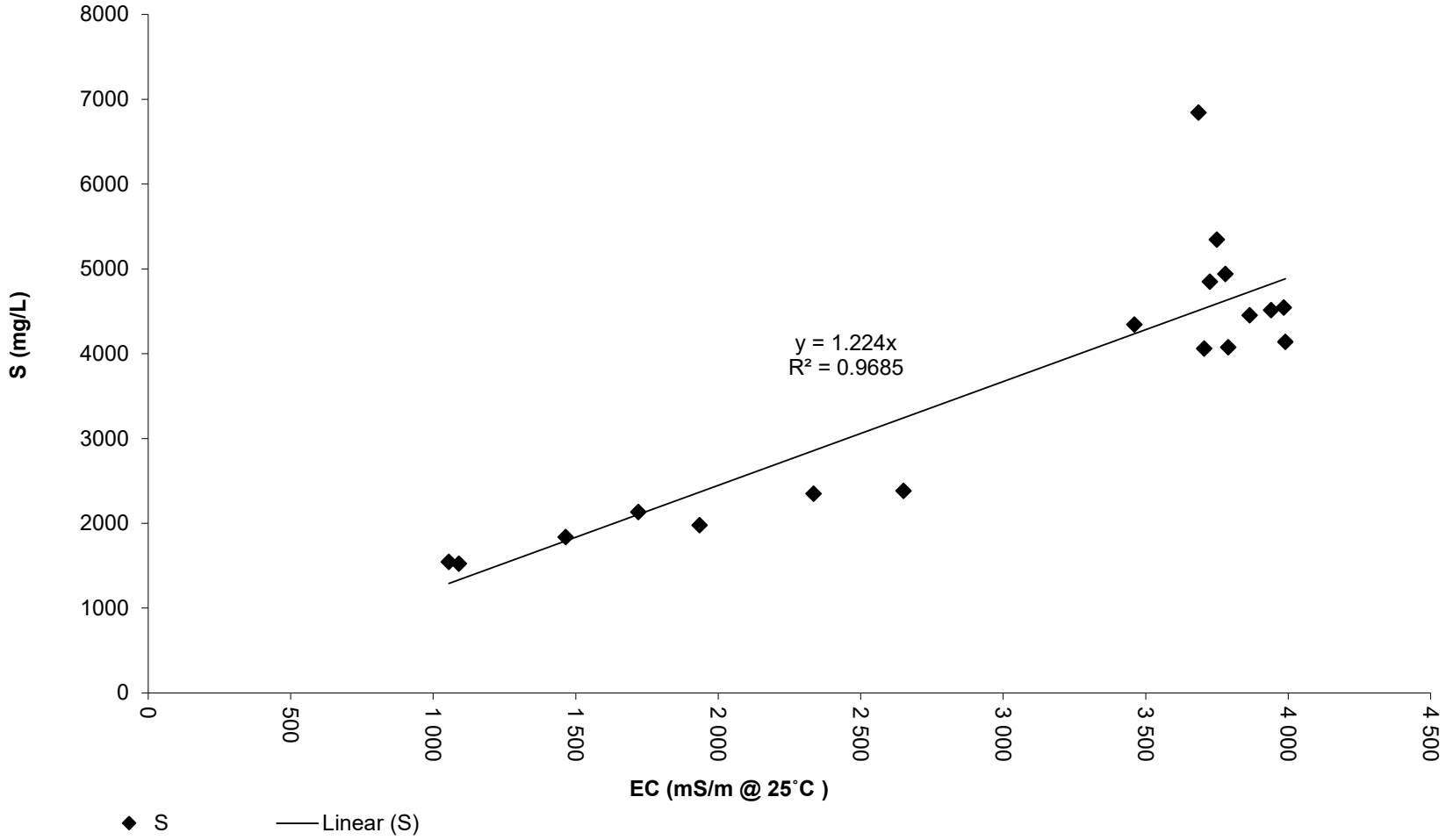


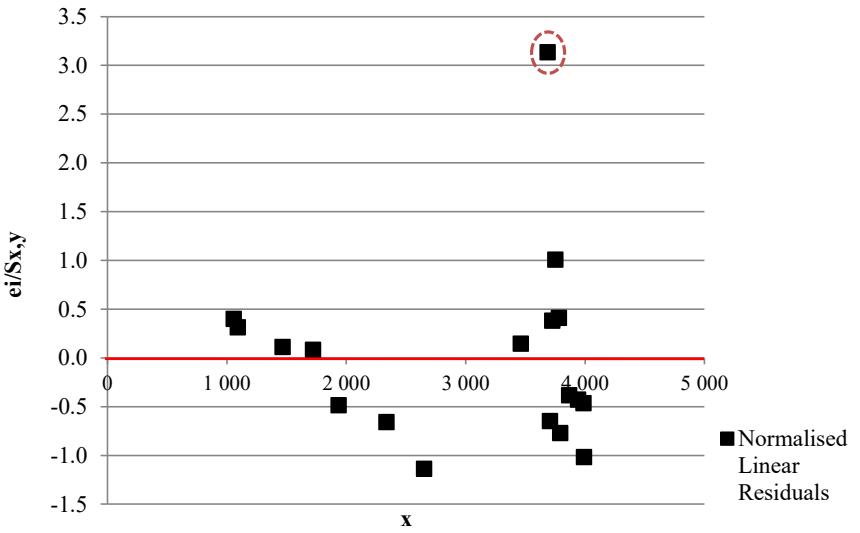
Figure F3.1. Dissolved Sulfur (S) vs Electrical Conductivity (EC) – All Data

Table F3.1. Dissolved Sulfur (S) vs Electrical Conductivity (EC) – All Data

S vs EC								
Regression Statistics			F critical value	F.INV.RT(0,05,1,16)	4.49	*Significance F*		
Multiple R	0.882829713			F-statistic	57	1.23E-06		
R Square	0.779388302		**R^2 Correlation is significant**		F value > F - critical	Significance F < 0,05		
Adjusted R Square	0.765600071		T critical value	T.INV.2T(0.05,16)	2.12	*P-value*	*Lower 95%*	*Upper 95%*
Standard Error	743.1021715			*t Stat*	7.52	1.23E-06	0.89	1.59
Observations	18		**Regression model is significant**		t Stat > t-critical	P-value < 0,05	Does not pass through zero	

ANOVA						
	df	*SS*	*MS*	*F*	*Significance F*	
Regression	1	31213494.2	31213494.2	56.52561912	1.22926E-06	
Residual	16	8835213.396	552200.8372			
Total	17	40048707.6				
	Coefficients	*Standard Error*	*t Stat*	*P-value*	*Lower 95%*	*Upper 95%*
Intercept	-63.81904158	525.3228453	-0.121485373	0.904819264	-1177.453725	1049.815642
EC	1.242915582	0.165317553	7.518352155	1.22926E-06	0.892458025	1.593373139

		RESIDUAL OUTPUT	Y	$e_i = Y_i - y_i$	$e_i/S_{x,y}$
			Linear	Linear	*Normalised*
EC	S	*Observation*	*Predicted S*	*Residuals*	*Normalised Linear Residuals*
3 460	4 345	1	4236.67	108.33	0.1458
3 685	6 845	2	4516.32	2328.68	3.1337
2 335	2 350	3	2838.39	-488.39	-0.6572
3 750	5 345	4	4597.11	748.03	1.0066
3 725	4 850	5	4566.04	283.96	0.3821
3 780	4 940	6	4634.40	305.60	0.4112
3 940	4 515	7	4833.27	-318.27	-0.4283
3 865	4 455	8	4740.05	-285.05	-0.3836
3 985	4 545	9	4889.20	-344.20	-0.4632
2 650	2 385	10	3229.91	-844.91	-1.1370
3 790	4 075	11	4646.83	-571.83	-0.7695
3 990	4 140	12	4895.41	-755.41	-1.0166
3 705	4 060	13	4541.18	-481.18	-0.6475
1 090	1 525	14	1290.96	234.04	0.3150
1 465	1 840	15	1757.05	82.95	0.1116
1 055	1 545	16	1247.46	297.88	0.4009
1 720	2 135	17	2074.00	61.00	0.0821
1 935	1 980	18	2341.22	-361.22	-0.4861



The normalized linear residual $e_i/Sx,y$ for data point 2 > 2 and the standard linear residuals are not consistent with neighbours – Reject data *pt.2*

F3.2 Dissolved Sulfur (S) vs Electrical Conductivity (EC) - Data point 4 rejected

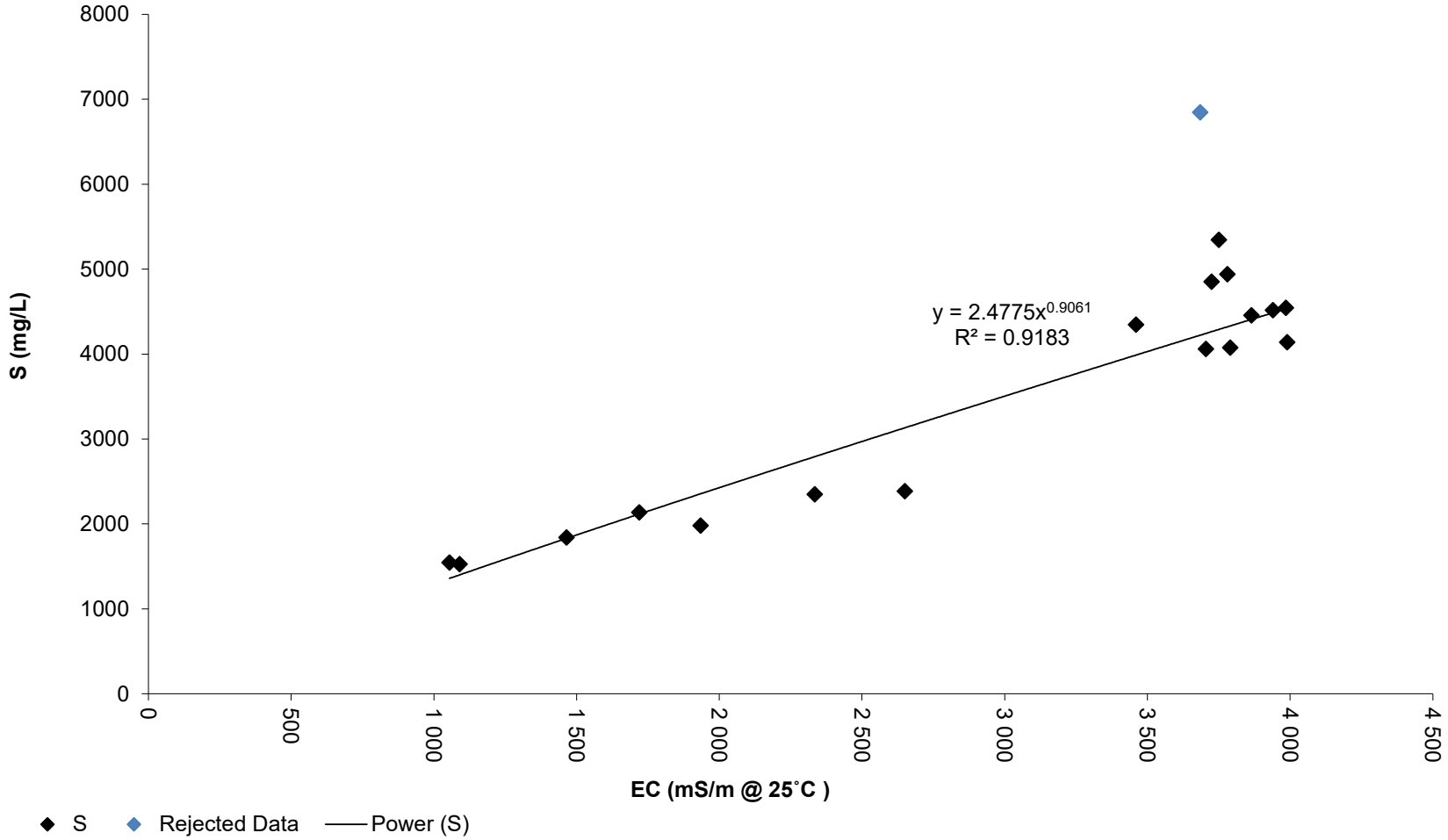
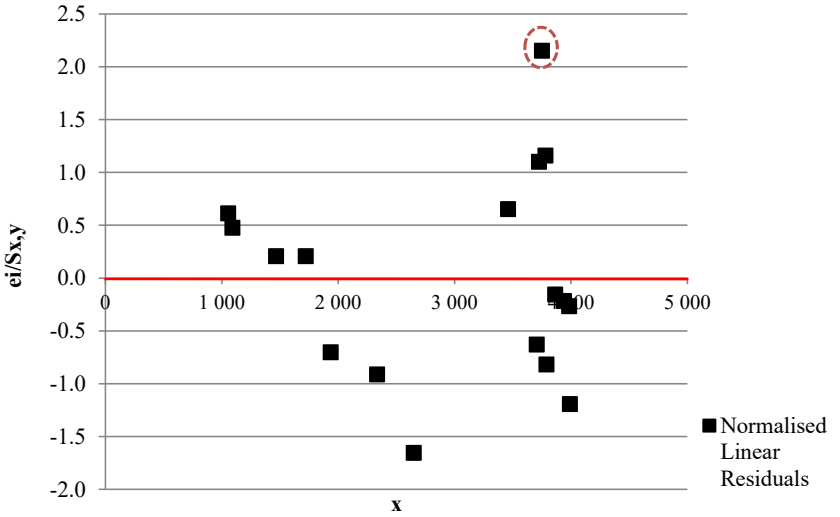


Figure F3.2. Dissolved Sulfur (S) vs Electrical Conductivity (EC) – Data pt. 2 rejected

Table F3.2. Dissolved Sulfur (S) vs Electrical Conductivity (EC) – Data pt. 2 rejected

		SUMMARY OUTPUT									
		S vs EC									
		Regression Statistics			F critical value	F.INV.RT(0,05,1,15)	4.54	*Significance F*			
		Multiple R	0.948389397			F-statistic	134	7.00E-09			
		R Square	0.899442448		**R^2 Correlation is significant**		F value > F - critical	Significance F < 0,05			
		Adjusted R Square	0.892738611		T critical value	T.INV.2T(0.05,15)	2.13	*P-value*	*Lower 95%*	*Upper 95%*	
		Standard Error	443.2415924			*t Stat*	11.58	7.00E-09	0.94	1.37	
		Observations	17		**Regression model is significant**		t Stat > t-critical	P-value < 0,05	Does not pass through zero		
		ANOVA									
			df	*SS*	*MS*	*F*	*Significance F*				
		Regression	1	26359123.11	26359123.11	134.1683088	6.99792E-09				
		Residual	15	2946946.638	196463.1092						
		Total	16	29306069.75							
			Coefficients	*Standard Error*	*t Stat*	*P-value*	*Lower 95%*	*Upper 95%*			
		Intercept	54.08515368	314.0810003	0.172201291	0.865581124	-615.3626517	723.532959			
		EC	1.156668638	0.099858258	11.58310445	6.99792E-09	0.943825799	1.369511478			

		RESIDUAL OUTPUT	Y	$e_i = Y_i - y_i$	$e_i/S_{x,y}$
			Linear	Linear	*Normalised*
EC	S	*Observation*	*Predicted S*	*Residuals*	*Normalised Linear Residuals*
3 460	4 345	1	4056.16	288.84	0.6517
2 335	2 350	2	2754.91	-404.91	-0.9135
3 750	5 345	3	4391.59	953.55	2.1513
3 725	4 850	4	4362.68	487.32	1.0995
3 780	4 940	5	4426.29	513.71	1.1590
3 940	4 515	6	4611.36	-96.36	-0.2174
3 865	4 455	7	4524.61	-69.61	-0.1570
3 985	4 545	8	4663.41	-118.41	-0.2671
2 650	2 385	9	3119.26	-734.26	-1.6566
3 790	4 075	10	4437.86	-362.86	-0.8186
3 990	4 140	11	4669.19	-529.19	-1.1939
3 705	4 060	12	4339.54	-279.54	-0.6307
1 090	1 525	13	1314.85	210.15	0.4741
1 465	1 840	14	1748.60	91.40	0.2062
1 055	1 545	15	1274.37	270.97	0.6113
1 720	2 135	16	2043.56	91.44	0.2063
1 935	1 980	17	2292.24	-312.24	-0.7044



The normalized linear residual $e_i/Sx,y$ for data point 4 > 2 and the standard linear residuals are not consistent with neighbours – Reject data *pt.4*

F3.3 Dissolved Sulfur (S) vs Electrical Conductivity (EC) - Graphs – Data point 2 & 4 rejected

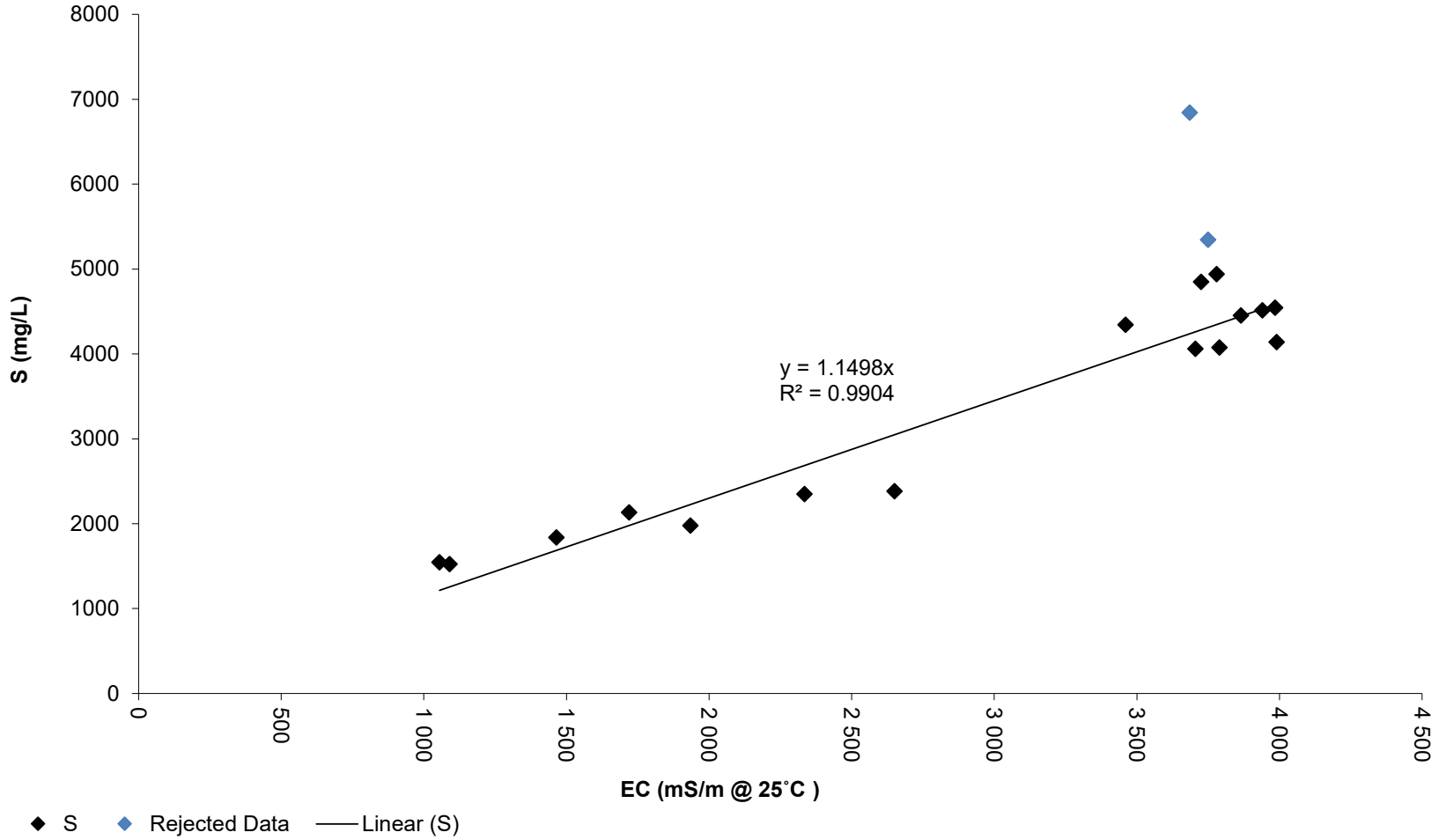
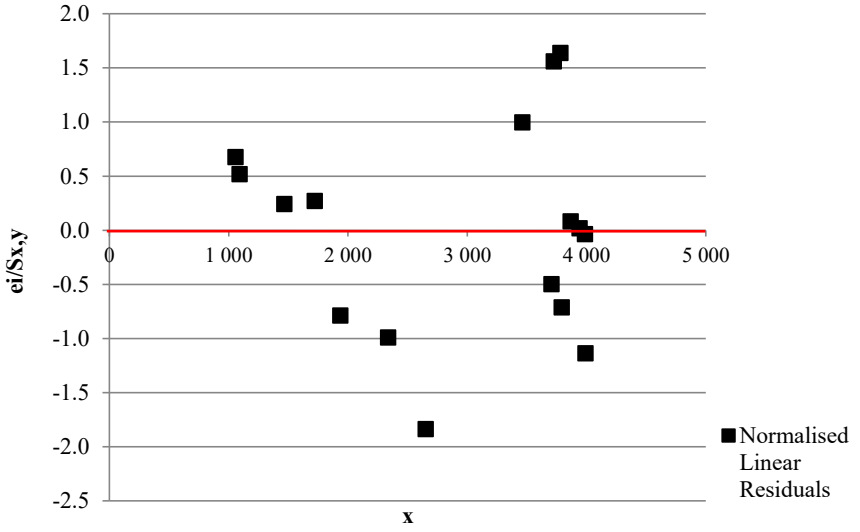


Figure F3.3. Dissolved Sulfur (S) vs Electrical Conductivity (EC) – Data pt. 2 and 4 rejected

Table F3.3. Dissolved Sulfur (S) vs Electrical Conductivity (EC) – Data pt. 2 and 4 rejected

		SUMMARY OUTPUT									
		S vs EC									
		Regression Statistics			F critical value	F.INV.RT(0,05,1,14)	4.60	*Significance F*			
		Multiple R	0.961193284			F-statistic	170	3.21E-09			
		R Square	0.923892529		**R^2 Correlation is significant**		F value > F - critical	Significance F < 0,05			
		Adjusted R Square	0.918456281		T critical value	T.INV.2T(0.05,14)	2.14	*P-value*	*Lower 95%*	*Upper 95%*	
		Standard Error	372.9038476			*t Stat*	13.04	3.21E-09	0.93	1.30	
		Observations	16		**Regression model is significant**		t Stat > t-critical	P-value < 0,05	Does not pass through zero		
		ANOVA									
			df	*SS*	*MS*	*F*	*Significance F*				
		Regression	1	23632840.62	23632840.62	169.9504024	3.20698E-09				
		Residual	14	1946801.914	139057.2796						
		Total	15	25579642.53							
			Coefficients	*Standard Error*	*t Stat*	*P-value*	*Lower 95%*	*Upper 95%*			
		Intercept	117.4171953	265.292811	0.442594712	0.664820234	-451.5792942	686.4136847			
		EC	1.114361473	0.085480094	13.03650269	3.20698E-09	0.931024906	1.29769804			

		RESIDUAL OUTPUT	Y	$e_i = Y_i - y_i$	$e_i/S_{x,y}$
			Linear	Linear	*Normalised*
EC	S	*Observation*	*Predicted S*	*Residuals*	*Normalised Linear Residuals*
3 460	4 345	1	3973.11	371.89	0.9973
2 335	2 350	2	2719.45	-369.45	-0.9907
3 725	4 850	3	4268.41	581.59	1.5596
3 780	4 940	4	4329.70	610.30	1.6366
3 940	4 515	5	4508.00	7.00	0.0188
3 865	4 455	6	4424.42	30.58	0.0820
3 985	4 545	7	4558.15	-13.15	-0.0353
2 650	2 385	8	3070.48	-685.48	-1.8382
3 790	4 075	9	4340.85	-265.85	-0.7129
3 990	4 140	10	4563.72	-423.72	-1.1363
3 705	4 060	11	4246.13	-186.13	-0.4991
1 090	1 525	12	1332.07	192.93	0.5174
1 465	1 840	13	1749.96	90.04	0.2415
1 055	1 545	14	1293.07	252.27	0.6765
1 720	2 135	15	2034.12	100.88	0.2705
1 935	1 980	16	2273.71	-293.71	-0.7876



All normalized linear residuals $e_i/Sx,y$ for all data are < 2 and standard linear residuals are consistent with neighbours – No further points to reject

F4. Dissolved Iron (Fe) vs Electrical Conductivity (EC)

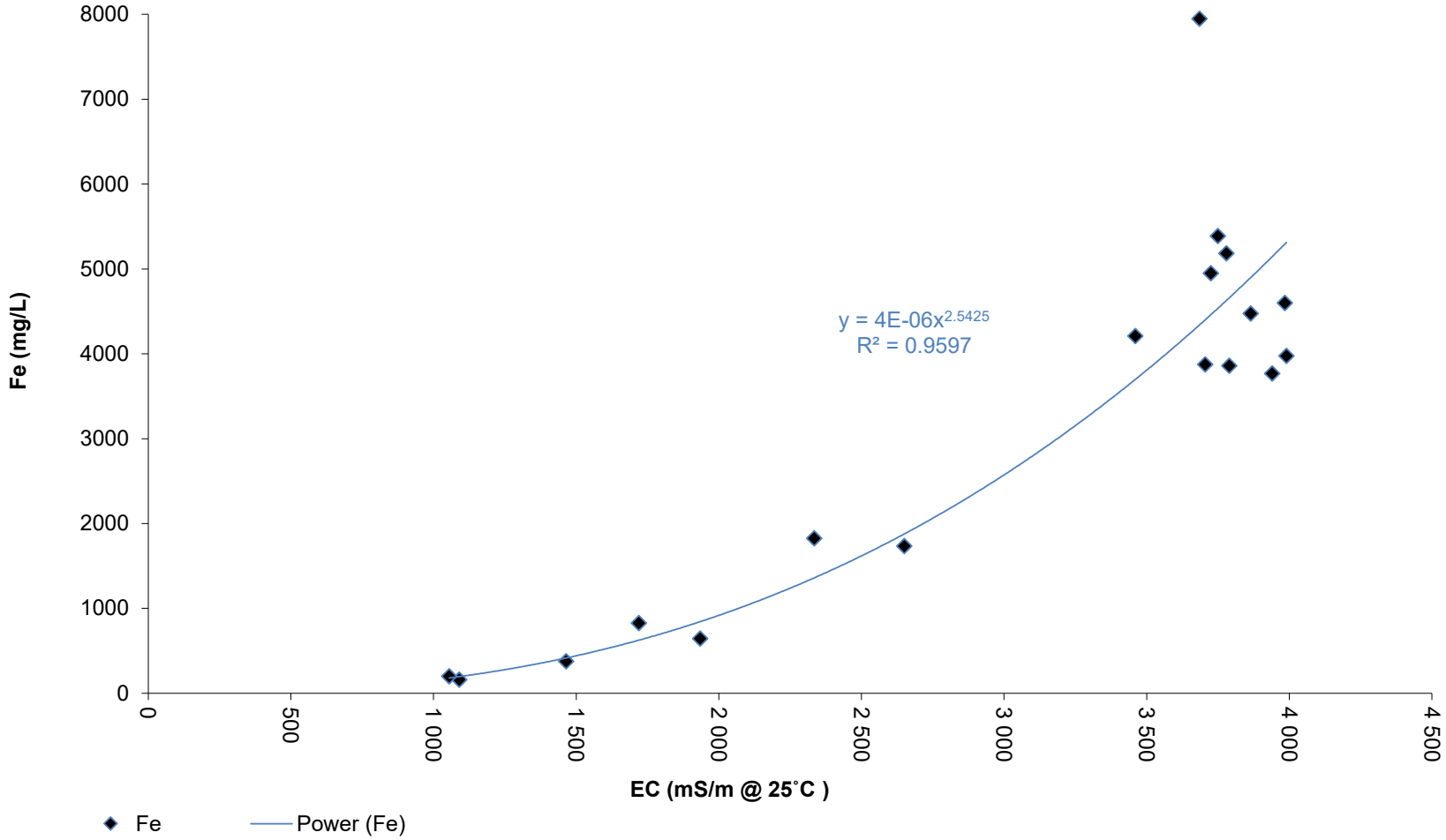
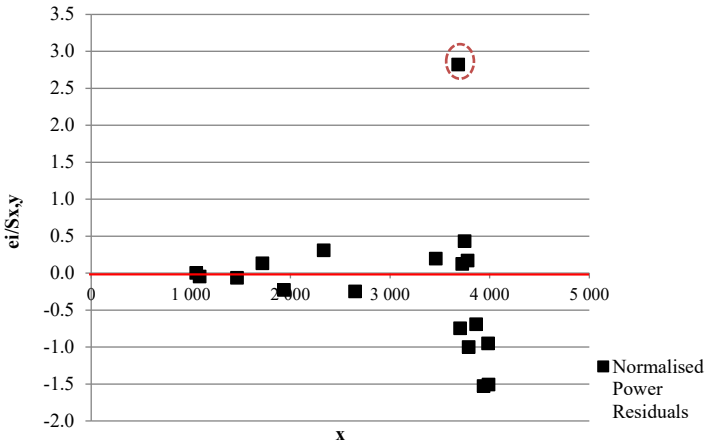


Figure F4.1. Dissolved Iron (Fe) vs Electrical Conductivity (EC) – All Data

Table F4.1. Dissolved Iron (Fe) vs Electrical Conductivity (EC)

		SUMMARY OUTPUT								
		Fe vs EC								
		Regression Statistics			F critical value	F.INV.RT(0,05,1,16)	4.49	*Significance F*		
		Multiple R	0.881112514			F-statistic	56	1.37E-06		
		R Square	0.776359262		**R^2 Correlation is significant**		F value > F - critical	Significance F < 0,05		
		Adjusted R Square	0.762381716		T critical value	T.INV.2T(0.05,16)	2.12	*P-value*	*Lower 95%*	*Upper 95%*
		Standard Error	1078.263027			*t Stat*	7.45	1.37E-06	1.28	2.30
		Observations	18		**Regression model is significant**		t Stat > t-critical	P-value < 0,05	Does not pass through zero	
		ANOVA								
			df	*SS*	*MS*	*F*	*Significance F*			
		Regression	1	64577500.61	64577500.61	55.54331608	1.37327E-06			
		Residual	16	18602418.49	1162651.155					
		Total	17	83179919.1						
			Coefficients	*Standard Error*	*t Stat*	*P-value*	*Lower 95%*	*Upper 95%*		
		Intercept	-2133.150116	762.2588428	-2.798458996	0.01288225	-3749.066676	-517.2335556		
		EC	1.787767568	0.239880614	7.45273883	1.37327E-06	1.279243383	2.296291753		

		RESIDUAL OUTPUT	$y = 0.000004x^{2.5425}$	$e_i = Y_i - y_i$	e_i^2	$e_i/S_{x,y}$
			Power	*Power*	*Power*	*Power*
EC	Fe	*Observation*	*Predicted Fe*	*Residuals*	*Residuals*	*Normalised Power Residuals*
3 460	4 210	1	3982.55	227.45	51734.61	0.1960
3 685	7 950	2	4674.42	3275.58	10729453.69	2.8223
2 335	1 825	3	1465.31	359.69	129377.18	0.3099
3 750	5 390	4	4886.91	503.09	253097.87	0.4335
3 725	4 950	5	4804.50	145.50	21169.11	0.1254
3 780	5 185	6	4986.93	198.07	39233.45	0.1707
3 940	3 770	7	5541.27	-1771.77	3139160.95	-1.5266
3 865	4 475	8	5277.01	-801.94	643101.40	-0.6910
3 985	4 600	9	5703.60	-1103.60	1217931.49	-0.9509
2 650	1 735	10	2021.45	-286.45	82052.59	-0.2468
3 790	3 860	11	5020.54	-1160.54	1346846.41	-0.9999
3 990	3 975	12	5721.81	-1746.81	3051351.91	-1.5051
3 705	3 875	13	4739.19	-864.49	747341.09	-0.7449
1 090	160	14	211.21	-51.32	2634.17	-0.0442
1 465	376	15	447.92	-71.67	5136.41	-0.0618
1055	199	16	194.39	5.07	25.66	0.0044
1 720	828	17	673.58	154.18	23772.42	0.1328
1 935	646	18	908.75	-262.72	69023.92	-0.2264
			For Power Normalised Residuals Sum ei2		**1347028**	
			Sy,x =SQURT[(ei)2/(n-2)]		**1161**	



The normalized power residual $e_i/Sx,y$ for data point 2 is > 2 and the standard power residual is not consistent with neighbours – Reject pt. 2

F4.2 Dissolved Iron (Fe) vs Electrical Conductivity (EC) – Data point 2 rejected

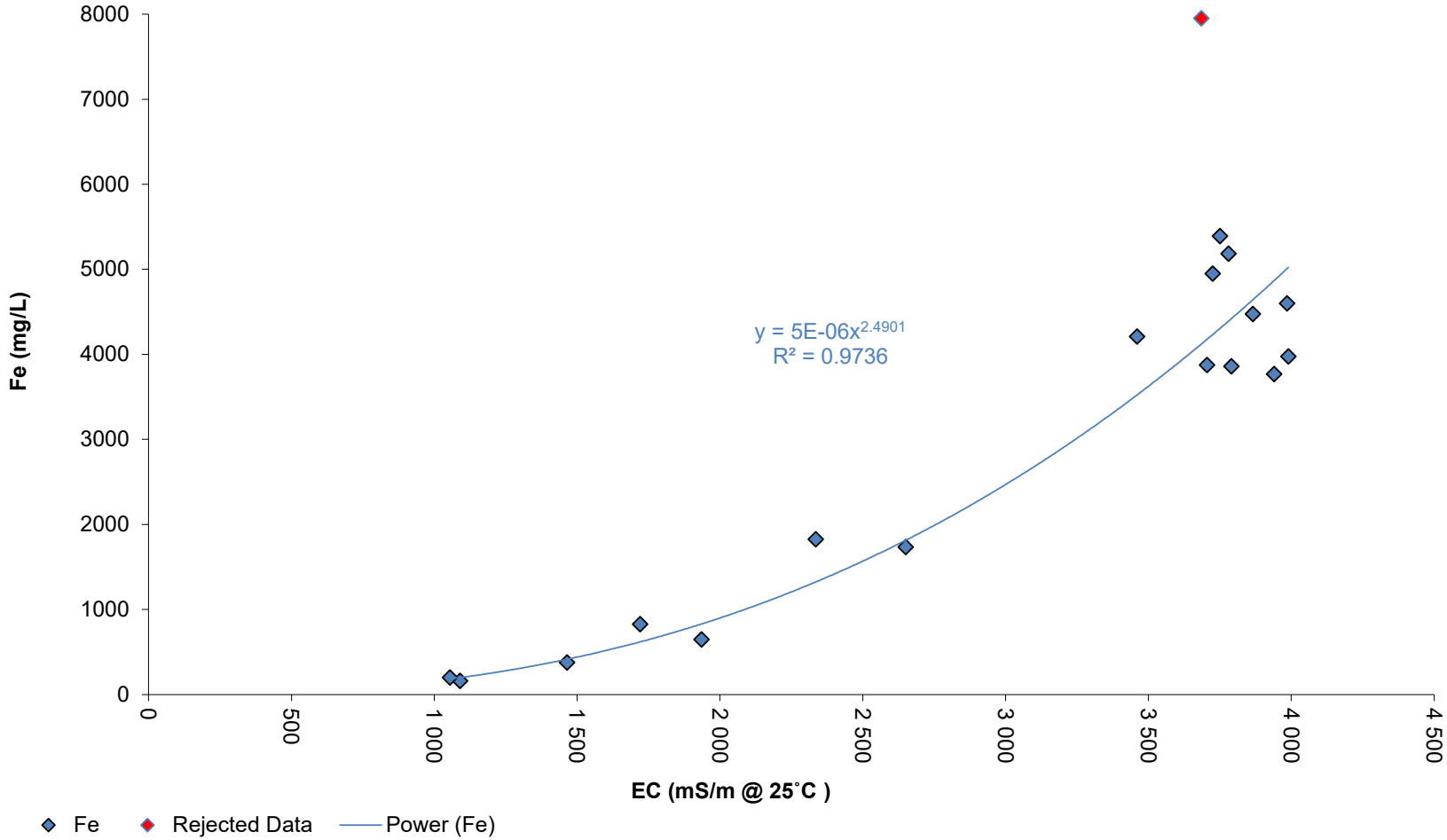
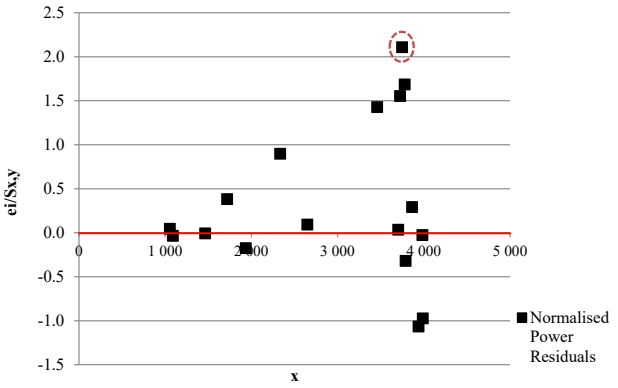


Figure F4.2. Dissolved Iron (Fe) vs Electrical Conductivity (EC) – Data point 2 rejected

Table F4.2. Dissolved Iron (Fe) vs Electrical Conductivity (EC) – Data point 2 rejected

		SUMMARY OUTPUT									
		Fe vs EC									
		Regression Statistics			F critical value	F.INV.RT(0,05,1,15)	4.54	*Significance F*			
		Multiple R	0.954111836			F-statistic	152	2.95E-09			
		R Square	0.910329396		**R^2 Correlation is significant**		F value > F - critical	Significance F < 0,05			
		Adjusted R Square	0.904351355		T critical value	T.INV.2T(0.05,15)	2.13	*P-value*	*Lower 95%*	*Upper 95%*	
		Standard Error	596.4907642			*t Stat*	12.34	2.95E-09	1.37	1.94	
		Observations	17		**Regression model is significant**		t Stat > t-critical	P-value < 0,05	Does not pass through zero		
		ANOVA									
			df	*SS*	*MS*	*F*	*Significance F*				
		Regression	1	54181020.03	54181020.03	152.2788995	2.94749E-09				
		Residual	15	5337018.476	355801.2317						
		Total	16	59518038.5							
			Coefficients	*Standard Error*	*t Stat*	*P-value*	*Lower 95%*	*Upper 95%*			
		Intercept	-1956.181728	422.6733661	-4.62811685	0.00032818	-2857.088682	-1055.274774			
		EC	1.658315155	0.134383889	12.34013369	2.94749E-09	1.371882676	1.944747634			

		RESIDUAL OUTPUT	Y	$y = 0.000005x^{2.4901}$	$e_i = Y_i - y_i$	e_i^2	$e_i/S_{x,y}$
			Linear	*Power*	*Power*	*Power*	*Power*
EC	Fe	*Observation*	*Predicted Fe*	*Predicted Fe*	*Residuals*	*Residuals*	*Normalised Power Residuals*
3 460	4 210	1	3781.59	3248.06	961.94	925337.85	1.4267
2 335	1 825	2	1915.98	1219.95	605.05	366088.41	0.8974
3 750	5 390	3	4262.50	3968.86	1421.14	2019652.29	2.1078
3 725	4 950	4	4221.04	3903.30	1046.70	1095588.13	1.5525
3 780	5 185	5	4312.25	4048.39	1136.61	1291882.47	1.6858
3 940	3 770	6	4577.58	4488.64	-719.14	517167.85	-1.0666
3 865	4 475	7	4453.21	4278.89	196.18	38487.18	0.2910
3 985	4 600	8	4652.20	4617.39	-17.39	302.42	-0.0258
2 650	1 735	9	2438.35	1671.84	63.16	3989.26	0.0937
3 790	3 860	10	4328.83	4075.11	-215.11	46272.98	-0.3190
3 990	3 975	11	4660.50	4631.83	-656.83	431425.66	-0.9742
3 705	3 875	12	4187.88	3851.32	23.38	546.65	0.0347
1 090	160	13	-148.62	183.01	-23.12	534.50	-0.0343
1 465	376	14	473.25	382.14	-5.89	34.65	-0.0087
1 055	199	15	-206.66	168.72	30.74	944.72	0.0456
1720	828	16	896.12	569.85	257.92	66521.45	0.3825
1 935	646	17	1252.66	764.07	-118.04	13933.91	-0.1751
				For Power Normalised Residuals Sum ei2		**454581**	
				Sy,x =SQURT[(ei)2/(n-2)]		**674**	



The normalized power residual $e_i/Sx,y$ for data point 4 is > 2 and the standard power residual is not consistent with neighbours – Reject pt. 2 and 4

F4.3: Dissolved Iron (Fe) vs Electrical Conductivity (EC) – Data points 2 and 4 rejected

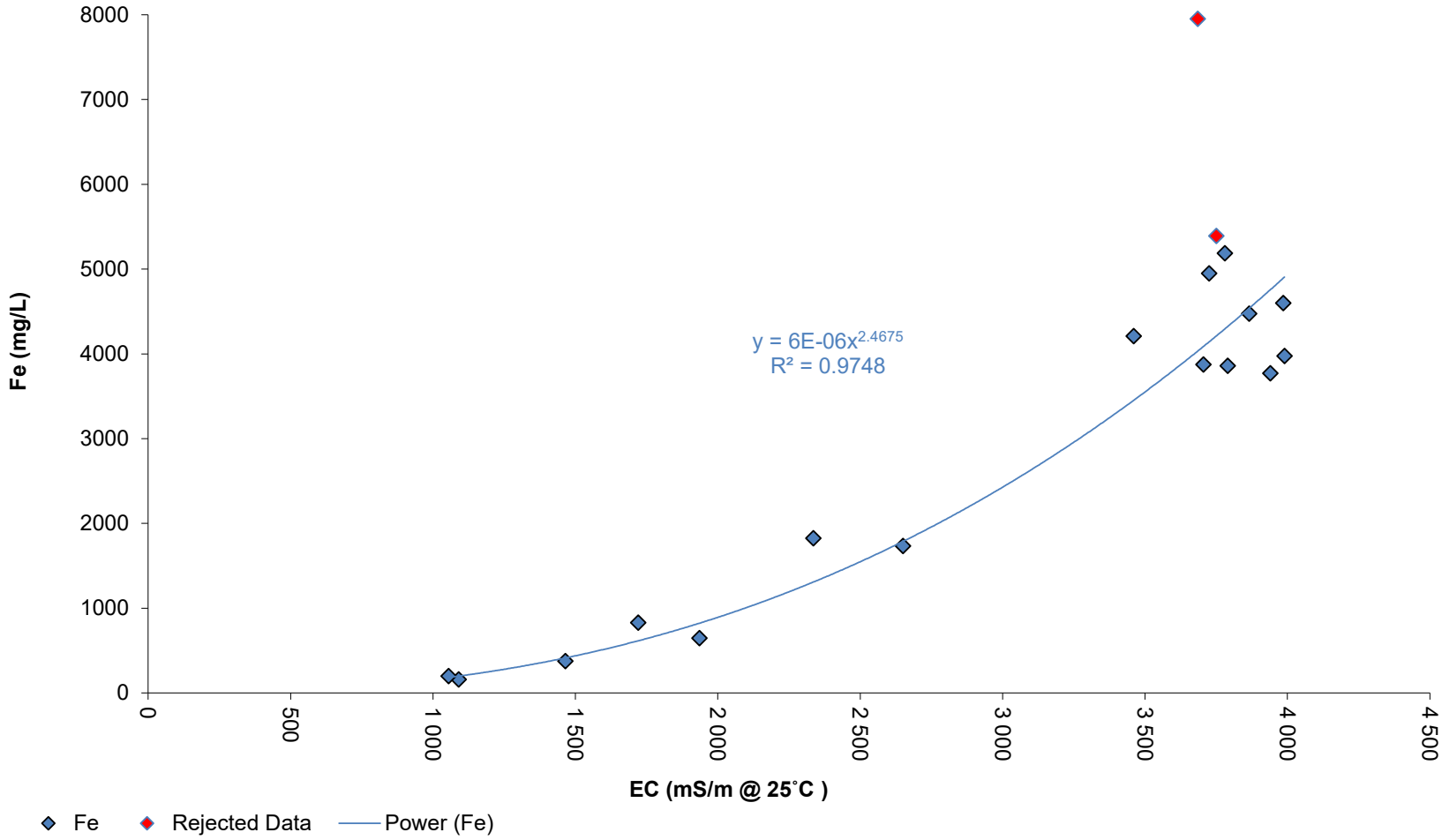


Figure F4.3. Dissolved Iron (Fe) vs Electrical Conductivity (EC) – Data points 2 and 4 rejected

Table F4.3. Dissolved Iron (Fe) vs Electrical Conductivity (EC) – Data points 2 and 4 rejected

SUMMARY OUTPUT	
Fe vs EC	
Regression Statistics	
Multiple R	0.962244819
R Square	0.925915092
Adjusted R Square	0.920623313
Standard Error	530.4097746
Observations	16

F critical value	F.INV.RT(0,05,1,14)	4.60	*Significance F*	
	F-statistic	175	2.65E-09	
R^2 Correlation is significant		F value > F - critical	Significance F < 0,05	
T critical value	T.INV.2T(0.05,14)	2.14	*P-value*	*Lower 95%*	*Upper 95%*
	t Stat	13.23	2.65E-09	1.35	1.87
Regression model is significant		t Stat > t-critical	P-value < 0,05	Does not pass through zero	

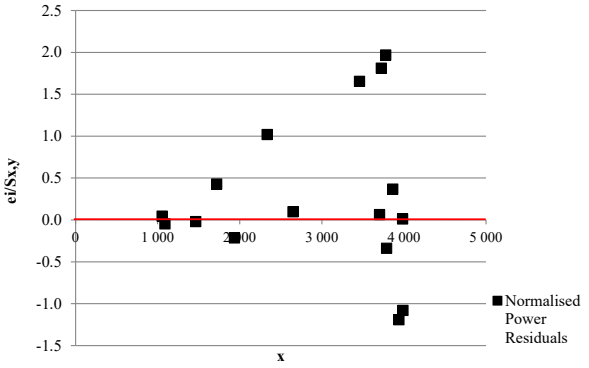
ANOVA

	df	*SS*	*MS*	*F*	*Significance F*
Regression	1	49225766.95	49225766.95	174.9723617	2.65339E-09
Residual	14	3938683.405	281334.529		
Total	15	53164450.35			

	Coefficients	*Standard Error*	*t Stat*	*P-value*	*Lower 95%*	*Upper 95%*
Intercept	-1881.296236	377.3463347	-4.985595626	0.000199784	-2690.623631	-1071.96884
EC	1.608290036	0.121584901	13.22771188	2.65339E-09	1.347516359	1.869063712

		RESIDUAL OUTPUT	Y
			Linear
EC	Fe	*Observation*	*Predicted Fe*
3 460	4 210	1	3683.39
2 335	1 825	2	1874.06
3 725	4 950	3	4109.58
3 780	5 185	4	4198.04
3 940	3 770	5	4455.37
3 865	4 475	6	4334.74
3 985	4 600	7	4527.74
2 650	1 735	8	2380.67
3 790	3 860	9	4214.12
3 990	3 975	10	4535.78
3 705	3 875	11	4077.42
1 090	160	12	-128.26
1 465	376	13	474.85
1 055	199	14	-184.55
1 720	828	15	884.96
1 935	646	16	1230.74

$y = 0.000006x^{2.4675}$	$e_i = Y_i - y_i$	e_i^2	$e_i/S_{x,y}$
Power	*Power*	*Power*	*Power*
Predicted Fe	*Residuals*	*Residuals*	*Normalised Power Residuals*
3242.06	967.94	936900.96	1.6525
1228.57	596.43	355731.33	1.0183
3889.60	1060.40	1124440.61	1.8104
4032.85	1152.15	1327445.40	1.9670
4467.23	-697.73	486825.21	-1.1912
4260.32	214.75	46115.81	0.3666
4594.18	5.82	33.86	0.0099
1678.84	56.16	3153.45	0.0959
4059.23	-199.23	39692.00	-0.3401
4608.42	-633.42	401218.45	-1.0814
3838.28	36.42	1326.73	0.0622
187.50	-27.61	762.47	-0.0471
388.92	-12.66	160.35	-0.0216
172.99	26.47	700.43	0.0452
577.85	249.91	62456.29	0.4267
772.75	-126.72	16056.84	-0.2163
For Power Normalised Residuals Sum ei2		**343073**	
Sy,x =SQURT[(ei)2/(n-2)]		**586**	



The normalized power residual $e_i/Sx,y$ for all data points are < 2 and the standard power residuals are consistent with neighbours – No further rejection

Appendix II - Supplementary data for Chapter 5

(with Figures and Tables in sub-Appendices A – D from the original published paper)

Appendix II-A:

Table A.1. Grass sample site identification and classification of grass samples collected in the Mpumalanga region

Grass Site Identification	Grass Type
G1	*Digitaria eriantha steud. (Stapf.) Koler MS, J48205*
G2	*Hyparrhenia hirta (L.) Stapf, J064238*
G3	*Eragrostis plana. Nees, J40177*
G4	*Eragrostis curvula (Schrad.) Nees, J071222*
G5	*Hyparrhenia filipendula (Hochst.) Stapf var. pilosa (Hochst.) Stapf, J075391*
G6	*Eragrostis curvula (Schrad.) Nees, J071222*
G7	*Eragrostis curvula (Schrad.) Nees, J071222*
G8	*Hyparrhenia hirta (L.) Stapf, J064238*
G9	*Hyparrhenia hirta (L.) Stapf, J064238*
G10	*Possible Hyparrhenia hirta (L.) Stapf, J064238 & Cynodon prectostachyas curly (KSchum.)Pilg, J48725*
G11	*Pogonarthria squarrosa (Licha.) Pilg C.F. Clinning No. 42*
G12	*Hyparrhenia hirta (L.) Stapf, J064238*
G13	*Hyparrhenia hirta (L.) Stapf, J064238*
G14	*Possible Hyparrhenia hirta (L.) Stapf, J064238 & Hyparrhenia filipendula (Hochst.) Stapf var. pilosa (Hochst.) Stapf, J075391*
G15	*Vetiveria zinanioldes (Linn.) Nash, and reclassified as Chrysopogon zizanioides (L.) Roberty*
G16	*Eragrostis curvula (Schrad.) Nees, J071222*

Table A.2. Data for structural analysis of grass including extractives, lignin, cellulose, hemicellulose, and ash content

Grass Site Identification	Grass Classification	Extractives (%)	Acid Soluble Lignin (%)	Acid insoluble Lignin (%)	Lignin (%)	Cellulose (%)	Hemicellulose (%)
G1	*Digitaria eriantha*	4.93 ± 1.33	1.15 ± 0.16	17.8 ± 1.53	18.96	36.6 ± 3.10	23.3 ± 1.87
G2	*Hyparrhenia hirta*	2.60 ± 1.02	1.01 ± 0.03	17.1 ± 0.39	18.09	32.8 ± 1.65	22.4 ± 2.71
G3	*Eragrostis plana*	3.79± 0.95	1.71 ± 0.06	16.3 ± 0.58	17.96	25.7 ± 3.46	22.2 ± 2.48
G4	*Eragrostis curvula*	3.47± 1.43	1.31 ± 0.07	19.2 ± 0.23	20.48	33.3 ± 2.62	28.3 ± 2.68
G5	*Hyparrhenia filipendula*	2.65 ± 0.38	1.15 ± 0.07	17.6 ± 0.74	18.74	34.6 ± 5.56	20.9 ± 0.92
G6	*Eragrostis curvula*	4.57 ± 1.37	1.10 ± 0.12	16.7 ± 0.85	17.75	34.9 ± 3.98	21.9 ± 0.81
G7	*Eragrostis curvula*	2.06 ± 0.79	1.49 ± 0.19	19.7 ± 4.61	21.20	33.4 ± 4.87	24.7 ± 3.58
G8	*Hyparrhenia hirta*	3.91 ± 2.83	1.34 ± 0.18	23.4 ± 5.05	24.71	28.4 ± 4.32	23.0 ± 1.71
G9	*Hyparrhenia hirta*	4.17 ± 2.51	1.27 ± 0.05	18.0 ± 0.55	19.25	31.4 ± 3.80	21.4 ± 0.92
G10	*Hyparrhenia hirta / Cynodon prectostachyas curly*	5.42 ± 2.31	1.55 ± 0.17	18.9 ± 2.75	20.49	31.6 ± 6.16	20.9 ± 1.05
G11	*Pogonarthria squarrosa*	5.16 ± 1.12	1.69 ± 0.10	20.9 ± 3.94	22.55	28.2 ± 4.78	22.3 ± 0.80
G12	*Hyparrhenia hirta*	5.46 ± 2.80	1.41 ± 0.04	17.8 ± 0.63	19.24	29.4 ± 4.46	21.4 ± 0.81
G13	*Hyparrhenia hirta*	6.05 ± 3.22	1.66 ± 0.18	17.7 ± 0.59	19.33	28.6 ± 1.18	23.3 ± 2.59
G14	*Hyparrhenia hirta / Hyparrhenia filipendula*	5.16 ± 0.93	1.74 ± 0.12	16.6 ± 0.61	18.30	22.5 ± 0.71	25.2 ± 4.04
G15	*Chrysopogon zizanioides*	4.80 ± 2.01	1.26 ± 0.14	17.5 ± 0.49	18.80	32.6 ± 2.81	25.2 ± 2.38
G16	*Eragrostis curvula*	5.97 ± 2.01	2.01 ± 0.19	15.5 ± 0.38	17.53	30.3 ± 4.18	23.0 ± 2.54

Table A.3. Data for Proximate analysis of grass including extractives, lignin, cellulose, hemicellulose, ash content and calorific value

Grass Site Identification	Grass Classification	Moisture (%)	Volatile Matter (%)	Fixed Carbon (%)	Ash Content TGA (%)	Average CV (MJ/kg)
G1	*Digitaria eriantha*	2.92 ± 1.59	79.6 ± 2.81	16.2 ± 0.94	1.25 ± 0.28	17.6 ± 0.22
G2	*Hyparrhenia hirta*	3.83 ± 0.32	77.5 ± 0.55	16.2 ± 1.78	2.40 ± 1.55	17.7 ± 0.76
G3	*Eragrostis plana*	3.81 ± 0.28	76.2 ± 0.66	15.1 ± 1.27	4.83 ± 0.34	16.8 ± 0.08
G4	*Eragrostis curvula*	4.07 ± 0.41	71.3 ± 1.53	17.0 ± 1.68	7.61 ± 0.56	16.7 ± 0.77
G5	*Hyparrhenia filipendula*	2.65 ± 0.28	76.8 ± 1.62	18.5 ± 1.35	2.07 ± 0.01	17.5 ± 0.23
G6	*Eragrostis curvula*	2.73 ± 0.24	76.3 ± 1.06	16.6 ± 1.32	4.38 ± 0.50	17.5 ± 1.36
G7	*Eragrostis curvula*	2.27 ± 1.42	81.3 ± 0.73	17.3 ± 1.59	0.35 ± 0.50	18.2 ± 1.36
G8	*Hyparrhenia hirta*	3.92 ± 0.06	76.4 ± 1.73	16.5 ± 1.73	3.11 ± 0.05	17.0 ± 0.06
G9	*Hyparrhenia hirta*	3.33 ± 0.24	74.3 ± 2.26	17.9 ± 1.47	4.57 ± 0.54	17.4 ± 0.18
G10	*Hyparrhenia hirta / Cynodon prectostachyas curly*	3.02 ± 0.37	75.6 ± 2.39	17.1 ± 2.07	4.28 ± 0.05	17.2 ± 0.03
G11	*Pogonarthria squarrosa*	4.01 ± 0.67	77.7 ± 0.66	15.3 ± 1.78	3.02 ± 0.45	17.3 ± 0.09
G12	*Hyparrhenia hirta*	2.88 ± 0.39	74.1 ± 2.05	16.3 ± 1.87	6.79 ± 0.21	16.8 ± 0.22
G13	*Hyparrhenia hirta*	2.93 ± 0.05	72.4 ± 2.59	17.0 ± 2.47	7.71 ± 0.16	16.7 ± 0.23
G14	*Hyparrhenia hirta / Hyparrhenia filipendula*	3.67 ± 0.63	58.9 ± 2.25	14.8 ± 1.53	22.60 ± *0.10*	13.7 ± 0.05
G15	*Chrysopogon zizanioides*	3.54 ± 0.15	75.6 ± 0.03	19.1 ± 1.61	1.75 ± 1.50	17.0 ± 0.10
G16	*Eragrostis curvula*	2.48 ± 1.29	80.9 ± 2.54	17.2 ± 0.75	0.00 ± 0.00	19.3 ± 0.04

Table A.4. Data for Ultimate analysis of grass including total carbon, hydrogen, nitrogen, total sulfur, and oxygen content

Grass Site Identification	Grass Classification	Total Carbon (%)	Hydrogen (%)	Nitrogen (%)	Total Sulfur (%)	Oxygen - calculated (%)
G1	Digitaria eriantha	44.6	6.35	0.11	0.23	48.8
G2	Hyparrhenia hirta	42.8	6.1	0.0	0.3	50.9
G3	Eragrostis plana	41.8	6.1	0.5	0.4	51.2
G4	Eragrostis curvula	39.8	5.7	0.5	0.3	53.8
G5	Hyparrhenia filipendula	41.8 ± 0.85	5.79 ± 0.11	0.38 *± 0.0*	0.13 ± 0.01	52.3
G6	Eragrostis curvula	41.7	5.8	0.0	0.1	52.3
G7	Eragrostis curvula	47.4	6.6	0.2	0.2	45.7
G8	Hyparrhenia hirta	39.8	5.7	0.3	0.2	54.0
G9	Hyparrhenia hirta	42.4	5.9	0.4	0.1	51.2
G10	Hyparrhenia hirta / Cynodon prectostachyas curly	41.3	5.7	0.0	0.1	52.8
G11	Pogonarthria squarrosa	39.9	5.7	0.3	0.2	53.9
G12	Hyparrhenia hirta	39.5	5.5	0.3	0.2	54.5
G13	Hyparrhenia hirta	38.2	5.5	1.0	0.5	54.8
G14	Hyparrhenia hirta / Hyparrhenia filipendula	32.6 ± 1.07	5.01 ± 0.07	0.69 ± 0.07	0.23 ± 0.01	61.5
G15	Chrysopogon zizanioides	41.1	5.7	0.5	0.1	52.5
G16	Eragrostis curvula	44.7	6.2	0.7	0.1	48.2

Appendix II-B

Table B.1. pH data for single grass addition test work to establish the suitability of grass for AMD remediation

Grass Site Identification	Grass Classification	Original pH	Day 1	Day 2	Day 3	Day 4	Day 5	Day 6	Day 7	Day 8
G9 – Synthetic	*Hyparrhenia hirta*	3.50	4.02	4.08	4.01	3.97	3.65	—	—	3.83
G13 Synthetic	*Hyparrhenia hirta*	3.50	4.42	4.58	4.34	4.26	4.05	—	—	4.19
G11 – Synthetic	*Pogonarthria squarrosa*	3.50	3.80	3.91	3.76	3.68	3.46	—	—	3.51
G12 – Synthetic	*Hyparrhenia hirta*	3.50	4.76	4.45	4.61	4.44	4.64	—	—	5.38
G6 – Synthetic	*Eragrostis curvula*	3.50	4.02	4.03	3.83	3.68	3.53	—	—	3.58
G10 – Synthetic	*Possible Hyparrhenia hirta & Cynodon prectostachyas curly*	3.50	3.97	4.03	3.76	3.67	3.51	—	—	3.58
G13 (2) – Synthetic	*Hyparrhenia hirta*	3.50	4.69	4.66	4.40	4.42	4.86	—	—	5.52
G5 – Synthetic	*Hyparrhenia filipendula*	3.50	4.30	4.33	4.15	4.08	3.78	—	—	3.85
G7 – Synthetic	*Eragrostis curvula*	3.50	4.02	4.06	3.92	3.84	3.63	—	—	3.66
G8 – Synthetic	*Hyparrhenia hirta*	3.50	4.14	4.28	4.02	3.85	3.64	—	—	3.75
G4 – Synthetic	*Eragrostis curvula*	3.50	3.96	4.19	3.97	3.96	3.74	—	—	3.89
G15 – Synthetic	*Chrysopogon zizanioides*	3.50	4.84	5.04	4.71	4.65	4.93	—	—	5.45
G15 – RD	*Chrysopogon zizanioides*	2.20	2.30	2.37	2.29	2.23	2.04	—	—	2.07
G6 – RD	*Hyparrhenia hirta*	2.20	2.21	2.33	2.26	2.19	1.99	—	—	1.92
Blank – Synthetic	*Blank – No grass*	3.50	3.50	3.41	3.36	3.33	3.04	—	—	2.98
Blank – RD	*Blank – No grass*	2.20	2.20	2.3	2.3	2.27	2.06	—	—	2.15

Table B.2. Oxidation-reduction potential data for single grass addition testwork to establish the suitability of grass for AMD remediation

Grass Site Identification	Grass Classification	Original ORP (mV)	Day 1 (mV)	Day 2 (mV)	Day 3 (mV)	Day 4 (mV)	Day 5 (mV)	Day 6 (mV)	Day 7 (mV)	Day 8 (mV)
G9 – Synthetic	*Hyparrhenia hirta*	224	104	109	125	145	158	—	—	158
G13 – Synthetic	*Hyparrhenia hirta*	224	96	87	107	130	139	—	—	132
G11 – Synthetic	*Pogonarthria squarrosa*	224	165	169	178	198	203	—	—	207
G12 – Synthetic	*Hyparrhenia hirta*	224	37	54	70	104	-48	—	—	6
G6 – Synthetic	*Eragrostis curvula*	224	146	161	181	196	206	—	—	202
G10 – Synthetic	*Possible Hyparrhenia hirta & Cynodon prectostachyas curly*	224	150	163	178	193	197	—	—	186
G13 (2) – Synthetic	*Hyparrhenia hirta*	224	85	79	123	103	-40	—	—	-163
G5 – Synthetic	*Hyparrhenia filipendula*	224	107	115	132	151	174	—	—	171
G7 – Synthetic	*Eragrostis curvula*	224	102	112	134	147	154	—	—	152
G8 – Synthetic	*Hyparrhenia hirta*	224	96	105	120	138	157	—	—	159
G4 – Synthetic	*Eragrostis curvula*	224	137	147	158	171	177	—	—	161
G15 – Synthetic	*Chrysopogon zizanioides*	224	-15	9	33	63	-318	—	—	-235
G15 – RD	*Chrysopogon zizanioides*	491	476	476	473	474	472	—	—	468
G6 – RD	*Hyparrhenia hirta*	491	470	480	478	478	477	—	—	471
Blank – Synthetic	*Blank – No grass*	224	224	258	265	290	288	—	—	318
Blank – Plant	*Blank – No grass*	491	491	493	497	503	512	—	—	590

Table B3. Dissolved oxygen data for single grass addition test work to establish the suitability of grass for AMD remediation

Grass Site Identification	Grass Classification	Original DO	Day 1	Day 2 (%)	Day 3 (%)	Day 4 (%)	Day 5 (%)	Day 6 (%)	Day 7 (%)	Day 8 (%)
G9 – Synthetic	*Hyparrhenia hirta*	—	—	21.9	11.0	18.2	20.0	—	—	22.0
G13 – Synthetic	*Hyparrhenia hirta*	—	—	7.2	13.2	16.8	8.5	—	—	10.0
G11 – Synthetic	*Pogonarthria squarrosa*	—	—	21.1	20.3	23.4	15.2	—	—	3.3
G12 – Synthetic	*Hyparrhenia hirta*	—	—	34.1	12.8	14.8	8.9	—	—	52.1
G6 – Synthetic	*Eragrostis curvula*	—	—	22.5	16.9	18.7	28.1	—	—	18.7
G10 – Synthetic	*Possible Hyparrhenia hirta & Cynodon prectostachyas curly*	—	—	11.7	9.2	21.2	10.2	—	—	7.6
G13 (2) – Synthetic	*Hyparrhenia hirta*	—	—	64.6	55.1	56.6	12.8	—	—	5.3
G5 – Synthetic	*Hyparrhenia filipendula*	—	—	9.4	27.0	18.7	28.0	—	—	22.4
G7 – Synthetic	*Eragrostis curvula*	—	—	53.2	39.8	14.9	12.7	—	—	13.2
G8 – Synthetic	*Hyparrhenia hirta*	—	—	28.3	25.3	19.3	23.3	—	—	6.7
G4 – Synthetic	*Eragrostis curvula*	—	—	9.9	34.3	23.0	38.2	—	—	17.8
G15 – Synthetic	*Chrysopogon zizanioides*	—	—	12.1	6.8	9.3	0.0	—	—	0.4
G15 – RD	*Chrysopogon zizanioides*	—	—	24.3	25.4	27.0	35.5	—	—	53.0
G6 – RD	*Hyparrhenia hirta*	—	—	56.7	66.7	64.2	57.3	—	—	61.1
Blank – Synthetic	*Blank – No grass*	—	—	64.5	64.8	65.2	69.9	—	—	68.5
Blank – Plant	*Blank – No grass*	—	—	61.5	16.6	15.6	16.4	—	—	46.4

Table B.4. Hydrogen ion (H+) data for single grass addition testwork to establish the suitability of grass for AMD remediation

Grass Site Identification	Grass Classification	Original H+ (mmol/L)	Day 1	Day 2	Day 3	Day 4	Day 5	Day 6	Day 7	Day 8
G9 – Synthetic	*Hyparrhenia hirta*	0.32	0.10	0.08	0.10	0.11	0.22	—	—	0.15
G13 – Synthetic	*Hyparrhenia hirta*	0.32	0.04	0.03	0.05	0.05	0.09	—	—	0.06
G11 – Synthetic	*Pogonarthria squarrosa*	0.32	0.16	0.12	0.17	0.21	0.35	—	—	0.31
G12 – Synthetic	*Hyparrhenia hirta*	0.32	0.02	0.04	0.02	0.04	0.02	—	—	0.00
G6 – Synthetic	*Eragrostis curvula*	0.32	0.10	0.09	0.15	0.21	0.30	—	—	0.26
G10 – Synthetic	*Possible Hyparrhenia hirta & Cynodon prectostachyas curly*	0.32	0.11	0.09	0.17	0.21	0.31	—	—	0.26
G13 (2) – Synthetic	*Hyparrhenia hirta*	0.32	0.02	0.02	0.04	0.04	0.01	—	—	0.00
G5 – Synthetic	*Hyparrhenia filipendula*	0.32	0.05	0.05	0.07	0.08	0.17	—	—	0.14
G7 – Synthetic	*Eragrostis curvula*	0.32	0.10	0.09	0.12	0.14	0.23	—	—	0.22
G8 – Synthetic	*Hyparrhenia hirta*	0.32	0.07	0.05	0.10	0.14	0.23	—	—	0.18
G4 – Synthetic	*Eragrostis curvula*	0.32	0.11	0.06	0.11	0.11	0.18	—	—	0.13
G15 – Synthetic	*Chrysopogon zizanioides*	0.32	0.01	0.01	0.02	0.02	0.01	—	—	0.00
G15 – RD	*Chrysopogon zizanioides*	6.31	5.01	4.27	5.13	5.89	9.12	—	—	8.51
G6 – RD	*Hyparrhenia hirta*	6.31	6.17	4.68	5.50	6.46	10.23	—	—	12.02
Blank – Synthetic	*Blank – No grass*	0.32	0.32	0.39	0.44	0.47	0.91	—	—	1.05
Blank – RD	*Blank – No grass*	6.31	6.31	5.01	5.01	5.37	8.71	—	—	7.08

Table B.5. Percentage change in hydrogen ion concentration (H+) between days for single grass addition testwork

Grass Site Identification	Grass Classification	% initial change in H^+ (Day 0-1)	% change in H^+ (Day 1-2)	% change in H^+ (Day 2-3)	% change in H^+ (Day 3-4)	% change in H^+ (Day 4-5)	% change in H^+ (Day 5-8)
G9 – Synthetic	*Hyparrhenia hirta*	-69.8	-12.9	17.5	9.6	108.9	-33.9
G13 – Synthetic	*Hyparrhenia hirta*	-88.0	-30.8	73.8	20.2	62.2	-27.6
G11 – Synthetic	*Pogonarthria squarrosa*	-49.9	-22.4	41.3	20.2	66.0	-10.9
G12 – Synthetic	*Hyparrhenia hirta*	-94.5	104	-30.8	47.9	-36.9	-81.8
G6 – Synthetic	*Eragrostis curvula*	-69.8	-2.3	58.5	41.3	41.3	-10.9
G10 – Synthetic	*Possible Hyparrhenia hirta & Cynodon prectostachyas curly*	-66.1	-12.9	86.2	23.0	44.5	-14.9
G13 (2) – Synthetic	*Hyparrhenia hirta*	-93.5	7.2	82.0	-4.5	-63.7	-78.1
G5 – Synthetic	*Hyparrhenia filipendula*	-84.2	-6.7	51.4	17.5	99.5	-14.9
G7 – Synthetic	*Eragrostis curvula*	-69.8	-8.8	38.0	20.2	62.2	-6.7
G8 – Synthetic	*Hyparrhenia hirta*	-77.1	-27.6	82.0	47.9	62.2	-22.4
G4 – Synthetic	*Eragrostis curvula*	-65.3	-41.1	66.0	2.3	66.0	-29.2
G15 – Synthetic	*Chrysopogon zizanioides*	-95.4	-36.9	113.8	14.8	-47.5	-69.8
G15 – RD	*Chrysopogon zizanioides*	-20.6	-14.9	20.2	14.8	54.9	-6.7
G6 – RD	*Hyparrhenia hirta*	-2.3	-24.1	17.5	17.5	58.5	17.5
Blank – Synthetic	*Blank – No grass*	0.0	23.0	12.2	7.2	95.0	14.8
Blank – RD	*Blank – No grass*	0.0	-20.6	0.0	7.2	62.2	-18.7

Table B.6. Percentage change in hydrogen ion concentration (H+) compared with initial H+ concentration for single grass addition testwork

Grass Site Identification	Grass Classification	% initial change in H^+ (Day 0-1)	% change in H^+ (Day 0-2)	% change in H^+ (Day 0-3)	% change in H^+ (Day 0-4)	% change in H^+ (Day 0-5)	% change in H^+ (Day 0-8)
G9 – Synthetic	*Hyparrhenia hirta*	-69.8	-73.7	-69.1	-66.1	-29.2	-53.2
G13 – Synthetic	*Hyparrhenia hirta*	-88.0	-91.7	-85.5	-82.6	-71.8	-79.6
G11 – Synthetic	*Pogonarthria squarrosa*	-49.9	-61.1	-45.0	-33.9	9.6	-2.3
G12 – Synthetic	*Hyparrhenia hirta*	-94.5	-88.8	-92.2	-88.5	-92.8	-98.7
G6 – Synthetic	*Eragrostis curvula*	-69.8	-70.5	-53.2	-33.9	-6.7	-16.8
G10 – Synthetic	*Possible Hyparrhenia hirta & Cynodon prectostachyas curly*	-66.1	-70.5	-45.0	-32.4	-2.3	-16.8
G13 (2) – Synthetic	*Hyparrhenia hirta*	-93.5	-93.1	-87.4	-88.0	-95.6	-99.0
G5 – Synthetic	*Hyparrhenia filipendula*	-84.2	-85.2	-77.6	-73.7	-47.5	-55.3
G7 – Synthetic	*Eragrostis curvula*	-69.8	-72.5	-62.0	-54.3	-25.9	-30.8
G8 – Synthetic	*Hyparrhenia hirta*	-77.1	-83.4	-69.8	-55.3	-27.6	-43.8
G4 – Synthetic	*Eragrostis curvula*	-65.3	-79.6	-66.1	-65.3	-42.5	-59.3
G15 – Synthetic	*Chrysopogon zizanioides*	-95.4	-97.1	-93.8	-92.9	-96.3	-98.9
G15 – RD	*Chrysopogon zizanioides*	-20.6	-32.4	-18.7	-6.7	44.5	34.9
G6 – RD	*Hyparrhenia hirta*	-2.3	-25.9	-12.9	2.3	62.2	90.5
Blank – Synthetic	*Blank – No grass*	0.0	23.0	38.0	47.9	188.4	231.1
Blank – RD	*Blank – No grass*	0.0	-20.6	-20.6	-14.9	38.0	12.2

Appendix II-C

Table C.1. pH data for multiple grass addition test work to establish whether incremental addition of fresh grass significantly affected the change in pH of the AMD

Grass Site Identification	Grass Classification	Day 0 Original pH	Day 1 After 1st grass addition	Day 3	Day 4 After 2nd grass addition	Day 7	Day 7.5 After 3rd grass addition	Day 8	Day 9	Day 10 1 day after 3rd grass removal
G6 – RD	*Eragrostis curvula*	1.98	1.95	1.93	2.21	2.23	2.18	2.20	2.20	2.14
G6 – Synthetic	*Eragrostis curvula*	2.93	3.19	3.22	3.50	3.58	3.87	3.85	3.80	3.75
G13 (2) – RD	*Hyparrhenia hirta*	1.98	1.97	1.99	2.25	2.29	2.29	2.29	2.26	2.23
G13 (2) – Synthetic	*Hyparrhenia hirta*	2.93	3.77	3.92	4.13	4.49	4.86	4.87	4.69	4.68
G15 – RD	*Chrysopogon zizanioides*	1.98	1.97	1.92	2.23	2.30	2.28	2.30	2.28	2.19
G15 – Synthetic	*Chrysopogon zizanioides*	2.93	4.07	4.10	4.28	4.48	4.65	4.59	4.51	4.33
G12 – RD	*Hyparrhenia hirta*	1.98	1.97	1.96	2.25	2.35	2.30	2.28	2.32	2.28
G12 – Synthetic	*Hyparrhenia hirta*	2.93	3.92	3.78	4.09	4.31	4.51	4.39	4.45	4.40
G5 – RD	*Hyparrhenia filipendula*	1.98	1.99	1.93	2.20	2.26	2.28	2.24	2.19	2.15
G5 – Synthetic	*Hyparrhenia filipendula*	2.93	3.36	3.36	3.58	3.76	4.14	4.10	4.07	3.83
G13 – RD	*Hyparrhenia hirta*	1.98	1.99	1.99	2.24	2.26	2.29	2.28	2.28	2.14
G13 – Synthetic	*Hyparrhenia hirta*	2.93	3.67	3.73	4.02	4.46	4.70	4.57	4.66	4.66
Blank – RD	*Blank – No grass*	1.98	1.98	1.94	2.25	2.28	2.31	2.30	2.29	2.22
Blank – Synthetic	*Blank – No grass*	2.93	2.93	2.84	3.12	3.10	3.05	3.04	3.00	2.87

Table C.2. Oxidation-reduction potential data for multiple grass addition test work to establish whether incremental addition of fresh grass significantly affected the change in pH of the AMD

Grass Site Identification	Grass Classification	Day 0 Original ORP (mV)	Day 1 After 1st grass addition	Day 3	Day 4 After 2nd grass addition	Day 7	Day 7.5 After 3rd grass addition	Day 8	Day 9	Day 10 1 day after 3rd grass removal
G6 – RD	*Eragrostis curvula*	489	492	486	490	483	482	476	476	476
G6 – Synthetic	*Eragrostis curvula*	321	304	254	262	243	154	183	187	193
G13 (2) – RD	*Hyparrhenia hirta*	489	492	488	493	484	483	479	480	480
G13 (2) – Synthetic	*Hyparrhenia hirta*	321	165	188	228	164	138	152	158	164
G15 – RD	*Chrysopogon zizanioides*	489	490	481	485	475	469	463	460	460
G15 – Synthetic	*Chrysopogon zizanioides*	321	111	118	150	101	72	83	109	143
G12 – RD	*Hyparrhenia hirta*	489	491	483	485	474	467	461	458	457
G12 – Synthetic	*Hyparrhenia hirta*	321	161	147	163	133	100	100	108	156
G5 – RD	*Hyparrhenia filipendula*	489		487	491	480	477	471	470	473
G5 – Synthetic	*Hyparrhenia filipendula*	321	193	223	248	195	130	133	196	191
G13 – RD	*Hyparrhenia hirta*	489	491	481	492	481	475	475	473	474
G13 – Synthetic	*Hyparrhenia hirta*	321	154	181	219	131	102	133	146	149
Blank – RD	*Blank – No grass*	489	489	498	509	243	469	533	473	580
Blank – Synthetic	*Blank – No grass*	321	321	311	312	321	477	323	337	353

Table C.3. DO data for multiple grass addition test work to establish whether incremental addition of fresh grass significantly affected the change in pH of the AMD

Grass Site Identification	Grass Classification	Day 0 Original DO (%)	Day 1 After 1st grass addition	Day 3	Day 4 After 2nd grass addition	Day 7	Day 7.5 After 3rd grass addition	Day 8	Day 9	Day 10 1 day after 3rd grass removal
G6 – RD	*Eragrostis curvula*	28.7	79.8	60.7	67.3	66.4	73.7	55.1	5.31	74.2
G6 – Synthetic	*Eragrostis curvula*	72.9	78.6	57.8	50	41.5	66.4	15.0	0.83	4.6
G13 (2) – RD	*Hyparrhenia hirta*	28.7	71.8	55.9	67.4	64	76.8	71.5	3.89	12
G13 (2) – Synthetic	*Hyparrhenia hirta*	72.9	72.1	64.5	52.3	61.1	64.2	19.5	0.86	13
G15 – RD	*Chrysopogon zizanioides*	28.7	76.3	62.5	51.6	60.5	64	42.5	3.24	65.8
G15 – Synthetic	*Chrysopogon zizanioides*	72.9	65.1	17.6	15.2	7.7	17.1	12.1	0.35	10.7
G12 – RD	*Hyparrhenia hirta*	28.7	80.7	58.1	66.7	68.3	74	64.1	4.45	72.6
G12 – Synthetic	*Hyparrhenia hirta*	72.9	73.2	40.8	37.1	33.4	50.1	15.8	0.19	12.9
G5 – RD	*Hyparrhenia filipendula*	28.7	76.8	66.9	67.1	62.7	77.6	71.8	4.41	73.7
G5 – Synthetic	*Hyparrhenia filipendula*	72.9	82.5	58.6	55.3	18.5	69.7	21.4	0.51	8.7
G13 – RD	*Hyparrhenia hirta*	28.7	74.9	70.7	67.7	68.7	74.2	65.8	4.93	77.2
G13 – Synthetic	*Hyparrhenia hirta*	72.9	75.8	20.1	62.9	4.5	68.9	10.9	0.61	5.3
Blank – RD	*Blank – No grass*	28.7	28.7	19.2	10.1	10.2	20.5	8.9	2	47.5
Blank – Synthetic	*Blank – No grass*	72.9	72.9	73.2	69.6	64.9	71	64.5	3.85	49.5

Table C.4. Hydrogen ion (H^+) data for multiple grass addition test work to establish whether incremental addition of fresh grass significantly affected the change in pH of the AMD

Grass Site Identification	Grass Classification	Day 0 Original H^+ (mmol/L)	Day 1 After 1st grass addition	Day 3	Day 4 After 2nd grass addition	Day 7	Day 7.5 After 3rd grass addition	Day 8	Day 9	Day 10 1 day after 3rd grass removal
G6 – RD	*Eragrostis curvula*	10.47	11.22	11.75	6.17	5.89	6.61	6.31	6.31	7.24
G6 – Synthetic	*Eragrostis curvula*	1.17	0.65	0.60	0.32	0.26	0.13	0.14	0.16	0.18
G13 (2) – RD	*Hyparrhenia hirta*	10.47	10.72	10.23	5.62	5.13	5.13	5.13	5.50	5.89
G13 (2) – Synthetic	*Hyparrhenia hirta*	1.17	0.17	0.12	0.07	0.03	0.01	0.01	0.02	0.02
G15 – RD	*Chrysopogon zizanioides*	10.47	10.72	12.02	5.89	5.01	5.25	5.01	5.25	6.46
G15 – Synthetic	*Chrysopogon zizanioides*	1.17	0.09	0.08	0.05	0.03	0.02	0.03	0.03	0.05
G12 – RD	*Hyparrhenia hirta*	10.47	10.72	10.96	5.62	4.47	5.01	5.25	4.79	5.25
G12 – Synthetic	*Hyparrhenia hirta*	1.17	0.12	0.17	0.08	0.05	0.03	0.04	0.04	0.04
G5 – RD	*Hyparrhenia filipendula*	10.47	10.23	11.75	6.31	5.50	5.25	5.75	6.46	7.08
G5 – Synthetic	*Hyparrhenia filipendula*	1.17	0.44	0.44	0.26	0.17	0.07	0.08	0.09	0.15
G13 – RD	*Hyparrhenia hirta*	10.47	10.23	10.23	5.75	5.50	5.13	5.25	5.25	7.24
G13 – Synthetic	*Hyparrhenia hirta*	1.17	0.21	0.19	0.10	0.03	0.02	0.03	0.02	0.02
Blank – RD	*Blank – No grass*	10.47	10.47	11.48	5.62	5.25	4.90	5.01	5.13	6.03
Blank – Synthetic	*Blank – No grass*	1.17	1.17	1.45	0.76	0.79	0.89	0.91	1.00	1.35

Table C.5. Percentage change in hydrogen ion concentration (H+) between days for multiple grass addition testwork

Grass Site Identification	Grass Classification	% initial change in H^+ (Day 1) After 1st grass addition	% change in H^+ (Day 1-3)	% change in H^+ (Day 3-4) After 2nd grass addition	% change in H^+ (Day 4-7)	% change in H^+ (Day 7-7.5) After 3rd grass addition	% change in H^+ (Day 7.5-8)	% change in H^+ (Day 8-9)	% change in H^+ (Day 9-10) After 3rd grass removal
G6 – RD	*Eragrostis curvula*	7.2	4.7	-47.5	-4.5	12.2	-4.5	0.0	14.8
G6 – Synthetic	*Eragrostis curvula*	-45.0	-6.7	-47.5	-16.8	-48.7	4.7	12.2	12.2
G13 (2) – RD	*Hyparrhenia hirta*	2.3	-4.5	-45.0	-8.8	0.0	0.0	7.2	7.2
G13 (2) – Synthetic	*Hyparrhenia hirta*	-85.5	-29.2	-38.3	-56.3	-57.3	-2.3	51.4	2.3
G15 – RD	*Chrysopogon zizanioides*	2.3	12.2	-51.0	-14.9	4.7	-4.5	4.7	23.0
G15 – Synthetic	*Chrysopogon zizanioides*	-92.8	-6.7	-33.9	-36.9	-32.4	14.8	20.2	51.4
G12 – RD	*Hyparrhenia hirta*	2.3	2.3	-48.7	-20.6	12.2	4.7	-8.8	9.6
G12 – Synthetic	*Hyparrhenia hirta*	-89.8	38.0	-51.0	-39.7	-36.9	31.8	-12.9	12.2
G5 – RD	*Hyparrhenia filipendula*	-2.3	14.8	-46.3	-12.9	-4.5	9.6	12.2	9.6
G5 – Synthetic	*Hyparrhenia filipendula*	-62.8	0.0	-39.7	-33.9	-58.3	9.6	7.2	73.8
G13 – RD	*Hyparrhenia hirta*	-2.3	0.0	-43.8	-4.5	-6.7	2.3	0.0	38.0
G13 – Synthetic	*Hyparrhenia hirta*	-81.8	-12.9	-48.7	-63.7	-42.5	34.9	-18.7	0.0
Blank – RD	*Blank – No grass*	0.0	9.6	-51.0	-6.7	-6.7	2.3	2.3	17.5
Blank – Synthetic	*Blank – No grass*	0.0	23.0	-47.5	4.7	12.2	2.3	9.6	34.9

Table C.6. Percentage change in hydrogen ion concentration (H+) compared with initial H+ concentration for multiple grass addition testwork

Grass Site Identification	Grass Classification	% initial change in H^+ (Day 0-1) 1st grass addition	% change in H^+ (Day 0-3)	% change in H^+ (Day 0-4) After 2nd grass addition	% change in H^+ (Day 0-7)	% change in H^+ (Day 0-7.5) After 3rd grass addition	% change in H^+ (Day 0-8)	% change in H^+ (Day 0-9)	% change in H^+ (Day 0-10) After 3rd grass removal
G6 – RD	*Eragrostis curvula*	7.2	12.2	-41.1	-43.8	-36.9	-39.7	-39.7	-30.8
G6 – Synthetic	*Eragrostis curvula*	-45.0	-48.7	-73.1	-77.6	-88.5	-88.0	-86.5	-84.9
G13 (2) – RD	*Hyparrhenia hirta*	2.3	-2.3	-46.3	-51.0	-51.0	-51.0	-47.5	-43.8
G13 (2) – Synthetic	*Hyparrhenia hirta*	-85.5	-89.8	-93.7	-97.2	-98.8	-98.9	-98.3	-98.2
G15 – RD	*Chrysopogon zizanioides*	2.3	14.8	-43.8	-52.1	-49.9	-52.1	-49.9	-38.3
G15 – Synthetic	*Chrysopogon zizanioides*	-92.8	-93.2	-95.5	-97.2	-98.1	-97.8	-97.4	-96.0
G12 – RD	*Hyparrhenia hirta*	2.3	4.7	-46.3	-57.3	-52.1	-49.9	-54.3	-49.9
G12 – Synthetic	*Hyparrhenia hirta*	-89.8	-85.9	-93.1	-95.8	-97.4	-96.5	-97.0	-96.6
G5 – RD	*Hyparrhenia filipendula*	-2.3	12.2	-39.7	-47.5	-49.9	-45.0	-38.3	-32.4
G5 – Synthetic	*Hyparrhenia filipendula*	-62.8	-62.8	-77.6	-85.2	-93.8	-93.2	-92.8	-87.4
G13 – RD	*Hyparrhenia hirta*	-2.3	-2.3	-45.0	-47.5	-51.0	-49.9	-49.9	-30.8
G13 – Synthetic	*Hyparrhenia hirta*	-81.8	-84.2	-91.9	-97.0	-98.3	-97.7	-98.1	-98.1
Blank – RD	*Blank – No grass*	0.0	9.6	-46.3	-49.9	-53.2	-52.1	-51.0	-42.5
Blank – Synthetic	*Blank – No grass*	0.0	23.0	-35.4	-32.4	-24.1	-22.4	-14.9	14.8

Appendix II-D

Table D.1. Elemental concentration data of grass samples

Units	**g/t**												
Element	**Na**	**Mg**	**K**	**Ca**	**P**	**S**	**B**	**Al**	**Mn**	**Co**	**Cu**	**Zn**	**Pb**
G13 - Synthetic - Original	368	2011	10877	4318	1915	4839	3.97	1187	296	1.16	12.1	72.9	2.19
Add 1	7015	171	786	568	1255	10053	10.1	736	59.7	0.82	8.07	22.5	1.77
Add 2	10608	396	2101	1338	1367	15026	1.28	973	108	0.93	9.51	31.3	1.70
Add 3	8084	466	2329	2093	1456	11529	1.51	837	126	1.05	11.7	42.7	2.97
G13 (2) - Synthetic - Original	408	3510	13601	6054	2876	6922	8.29	7894	465	4.71	26.4	78.6	6.06
Add 1	7050	237	576	697	1345	9933	1.82	4147	90.2	1.79	12.1	20.1	2.86
Add 2	11954	583	1682	1777	1308	18095	10.8	4040	164	2.15	9.84	30.9	3.02
Add 3	7611	555	1532	2358	1470	11839	2.23	3370	173	2.19	11.1	36.8	3.99
G6 - Synthetic - Original	7.87	489	4897	2417	592	1065	2.07	240	40.7	0.36	6.77	20.4	21.17
Add 1	3868	281	1952	476	448	5292	0.81	498	28.6	0.45	8.30	9.85	0.92
Add 2	3962	331	1373	915	508	5388	10.4	257	22.4	0.38	7.18	25.3	2.34
Add 3	3172	67.5	562	351	301	4497	0.50	274	16.2	0.29	7.88	7.25	1.36
G5 - Synthetic - Original	5.54	1106	11052	2201	1272	1530	3.71	384	92.0	0.54	3.84	21.5	1.10
Add 1	4224	681	614	3904	1811	6558	13.2	1086	120	2.06	23.7	194	20.1
Add 2	8328	315	1903	666	695	13062	1.19	499	59.8	0.85	4.78	12.2	2.30
Add 3	5865	213	1884	552	604	7947	1.21	318	33.6	0.42	6.97	9.73	0.78
G15 - Synthetic - Original	221 ±11	3234 ±117	11935 ±554	6734 ±283	1817 ±198	1814 ±45.1	6.80 ±0.21	355 ±64.6	45.6 ±3.09	0.42 ±0.13	10.8 ±1.13	79.3 ±3.41	4.88 ±0.73

Units	**g/t**												
Element	**Na**	**Mg**	**K**	**Ca**	**P**	**S**	**B**	**Al**	**Mn**	**Co**	**Cu**	**Zn**	**Pb**
Add 1	*5362 ±265*	261 ±1.66	843 ±3.88	*2416 ±51*	1173 ±24.5	7557 ±89.3	1.20 ±0.007	385 ±3.41	24.7 ±0.14	0.41 ±0.00	7.67 ±0.16	13.3 ±0.03	1.18 ±0.06
Add 2	4736	389	1273	3386	1141	6456	11.1	298	22.5	0.28	5.66	14.3	1.45
Add 3	4099	476	1600	3728	888	5844	8.34	309	21.9	0.28	8.51	14.3	0.02
G12 - Synthetic - Original	42.7	3900	27542	4360	2970	4022	7.82	3156	181	1.94	12.8	57.0	3.14
Add 1	6732	672	2423	1148	2240	9088	2.73	3671	73.5	1.93	10.9	42.8	3.15
Add 2	9810	1143	5312	2969	2403	14155	13.2	3987	114	2.21	13.4	36.0	3.35
Add 3	4896	961	4285	4019	2110	6750	3.47	3298	97.5	1.97	14.6	40.1	3.65
G12 - RD - Original	42.7	3900	27542	4360	2970	4022	7.82	3156	181	1.94	12.8	57.0	3.14
Add 1	128	1208	2145	1608	998	14749	2.07	3859	218	4.42	14.3	39.0	6.32
Add 2	157	1333	3164	1615	1339	14842	2.73	5088	222	4.69	16.1	42.8	4.16
Add 3	73.9	958	2572	1251	1958	9388	2.73	3654	144	3.30	14.9	29.3	2.68
CRM - Tea Leaves CRM	6.76 ±0.00	2261 ±48.9	15729 ±88.7	5711 ±28.7	2418 *±8.50*	2606 ±12.7	28.1 *±0.26*	2131 ±15.6	1505 ±17.4	0.30 ±0.002	21.3 ±1.45	32.2 ±0.30	1.68 ±0.13
CRM – True values	24.7 *±3.2*	2240 *±170*	17000 *±1200*	5820 *±520*	—	2470 *±250%*	—	2290 *±250*	1570 *±110*	0.387 *±0.042*	20.4 *±1.5*	34.7 *±2.7*	1.78 ±0.024

Appendix III - Supplementary data for Chapter 6

(with Figures and Tables from the original published paper)

Table S1. Experimental data for test work performed at pH2 for parameters pH, sulfide (S^{2-}), sulfate (SO_4^{2-}), and chemical oxygen demand (COD) concentrations.

pH2	pH						
Day	**Blk**	**AMD**	**MW**	**RS**	**CD**	**MUD**	**RM**
1	2.09	2.07	2.45	2.16	2.03	2.24	2.23
4	2.07	2.03	2.61	2.09	1.98	2.29	2.26
7	2.32	2.34	2.88	2.13	2.01	2.44	2.33
14	2.13	2.14	2.70	2.08	1.95	2.51	2.3
21	2.08	2.12	2.67	1.98	1.83	2.44	2.21
28	2.11	2.14	2.69	2.17	2.04	2.72	2.46
35	2.08	2.12	2.70	2.06	1.93	2.67	2.36
42	1.98	2.01	2.61				
49	1.98	2.01	2.64				
57							
pH2	COD (mg/L)						
Day	**Blk**	**AMD**	**MW**	**RS**	**CD**	**MUD**	**RM**
1	2475	2570	2875	3025	3170	2625	2735
4							
7	2845	2619	5204	2565	3575	2495	3910
14	2790	2720	4540	2530	2885	2740	2240
21	2820	2525	4655	2400	3330	2785	1815
28	2680	2225	4285	2415	3015	2825	1975
35	4265	2355	4600	2410	3125	3565	1720
42							
49	1775	1605	3865				
57							
pH2	SO_4^{2-} *(mg/L)*						
Day	**Blk**	**AMD**	**MW**	**RS**	**CD**	**MUD**	**RM**
1	2086	3156	2003	2143	2048	2796	2204
4							
7				1804	1839	2152	2111
14				2017	2010	2540	2363
21				2094	2116	2698	2578
28	852	2930	1913	1982	2017	2596	2448
35				2131	2113	2778	2505
42	1856	2674	1745				
49	2123	3227	2075				
57							
pH2	S^{2-}(mg/L)						
Day	**Blk**	**AMD**	**MW**	**RS**	**CD**	**MUD**	**RM**
1	0.000	0.000	0.020	0.014	0.021	0.009	0.016
4	0.002	0.009	0.054		0.033	0.036	0.025
7	0.035	0.056	0.006	0.008	0.027	0.004	0.000
14	0.009	0.001	0.012	0.009	0.002	0.056	0.0094
21	0.036	0.030	0.018	0.014	0.026	0.005	0.006
28	0.040	0.022	0.090	0.001	0.031	0.008	0.001
35	0.009	0.000	0.015	0.286	0.038	0.023	0.036
42	0.023	0.005	0.017				
49	0.029	0.020	0.040				
57							

Table S2. Experimental data for test work performed at pH4 for parameters pH, sulfide (S^{2-}), sulfate (SO_4^{2-}), and chemical oxygen demand (COD) concentrations.

pH4	pH						
Day	**Blk**	**AMD**	**MW**	**RS**	**CD**	**MUD**	**RM**
1	3.98	2.87	4.07	5.11	4.41	6.27	4.62
4	3.94	2.95	4.9	4.44	4.25	5.50	4.68
7	4.09	3.29	5.12	5.35	4.43	5.98	5.06
14	3.92	3.18	4.61	6.49	4.50	7.04	6.17
21	3.91	3.18	4.65	7.07	4.47	7.27	6.50
28	3.87	3.29	4.70	7.24	4.61	7.67	7.27
35	3.89	3.33	4.79	7.49	4.55	7.72	6.93
42	3.75	3.30	4.85				
49	3.80	3.32	5.18				7.10
57				7.8		8.3	7.40
pH4	COD (mg/L)						
Day	**Blk**	**AMD**	**MW**	**RS**	**CD**	**MUD**	**RM**
1	2650	2860	3125	2765	3555	2635	2765
4							
7	4419	2869	4169	2125	2860	3555	2165
14	2410	2740	4545	935	2835	1735	2195
21	2205	2575	4745	840	3145	950	1780
28	2015	1990	4335	1360	3215	755	1665
35	2160	2025	4040	770	3050	725	1740
42							
49	1670	1710	3980				
57				705		700	1705
pH4	SO_4^{2-} (mg/L)						
Day	**Blk**	**AMD**	**MW**	**RS**	**CD**	**MUD**	**RM**
1	1983	3009	1984	2035	2048	2243	2210
4							
7				1722	1842	2129	2043
14				1905	1910	2364	2024
21				1922	2036	2191	1808
28	1809	3009	1899	1887	1877	1979	1447
35				1928	2050	2173	1330
42	1777	2774	1765				
49	2026	3099	2114				1326
57				1844		2108	1335
pH4	S^{2-} (mg/L)						
Day	**Blk**	**AMD**	**MW**	**RS**	**CD**	**MUD**	**RM**
1	0.000	0.000	0.017	0.027	0.020	0.02	0.020
4	0.033	0.015	0.072	0.089	0.045	0.10	0.065
7	0.000	0.015	0.006	0.357	0.056	0.86	0.10
14	0.003	0.018	0.234	1.424	0.048	1.0	1.0
21	0.033	0.005	0.355	0.190	0.125	2.8	14
28	0.039	0.027	0.100	0.027	0.085	1.1	13
35	0.007	0.002	0.018	0.328	0.300	0.59	36
42	0.027	0.476	0.035				
49	0.032	0.296	0.056				30
57				0.053		0.02	0.015

Table S3. Experimental data for test work performed at pH7.5 for parameters pH, sulfide (S^{2-}), sulfate (SO_4^{2-}), and chemical oxygen demand (COD) concentrations.

pH7.5	pH						
Day	**Blk**	**AMD**	**MW**	**RS**	**CD**	**MUD**	**RM**
1	7.02	3.4	6.37	7.07	6.92	7.10	6.94
4	6.26	3.47	5.75	5.62	5.50	5.88	5.52
7	5.85	3.72	6.03	5.97	5.73	6.22	5.81
14	5.17	3.71	5.82	6.21	6.76	6.68	6.37
21	5.42	4.50	6.02	6.24	6.94	6.99	6.45
28	5.54	5.35	6.03	6.58	7.34	7.10	6.70
35	5.51	5.50	5.99	6.59	7.51	7.28	6.60
42	5.71	5.44	6.07				
49	5.96	5.74	6.38	6.75		7.77	6.78
57				6.62		7.64	7.79
pH7.5	**COD**						
Day	**Blk**	**AMD**	**MW**	**RS**	**CD**	**MUD**	**RM**
1	3065	2500	3025	3485	3510	2580	2780
4							
7	2214	3034	4184	2300	2600	2160	2185
14	2490	2590	4455	2505	1985	2165	2250
21	2115	2665	4455	4095	1725	1815	1975
28	2105	2130	4310	2810	2385	1625	2090
35	2125	2755	4415	2315	1130	1350	1870
42							
49	1660	2030	4095				
57				2525		1115	2065
pH7.5	SO_4^{2-}						
Day	**Blk**	**AMD**	**MW**	**RS**	**CD**	**MUD**	**RM**
1	2026	2983	1964	1875	2064	2058	2063
4							
7				1660	1761	2199	2034
14				1721	1889	2203	1949
21				1564	1906	2090	1723
28	1890	2891	1948	1112	1875	1938	1470
35				1087	2078	1860	1435
42	1734	2719	1829				
49	2102	3076	2120	1289		1430	1418
57				1053		1288	1482
pH7.5	S^{2-}						
Day	**Blk**	**AMD**	**MW**	**RS**	**CD**	**MUD**	**RM**
1	0.000	0.000	0.016	0.022	0.046	0.022	0.028
4	0.010	0.000	0.067	0.79	0.071	0.062	0.048
7	0.025	0.003	0.000	6.5	0.099	0.99	2.4
14	0.028	0.009	0.280	28	0.363	1.20	15
21	0.030	0.069	0.178	50	0.263	8.5	26
28	0.059	0.053	0.178	89	0.405	3.5	99
35	0.018	0.011	0.069	108	0.113	1.9	58
42	0.026	0.022	0.120	91			52
49	0.044	0.068	0.125	114		35	77
57				99		25	61

Table S4. Quality Control samples analysed with each sample batch with averages and percentage error

pH	Day 1	Day 4	Day 7	Day 14	Day 21	Day 28	Day 35	Day 42	Day 49	Day 57
Control pH 7	7.02	7.01	6.98	7.01	6.99	6.99	6.98	6.98	7.01	–
Control pH 7	6.98	7.02	7.00	7.03	6.98	6.96	6.99	–	6.99	7.03
Average	7.00	7.02	6.99	7.02	6.99	6.98	6.99	6.98	7.00	7.03
% Error	0.00	0.21	-0.14	0.29	-0.21	-0.36	-0.21	-0.29	0.00	0.43
Control pH 4	4.02	4.01	3.97	3.97	3.99	4.03	3.98	–	–	–
Control pH 4	4.04	4.06	4.01	3.98	3.98	4.04	3.99	3.99	3.97	3.99
Average	4.03	4.04	3.99	3.98	3.99	4.04	3.99	3.99	3.97	3.99
% Error	0.75	0.88	-0.25	-0.62	-0.37	0.88	-0.37	-0.25	-0.75	-0.25

Table S5. COD - Quality Control samples analysed with each sample batch with averages and percentage error

COD	Day 1	Day 4	Day 7	Day 14	Day 21	Day 28	Day 35	Day 42	Day 49	Day 57
1000 mg/L - control	1010	–	840	1075	1140	1090	1090	–	1075	–
1000 mg/L - control	1090	–	–	–	–	–	–	–	–	–
Average	1050	–	840	1075	1140	1090	1090	–	1075	–
% Error	1.00	–	-16.00	7.50	14.00	9.00	9.00	–	7.50	–

Table S6. Sulfide - Quality Control samples analysed with each sample batch with averages and percentage error

Sulfide	Day 1	Day 4	Day 7	Day 14	Day 21	Day 28	Day 35	Day 42	Day 49	Day 57
0.5 mg/L control	0.53	0.51	0.42	0.43	0.47	–	0.45	0.409	–	0.45
% Error	6.84	1.38	-16.83	-14.44	-6.42	–	-10.28	-18.26	–	-10.09
1.0 mg/L control	1.07	1.04	0.98	1.01	0.98	0.73	1.03	0.986	1.00	1.02
% Error	6.73	3.80	-1.60	0.97	-1.73	-27.30	3.41	-1.43	0.27	2.02

Table S7. Sulfate - Quality Control samples analysed with each sample batch with averages and percentage error

Sulfate	Day 1	Day 4	Day 7	Day 14	Day 21	Day 28	Day 35	Day 42	Day 49	Day 57
10 mg/L - control	–	–	–	10.1	–	10.0	10.0	10.8	9.06	9.68
10 mg/L - control	–	–	–	9.89	–	10.1	–	–	10.4	–
Average	–	–	–	10.0	–	10.1	10.0	10.8	9.74	9.68
% Error	–	–	–	0.06	–	0.54	0.32	7.75	-2.58	-3.20
20 mg/L - control	21.09	–	–	20.6	20.6	20.9	20.9	21.4	21.3	–
% Error	5.44	–	–	2.75	2.75	4.44	4.29	7.13	6.25	–
25 mg/L - control	–	–	24.1	–	–	–	–	24.1	–	–
25 mg/L - control	–	–	24.3	–	–	–	–	24.3	–	–
Average	–	–	24.2	–	–	–	–	24.2	–	–
% Error	–	–	-3.10	–	–	–	–	-3.10	–	–

Table S8. Sulfate – Sample replicate analysis with averages and standard deviations

Sulfate - replicate analysis	Day 1	Day 4	Day 7	Day 14	Day 21	Day 28	Day 35	Day 42	Day 49	Day 57
AMD pH 2	3156	–	–	–	–	–	–	–	–	–
AMD pH 2	3143	–	–	–	–	–	–	–	–	–
Average	3149	–	–	–	–	–	–	–	–	–
Std dev	9.12	–	–	–	–	–	–	–	–	–
Blk pH 4	1983	–	–	–	–	–	–	–	–	–
Blk pH 4	1990	–	–	–	–	–	–	–	–	–
Average	1987	–	–	–	–	–	–	–	–	–
Std dev	4.77	–	–	–	–	–	–	–	–	–
Sewage 7.5	–	–	–	1721	–	–	1087	–	–	–
Sewage 7.5	–	–	–	1797	–	–	1154	–	–	–
Average	–	–	–	1759	–	–	1121	–	–	–
Std dev	–	–	–	53.54	–	–	47.38	–	–	–
Reed Mud 7.5	–	–	–	–	1470	–	–	–	1326	1335
Reed Mud 7.5	–	–	–	–	1458	–	–	–	1418	1482
Average	–	–	–	–	1464	–	–	–	1372	1408
Std dev	–	–	–	–	8.32	–	–	–	65.47	104.13

Appendix IV - Supplementary data for Chapter 7

(with Figures and Tables from the original paper)

Table S1.1 Glucose data for pre-treatment of grass test work performed at different retention times *(mg/L)*

Day (HRT)	non-amended Blk	SRB-amended Blk	non-amended grass	SRB-amended grass	Non-amended grass (Std Dev)	SRB-amended grass (Std Dev)
0	0.00	0.00	118	120	10.7	5.6
1	0.00	0.00	297	245	7.15	20.1
4	0.00	0.00	236	289	15.1	36.8
7	0.00	0.00	197	154	—	4.65
11	0.00	0.00	—	205	—	—
13	0.00	0.00	—	—	—	—

Table S1.2 Glucose concentrations of filtrate samples after grass removal *(mg/L)*

No of days after grass removal	Glucose	(Std Dev)	Glucose - SRB	(Std Dev) - SRB
Initial Glucose	0.00		0.00	
HRT Day 1	**Glucose**	**(Std Dev)**	**Glucose - SRB**	**(Std Dev) - SRB**
0	297	7.2	245	20.1
3	—	—	—	—
6	153	15.4	223	2.34
10	98.7	—	—	—
12	—	—	16.7	—
26	—	—	—	—
HRT Day 4	**Glucose**	**(Std Dev)**	**Glucose - SRB**	**(Std Dev) - SRB**
0	236	15.1	289	36.8
3	117	59.3	255	9.02
7	81.9	—	199	—
9	47.8	—	40.4	27.2
23	—	—	47.9	—
HRT Day 7	**Glucose**	**(Std Dev)**	**Glucose - SRB**	**(Std Dev) - SRB**
0	197	—	154	4.65
4	—	—	49.3	2.02
6	—	—	22.7	0.10
20	42.9	—	55.4	—
HRT Day 11	**Glucose**	**(Std Dev)**	**Glucose - SRB**	**(Std Dev) - SRB**
0	—	—	205	—
2	—	—	182	—
16	—	—	—	—
HRT Day 13	**Glucose**	**(Std Dev)**	**Glucose - SRB**	**(Std Dev) - SRB**
0	—	—	—	—
14	—	—	—	—

Table S1.3 – Xylose data for pre-treatment of grass test work performed at different retention times *(mg/L)*

Day (HRT)	non-amended Blk	SRB-amended Blk	non-amended grass	SRB-amended grass	Non-amended grass (Std Dev)	SRB-amended grass (Std Dev)
0	0.00	0.00	151	121	21.1	24.4
1	0.00	0.00	336	295	68.2	61.4
4	0.00	0.00	266	299	94.0	93.2
7	0.00	0.00	217	180	171	2.99
11	0.00	0.00	56.5	160	8.49	137
13	0.00	0.00	37.8	42.2	5.06	—

Table S1.4 Xylose data showing Xylose concentrations of filtrate samples after grass removal *(mg/L)*

No of days after grass removal	Xylose	(Std Dev)	Xylose - SRB	(Std Dev) - SRB
Initial Xylose	0.00		0.00	
HRT Day 1	**Xylose**	**(Std Dev)**	**Xylose - SRB**	**(Std Dev) - SRB**
0	336	68.2	295	61.4
3	—	—	—	—
6	304	17.9	144	9.73
10	163	90.9	87.8	4.72
12	74.0	3.52	50.1	2.38
26	—	—	—	—
HRT Day 4	**Xylose**	**(Std Dev)**	**Xylose - SRB**	**(Std Dev) - SRB**
0	266	94.0	299	93.2
3	249	83.2	249	82.5
7	166	130	172	111
9	128	105	71.7	24.6
23	—	—	—	—
HRT Day 7	**Xylose**	**(Std Dev)**	**Xylose - SRB**	**(Std Dev) - SRB**
0	217	171	180	2.99
4	53.5	3.30	82.4	9.61
6	54.4	6.51	60.7	8.38
20	—	—	—	—
HRT Day 11	**Xylose**	**(Std Dev)**	**Xylose - SRB**	**(Std Dev) - SRB**
0	56.5	8.49	160	137
2	63.3	4.36	135	131
16	—	—	—	—
HRT Day 13	**Xylose**	**(Std Dev)**	**Xylose - SRB**	**(Std Dev) - SRB**
0	37.80	5.06	42.2	—
14	—	—	—	—

Table S1.5 Acetate data for pre-treatment of grass test work performed at different retention times *(mg/L)*

Day (HRT)	non-amended Blk	SRB-amended Blk	non-amended grass	SRB-amended grass	Non-amended grass (Std Dev)	SRB-amended grass (Std Dev)
0	0.00	0.00	227	228	27.2	20.6
1	0.00	0.00	449	662	61.6	215
4	0.00	0.00	268	259	16.1	17.6
7	0.00	0.00	435	311	61.2	53.4
11	0.00	0.00	386	309	51.6	55.1
13	0.00	0.00	382	386	35.8	10.0

Table S1.6 Acetate concentrations of filtrate samples after grass removal *(mg/L)*

No of days after grass removal	Acetate	(Std Dev)	Acetate - SRB	(Std Dev) - SRB
Initial Acetate	0.00		0.00	
HRT Day 1	**Acetate**	**(Std Dev)**	**Acetate - SRB**	**(Std Dev) - SRB**
0	449	61.6	662	215
3	—	—	—	—
6	299	10.3	289	11.0
10	282	14.0	412	67.5
12	288	25.8	256	9.22
26	212	74.3	226	1.85
HRT Day 4	**Acetate**	**(Std Dev)**	**Acetate - SRB**	**(Std Dev) - SRB**
0	268	16.1	259	17.6
3	343	53.5	287	5.0
7	379	142	248	35.6
9	298	43.7	216	46.3
23	214	8.24	195	11.7
HRT Day 7	**Acetate**	**(Std Dev)**	**Acetate - SRB**	**(Std Dev) - SRB**
0	435	61.2	311	53.4
4	248	71.7	287	20.1
6	325	38.3	307	3.78
20	187	3.97	194	24.1
HRT Day 11	**Acetate**	**(Std Dev)**	**Acetate - SRB**	**(Std Dev) - SRB**
0	386	51.6	309	55.1
2	405	11.6	323	89.2
16	403	17.2	307	107
HRT Day 13	**Acetate**	**(Std Dev)**	**Acetate - SRB**	**(Std Dev) - SRB**
0	382	35.8	386	10.0
14	443	61.5	352	6.20

Table S1.7 – Propionate data for pre-treatment of grass test work performed at different retention times *(mg/L)*

Day (HRT)	non-amended Blk	SRB-amended Blk	non-amended grass	SRB-amended grass	Non-amended grass (Std Dev)	SRB-amended grass (Std Dev)
0	0.00	26.4	31.3	31.8	0.9	2.4
1	0.00	0.00	77.3	136	30.4	65.2
4	0.00	0.00	47.5	42.0	0.42	3.26
7	32.2	33.4	106	50.0	45.1	19.1
11	27.5	30.6	102	51.5	28.0	20.9
13	30.0	30.1	125	137	15.2	11.8

Table S1.8 – Propionate concentrations of filtrate samples after grass removal *(mg/L)*

No of days after grass removal	Propionate	(Std Dev)	Propionate - SRB	(Std Dev) - SRB
Initial Acetate	0.00		0.00	
HRT Day 1	**Propionate**	**(Std Dev)**	**Propionate - SRB**	**(Std Dev) - SRB**
0	77.3	30.4	136	65.2
3	—	—	—	—
6	38.5	2.57	33.7	4.52
10	40.6	0.65	58.7	21.3
12	48.4	0.08	34.0	3.08
26	36.4	2.91	35.0	0.00
HRT Day 4	**Propionate**	**(Std Dev)**	**Propionate - SRB**	**(Std Dev) - SRB**
0	47.5	0.42	42.0	3.26
3	62.3	17.8	38.4	1.37
7	94.8	23.1	72.8	48.6
9	76.4	55.0	63.3	29.5
23	42.2	1.38	29.7	6.56
HRT Day 7	**Propionate**	**(Std Dev)**	**Propionate - SRB**	**(Std Dev) - SRB**
0	106	45.1	50.0	19.1
4	95.0	9.06	104	5.66
6	123	0.90	108	21.2
20	48.4	1.49	33.8	—
HRT Day 11	**Propionate**	**(Std Dev)**	**Propionate - SRB**	**(Std Dev) - SRB**
0	102	28.0	51.5	20.9
2	119	8.86	54.2	34.2
16	130	38.6	35.7	
HRT Day 13	**Propionate**	**(Std Dev)**	**Propionate - SRB**	**(Std Dev) - SRB**
0	125	15.2	137	11.8
14	155	4.00	46.0	2.35

Table S1.9 – Average pH data and standard deviations for pre-treatment of grass test work performed at different retention times

Day (HRT)	non-amended Blk	SRB-amended Blk	non-amended grass	SRB-amended grass	Non-amended grass (Std Dev)	SRB-amended grass (Std Dev)
0	3.06	3.06	3.92	3.83	0.049	0.035
1	3.03	3.04	4.02	3.91	0.035	0.021
4	3.01	3.01	3.99	3.97	0.071	0.007
7	3.04	3.07	4.12	4.12	0.120	0.007
11	2.98	2.96	4.45	4.18	0.042	0.212
13	2.99	2.92	4.57	4.46	0.021	0.057

Table S1.10 – pH values of filtrate samples after grass removal

No of days after grass removal	pH	(Std Dev)	pH - SRB	(Std Dev) - SRB
Initial pH	3.01	—	3.01	—
HRT Day 1	**pH**	**(Std Dev)**	**pH - SRB**	**(Std Dev) - SRB**
0	4.02	0.04	3.91	0.02
3	3.92	0.03	3.90	0.01
6	4.07	0.04	4.09	0.01
10	4.30	0.08	4.30	0.04
12	4.53	0.21	4.56	0.04
26	5.41	0.05	5.53	0.48
HRT Day 4	**pH**	**(Std Dev)**	**pH - SRB**	**(Std Dev) - SRB**
0	3.99	0.07	3.97	0.01
3	3.99	0.16	3.99	0.01
7	4.29	0.35	4.20	0.18
9	4.43	0.43	4.40	0.27
23	5.17	0.30	5.26	0.28
HRT Day 7	**pH**	**(Std Dev)**	**pH - SRB**	**(Std Dev) - SRB**
0	4.12	0.12	4.12	0.01
4	4.50	0.04	4.07	0.04
6	4.72	0.04	4.26	0.05
20	5.28	0.03	5.68	0.14
HRT Day 11	**pH**	**(Std Dev)**	**pH - SRB**	**(Std Dev) - SRB**
0	4.45	0.04	4.18	0.21
2	4.40	0.20	4.19	0.43
16	5.04	0.12	5.01	—
HRT Day 13	**pH**	**(Std Dev)**	**pH - SRB**	**(Std Dev) - SRB**
0	4.57	0.02	4.46	0.06
14	5.13	0.05	5.66	0.25

Table S1.11 – COD data for pre-treatment of grass test work performed at different retention times *(mg/L)*

Day (HRT)	non-amended Blk	SRB-amended Blk	non-amended grass	SRB-amended grass	Non-amended grass (Std Dev)	SRB-amended grass (Std Dev)
0	0.00	0.00	901	865	87.4	104
1	261	156	1544	1319	138	38.9
4	828.5	33.5	1211	1349	138	84.9
7	133	438	1233	1306	28.3	81.3
11	1265	665	2155	1458	1131	463
13	191	286	1439	1426	103	63.6

Table S1.12 – COD concentrations of filtrate samples after grass removal *(mg/L)*

No of days after grass removal	COD	(StdDev)	COD - SRB	(StdDev) - SRB
Initial COD	195		293	
HRT Day 1	**COD**	**(StdDev)**	**COD - SRB**	**(StdDev) - SRB**
0	1544	138	1319	38.9
3	904	127	1151	38.9
6	1251	138	1121	110
10	1568	53.0	1230	120
12	1184	145	1196	0.0
26	1098	255	1006	159
HRT Day 4	**COD**	**(StdDev)**	**COD - SRB**	**(StdDev) - SRB**
0	1211	138	1349	84.9
3	1073	304	1178	49.5
7	1450	21.2	1583	31.8
9	1294	24.7	1261	99.0
23	1213	120	1056	124
HRT Day 7	**COD**	**(StdDev)**	**COD - SRB**	**(StdDev) - SRB**
0	1233	28.3	1306	81.3
4	2060	636	1413	3.54
6	1416	49.5	1219	46.0
20	1188	127	948	28.3
HRT Day 11	**COD**	**(StdDev)**	**COD - SRB**	**(StdDev) - SRB**
0	2155	1131	1458	463
2	1446	49.5	1324	180
16	1163	113	1046	46.0
HRT Day 13	**COD**	**(StdDev)**	**COD - SRB**	**(StdDev) - SRB**
0	1439	103	1426	63.6
14	1153	746	1058	141

Table S1.13 – Sulfide data for pre-treatment of grass test work performed at different retention times *(mg/L)*

Day (HRT)	non-amended Blk	SRB-amended Blk	non-amended grass	SRB-amended grass	Non-amended grass (Std Dev)	SRB-amended grass (Std Dev)
0	0.033	0.067	0.044	0.066	0.007	0.008
1	0.051	0.049	0.205	0.091	0.175	0.062
4	0.029	0.034	0.075	0.056	0.020	0.012
7	0.071	0.097	0.120	0.077	0.005	0.007
11	0.071	0.080	0.125	0.113	0.008	0.016
13	0.075	0.081	0.176	0.131	0.045	0.018

Table S1.14 – Sulfide concentrations of filtrate samples after grass removal *mg/L)*

No of days after grass removal	Sulfide	(Std Dev)	Sulfide - SRB	(Std Dev) - SRB
Initial Sulfide	0.055		0.068	
HRT Day 1	**Sulfide**	**(Std Dev)**	**Sulfide - SRB**	**(Std Dev) - SRB**
0	0.205	0.175	0.091	0.062
3	0.228	0.110	0.148	0.081
6	0.344	0.119	0.256	0.029
10	0.500	0.226	0.369	0.062
12	0.541	0.175	0.482	0.003
26	0.531	0.178	1.297	—
HRT Day 4	**Sulfide**	**(Std Dev)**	**Sulfide - SRB**	**(Std Dev) - SRB**
0	0.075	0.020	0.056	0.012
3	0.194	0.031	0.117	0.024
7	0.305	0.037	0.201	0.085
9	0.345	0.058	0.291	0.052
23	0.298	0.011	0.737	0.458
HRT Day 7	**Sulfide**	**(Std Dev)**	**Sulfide - SRB**	**(Std Dev) - SRB**
0	0.120	0.005	0.077	0.007
4	0.344	0.065	0.178	0.038
6	0.364	0.002	0.274	0.049
20	0.354	0.003	0.934	0.142
HRT Day 11	**Sulfide**	**(Std Dev)**	**Sulfide - SRB**	**(Std Dev) - SRB**
0	0.125	0.008	0.113	0.016
2	0.239	0.159	0.256	0.213
16	0.311	0.108	1.810	—
HRT Day 13	**Sulfide**	**(Std Dev)**	**Sulfide - SRB**	**(Std Dev) - SRB**
0	0.176	0.045	0.131	0.018
14	0.380	0.179	2.623	0.429

Table S1.15 – Fe data for pre-treatment of grass test work performed at different retention times *(mg/L)*

Day (HRT)	non-amended Blk	SRB-amended Blk	non-amended grass	SRB-amended grass	Non-amended grass (Std Dev)	SRB-amended grass (Std Dev)
0	334	389	291	325	2.22	17.4
1	302	371	255	304	15.6	13.8
4	301	370	218	296	7.10	5.71
7	306	367	261	325	9.70	0.01
11	353	410	286	406	0.43	37.5
13	304	374	277	347	4.24	3.43

Table S1.16 – Iron (Fe) concentrations of filtrate samples after grass removal *(mg/L)*

No of days after grass removal	Iron (Fe)	(Std Dev)	Iron (Fe) - SRB	(Std Dev) - SRB
Initial Iron	0.060		0.068	
HRT Day 1	**Iron (Fe)**	**(Std Dev)**	**Iron (Fe) - SRB**	**(Std Dev) - SRB**
0	255	15.6	304	13.8
3	242	12.2	299	12.8
6	255	8.49	300	22.7
10	305	8.98	367	15.4
12	253	8.77	285	15.1
26	298	8.60	328	36.4
HRT Day 4	**Iron (Fe)**	**(Std Dev)**	**Iron (Fe) - SRB**	**(Std Dev) - SRB**
0	218	7.10	296	5.71
3	211	14.2	296	15.9
7	294	22.7	387	0.48
9	232	10.5	313	0.74
23	263	12.3	361	7.90
HRT Day 7	**Iron (Fe)**	**(Std Dev)**	**Iron (Fe) - SRB**	**(Std Dev) - SRB**
0	261	9.70	325	0.01
4	278	4.89	342	0.04
6	247	13.4	323	0.05
20	294	26.1	364	0.14
HRT Day 11	**Iron (Fe)**	**(Std Dev)**	**Iron (Fe) - SRB**	**(Std Dev) - SRB**
0	286	0.43	406	37.5
2	268	5.62	386	34.6
16	300	7.49	—	
HRT Day 13	**Iron (Fe)**	**(Std Dev)**	**Iron (Fe) - SRB**	**(Std Dev) - SRB**
0	277	4.24	347	3.43
14	303	10.6	382	0.20

Table S2.1 – Glucose data for hydrolysis and fermentation test work *(mg/L)*

Glucose	Day	Sample	No SRB	Std Dev - No SRB	SRB Added	Std Dev - SRB
No grass	0	Blank	2059	27	-	-
grass	0	HRT Day 1	1941	303	2031	8.86
grass	0	HRT Day 4	2023	92.8	2034	248
grass	0	HRT Day 7	1991	281	1930	51
grass	0	HRT Day 11	2078	11.3	1961	89.2
grass	0	HRT Day 13	2030	10.8	1886	240
grass	0	Untreated	2126	18.4	-	-
No grass	1	Blank	-	-	-	-
grass	1	HRT Day 1	0	-	0	-
grass	1	HRT Day 4	0	-	0	-
grass	1	HRT Day 7	0	-	0	-
grass	1	HRT Day 11	0	-	0	-
grass	1	HRT Day 13	0	-	0	-
grass	1	Untreated	0	-	-	-
No grass	2	Blank	0	-	-	-
grass	2	HRT Day 1	0	-	0	-
grass	2	HRT Day 4	0	-	0	-
grass	2	HRT Day 7	0	-	0	-
grass	2	HRT Day 11	0	-	0	-
grass	2	HRT Day 13	0	-	0	-
grass	2	Untreated	0	-	-	-
No grass	4	Blank	0.45	-	0.45	-
grass	4	HRT Day 1	0	-	0	-
grass	4	HRT Day 4	0	-	0	-
grass	4	HRT Day 7	0	-	0	-
grass	4	HRT Day 11	0	-	0	-
grass	4	HRT Day 13	0	-	0	-
grass	4	Untreated	0	-	-	-
No grass	6	Blank	-	-	-	-
grass	6	HRT Day 1	0	-	0	-
grass	6	HRT Day 4	0	-	0	-
grass	6	HRT Day 7	0	-	0	-
grass	6	HRT Day 11	0	-	0	-
grass	6	HRT Day 13	0	-	0	-
grass	6	Untreated	0	-	-	-
No grass	8	Blank	-	-	-	-
grass	8	HRT Day 1	0	-	0	-
grass	8	HRT Day 4	0	-	0	-
grass	8	HRT Day 7	0	-	0	-
grass	8	HRT Day 11	0	-	0	-
grass	8	HRT Day 13	0	-	0	-
grass	8	Untreated	0	-	-	-
No grass	12	Blank	-	-	-	-
grass	12	HRT Day 1	0	-	0	-
grass	12	HRT Day 4	0	-	0	-
grass	12	HRT Day 7	0	-	0	-
Grass	12	HRT Day 11	660	-	0	-
Grass	12	HRT Day 13	0	-	0	-
Grass	12	Untreated	0	-	-	-

Table S2.2 –D-Glucose isomer data for hydrolysis and fermentation test work *(mg/L)*

Glucose Isomer	Day	Sample	No SRB	Std Dev - No SRB	SRB Added	Std Dev - SRB
No grass	0	Blank	3000	371	-	-
grass	0	HRT Day 1	2588	371	2813	53
grass	0	HRT Day 4	2738	159	2738	265
grass	0	HRT Day 7	2663	371	2625	106
grass	0	HRT Day 11	2850	0	2738	159
grass	0	HRT Day 13	2775	-	2588	265
grass	0	Untreated	2888	53	-	-
No grass	1	Blank	3188	159	-	-
grass	1	HRT Day 1	3113	159	3150	106
grass	1	HRT Day 4	2370	1527	2925	-
grass	1	HRT Day 7	2925	212	3113	53
grass	1	HRT Day 11	3000	106	2850	318
grass	1	HRT Day 13	2813	371	2813	53
grass	1	Untreated	2700	0	-	-
No grass	2	Blank	2363	53	-	-
grass	2	HRT Day 1	2363	53	2250	0
grass	2	HRT Day 4	2100	212	1763	265
grass	2	HRT Day 7	2138	159	2325	0
grass	2	HRT Day 11	2175	212	2325	0
grass	2	HRT Day 13	3150	318	3038	371
grass	2	Untreated	1688	477	-	-
No grass	4	Blank	2475	-	-	-
grass	4	HRT Day 1	2475	-	1838	795
grass	4	HRT Day 4	1913	795	1763	902
grass	4	HRT Day 7	2025	636	2100	530
grass	4	HRT Day 11	1725	106	2475	0
grass	4	HRT Day 13	2213	265	1781	981
grass	4	Untreated	1200	-	-	-
No grass	6	Blank	2550	-	-	-
grass	6	HRT Day 1	2475	-	2475	-
grass	6	HRT Day 4	1763	1008	2475	-
grass	6	HRT Day 7	1913	902	1988	689
grass	6	HRT Day 11	1725	318	2400	212
grass	6	HRT Day 13	2475	0	2550	-
grass	6	Untreated	1350	-	-	-
No grass	8	Blank	2625	-	-	-
grass	8	HRT Day 1	2475	-	2550	-
grass	8	HRT Day 4	1838	1008	1725	-
grass	8	HRT Day 7	1725	849	1950	636
grass	8	HRT Day 11	1650	318	2400	212
grass	8	HRT Day 13	2363	53	2475	-
grass	8	Untreated	1350	-	-	-
No grass	12	Blank	2250	-	-	-
grass	12	HRT Day 1	2175	-	2100	-
grass	12	HRT Day 4	1500	849	900	-
grass	12	HRT Day 7	1556	875	1688	689
grass	12	HRT Day 11	1013	159	2175	-
grass	12	HRT Day 13	2175	0	2025	-
grass	12	Untreated	1275	-	-	-

Table S2.3 – Xylose data for hydrolysis and fermentation test work *(mg/L)*

Xylose	Day	Sample	No SRB	Std Dev - No SRB	SRB Added	Std Dev - SRB
No grass	0	Blank	378	-	-	-
Grass	0	HRT Day 1	0.00	-	0.00	-
Grass	0	HRT Day 4	0.00	-	0.00	-
Grass	0	HRT Day 7	0.00	-	0.00	-
Grass	0	HRT Day 11	0.00	-	0.00	-
Grass	0	HRT Day 13	0.00	-	0.00	-
Grass	0	Untreated	642	11.8	-	-
No grass	1	Blank	364	19.2	-	-
Grass	1	HRT Day 1	602	37.8	584	6.38
Grass	1	HRT Day 4	476	312	584	
Grass	1	HRT Day 7	575	38.2	584	35.3
Grass	1	HRT Day 11	583	13.0	534	50.0
Grass	1	HRT Day 13	518	64.2	606	47.3
Grass	1	Untreated	987	108	-	-
No grass	1	Blank	262	4.72	-	-
Grass	2	HRT Day 1	356	1.74	340	37.4
Grass	2	HRT Day 4	348	1.32	348	57.6
Grass	2	HRT Day 7	337	2.86	336	18.4
Grass	2	HRT Day 11	329	11.3	325	6.73
Grass	2	HRT Day 13	468	52.9	693	112
Grass	2	Untreated	839	31.9	-	-
No grass	4	Blank	264	50.0	-	-
Grass	4	HRT Day 1	368	4.51	375	32.2
Grass	4	HRT Day 4	383	44.1	446	107
Grass	4	HRT Day 7	385	19.7	378	16.6
Grass	4	HRT Day 11	366	53.4	359	22.9
Grass	4	HRT Day 13	317	44.9	446	138
Grass	4	Untreated	730	-	-	-
No grass	6	Blank	210	99.2	-	-
Grass	6	HRT Day 1	403	22.1	380	42.6
Grass	6	HRT Day 4	449	97.5	502	104
Grass	6	HRT Day 7	469	61.9	459	50.3
Grass	6	HRT Day 11	430	95.8	380	52.8
Grass	6	HRT Day 13	390	21.9	393	-
Grass	6	Untreated	738	-	-	-
No grass	8	Blank	205	91.0	-	-
Grass	8	HRT Day 1	320	196	400	103
Grass	8	HRT Day 4	481	199	462	112
Grass	8	HRT Day 7	485	60.1	501	75.0
Grass	8	HRT Day 11	467	122	422	40.7
Grass	8	HRT Day 13	414	14.4	471	167
Grass	8	Untreated	499	179	-	-
No grass	12	Blank	177	97.7	-	-
Grass	12	HRT Day 1	609	-	435	130
Grass	12	HRT Day 4	412	118	221	50
Grass	12	HRT Day 7	587	3.15	454	142
Grass	12	HRT Day 11	-	-	554	-
Grass	12	HRT Day 13	516	62.8	406	119
Grass	12	Untreated	404	162	-	-

Table S2.4– Lactate data for hydrolysis and fermentation test work *(mg/L)*

Lactate	Day	Sample	No SRB	Std Dev - No SRB	SRB Added	Std Dev - SRB
No grass	0	Blank	408	14.1	-	-
grass	0	HRT Day 1	412	48.1	423	5.16
grass	0	HRT Day 4	418	24.7	412	47.1
grass	0	HRT Day 7	415	51.5	399	17.9
grass	0	HRT Day 11	425	6.29	427	-
grass	0	HRT Day 13	415	-	385	34.1
grass	0	Untreated	406	11.2	-	-
No grass	1	Blank	435	20.5	-	-
grass	1	HRT Day 1	392	9.43	435	20.7
grass	1	HRT Day 4	327	206	410	-
grass	1	HRT Day 7	377	23.3	418	11.9
grass	1	HRT Day 11	387	18.9	365	42.1
grass	1	HRT Day 13	368	58.4	363	6.59
grass	1	Untreated	523	1.73	-	-
No grass	2	Blank	337	2.22	-	-
grass	2	HRT Day 1	402	-	375	14.5
grass	2	HRT Day 4	358	4.29	365	80.9
grass	2	HRT Day 7	332	54.4	384	27.3
grass	2	HRT Day 11	361	51.5	387	1.84
grass	2	HRT Day 13	517	30.8	506	10
grass	2	Untreated	1902	149	-	-
No grass	4	Blank	299	98.8	-	-
grass	4	HRT Day 1	914	250	1022	90.7
grass	4	HRT Day 4	545	21.3	981	352
grass	4	HRT Day 7	549	114	802	458
grass	4	HRT Day 11	742	197	740	192
grass	4	HRT Day 13	852	203	793	363
grass	4	Untreated	2118	-	-	-
No grass	6	Blank	470	65	-	-
grass	6	HRT Day 1	1231	202	1474	128
grass	6	HRT Day 4	932	477	1149	436
grass	6	HRT Day 7	938	537	1011	602
grass	6	HRT Day 11	1239	119	1183	103
grass	6	HRT Day 13	1102	219	1056	579
grass	6	Untreated	2728	-	-	-
No grass	8	Blank	780	102	-	-
grass	8	HRT Day 1	1513	-	1591	44.4
grass	8	HRT Day 4	1166	728	1005	691
grass	8	HRT Day 7	1140	83.3	1506	104
grass	8	HRT Day 11	1642	162	1101	-
grass	8	HRT Day 13	1187	47.8	1230	430
grass	8	Untreated	2786	-	-	-
No grass	12	Blank	810	70.6	-	-
grass	12	HRT Day 1	1866	-	1887	196
grass	12	HRT Day 4	1947	361	-	-
grass	12	RT Day 7	1367	158	1616	331
grass	12	HRT Day 11	1962	-	1770	-
grass	12	HRT Day 13	1469	111	1520	-
grass	12	Untreated	-	-	-	-

Table S2.5 – Acetate data for hydrolysis and fermentation test work *(mg/L)*

Acetate	Day	Sample	No SRB	Std Dev - No SRB	SRB Added	Std Dev - SRB
No grass	0	Blank	854	2.3	-	-
Grass	0	HRT Day 1	868	123	848	1.54
Grass	0	HRT Day 4	846	37.2	834	86.3
Grass	0	HRT Day 7	861	90.8	837	17.3
Grass	0	HRT Day 11	861	2.02	842	3.07
Grass	0	HRT Day 13	881	-	797	79.6
Grass	0	Untreated	1331	34.4	-	-
No grass	1	Blank	1006	92.2	-	-
Grass	1	HRT Day 1	1383	63.6	1494	72.7
Grass	1	HRT Day 4	1502	-	1595	-
Grass	1	HRT Day 7	1230	57.1	1470	253
Grass	1	HRT Day 11	1376	68	1167	150
Grass	1	HRT Day 13	1203	254	1174	77.2
Grass	1	Untreated	8825	793	-	-
No grass	2	Blank	882	38	-	-
Grass	2	HRT Day 1	2683	515	2699	-
Grass	2	HRT Day 4	2291	-	1742	-
Grass	2	HRT Day 7	2447	307	2936	103
Grass	2	HRT Day 11	3546	804	2875	163
Grass	2	HRT Day 13	3628	365	2602	-
Grass	2	Untreated	17652	3663	-	-
No grass	4	Blank	11661	15148	-	-
Grass	4	HRT Day 1	10927	10146	9037	7615
Grass	4	HRT Day 4	8749	7347	10248	8374
Grass	4	HRT Day 7	7947	5393	7176	4756
Grass	4	HRT Day 11	9376	2196	4302	1129
Grass	4	HRT Day 13	4695	427	10179	7801
Grass	4	Untreated	17306	4432	-	-
No grass	6	Blank	18627	16681	-	-
Grass	6	HRT Day 1	13075	13161	10634	9783
Grass	6	HRT Day 4	9558	8210	11952	10520
Grass	6	HRT Day 7	9369	7484	8314	6316
Grass	6	HRT Day 11	11628	1881	4054	118
Grass	6	HRT Day 13	4941	1138	10933	10004
Grass	6	Untreated	14601	1759	-	-
No grass	8	Blank	16188	18531	-	-
Grass	8	HRT Day 1	9791	8734	9743	8465
Grass	8	HRT Day 4	10206	8833	12088	11201
Grass	8	HRT Day 7	8701	7130	8426	6826
Grass	8	HRT Day 11	12724	2406	3988	1444
Grass	8	HRT Day 13	4212	604	11206	10775
Grass	8	Untreated	14619	-	-	-
No grass	12	Blank	15955	17422	-	-
Grass	12	HRT Day 1	11543	9398	10729	9108
Grass	12	HRT Day 4	10379	7911	18120	4861
Grass	12	HRT Day 7	9080	6136	8753	5657
Grass	12	HRT Day 11	15111	2686	16833	15775
Grass	12	HRT Day 13	5203	430	10554	9817
Grass	12	Untreated	18537	-	-	-

Table S2.6 – Propionate data for hydrolysis and fermentation test work *(mg/L)*

Propionate	Day	Sample	No SRB	Std Dev - No SRB	SRB Added	Std Dev - SRB
No grass	0	Blank	1564	5.02	-	-
grass	0	HRT Day 1	1492	213	1502	46.4
grass	0	HRT Day 4	1467	89.8	1463	172
grass	0	HRT Day 7	1493	204	1451	45.8
grass	0	HRT Day 11	1517	15.7	1473	31.5
grass	0	HRT Day 13	1519	-	1374	162
grass	0	Untreated	1662	8.39	-	-
No grass	1	Blank	1719	126	-	-
grass	1	HRT Day 1	1856	51.6	1886	34.3
grass	1	HRT Day 4	1380	993	1811	-
grass	1	HRT Day 7	1695	87.5	1854	15.9
grass	1	HRT Day 11	1706	33.1	1629	190
grass	1	HRT Day 13	1604	268	1577	27
grass	1	Untreated	2503	558	-	-
No grass	2	Blank	1304	5.13	-	-
grass	2	HRT Day 1	2526	869	1843	362
grass	2	HRT Day 4	1677	26.1	1605	48.3
grass	2	HRT Day 7	1607	68.1	1698	135
grass	2	HRT Day 11	1644	146	1614	36.1
grass	2	HRT Day 13	2238	189	2060	178
grass	2	Untreated	2950	649	-	-
No grass	4	Blank	1526	209	-	-
grass	4	HRT Day 1	2830	1004	2149	287
grass	4	HRT Day 4	2075	175	2387	520
grass	4	HRT Day 7	2150	212	2032	179
grass	4	HRT Day 11	2078	93.7	1880	17.4
grass	4	HRT Day 13	1892	52.3	1957	242
grass	4	Untreated	2589	557	-	-
No grass	6	Blank	2028	793	-	-
grass	6	HRT Day 1	2941	888	2289	95.4
grass	6	HRT Day 4	2106	374	2354	676
grass	6	HRT Day 7	2220	87.8	2111	293
grass	6	HRT Day 11	2143	162	1989	177
grass	6	HRT Day 13	2339	348	1986	330
grass	6	Untreated	2615	651	-	-
No grass	8	Blank	2334	941	-	-
grass	8	HRT Day 1	3083	1249	2083	254
grass	8	HRT Day 4	2155	260	2461	1053
grass	8	HRT Day 7	2003	102	2003	258
grass	8	HRT Day 11	2197	126	2269	59.1
grass	8	HRT Day 13	2271	469	2219	729
grass	8	Untreated	6659	2373	-	-
No grass	12	Blank	1579	-	-	-
grass	12	HRT Day 1	5234	4225	2110	148
grass	12	HRT Day 4	2506	777	3343	1353
grass	12	HRT Day 7	2009	103	2288	237
grass	12	HRT Day 11	2231	72.4	2660	274
grass	12	HRT Day 13	2317	338	2524	460
grass	12	Untreated	6434	3123	-	-

Table S2.7 – Isovalerate data for hydrolysis and fermentation test work *(mg/L)*

Isovalerate	Day	Sample	No SRB	Std Dev - No SRB	SRB Added	Std Dev - SRB
No grass	0	Blank	102	6.66	-	-
grass	0	HRT Day 1	86.6	99.1	99.0	1.67
grass	0	HRT Day 4	93.8	7.50	92.8	13.8
grass	0	HRT Day 7	118	29.2	108	22.7
grass	0	HRT Day 11	101	4.46	113	18.7
grass	0	HRT Day 13	141	-	89.4	13.3
grass	0	Untreated	133	24.8	-	-
No grass	1	Blank	117	27.6	-	-
grass	1	HRT Day 1	142	26.7	158	0.58
grass	1	HRT Day 4	141	151	205	-
grass	1	HRT Day 7	123	13.6	140	30.3
grass	1	HRT Day 11	113	0.81	101	17.2
grass	1	HRT Day 13	126	47.1	105	10.9
grass	1	Untreated	175	1.24	-	-
No grass	2	Blank	151	2.70	-	-
grass	2	HRT Day 1	128	3.35	104	18.2
grass	2	HRT Day 4	111	5.55	98.6	18.7
grass	2	HRT Day 7	92.1	14.4	106	1.88
grass	2	HRT Day 11	117	7.66	117	10.7
grass	2	HRT Day 13	156	34.6	185	46.5
grass	2	Untreated	203	15.5	-	-
No grass	4	Blank	91.7	0.32	-	-
grass	4	HRT Day 1	112	20.1	116	9.80
grass	4	HRT Day 4	118	6.04	109	41.8
grass	4	HRT Day 7	121	6.27	121	0.23
grass	4	HRT Day 11	213	127	91.0	25.0
grass	4	HRT Day 13	100	26.7	130	22.4
grass	4	Untreated	154	21.2	-	-
No grass	6	Blank	87.8	12.5	-	-
grass	6	HRT Day 1	117	6.64	117	4.85
grass	6	HRT Day 4	106	8.86	86.4	17.5
grass	6	HRT Day 7	107	16.3	108	3.24
grass	6	HRT Day 11	113	3.35	104	5.99
grass	6	HRT Day 13	132	28.1	113	4.19
grass	6	Untreated	328	127	-	-
No grass	8	Blank	128	60	-	-
grass	8	HRT Day 1	86.0	-	112	21.1
grass	8	HRT Day 4	120	0.73	118	34.5
grass	8	HRT Day 7	108	3.03	101	4.68
grass	8	HRT Day 11	95.2	2.21	118	0.21
grass	8	HRT Day 13	128	39.6	121	8.93
grass	8	Untreated	191	-	-	-
No grass	12	Blank	81.3	-	-	-
grass	12	HRT Day 1	990	-	123	-
grass	12	HRT Day 4	-	-	1106	416
grass	12	HRT Day 7	-	-	136	7.13
grass	12	HRT Day 11	109	12.0	141	-
grass	12	HRT Day 13	-	-	739	-
grass	12	Untreated	524	-	-	-

Table S2.8 – Valerate data for hydrolysis and fermentation test work *(mg/L)*

Valerate	Day	Sample	No SRB	Std Dev - No SRB	SRB Added	Std Dev - SRB
No grass	0	Blank	316	1.58	-	-
Grass	0	HRT Day 1	344	44.8	310	8.40
Grass	0	HRT Day 4	302	14.6	293	25.1
Grass	0	HRT Day 7	341	50.9	325	33.2
Grass	0	HRT Day 11	323	0.34	340	35.3
Grass	0	HRT Day 13	314	-	291	28.2
Grass	0	Untreated	349	37.9	-	-
No grass	1	Blank	338	79.8	-	-
Grass	1	HRT Day 1	301	1.62	392	110
Grass	1	HRT Day 4	527	-	-	-
Grass	1	HRT Day 7	362	69.3	407	121
Grass	1	HRT Day 11	314	6.37	308	47.0
Grass	1	HRT Day 13	379	160	295	13.4
Grass	1	Untreated	457	17.3	-	-
No grass	2	Blank	272	5.03	-	-
Grass	2	HRT Day 1	325	15.8	298	49.3
Grass	2	HRT Day 4	290	27.6	282	60.4
Grass	2	HRT Day 7	251	31.9	304	11.3
Grass	2	HRT Day 11	334	24.8	327	10.8
Grass	2	HRT Day 13	425	93.7	413	10.7
Grass	2	Untreated	515	28.6	-	-
No grass	4	Blank	286	4.98	-	-
Grass	4	HRT Day 1	295	111	354	46.9
grass	4	HRT Day 4	343	22.9	368	27.2
grass	4	HRT Day 7	346	11.9	352	0.33
grass	4	HRT Day 11	421	159	266	47.3
grass	4	HRT Day 13	300	47.2	351	39.6
grass	4	Untreated	370	47.7	-	-
No grass	6	Blank	292	62.8	-	-
grass	6	HRT Day 1	308	1.05	299	33.5
grass	6	HRT Day 4	266	17.1	293	33.8
grass	6	HRT Day 7	279	56.3	296	4.71
grass	6	HRT Day 11	303	8.49	289	19.9
grass	6	HRT Day 13	292	14.5	281	0.15
grass	6	Untreated	319	60.5	-	-
No grass	8	Blank	383	83.3	-	-
grass	8	HRT Day 1	404	94.2	262	42.8
grass	8	HRT Day 4	293	2.92	238	1.30
grass	8	HRT Day 7	298	57.4	253	5.09
grass	8	HRT Day 11	240	5.68	268	27.5
grass	8	HRT Day 13	271	3.09	271	2.09
grass	8	Untreated	705	147	-	-
No grass	12	Blank	263	-	-	-
grass	12	HRT Day 1	411	140	264	18.8
grass	12	HRT Day 4	272	18.7	557	50.4
grass	12	HRT Day 7	242	92.4	307	5.62
grass	12	HRT Day 11	252	22.6	303	24.6
grass	12	HRT Day 13	317	28.5	281	40.3
grass	12	Untreated	1514	339	-	-

Table S2.9 – Ethanol data for hydrolysis and fermentation test work *(mg/L)*

Ethanol	Day	Sample	No SRB	Std Dev - No SRB	% RSD No SRB	SRB Added	Std Dev - SRB	% RSD SRB Added
No grass	0	Blank	408	14.1	3.45	-	-	-
grass	0	HRT Day 1	508	71.5	14.07	434	7.93	1.83
grass	0	HRT Day 4	434	24.9	5.73	459	67.3	14.7
grass	0	HRT Day 7	471	44.9	9.53	449	21.1	4.70
grass	0	HRT Day 11	423	14.7	3.48	424	16.1	3.81
grass	0	HRT Day 13	466	-	-	415	58.7	14.2
grass	0	Untreated	499	38.3	7.68	-	-	-
No grass	1	Blank	989	92.0	9.30	-	-	-
grass	1	HRT Day 1	1358	293	21.6	1622	89.3	5.50
grass	1	HRT Day 4	1794	-	-	1560	-	-
grass	1	HRT Day 7	1463	86.1	5.88	1603	17.7	1.10
grass	1	HRT Day 11	1511	39.6	2.62	1289	355	27.5
grass	1	HRT Day 13	1305	397	30.4	1499	122	8.12
grass	1	Untreated	2220	188	8.46	-	-	-
No grass	2	Blank	665	6.56	0.99	-	-	-
grass	2	HRT Day 1	1807	404	22.4	1932	158	8.19
grass	2	HRT Day 4	1868	79.8	4.27	1546	112	7.25
grass	2	HRT Day 7	1588	384	24.2	1895	13.8	0.73
grass	2	HRT Day 11	1704	378	22.2	1904	16.3	0.86
grass	2	HRT Day 13	2429	216	8.89	2351	48.9	2.08
grass	2	Untreated	2405	235	9.78	-	-	-
No grass	4	Blank	1052	297	28.2	-	-	-
grass	4	HRT Day 1	1843	360	19.5	1957	38.0	1.94
grass	4	HRT Day 4	2109	28.0	1.33	2066	-	-
grass	4	HRT Day 7	2089	232	11.1	2171	52.2	2.41
grass	4	HRT Day 11	2168	57.8	2.66	2178	92.1	4.23
grass	4	HRT Day 13	2263	4.19	0.19	2255	21.1	0.94
grass	4	Untreated	2436	160	6.59	-	-	-
No grass	6	Blank	1502	321	21.4	-	-	-
grass	6	HRT Day 1	1880	342	18..2	2026	201	9.94
grass	6	HRT Day 4	2020	111	5.50	1760	-	-
grass	6	HRT Day 7	2083	156	7.49	2168	120	5.52
grass	6	HRT Day 11	2074	9.79	0.47	2046	305	14.90
grass	6	HRT Day 13	2409	311	12.9	2170	51.5	2.38
grass	6	Untreated	2184	-	-	-	-	-
No grass	8	Blank	1689	-	-	-	-	-
grass	8	HRT Day 1	1410	575	40.8	1726	266	15.4
grass	8	HRT Day 4	2123	104	4.88	1321	324	24.5
grass	8	HRT Day 7	1883	174	9.26	1892	180	9.50
grass	8	HRT Day 11	2013	2.62	0.13	2191	-	-
grass	8	HRT Day 13	2072	157	7.58	2168	683	31.5
grass	8	Untreated	2314	-	-	-	-	-
No grass	12	Blank	1515	-	-	-	-	-
grass	12	HRT Day 1	1972	-	-	1749	122	6.95
grass	12	HRT Day 4	1971	259	13.1	1754	-	-
grass	12	HRT Day 7	2036	276	13.5	1981	163	8.25
grass	12	HRT Day 11	2142	102	4.75	2594	-	-
grass	12	HRT Day 13	2740	52.1	1.90	3019	-	-
grass	12	Untreated	2557	-	-	-	-	-